



Michigan Technological University
Create the Future Digital Commons @ Michigan Tech

Dissertations, Master's Theses and Master's
Reports - Open

Dissertations, Master's Theses and Master's
Reports

2013

Novel Automotive Waste Heat Recovery Techniques

John Randall Armstead
Michigan Technological University

Follow this and additional works at: <https://digitalcommons.mtu.edu/etds>



Part of the [Mechanical Engineering Commons](#)

Copyright 2013 John Randall Armstead

Recommended Citation

Armstead, John Randall, "Novel Automotive Waste Heat Recovery Techniques", Dissertation, Michigan Technological University, 2013.

<https://doi.org/10.37099/mtu.dc.etds/451>

Follow this and additional works at: <https://digitalcommons.mtu.edu/etds>



Part of the [Mechanical Engineering Commons](#)

NOVEL AUTOMOTIVE WASTE HEAT RECOVERY TECHNIQUES

By

John Randall Armstead

A DISSERTATION

Submitted in partial fulfillment of the requirements for the degree of

DOCTOR OF PHILOSOPHY

In Mechanical Engineering-Engineering Mechanics

MICHIGAN TECHNOLOGICAL UNIVERSITY

2013

© 2013 John Randall Armstead

This dissertation has been approved in partial fulfillment of the requirements for the Degree
of DOCTOR OF PHILOSOPHY in Mechanical Engineering-Engineering Mechanics.

Department of Mechanical Engineering-Engineering Mechanics

Dissertation Advisor: *Dr. Scott A. Miers*

Committee Member: *Dr. Jason R. Blough*

Committee Member: *Dr. Charles H. Margraves*

Committee Member: *Dr. Peter D. Moran*

Department Chair: *Dr. William W. Predebon*

To my wife, Teresa.

Table of Contents

Title Page	i
List of Figures	xiii
List of Tables	xxiii
Lists of Abbreviations	xxx
Preface	xxxii
Acknowledgments	xxxiii
Abstract	xxxv
1 Introduction	1
1.1 Fuel Usage and CAFE Standards	1
1.2 Dissertation Aim and Motivation	4
1.3 Organization of Dissertation	5
2 Waste Heat Recovery Background	9
2.1 Abstract	10

2.2	Introduction	11
2.3	Background	14
2.3.1	Thermoelectric Principles	14
2.3.2	Rankine Cycle Principles	17
2.4	Design Considerations to Address	18
2.4.1	Common Issues Related to WHR Systems	19
2.4.1.1	Backpressure	19
2.4.1.2	Weight	20
2.4.1.3	Thermal Power Fluctuations	22
2.4.1.4	Cold Reservoir Reliability	22
2.4.1.5	Type of Engine	23
2.4.1.6	Coolant or Exhaust Energy Streams	23
2.4.1.7	Expense / Complexity / Size	24
2.4.2	Thermoelectric Device Issues	24
2.4.2.1	Thermoelectric Materials	24
2.4.2.2	Longevity	25
2.4.2.3	Stress	26
2.4.2.4	DC-DC Converter Loses	26
2.4.3	Rankine Cycle System Issues	27
2.4.3.1	Working fluid selection	27
2.4.3.2	Components design	27

2.4.3.3	System pressure	28
2.4.3.4	Safety	28
2.5	Technology Advancements / Studies	29
2.5.1	Thermoelectric	29
2.5.2	Rankine Cycle	35
2.6	Conclusions	39
3	Rankine Cycle: Steam Assisted Engine	41
3.1	Abstract	42
3.2	Introduction	43
3.3	Experimental Design	44
3.3.1	Steam Chamber	47
3.3.2	Working Fluid	48
3.3.3	Coolant Heat Exchanger:	48
3.3.4	Exhaust Heat Exchanger:	49
3.3.5	Condenser, Pump, and Piping	50
3.4	Compression Ignition Engine	51
3.5	Data Analysis	53
3.5.1	Steam Generation	53
3.5.2	Steam Chamber Analysis	55
3.5.3	Power Generation	57
3.6	Conclusions	59

4	Thermoelectric Generators: Cylinder Walls	61
4.1	Abstract	63
4.2	Introduction / Background	64
4.3	Experimental Design	68
4.3.1	TEG / Surrogate Selection and Installation	70
4.4	Test Matrix / Procedure	72
4.5	Fuel Energy Distribution	74
4.5.1	In-Cylinder Heat Transfer	77
4.5.2	Gross Indicated Work	82
4.5.2.1	Remaining Friction Energy and Pumping Work	84
4.5.3	Exhaust Gas Energy	89
4.5.4	Miscellaneous Energy	93
4.6	TEG Energy Conversion	94
4.6.1	TEG Malfunction	95
4.7	Conclusions	100
5	Conclusions and Recommendations	103
5.1	Conclusions	103
5.2	Recommendations for Future Work	106
5.2.1	Rankine Cycle: Steam Assisted Engine	106
5.2.2	Thermoelectric Generators: Cylinder Walls	107
	References	109

A	Supplemental Information	119
A.1	Engine Specifications	119
A.2	Laboratory Test Cell	121
A.2.1	Cooling System	122
A.2.1.1	Cylinder Walls	126
A.2.1.2	Cold-Junction Compensation	129
A.2.2	Exhaust System	131
A.2.3	Mechanical System	132
A.3	Oil Analysis	134
A.4	Test Variable Nomenclature / Data	136
A.4.1	Raw Data Statistics	144
B	Copyrights	161
B.1	Copyright Not Required	161
B.2	Copyright Permission	173

List of Figures

1.1	The estimated yearly consumption of common fuels in the United States. Gasoline consumption includes ethanol in gasohol and Methyl Tertiary Butyl Ether (MTBE). Diesel includes biodiesel. [1, 2, 3, 4, 5, 6]	2
1.2	The trends and projections of the United States liquid fuel consumptions and the world oil prices [1]	2
(a)	United States liquid fuels consumption by sector, 1990 – 2040, in million barrels per day	2
(b)	Average annual world oil prices from 1990 – 2011 and three predictive cases from 2011 – 2040 (2011 dollars per barrel)	2
1.3	Schematic of the waste heat recovery piston in piston design	7
1.4	Engine block water-jacket with the TEG (magenta) and the TEG surrogate material (orange) installed.	8
(a)	Top view	8
(b)	Isometric view	8

2.1	Heat balance of a 1.4 liter spark ignition internal combustion engine. Reprinted with permission from SAE Paper No. 2005-01-1171 © 2005 SAE International. [25]	12
2.2	Exhaust gas temperatures from a four cylinder gasoline engine with stoichiometric combustion. Reprinted with permission from SAE Paper No. 2009-01-0174 © 2009 SAE International. [20]	12
2.3	Effect of external electric power supplied to a 2.0 liter midsize production vehicle. Reprinted with permission from SAE Paper No. 2009-01-0170 © 2009 SAE International. [31]	14
2.4	Schematic of a TE system demonstrating the Seebeck and Peltier effect [32]	15
2.5	Schematic showing cross-section of a typical multi-couple thermo-electric module. Reprinted with permission from SAE Paper No. 2009-01-1333 © 2009 SAE International. [30]	15
2.6	Electrical and thermal conduction paths of a multi-couple thermo-electric module. Reprinted with permission from SAE Paper No. 2009-01-1333 © 2009 SAE International. [30]	15
2.7	Rankine cycle system and its ideal - actual cycle. Reprinted with permission from SAE Paper No. 2005-01-1171 © 2005 SAE International. [25]	17

2.8	Rankine cycle efficiency for various turbine inlet temperatures. Reprinted with permission from SAE Paper No. 2005-01-1171 © 2005 SAE International. [25]	19
2.9	T-s diagram for dry, wet, and isentropic fluids. Reprinted with permission from SAE Paper No. 2005-01-1171 © 2005 SAE International. [25] . .	19
2.10	Effect of backpressure supplied to a 2.0 liter midsize production vehicle. Reprinted with permission from SAE Paper No. 2009-01-0170 © 2009 SAE International. [31]	20
2.11	Percent change of road load power as the percent mass increases	22
2.12	“ZT versus T for state-of-the-practice (symbols with lines) and state-of-the-art materials (lines only)” [27]	25
2.13	The heating-cooling cycle performed [28]	29
2.14	“TEG’s maximum gained power (P) and EMF (U_0) during the reliability test” [28]	30
2.15	Scanning electron microscope micrograph for a TEG before 6,000 thermal cycles [28]	31
2.16	Scanning electron microscope micrograph for a TEG after 6,000 thermal cycles [28]	31
2.17	Schematic diagram of a multiple section TE power generator system without an intermediate loop [41]	32

2.18	The schematic for a multiple TE power generator system with an intermediate loop between the exhaust pipe and the TE generator [41] .	32
2.19	The power output improvement (%) for a given exhaust gas mass flow (g/s) by using a three section system compared to a single section system [41]	33
2.20	Comparing the total cycle energy recovered (W/hr) for four different drive cycles that used a single section system (optimized at 25 g/s) to that of a three section system (optimized at 5, 10, and 20 g/s) [41]	34
2.21	The percent improvement of energy recovered for the four drive cycles for the three section system over the single section system [41]	34
2.22	Schematic showing layout of sub-section of thermoelectric heat exchanger [29]	35
2.23	Schematic of counter flow TE heat exchanger [29]	35
2.24	Schematic of the Rankine cycle utilizing the engine and exhaust gas waste heat. Reprinted with permission from SAE Paper No. 2006-01-1605 © 2006 SAE International. [48]	36
2.25	An ORC-WHR system with integrated low-temperature cooling loop [49]	37
2.26	Schematic of a regenerative ORC [50]	38
3.1	Schematic of the proposed waste heat recovery engine setup	44
3.2	Schematic of the proposed waste heat recovery piston in piston design .	46
3.3	The steam inlet and exhaust valve profiles with the steam cylinder clearance height.	46

3.4	Exhaust gas temperature and mass flow rate located in the exhaust system between after-treatment devices and the muffler for the C-13 diesel engine operating at full load	52
3.5	Exhaust gas specific heat and density located in the exhaust system between after-treatment devices and the muffler for the C-13 diesel engine operating at full load	52
3.6	The amount of waste heat recovered and the percentage of the total rejected in-cylinder heat transfer from 100 kW over a range of starting working fluid temperatures.	54
3.7	Steam chamber valve lift profiles and trapped working fluid mass within the steam chamber	56
3.8	Steam chamber pressure and working fluid temperature	56
3.9	The steam chamber pressure and steam quality throughout the four engine cycles. (Quality of 1 correlates to 100% steam per mass ratio and a quality of 0 correlates to 0% steam per mass ratio.)	57
3.10	Net power generated from WHR and corresponding fuel conversion efficiency over a range of exhaust back pressures resulting from an exhaust heat exchanger.	59
4.1	Energy and exergy (availability) for a SI engine. [57]	65
4.2	Engine block water-jacket with a TEG (magenta) and a TEG surrogate material (orange) installed.	71

(a) Top view	71
(b) Isometric view	71
4.3 Fuel energy distribution flowchart	74
4.4 Combustion efficiency and lambda for the baseline testing and the resulting change after TEG installation	76
(a) Combustion Efficiency	76
(b) Lambda	76
4.5 Relations between combustion efficiency and lambda	77
(a) Baseline data	77
(b) TEG addition	77
4.6 Upper (3mm) and lower (15mm) outer cylinder wall temperatures	79
(a) Baseline testing	79
(b) TEG testing	79
(c) Change of outer cylinder wall temperatures due to TEG material .	79
4.7 Heat transfer to the coolant system for the baseline testing and the resulting change after TEG installation	81
4.8 Percentage of the heat energy within the coolant system that was transferred through the TEG material	82
4.9 Gross indicated and brake work and BSFC for the baseline testing and the resulting change after TEG installation	83
(a) Gross indicated and brake work	83

(b) Brake specific fuel consumption	83
4.10 Remaining friction energy and pumping work for the baseline testing and the resulting change after TEG installation	85
(a) Remaining friction energy	85
(b) Pumping work	85
4.11 Oil to friction relations	87
(a) Oil temperature for the baseline testing and the resulting change after TEG installation	87
(b) Oil viscosity over a range of temperatures including 8.7% reduction in viscosity for BL oil fuel dilution	87
(c) Stribeck diagram [73]	87
4.12 Air density and throttle position for the baseline testing and the resulting change after TEG installation	89
(a) Air density	89
(b) Throttle position	89
4.13 Exhaust gas energy and temperature for the baseline testing and the resulting change after TEG installation	90
(a) Exhaust gas energy	90
(b) Exhaust gas temperature	90
4.14 Combustion duration for the baseline testing and the resulting change after TEG installation and the relation to the change in exhaust gas energy . .	92

(a) Combustion duration	92
(b) Change in exhaust gas energy and change in combustion duration correlation	92
4.15 Cylinder pressure trace and the total change after TEG installation for engine speed of 3000 <i>RPM</i> and 40 <i>Nm</i>	92
4.16 Miscellaneous power for the baseline testing and the resulting change after TEG installation	93
4.17 Scaled TEG energy output and fuel energy conversion	95
(a) From experimental TEG data	95
(b) From predicted TEG data	95
4.18 TEG validation test without compression	97
4.19 Location for coolant penetration into TEG	97
4.20 TEG measured voltage compared to the predicted TEG voltage	99
4.21 Comparison of cylinder wall temperatures for cylinder 2 using the TEG as a thermal insulator and using the TEG surrogate material as a thermal insulator	99
(a) TEG location with TEG	99
(b) TEG location with surrogate	99
A.1 Kohler AEGIS LH690 Liquid-Cooled Horizontal Crankshaft Engine [71]	121
(a) View one	121
(b) View two	121

A.2	View 1 of the coolant system.	122
A.3	View 2 of the coolant system	125
A.4	View 3 of the coolant system	126
A.5	TEG performance output in Watts over a range of hot and cold-side temperatures [76]	127
A.6	Cylinder #1 outer wall thermocouple installation	128
	(a) Location of thermocouples within cylinder wall (exhaust side) . .	128
	(b) Thermocouples installed with JB Weld	128
A.7	Cylinder #1 TEG and TEG surrogate installation	129
	(a) TEG surrogate (light blue) installed	129
	(b) TEG and TEG thermocouple installed (close up)	129
A.8	Terminal block of the K-type thermocouple to copper wire connections. Bag is filled with a dielectric fluid.	130
A.9	Exhaust system schematic	131
A.10	Transducer locations	136

List of Tables

1.1	NHTSA CAFE standards and EPA CO_2 equivalent emissions standard from 2012 – 2016 [23]	4
4.1	Data summary of the combustion efficiency and lambda	76
4.2	Data summary of the Upper (3mm) and Lower (15mm) outer cylinder wall temperature	78
4.3	Data summary of the energy to coolant	80
4.4	Data summary of the percentage of the energy within the coolant system that was transferred through the TEG material data summary	82
4.5	Data summary of the gross indicated work, brake work, and brake specific fuel consumption	84
4.6	Data summary of the remaining friction energy and pumping work	85
4.7	Data summary of the oil temperature	87
4.8	Data summary of the air density and throttle position	89
4.9	Data summary of the exhaust gas energy and temperature	91
4.10	Data summary of the combustion duration	92
4.11	Miscellaneous energy and temperature data summary	94

4.12	Data summary of the TEG energy output and fuel energy conversion . .	95
4.13	TEG voltage output validation with and without compression	96
A.1	Engine specifications for the Kohler LH690 horizontal-shaft, liquid-cooled SI engine. NOTE: All listed dimensions and tolerances are measured at 20°C. [71]	120
A.2	9" water brake dynamometer information [77]	133
A.3	Engine testing mode numbers and the corresponding engine speed and load	137
B.1	List of figures and that do not require copyright permission	162
B.2	List of figures and that require copyright permission	173

Lists of Abbreviations

Initialisms

AFR. air fuel ratio

BDC. bottom dead center

BL. baseline

BSFC. brake specific fuel consumption

BSFC. brake specific fuel consumption

BTDC. before top dead center

CAC. Charge Air Cooler

CAD. crank angle degrees

CAFE. Corporate Average Fuel Economy

CI. compression ignition

CJC. cold-junction compensation

DAQ. data acquisition

EES. Engineering Equation Solver

EGR. exhaust gas recirculation

EIA. Energy Information Administration

EMF. electromotive force

EPA. Environmental Protection Agency

exh. exhaust

g. acceleration due to gravity

HT. high temperature

IC. internal combustion

LHR. low heat rejection

LHV. lower heating value of the fuel

LT. low temperature

MTBE. Methyl Tertiary Butyl Ether

N. rotational speed of the crankshaft

NHTSA. National Highway Traffic Safety Administration

ORC. Organic Rankine Cycle

P. power

PID. proportional-integral-derivative

RPM. revolutions per minute

S. Seebeck coefficient

SG. specific gravity

T. average operating temperature

TDC. top dead center

TE. thermoelectric

TEG. thermoelectric generator(s)

WHR. waste heat recovery

ZT. dimensionless figure of merit

Mathematical Symbols

A_v . frontal area of the vehicle

C_D . drag coefficient

$C_{p,f}$. specific heat of fluid

$C_{p,g}$. specific heat of gas

C_R . coefficient of rolling resistance

C_V . flow coefficient

$cp_{cool,95C}$. specific heat of a 50/50 mixture of water and ethylene glycol at 95°C

$Heat_{cool}$ coolant energy

\dot{m}_f . mass flow rate of fuel

M_v . mass of vehicle

n_R . number of crankshaft revolutions per cycle

P_r . road-load power

Q . volumetric flow rate

Q_{LHV} . lower heating value of a fuel

R_{JBWeld} . thermal resistance of JB Weld

$R_{surrogate}$. thermal resistance of TEG surrogate material

S_v . vehicle speed

T_C . cold-side temperature

T_H . hot-side temperature

$T_{Head,Out}$. coolant temperature leaving cylinder head

T_{lower} . lower position cylinder wall temperature

T_{TEG} . cold-side temperature from TEG

$T_{WJ,In}$. coolant temperature entering the water-jacket

U_0 . electromotive force

\dot{V}_{cool} . volumetric flow rate of the coolant

ΔH_{vap} . enthalpy of vaporization

ΔP_{press} . pressure drop

ΔT_f . change in fluid temperature

ΔT_g . change in gas temperature

η_f . fuel conversion efficiency

η_{HE} . efficiency of heat exchanger

η_v . volumetric efficiency

κ . thermal conductivity

λ . relative air/fuel ratio

ρ_a . ambient air density

$\rho_{cool,95C}$. density of 50/50 mixture of water and ethylene glycol at 95°C

σ . electrical conductivity

Preface

This dissertation is a compilation of journal articles that were authored by myself and my advisor, Dr. Scott Miers.

Chapter 2: “Review of Waste Heat Recovery Mechanisms for Internal Combustion Engines”, was originally published from the ASME 2010 Internal Combustion Engine Division Fall Technical Conference. The manuscript was submitted and accepted in 2013 to the Journal of Thermal Science and Engineering Application. As the primary author, I performed the literature review and wrote the article while Dr. Miers edited and helped to develop the paper.

Chapter 3: “Waste Heat Recovery Rankine Cycle: Steam Assisted Engine Piston-in-Piston Assembly”, was written in preparation to be submitted as a journal article. CarbonTec, Inc. solicited a simulation-based evaluation of their waste heat recovery patent. I developed the GT-Power simulations and authored the article. This project and article required feedback and guidance from my advisor.

Chapter 4: “Automotive Cylinder Wall Waste Heat Recovery with Thermoelectric Generators”, was written in preparation to be submitted as a journal article. I developed this original idea from my previous research. The experimental-based project required significant time and effort from Dr. Miers and myself to setup the engine test cell. I

performed the data analysis and wrote the article. Dr. Miers helped to edit and refine the paper.

Acknowledgments

I would like start by acknowledging that my advisor, Dr. Miers, has been a very influential mentor since the moment I returned to Michigan Tech for my graduate studies. I cannot thank him enough for his near tireless efforts and for his time that he had invested in me. I want to thank the rest of my committee members: Dr. Blough, Dr. Margraves, and Dr. Moran. Your insight and suggestions helped me to create an even better dissertation. I have had the pleasure of being a graduate teaching assistant for most of my committee. Through those interactions, I have had many long conversations that I will always cherish. Nancy Barr has been invaluable, not only for her feedback on my writing, but also for her friendship throughout the years. Thank you to all of my office-mates, especially Andrew Wiegand, for their friendship and support. I am also extremely thankful for the engine lab support that I received from my colleague, Swaroop Kumar Gurram. Without Swaroop's assistance, I might still be in the lab taking data today!

I want to thank my family, which has always held a positive role in my life. My dad, Randy, has always been the man that I look up to the most. It has been inspiring that he is frustratingly good at everything he attempts and yet he refuses to become complacent. His determination and resolve has helped to give me the courage to strive to become the man that he sees in me. My mom, Sue, has always been the one that I could count on for guidance and she still has an ability to give me confidence when I felt I had none. My older

brother and sister (Dan and Jen) are both brilliant, compassionate, and determined people and I cannot describe how much they have influenced my life for the better.

I saved my closest family member for last. My wife, Teresa, has inspired me in ways that no one else has done before. She is everything I ever wanted and needed in this life. I could always count on her to shower me with love and support when I need it... but I can also count on her to give me the swift kick-to-the-bum when I need that too! She keeps me humble and thankful for every achievement that I attain. Thank you!

Abstract

The United States transportation industry is predicted to consume approximately 13 million barrels of liquid fuel per day by 2025. If one percent of the fuel energy were salvaged through waste heat recovery, there would be a reduction of 130 thousand barrels of liquid fuel per day. This dissertation focuses on automotive waste heat recovery techniques with an emphasis on two novel techniques.

The first technique investigated was a combination coolant and exhaust-based Rankine cycle system, which utilized a patented piston-in-piston engine technology. The research scope included a simulation of the maximum mass flow rate of steam (700 K and 5.5 MPa) from two heat exchangers, the potential power generation from the secondary piston steam chambers, and the resulting steam quality within the steam chamber. The secondary piston chamber provided supplemental steam power strokes during the engine's compression and exhaust strokes to reduce the pumping work of the engine. A Class-8 diesel engine, operating at $1,500\text{ RPM}$ at full load, had a maximum increase in the brake fuel conversion efficiency of 3.1%.

The second technique investigated the implementation of thermoelectric generators on the outer cylinder walls of a liquid-cooled internal combustion engine. The research scope focused on the energy generation, fuel energy distribution, and cylinder wall temperatures.

The analysis was conducted over a range of engine speeds and loads in a two cylinder, 19.4 kW, liquid-cooled, spark-ignition engine. The cylinder wall temperatures increased by 17% to 44% which correlated well to the 4.3% to 9.5% decrease in coolant heat transfer. Only 23.3% to 28.2% of the heat transfer to the coolant was transferred through the TEG and TEG surrogate material. The gross indicated work decreased by 0.4% to 1.0%. The exhaust gas energy decreased by 0.8% to 5.9%. Due to coolant contamination, the TEG output was not able to be obtained. TEG output was predicted from cylinder wall temperatures and manufacturer documentation, which was less than 0.1% of the cumulative heat release. Higher TEG conversion efficiencies, combined with greater control of heat transfer paths, would be needed to improve energy output and make this a viable waste heat recovery technique.

Chapter 1

Introduction

1.1 Fuel Usage and CAFE Standards

Fossil fuels, which includes coal, natural gas, and petroleum, accounted for approximately 95.5% of the primary sources of energy for transportation in the United States in 2011 [1]. The estimated yearly amount of gasoline and diesel fuel consumed in the United States from 1992 to 2011, as seen in Figure 1.1, indicates that even minor improvements in vehicle fuel economy have the potential to save significant quantities of fossil fuels. The U.S. Energy Information Administration (EIA) has projected that liquid fuels consumption for transportation will stabilize around 13 million barrels per day in the United States from 2025 to 2040, seen in Figure 1.2(a) and the average annual world oil price will reach 162

dollars per barrel by 2040, seen in Figure 1.2(b). The combination of the projected increase in fuel consumption and cost is a cause for concern. This will lead to a faster depletion of non-renewable fossil fuels and an increase in the financial strain on the economy.

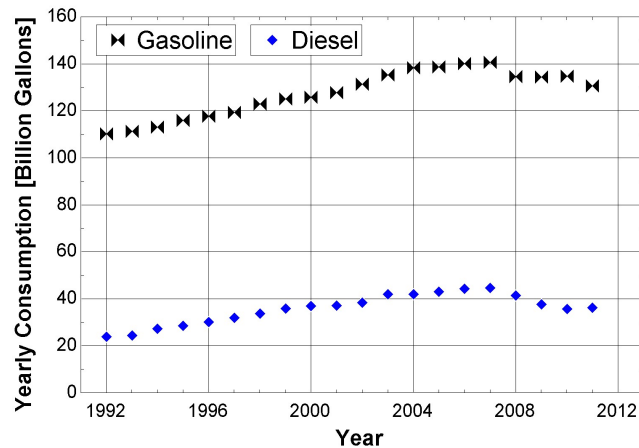


Figure 1.1: The estimated yearly consumption of common fuels in the United States. Gasoline consumption includes ethanol in gasohol and Methyl Tertiary Butyl Ether (MTBE). Diesel includes biodiesel. [1, 2, 3, 4, 5, 6]

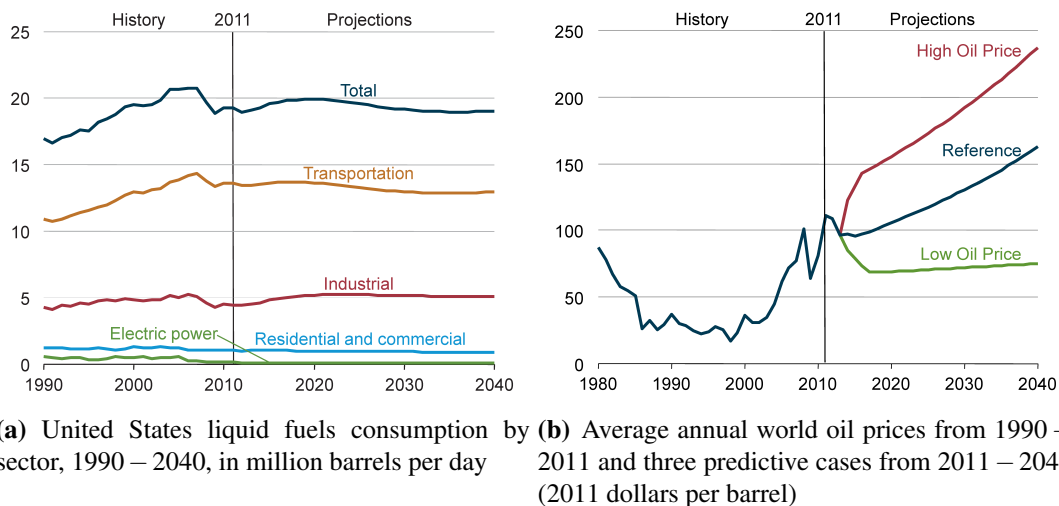


Figure 1.2: The trends and projections of the United States liquid fuel consumptions and the world oil prices [1]

The United States Congress in 1975, in an attempt to address the issue of fuel usage, created the Corporate Average Fuel Economy (CAFE). The mission statement of the CAFE is to reduce the United States energy consumption by increasing the fuel economy of cars and light trucks (less than 8,500 lbs) that are sold within the United States. The mission is implemented by the National Highway Traffic Safety Administration (NHTSA) which is responsible for setting the fuel economy standards and the Environmental Protection Agency (EPA) which calculates the average fuel economy for each manufacturer. Between the year 2012 and 2016, the CAFE standards for fuel economy and CO_2 will become increasingly strict, as seen in Table 1.1.

The internal combustion (IC) engine converts approximately one third of the chemical energy in fuel to mechanical work. This fuel conversion efficiency (η_f) is calculated with Equation (1.1), where P is power, \dot{m}_f is the mass flow rate of fuel, and Q_{LHV} is the lower heating value of fuel. To help achieve the CAFE standards, there is continuous research to improve the overall fuel conversion efficiency in a number of different areas including friction reduction [7, 8, 9], volumetric efficiency (η_v) improvements [10, 11, 12, 13], advanced combustion systems [14, 15, 16, 17, 18], and waste heat recovery (WHR) [19, 20, 21, 22]. By increasing the fuel conversion efficiency and meeting the CAFE standards, the depletion of the global fuel supply could be decelerated and the fuel expenditure by the end user could be decreased.

Table 1.1
NHTSA CAFE standards and EPA CO_2 equivalent emissions standard
from 2012 – 2016 [23]

Model Year	Passenger Car	Light Truck	Combined
NHTSA CAFE standard (miles per gallon)			
2012	33.3	25.4	29.7
2013	34.2	26.0	30.5
2014	34.9	26.6	31.5
2015	36.2	27.5	32.6
2016	37.5	28.8	34.1
EPA CO_2 -equivalent emissions standard (grams per mile)			
2012	263	346	295
2013	256	337	286
2014	247	326	276
2015	236	312	263
2016	225	298	250

$$\eta_f = \frac{P}{\dot{m}_f * Q_{LHV}} \quad (1.1)$$

1.2 Dissertation Aim and Motivation

This dissertation focused on the potential energy recovery, engineering challenges, and the new advancements in automotive waste heat recovery methods. This was accomplished through three main goals. The first goal was to clearly define current waste heat recovery techniques using Rankine cycles and thermoelectric generators while building an understanding of the engineering obstacles that are hindering their widespread application. The second goal explored the potential of harnessing the coolant and exhaust energy stream

for a unique Rankine cycle design while the third goal explores the effects of utilizing thermoelectric generators within the coolant energy stream.

The United States transportation industry is predicted to consume approximately 13 million barrels of liquid fuel per day by 2025, shown in Figure 1.2(a). Considering that the IC engine converts more of the chemical fuel energy into heat than mechanical energy, the ability to recover this heat energy and convert it into useable mechanical or electrical energy would be valuable. If one percent of the fuel energy is salvaged through waste heat recovery, there would be a reduction of 130 thousand barrels of liquid fuel per day from the predicted 2025 transportation industry fuel consumption. That would be a savings of approximately 47 million barrels of liquid fuel per year!

1.3 Organization of Dissertation

This dissertation is comprised of journal articles that are either published or are in the process of being reviewed. Each of the following chapters were used to satisfy the dissertation aim by accomplishing all three of the dissertation goals. The description of each of the chapters along with the chapter objectives are described below:

The objective of Chapter 2 is a literature review that provides a thorough overview of the automotive waste heat recovery techniques using thermoelectric generators and Rankine

cycles. There are a number of engineering obstacles hindering these fuel saving techniques which are evaluated. This chapter also highlights recent advancements in these fields that do address the engineering challenges.

The objective of Chapter 3 is to quantify the potential improvement in vehicle fuel economy with a coolant and exhaust-based Rankine cycle which utilized a recently patented piston-in-piston engine technology, shown in Figure 1.3. Two GT-Power (from Gamma Technologies) simulations were used to evaluate this WHR technique. The first simulation recreated a representative version of a Caterpillar Inc. C-13 on-highway diesel engine with ACERT Technology. This simulation determined the operational characteristics of the engine's power distribution (thermal and mechanical) as well as exhaust gas characteristics (temperature, mass flow rate, and specific heat). The second GT-Power simulation investigated a steam chamber, which was designed with the calculated values of the maximum mass and volumetric flow rate of the working fluid (steam) which had a temperature of 700 K and a pressure of 5.5 MPa . This steam chamber had power strokes during the engine's compression and exhaust strokes to reduce the pumping work of the C-13 engine. The hypotheses of this research project was that there would be enough steam generation that all six cylinders of the C-13 diesel engine could be equipped with a secondary steam chamber and that fuel conversion efficiency would increase by 2.0%.

The objective of Chapter 4 was to investigate the impact of implementing thermoelectric generators (TEG) on the outer cylinder walls of a liquid-cooled internal combustion engine.

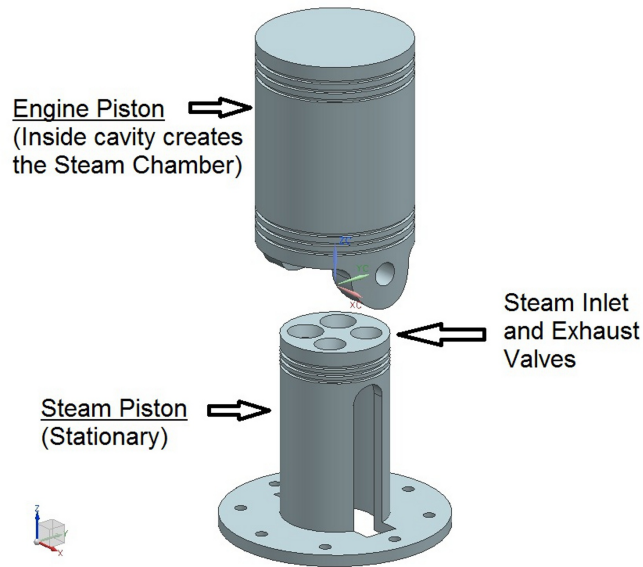


Figure 1.3: Schematic of the waste heat recovery piston in piston design

The research scope focused on the empirical trends in TEG power generation, fuel energy distribution, and cylinder wall temperatures with the addition of the TEG / TEG surrogate material over a range of engine speeds and loads utilizing a 19.4 kW liquid-cooled spark ignition engine. One 30 mm x 30 mm TEG was installed on each cylinder and a TEG surrogate material (similar thermal resistance) covered the remaining cylinder surface area. With the increased cylinder wall temperatures from the TEG/surrogate insulating effect, an engine oil analysis was performed to assess the effects of increased cylinder wall temperature on oil quality and potential degradation. A model of the engine block with the TEG and TEG surrogate installed in the water-jacket is shown in 1.4(a) and 1.4(b). The installation location of the TEG was identical for both cylinders. The electrical power generated from the TEGs was scaled to simulate the effect of covering the entire cylinder surface with TEGs. The hypotheses of this research was that the fuel conversion efficiency

will improve by 0.5% and that the majority of the displaced cylinder wall heat transfer will be expelled through the exhaust system.

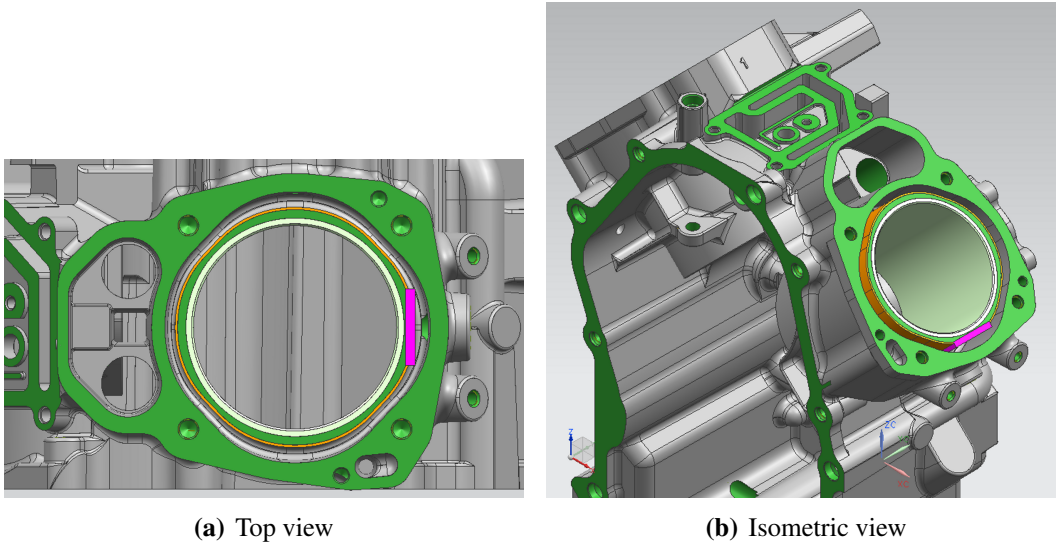


Figure 1.4: Engine block water-jacket with the TEG (magenta) and the TEG surrogate material (orange) installed.

Chapter 2

Waste Heat Recovery Background

*This chapter was originally published in the ASME 2010 Internal Combustion Engine Division Fall Technical Conference [24]. The manuscript was submitted and accepted in 2013 to the Journal of Thermal Science and Engineering Application. It is an overview of automotive-based waste heat recovery techniques which were primarily focused on the use of thermoelectric generators and Rankine cycles. While both of these waste heat recovery techniques have potential, there are several engineering complications that need to be addressed. The end of this chapter also emphasizes recent advancements in these technologies which concentrate on the engineering challenges.*¹

¹The material contained in this chapter been accepted for publication in the Journal of Thermal Science and Engineering Applications.

ICEF2010-35142

Review of Waste Heat Recovery Mechanisms for Internal Combustion Engines

John R. Armstead

Michigan Technological University
Houghton, Michigan, USA

Scott A. Miers

Michigan Technological University
Houghton, Michigan, USA

2.1 Abstract

The demand for more fuel efficient vehicles has been growing steadily and will only continue to increase given the volatility in the commodities market for petroleum resources. The internal combustion engine utilizes approximately one third of the chemical energy released during combustion. The remaining two-thirds are rejected from the engine via the cooling and exhaust systems. Significant improvements in fuel conversion efficiency are possible through the capture and conversion of these waste energy streams. Promising waste heat recovery techniques include turbocharging, turbo compounding, Rankine engine compounding, and thermoelectric generators. These techniques have shown increases in

engine thermal efficiencies that range from 2% to 20%, depending on system design, quality of energy recovery, component efficiency, and implementation. The purpose of this paper is to provide a broad review of the advancements in the waste heat recovery methods; thermoelectric generators and Rankine cycles for electricity generation, which have occurred over the past 10 years as these two techniques have been at the forefront of current research for their untapped potential. The various mechanisms and techniques, including thermodynamic analysis, employed in the design of a waste heat recovery system are discussed.

2.2 Introduction

The internal combustion (IC) engine is approximately one third efficient at converting the energy in fuel to mechanical work. The remaining energy is lost through waste heat that is predominantly rejected from the engine through the cooling and exhausts systems [25]. To improve the fuel economy in automobiles with IC engines, various techniques to recover this waste heat energy are being investigated. Two of the most promising techniques that will be discussed in this paper are thermoelectric generators and the Rankine cycle.

Depending on operating conditions, engine type, and location of the temperature measurement, exhaust gas temperatures average between 500°C and 600°C, with maximum values up to 1000°C [25, 26, 27, 28] while the coolant fluid temperatures range between

100 and 130°C [25, 29]. The heat energy found in the exhaust ranges from 4.6 to 120 kW and from 9 to 48 kW for the coolant system. An illustration of the heat balance of a 1.4 liter gasoline engine at two operating conditions can be seen in Figure 2.1 while a graph showing exhaust gas temperatures over different engine speeds and torque from a four cylinder gasoline engine can be seen in Figure 2.2. [25]

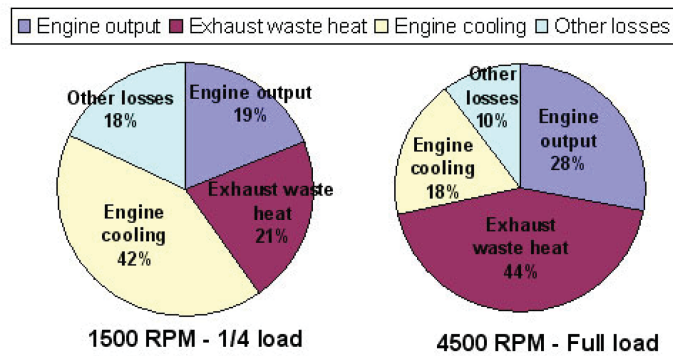


Figure 2.1: Heat balance of a 1.4 liter spark ignition internal combustion engine. Reprinted with permission from SAE Paper No. 2005-01-1171 © 2005 SAE International. [25]

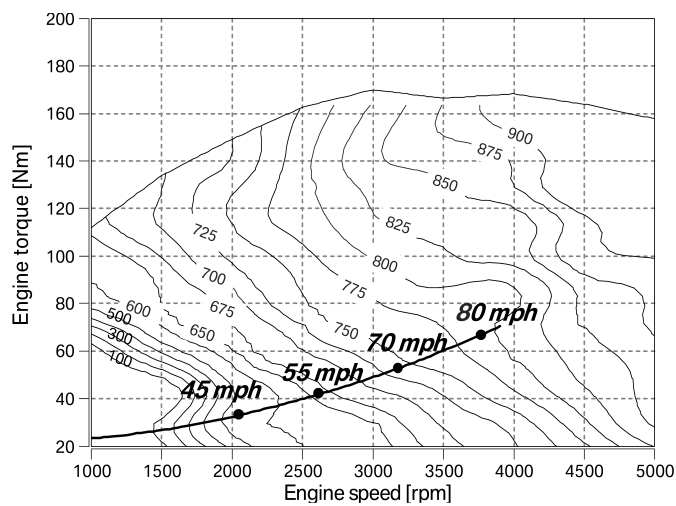


Figure 2.2: Exhaust gas temperatures from a four cylinder gasoline engine with stoichiometric combustion. Reprinted with permission from SAE Paper No. 2009-01-0174 © 2009 SAE International. [20]

The Carnot cycle, that takes into account the average exhaust gas/coolant fluid temperatures with ambient air temperatures, states that the maximum amount of energy that ideally can be recovered ranges from 1.7 to 45 *kW* for the exhaust and from 0.9 to 4.8 *kW* for the coolant system [25].

The recovered exergy or, available useful energy, can be recycled back into the vehicle system either mechanically or electrically. This paper will focus on the use of thermoelectric generators and Rankine cycles as waste heat recovery (WHR) systems that generate electricity. It has been estimated that a WHR system that produces 1.3 *kW* of electricity can replace the alternator of a small passenger vehicle [30]. Reduction of the engine's mechanical load needed to operate the alternator would result in an increase in vehicle fuel economy. The potential energy that could be recovered would indicate that the net fuel consumption of hybrid vehicles can be improved by as much as 32% [25].

A 2.0 liter midsize production vehicle was tested on a chassis dynamometer by Mori, et al. [31]. Figure 2.3 shows the proof of concept of supplying external electric power to the electrical system over three different driving cycles. The improvement in fuel economy could exceed 15% for certain cases. The improvement in the fuel economy was the direct result of supplementing the electrical load on the engine from the alternator and thus reducing the mechanical load on the engine.

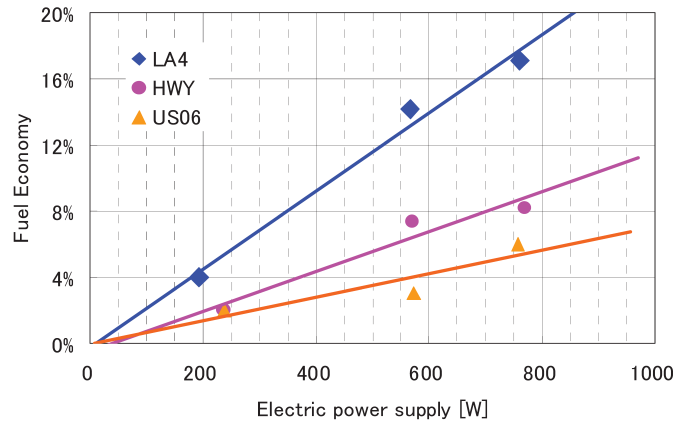


Figure 2.3: Effect of external electric power supplied to a 2.0 liter midsize production vehicle. Reprinted with permission from SAE Paper No. 2009-01-0170 © 2009 SAE International. [31]

2.3 Background

2.3.1 Thermoelectric Principles

Thermoelectric systems are solid state devices that can be used in two basic modes based on either the Peltier effect or the Seebeck effect [32], shown in Figure 2.4. The mode that uses the Peltier effect has current going through the TE (thermoelectric) module which causes absorption of heat on one side of the device and an expulsion of heat on the other. The mode that uses the Seebeck effect has a temperature gradient across a TE module that causes the TE module to generate an electric current. Thermoelectric (TE) modules are made from alternating elements of n-type (negative) and p-type (positive) semiconductors connected electrically in series and thermally in parallel [33]. This can be seen in Figure 2.5

and Figure 2.6.

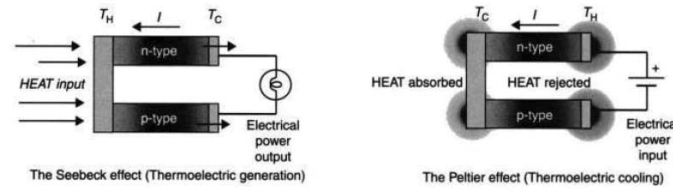


Figure 2.4: Schematic of a TE system demonstrating the Seebeck and Peltier effect [32]

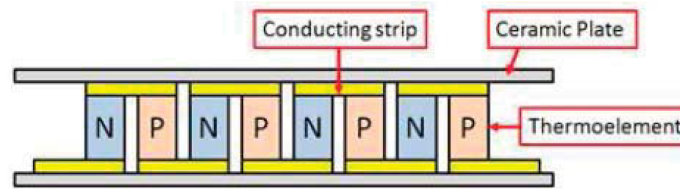


Figure 2.5: Schematic showing cross-section of a typical multi-couple thermo-electric module. Reprinted with permission from SAE Paper No. 2009-01-1333 © 2009 SAE International. [30]

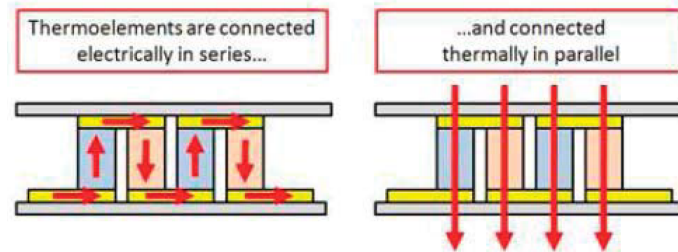


Figure 2.6: Electrical and thermal conduction paths of a multi-couple thermo-electric module. Reprinted with permission from SAE Paper No. 2009-01-1333 © 2009 SAE International. [30]

To measure the efficiencies of these TE modules to generate electricity, a term is defined called the dimensionless figure of merit (ZT) [34]. The equation to calculate the ZT value can be found in Eq. (2.1). Where S is the Seebeck coefficient, σ is the electrical

conductivity, T is the average operating temperature, and κ is the thermal conductivity.

$$ZT = \frac{S^2 * \sigma * T}{\kappa} \quad (2.1)$$

The current value of ZT for TE systems is around 1.0. To be competitive with current mechanical recovery systems, such as turbochargers, the ZT value for TE systems needs to be around 34 [34]. It should be noted that Srinivasan and Praslad [35] have stated that the ZT needs to be equal to or greater than 8 to compete with conventional electricity generators or vapor compression refrigerators. Although these levels of ZT are not available at this time, lab studies of TE systems that use new materials have been recording ZT values that have exceeded 2 with evidence that it could be improved with additional research. It was estimated in 2008 by Heading, et al. [33] that higher efficiency TE systems will be commercially available within the next five to ten years. This rapid advancement of TE materials that has increased the ZT for operation around 500°C has made thermoelectric generators (TEG) good candidates for waste heat recovery for automotive purposes [33].

The thermal efficiency of any exhaust-based TEG is controlled by four main factors; heat exchanger geometry, heat exchanger materials, the installation site of the exhaust-based TEG, and the coolant system of the exhaust-based TEG [36].

2.3.2 Rankine Cycle Principles

The Rankine cycle is a thermodynamic cycle dedicated to generate mechanical work from heat. This mechanical work can be converted into electrical energy [25].

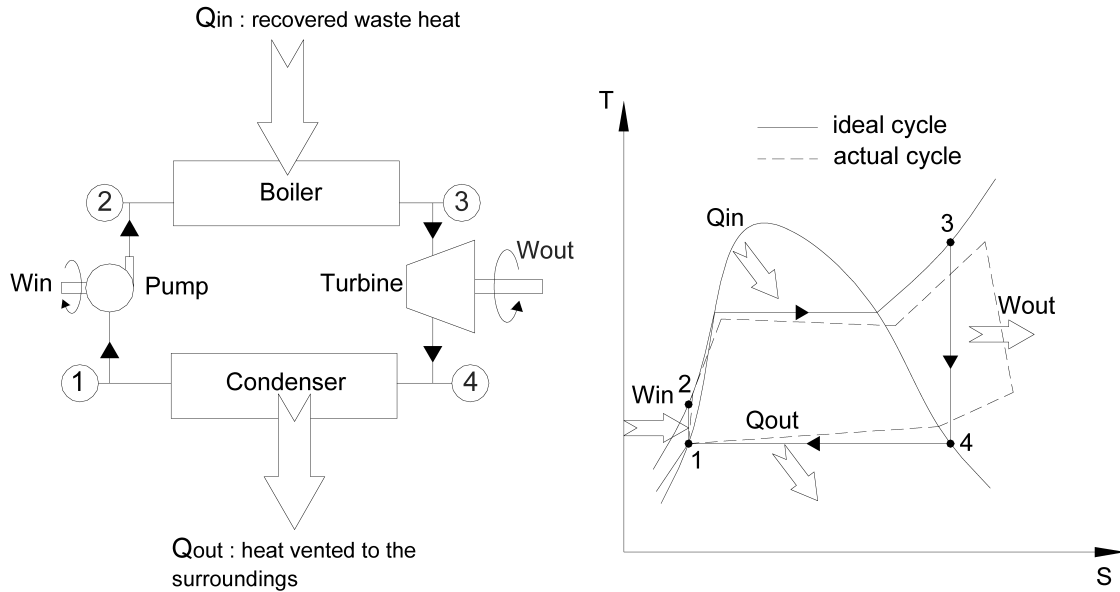


Figure 2.7: Rankine cycle system and its ideal - actual cycle. Reprinted with permission from SAE Paper No. 2005-01-1171 © 2005 SAE International. [25]

The ideal Rankine cycle, seen in Figure 2.7, consists of the following processes: [25]

- 1 – 2: compression of a working fluid in a pump
- 2 – 3: constant pressure heat addition in a boiler
- 3 – 4: isentropic expansion through a turbine
- 4 – 1: constant pressure heat rejection in a condenser

Irreversibilities, such as fluid friction and heat transfer, contribute to differences between

the actual cycle efficiency and the ideal Rankine cycle prediction.

The choice of the working fluid in the Rankine cycle for automotive WHR systems is important. The use of water as the working fluid becomes inefficient for WHR at temperatures below 370°C [37, 38]. The use of an organic fluid instead of water to recover heat energy at temperatures below 370°C increases the Rankine cycle efficiency [37, 38, 39]. A graph of efficiencies of numerous working fluids over a range of the inlet temperature of the turbine can be seen in Figure 2.8. A Rankine cycle that utilizes organic fluid is termed an Organic Rankine Cycle (ORC). The three categories of working fluid are dry, wet, and isentropic. They are determined by the slope (dT/ds) of the saturated vapor line on the temperature-entropy (T-s) diagram; dry is positive, wet is negative, and isentropic is infinite as shown in Figure 2.9. ORC systems use dry or isentropic type for the working fluid because they are superheated after isentropic expansion. This eliminates the need of a superheated apparatus because there is no longer a concern that liquid droplets would form on the turbine blades [38].

2.4 Design Considerations to Address

There is a considerable number of design and technological issues within these two WHR techniques but these techniques also have unique issues of their own.

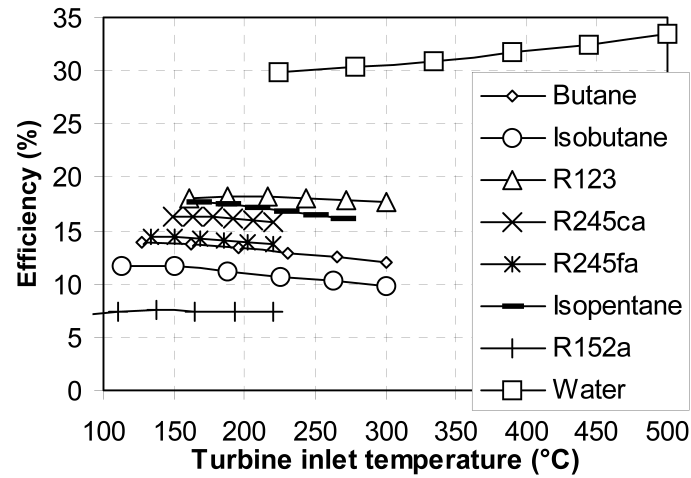


Figure 2.8: Rankine cycle efficiency for various turbine inlet temperatures. Reprinted with permission from SAE Paper No. 2005-01-1171 © 2005 SAE International. [25]

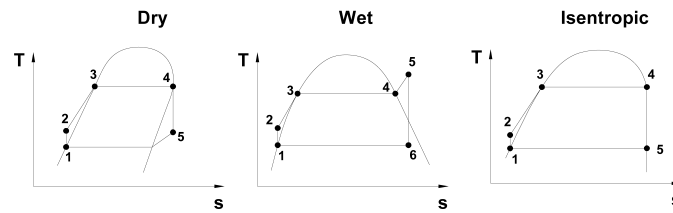


Figure 2.9: T-s diagram for dry, wet, and isentropic fluids. Reprinted with permission from SAE Paper No. 2005-01-1171 © 2005 SAE International. [25]

2.4.1 Common Issues Related to WHR Systems

2.4.1.1 Backpressure

With the installation of a WHR system in a vehicle exhaust system, the engine backpressure will increase resulting in reduced engine volumetric efficiency and thus reduced fuel

conversion efficiency. This restriction is caused by direct obstruction of the exhaust gas flow, or by the reduction in temperature of the exhaust gas or by a combination of both [31]. An experiment conducted by Mori, et al. [31] on a 2.0 liter mid-size production vehicle showed the effect of additional mean backpressure to the fuel economy during three different driving modes. The results of the study are shown in Figure 2.10.

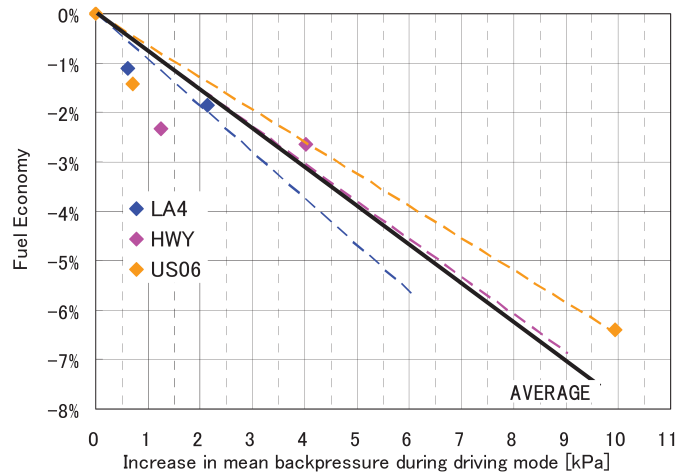


Figure 2.10: Effect of backpressure supplied to a 2.0 liter midsize production vehicle. Reprinted with permission from SAE Paper No. 2009-01-0170 © 2009 SAE International. [31]

However, the effect of increased back pressure within the coolant system on fuel economy was negligible [31].

2.4.1.2 Weight

The added weight of automotive WHR systems could result in a reduction of fuel economy, which has been a widely published concern although the range of additional weights

of these systems have not been disclosed. The additional weight increases the required road-load power to keep a vehicle at a constant speed. The equation for road-load power, P_r can be seen in Equation (2.2) [40]. The nomenclature for the variables are; C_R is the coefficient of rolling resistance, M_v is the mass of vehicle, g is the acceleration due to gravity, ρ_a is the ambient air density, C_D is the drag coefficient, A_v is the frontal area of the vehicle, and S_v is the vehicle speed. The possible effects of additional weight on the fuel economy is not easily determined because every engine design would have a unique brake specific fuel consumption (BSFC), map. This means there will be situations where the increased road-load power could result in a lower BSFC and thus have an improved fuel economy. This generally is not the case as increased vehicle weight is not desired in regards to fuel economy.

$$P_r = \left(C_R M_v g + \frac{1}{2} \rho_a C_D A_v S_v^2 \right) S_v \quad (2.2)$$

To further explain the concern of additional weight on a road load power, a vehicle was set to the following attributes: coefficient of rolling resistance = 0.0138, mass of vehicle = 5000lb, drag coefficient = 0.038, frontal area of vehicle = 33ft², and the vehicle speed = 55mph. The results, Figure 2.11, show that the change in required road load power increases by 0.42 multiplied by the percent increase in the vehicle weight.

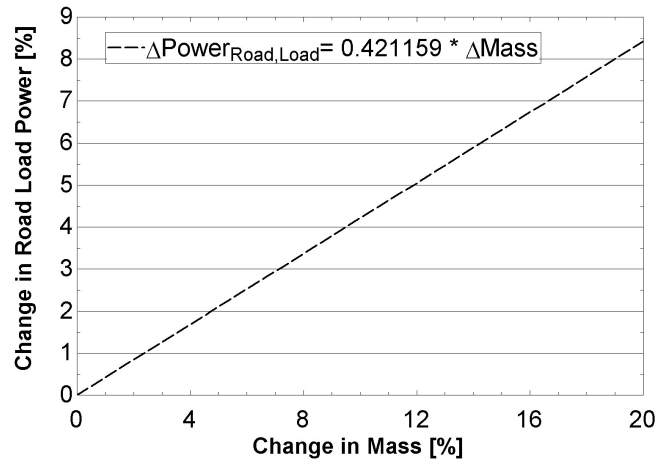


Figure 2.11: The percent change of road load power as the percent mass increases for a 5000lb vehicle with a coefficient of rolling resistance = 0.0138, drag coefficient = 0.038, frontal area of vehicle = 33ft², and the vehicle speed = 55mph

2.4.1.3 Thermal Power Fluctuations

The thermal power sources of waste heat in an IC engine are highly dynamic. They are a function of mass flow rate and temperature. The dynamic changes that occur with the mass flow rate and temperature will greatly affect the heat transfer to the WHR system. This will cause the overall performance of the WHR system to degrade from its optimum [41].

2.4.1.4 Cold Reservoir Reliability

To properly recover the wasted heat from the exhaust, a compact heat exchanger similar to a radiator would need to be integrated. The air flow on the underside of the car is not

consistent compared to the airflow that is being applied to the coolant system radiator. Due to this fact, it is difficult to regulate dependable heat transfer to the cold reservoir (ambient air) which will diminish the efficiency of the system [42].

2.4.1.5 Type of Engine

The comparison of two engine types for light-duty vehicles concluded that spark ignition engines are more favorable for WHR systems because they generally have higher exhaust gas temperatures and lower exhaust gas flow rates [43].

2.4.1.6 Coolant or Exhaust Energy Streams

As was stated earlier, the exhaust system has a greater potential to convert waste heat into mechanical work compared to the cooling system. Thus, the location of the WHR system generally resides in the exhaust system [44].

The highest temperatures and heat energy in the exhaust system would be found before and in the catalytic converter. Although this would permit larger amounts of WHR, it is not recommended to remove heat from the catalytic converter since this could decrease its conversion efficiency if enough energy was extracted. [31]

2.4.1.7 Expense / Complexity / Size

The added expense, complexity, and size of WHR systems have hindered significant implementation. Generally, to utilize a larger quantity of waste heat would require an increase in the system complexity and thus increased expense and size [25, 20].

As was stated by Smith and Thornton [45], “Current TE system costs of \$3,000 to 6,000/ kW must be reduced substantially, to about \$450/ kW for the Class 8 truck platform application, to become economically justifiable.” They went on to mention that this reduction in cost might come as a result of using thin-film devices that use expensive TE junction materials more efficiently.

2.4.2 Thermoelectric Device Issues

2.4.2.1 Thermoelectric Materials

A high ZT value of TE materials over certain temperature ranges is crucial to the success of TEG as WHR systems. The key to this WHR technique will continue to be the development of new TE materials with increased TE efficiency [46].

2.4.2.2 Longevity

Although thermoelectrics have been known to have long productive life spans in certain applications, a great deal of planning must be done to get the most power out of these devices while protecting their durability. “Efficient operation of the TEG heat exchangers over the life of 10 years to 30 years of a vehicle is a concern. The effect of material buildup on the heat exchanger surfaces from exhaust gas, coolant, or air is basically unknown and needs research to ensure that it does not excessively degrade system operation” [27].

As seen in Figure 2.12, the ZT values of high- ZT materials peak only relatively lower than the material degradation (melting, sublimation, etc) temperatures. This is a cause for

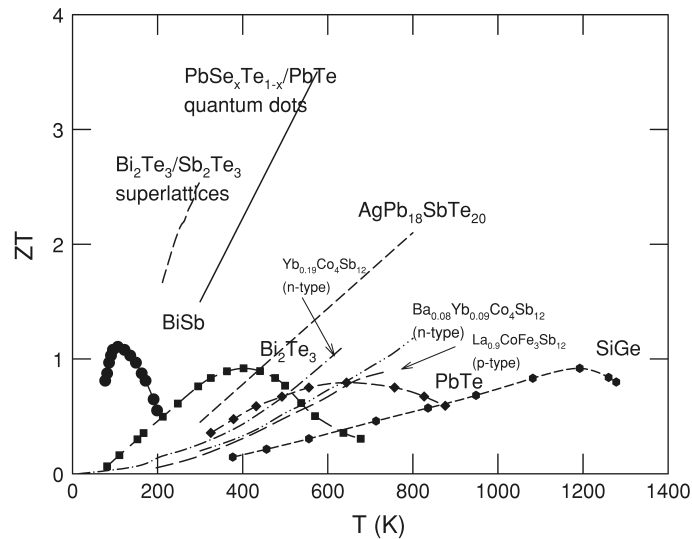


Figure 2.12: “ ZT versus T for state-of-the-practice (symbols with lines) and state-of-the-art materials (lines only)” [27]

concern since the goal of TEGs as WHR systems is to maximize the amount of electrical

energy generated. As the temperature decreases from the optimum setting, the ZT value decreases significantly. Therefore, the efficiency of the TEG will be proportionally lower at these lower temperatures. The materials in the TEG must be able to either withstand the highest possible temperatures found in either the coolant or exhaust systems or must be protected from these potentially devastating high temperatures by other means [28, 41].

2.4.2.3 Stress

Most thermoelectric materials are brittle semiconductors. Any micro fractures in the thermoelectric materials will reduce the TEG's ability to generate electricity. In the case of using TEG's in automotive applications, the stresses from thermal gradient, thermal cycling, and vibrations may cause; fractures within the TE materials, increases in the electrical resistivity, decreases in the material's ZT value, and reduction in the lifetime of the TEG [27, 28].

2.4.2.4 DC-DC Converter Losses

The relatively low output voltages of thermoelectric WHR systems will need to be raised to a level that is compatible with the vehicle's electrical system. The DC-DC converter losses will affect the total increase in fuel economy. The issue of DC-DC converter losses becomes more important when high voltages are needed for Hybrid Electric Vehicle

applications [47].

2.4.3 Rankine Cycle System Issues

2.4.3.1 Working fluid selection

Most organic fluids suffer chemical decomposition and deterioration at high temperatures and pressures. Although water does not have this issue, it does have shortcomings of high operating boiling pressure, low condensing pressures, and high triple-point temperatures that does not make it an ideal fluid for Rankine bottoming cycles for automotive applications [25].

The environmental aspects of the organic working fluid such as global warming potential and ozone depletion potential have to be a consideration in selecting the working fluid [25]. Organic fluids prevent freezing and air infiltration problems that can occur in similarly designed steam Rankine systems [25].

2.4.3.2 Components design

The working fluid and operating conditions can greatly influence the design of the turbine since they influence the power density, pressure ratio, volumetric flow, and maximum

operating pressure [25]. The heat exchanger (boiler and condenser) dimensions and cost are dependent on the thermal properties of the operating fluid, mass flow rates, operating pressures, and the Rankine cycle system efficiency. The mass flow rate is significant because higher mass flow rates require large collectors and flow passages in order to avoid excessive pressure drop. The operating pressure of the working fluid is influential as it will affect the heat exchanger mass due to the metal thickness that will be required [25].

2.4.3.3 System pressure

The efficiency of the system increases as the system pressure increases, however, it may not be realistic to pursue this direction due to cost, complexity, and material selection of the components [25].

2.4.3.4 Safety

The safety aspects of toxicity, maximum operating pressure, and flammability have to be considered [25].

2.5 Technology Advancements / Studies

2.5.1 Thermoelectric

There was a study performed by Hatzikraniotis, et al. [28] to determine the longevity of a TEG in an environment similar to that found in vehicles. This test involved 6,000 sequential heating-cooling cycles over a time period of 3,000 hours. The TE material used was $2.5\text{cm} \times 2.5\text{cm}$ Bi_2Te_3 -based modules (Melcor HT9 – 3 – 25) and the module consisted of 31 thermocouples. The hot reservoir fluctuated from 30°C to 200°C while the cold reservoir stayed constant at 24°C . The graph of the thermal cycle and the generated amperage and volts can be seen in Figure 2.13.

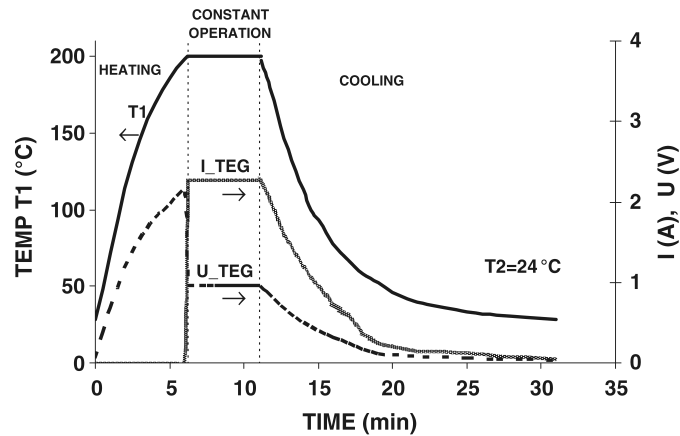


Figure 2.13: The heating-cooling cycle performed [28]

The abrupt changes in the first 15 cycles could have been the contribution by the thermal

grease being deteriorated caused by the elevated temperatures. The ZT value decreased from 0.74 to 0.63 and was accompanied by a 6.6% decrease in the average leg thermal conductivity, a 3.8% decrease in the Seebeck coefficient, and a 16.1% increase in resistivity. The gained power and electromotive force (EMF) was reduced by 14% and 3.3%, respectively [28]. These results of the experiment can be found in Figure 2.14.

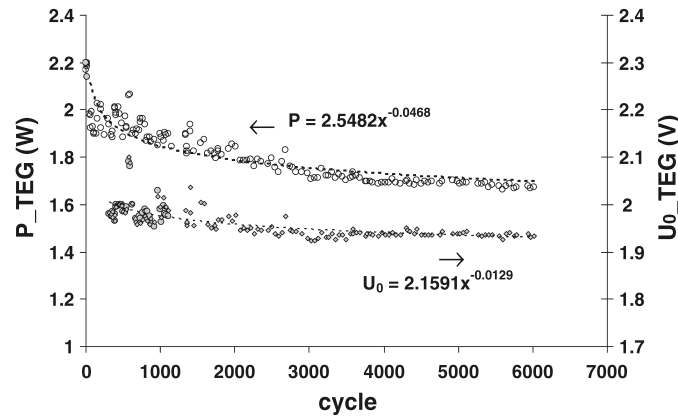


Figure 2.14: “TEG’s maximum gained power (P) and EMF (U_0) during the reliability test” [28]

Using a scanning electron microscope, Figures 2.15 and 2.16 reveal the physical effects of 6,000 thermal cycles on the tested TEG. Notice how the TE material degraded and there is evidence of a micro fracture in the connecting metal.

Realizing that TE systems are only optimized for a small range of temperature and mass flow rate, an experiment by Crane and Bell [41] utilized a three section system that had each section optimized for different operating conditions. The multiple sections allowed for the TE system to adjust to the constantly changing environment to insure the maximum amount of electricity could be generated. This system would be regulated with a controller

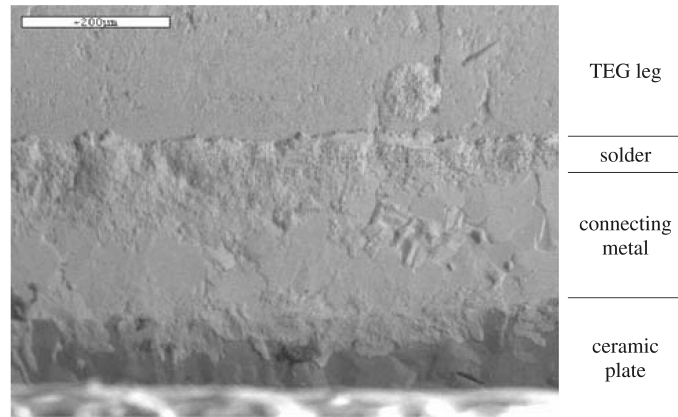


Figure 2.15: Scanning electron microscope micrograph for a TEG before 6,000 thermal cycles [28]

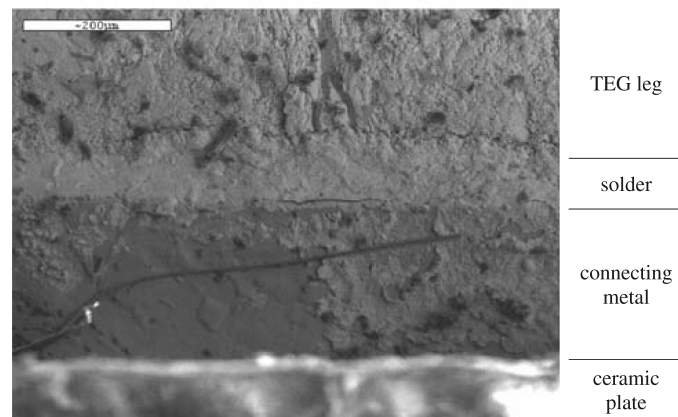


Figure 2.16: Scanning electron microscope micrograph for a TEG after 6,000 thermal cycles [28]

and valves. An example of such a system can be seen in Figure 2.17. To minimize the influence of fluctuations in the operating conditions, an intermediate loop was added to the system, which is shown in Figure 2.18.

Improvement in the power output percentage was consistently increased over an exhaust gas mass flow rate range of 5 – 40 g/s. The largest increases occurred when the exhaust gas mass flow was very low (5 g/s). The lowest improvement was around the exhaust gas mass

flow rate of 20 – 25 g/s but increased as the mass flow rate increased or decreased from this amount. The performance improvements over traditional single section TE devices are in the range of 90% at low mass flow rates and 25% for high mass flow rates. This data can be found in Figure 2.19.

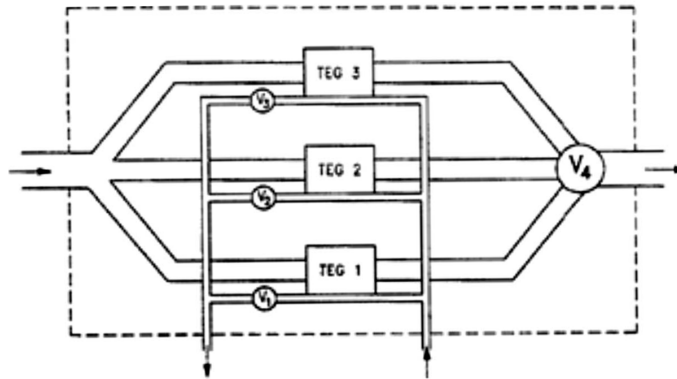


Figure 2.17: Schematic diagram of a multiple section TE power generator system without an intermediate loop [41]

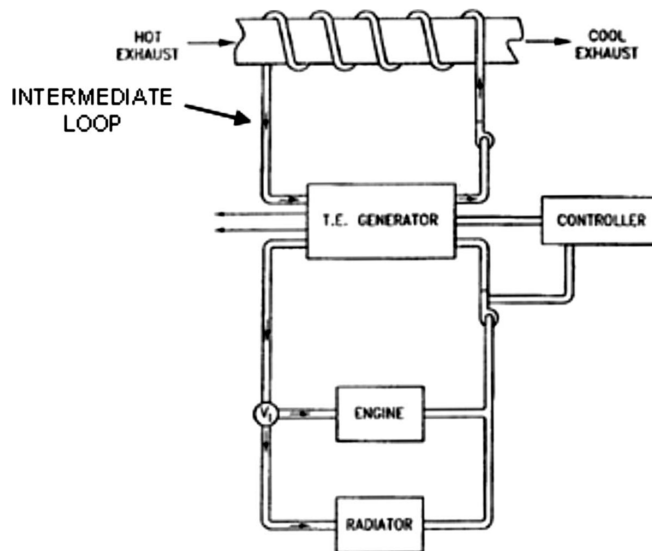


Figure 2.18: The schematic for a multiple TE power generator system with an intermediate loop between the exhaust pipe and the TE generator [41]

The total cycle energy recovered was measured on four different drive cycles for both a

single section TE system and a three section TE system. These drive cycles were FTP–75 city cycle, the HWFET highway cycle, the combined city and highway cycle, and the European NEDC drive cycle. The results found in Figure 2.20 show that the three section TE system outperforms the single section TE system for all four drive cycles because the three section TE system can be optimized for three different heat energy conditions instead of just one.

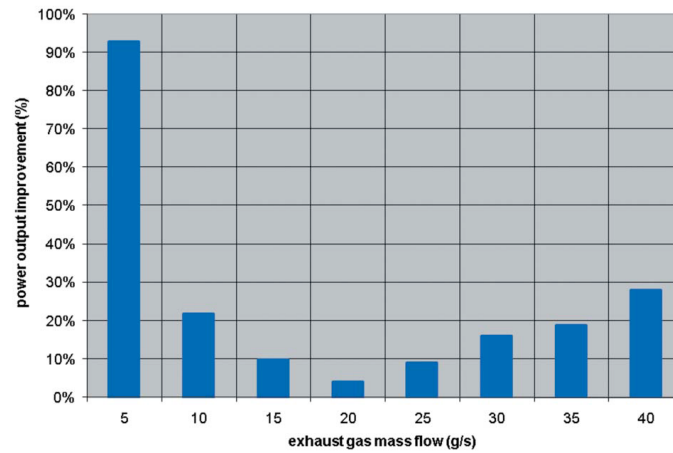


Figure 2.19: The power output improvement (%) for a given exhaust gas mass flow (g/s) by using a three section system compared to a single section system [41]

The performance improvement for the four different drive cycles can be found in Figure 2.21, which illustrates an increase from roughly 9% – 18%.

A system level optimization study by Mori, et al. [29] that used a validated model was performed to find the potential of a cross flow heat exchanger that had hot reservoir characteristics of the coolant flows of an IC engine. The system would take the place of a traditional radiator and thus would have the cold reservoir consisting of ambient air

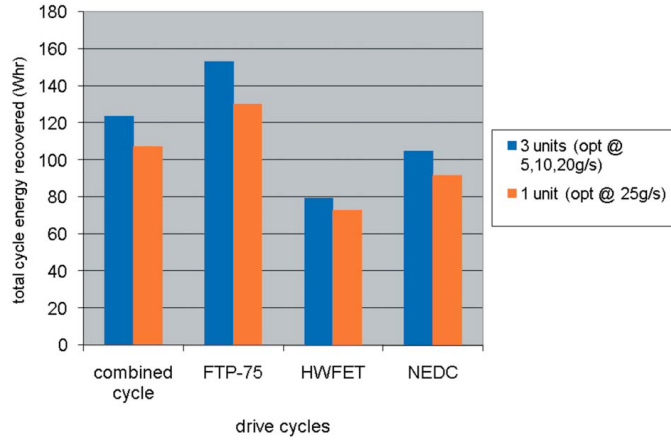


Figure 2.20: Comparing the total cycle energy recovered (W/hr) for four different drive cycles that used a single section system (optimized at 25 g/s) to that of a three section system (optimized at 5, 10, and 20 g/s) [41]

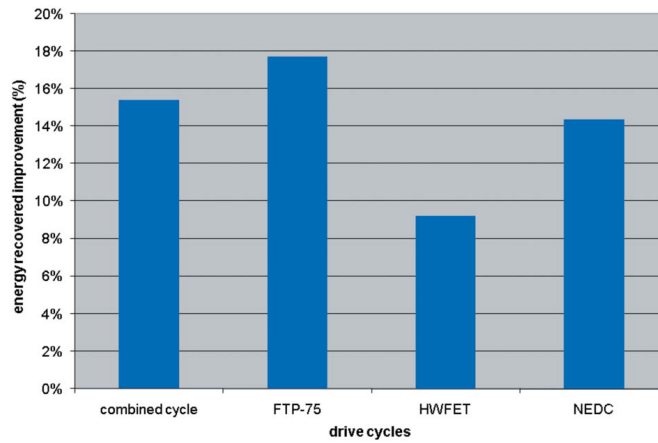


Figure 2.21: The percent improvement of energy recovered for the four drive cycles for the three section system over the single section system [41]

flowing over the heat exchanger. The schematics of the simulated system can be seen in Figure 2.22 and 2.23. “The results show that a net power output of 1 kW can be achieved for a modestly sized heat exchanger core such that the net power density based on heat exchanger volume is 45 kW/m³. Optimization for a power/cost ratio objective function with a minimum net power requirement of 1 kW indicated that the power per cost can

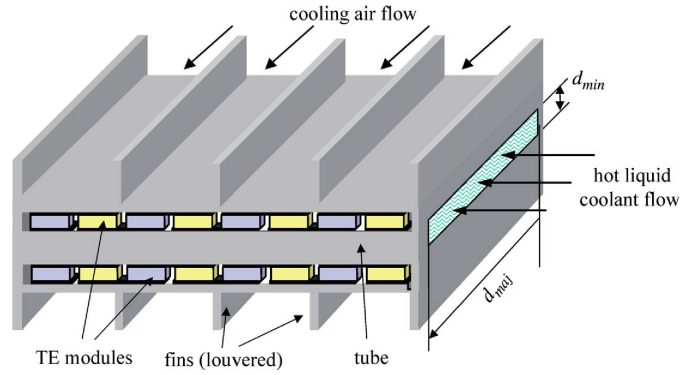


Figure 2.22: Schematic showing layout of sub-section of thermoelectric heat exchanger [29]

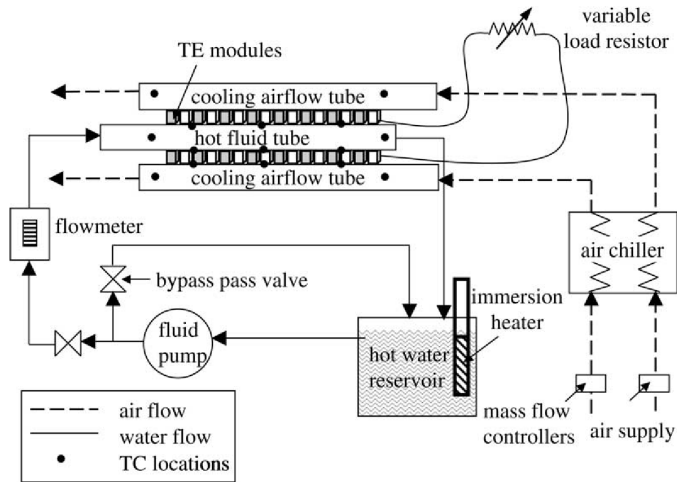


Figure 2.23: Schematic of counter flow TE heat exchanger [29]

reach as high as $1.1\text{ kW}/10,000''$ [29].

2.5.2 Rankine Cycle

A study conducted by Arias, et al. [48] evaluated the potential energy recovery in a practical hybrid implementation. The Toyota Prius hybrid was used as inputs for the vehicle/energy

recovery model. It was found that the exhaust temperatures for this vehicle were lower than what was expected. This lower temperature accounted for a poor average recovery rate of 0.8% of the total fuel energy and about 1.8% of the total available waste heat. The system was modified to utilize the heat from the engine block, seen in Figure 2.24. The

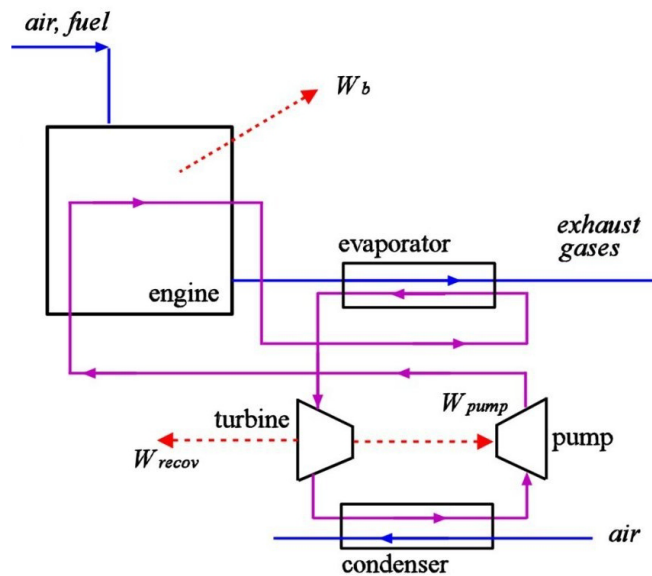


Figure 2.24: Schematic of the Rankine cycle utilizing the engine and exhaust gas waste heat. Reprinted with permission from SAE Paper No. 2006-01-1605 © 2006 SAE International. [48]

engine block was used to boil the working fluid in the power cycle and the high temperature exhaust gases were then used to superheat the fluid. This combination of WHR resulted in an average recovery rate of 5.5% of the total fuel energy and about 7.5% of the total available waste heat.

In a study from Teng, et al. [49], an ORC system was proposed for a heavy-duty diesel engine. The working fluid that was used was categorized as a dry fluid with a critical

pressure less than 70 bar. This ORC WHR system had different pressures in the Charge Air Cooler (CAC), the low temperature exhaust gas recirculation (LT-EGR), the exhaust cooler, and the high temperature exhaust gas recirculation (HT-EGR) cooler. This was done to improve system performance, reduce system cost, and avoid possible phase change in the EGR coolers. It was decided that heat rejection from the radiator would be excluded in the WHR system because its energy level was close to that of the ambient. The negative effect of requiring a larger condenser size, if the heat rejection from the radiator was included, also helped the decision to exclude it. A schematic of the proposed system can be found in Figure 2.25.

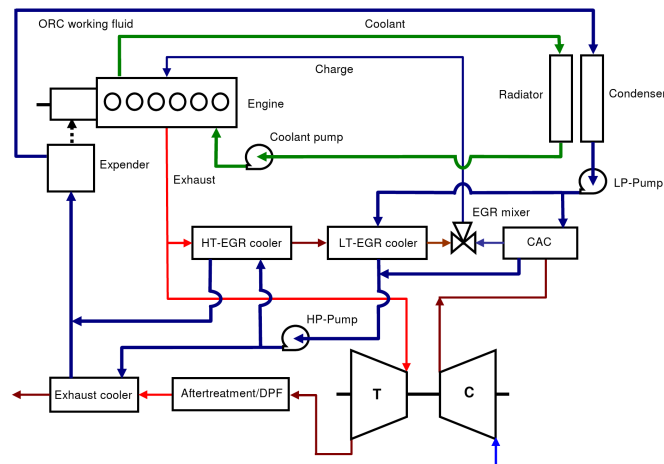


Figure 2.25: An ORC-WHR system with integrated low-temperature cooling loop [49]

“The case study showed that up to 20% increase in the engine power could be achieved by the WHR system without additional fuel consumption. It was demonstrated that, with the hybrid power system of the diesel engine and the Rankine engine operated with waste heat, substantial enhancement in the engine power, improvement in fuel economy, and deduction

in specific emissions can be achieved” [49].

A study by Mago, et al. [50], explored how the use of regenerative ORC over a basic ORC would affect the amount of exergy destroyed during the Rankine cycle process. Reducing the amount of exergy destroyed during the Rankine cycle would help increase the efficiency of the entire WHR system. The schematic of a regenerative ORC can be found in Figure 2.26.

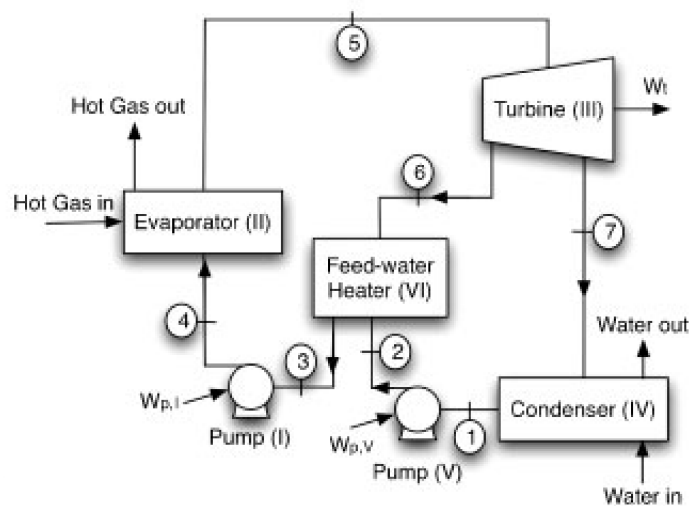


Figure 2.26: Schematic of a regenerative ORC [50]

The regenerative ORC produced higher thermal/exergy efficiencies, a higher degree of thermodynamic perfection, and a lower total system exergy loss compared to the basic ORC system.

It was found that the evaporator is the component, in ORC systems, with the highest influence coefficient and highest exergy loss with respect to the overall system exergy loss. The exergy loss was reduced in regenerative ORC systems from 77% to 40.4% because the

working fluid was more gradually warmed up by the presence of the feed-water heater.

The thermal and exergy efficiencies increase along with a decrease in system total exergy loss with the increase in the evaporator pressure. The increased evaporator pressure will bring the temperature of the organic fluid closer to the temperature of the hot gas entering the evaporator with heat transfer occurring over a lower temperature difference.

2.6 Conclusions

The use of waste heat recovery systems in automobiles has shown substantial potential to increase fuel economy. The two main WHR systems for automotive applications were found to be thermoelectric generators and Rankine cycle electrical generators. The design considerations for these systems include; backpressure, weight, thermal power fluctuations, cold reservoir reliability, DC-DC converter losses, type of engine, coolant or exhaust energy streams, expense, complexity, and size. Additional considerations for thermoelectric material, longevity, and stress are needed for thermoelectric generators while working fluid selection, component design, system pressure, and safety are needed for Rankine cycles. Over the past ten years, these issues have been addressed by a number of different case studies and advances in technology which will assist in making these techniques for waste heat recovery in automobiles economically and technologically a reality.

Chapter 3

Rankine Cycle: Steam Assisted Engine

This chapter was written in preparation to be submitted as a journal article ¹. The goal of this project was to quantify the potential improvement in vehicle fuel economy with a combination of a coolant and exhaust-based Rankine cycle which utilizes a recently patented piston in piston engine technology. This was done with the aid of two GT-Power simulations. One simulation was of a Class-8 diesel engine and the other simulation was on a uniquely designed steam chamber.

¹The material contained in this chapter was written/designed for a journal article submission.

Waste Heat Recovery Rankine Cycle: Steam Assisted Engine Piston-in-Piston Assembly

John R. Armstead

Michigan Technological University
Houghton, Michigan, USA

Scott A. Miers

Michigan Technological University
Houghton, Michigan, USA

Keywords Waste Heat Recovery, Rankine Cycle, Exhaust Heat Exchanger, Coolant Heat Exchanger, Automotive

3.1 Abstract

The reciprocating internal combustion engine converts more of the chemical energy in fuel to thermal energy than mechanical energy. Waste heat recovery methods are currently being evaluated for transforming the generally unutilized thermal energy into either mechanical or electrical energy that can be used to improve overall fuel economy. This article focused on the feasibility of using a Rankine cycle waste heat recovery method in an automotive setting. The engine simulation has modified piston assemblies to incorporate a second piston within the existing piston that is powered by high temperature, high pressure steam that is generated from the collected thermal energies within the coolant and exhaust systems. The simulation showed that a Class-8 diesel engine would produce sufficient recoverable waste heat to operate this engine technology under specific operating

conditions. The Class-8 diesel engine running at 1,500 *RPM* at full load with the waste heat recovery system had a net power increase of up to 26.7 *kW* with the addition of the engine technology which equated to an increase of the brake fuel conversion efficiency from 34.4% up to a maximum of 37.5% for a total of a 3.1% increase.

3.2 Introduction

Waste heat recovery (WHR) is a concept of collecting unused thermal energy and converting it into usable electrical energy or mechanical work. Utilizing WHR on internal combustion (IC) engines will improve the approximately thirty three percent fuel conversion efficiency and thus reduce the consumption of fossil fuels. The fuel energy that is not converted to mechanical work is predominantly rejected from the combustion chamber as heat through the cooling and exhaust systems [25]. Although the amount of thermal energy expelled by the coolant and exhaust system may be significant, the maximum amount of useful energy, or exergy, is determined based on the differences in temperature between the defined hot and cold reservoirs. This paper evaluated the validity and potential of an automotive Rankine cycle which recovered waste heat from both the coolant and exhaust systems from a Class-8 diesel engine to power reciprocating pistons that supplemented the engine power during the compression and exhaust strokes. The Class-8 diesel engine, used in trucks categorized by the gross vehicle weight rating of 14,968 *kg* and over [51], and the steam chamber were modeled in the engine simulation

software GT-Power and the desired thermodynamic properties and calculations were performed using Engineering Equation Solver (EES).

3.3 Experimental Design

The automotive WHR technique evaluated with a piston-in-piston design is modeled after the United States Patent No. 7,997,080 [52]. The schematic of the proposed WHR engine setup is shown in Figure 3.1. Starting at the pump, the working fluid in liquid form is

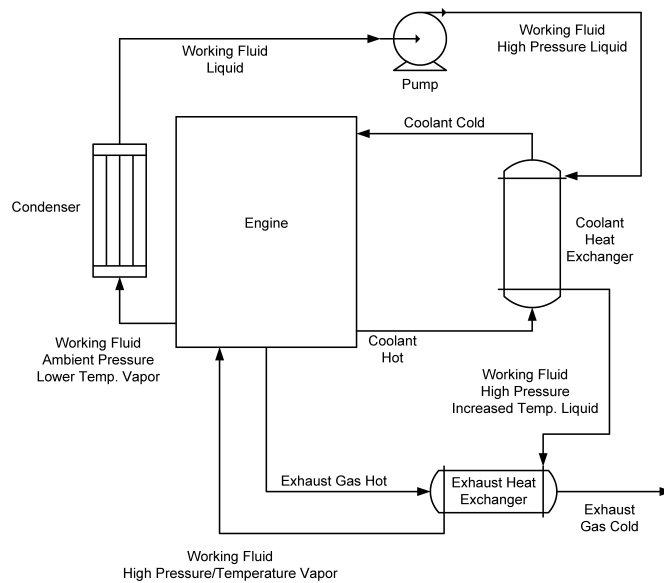


Figure 3.1: Schematic of the proposed waste heat recovery engine setup

pressurized to a pressure of 7.1 MPa . The high pressure working fluid flows through an engine coolant heat exchanger until it reaches the engine temperature of 393 K . Due to the high pressure, the working fluid remains in liquid form as it flows into the exhaust

heat exchanger. The working fluid increases in temperature, evaporates, and becomes a superheated vapor. The high temperature, high pressure vapor (in this study; steam) is utilized in reciprocating pistons that are located directly below a traditional engine piston assembly that is modified to accept a piston-in-piston configuration. A schematic of the piston-in-piston design is shown in Figure 3.2. The engine piston and the steam piston have the same stroke length while the steam piston bore diameter is less than the engine piston bore. This allows the smaller steam piston to fit within the inside cavity of the engine piston. Since the steam piston is stationary, the maximum volume of the steam chamber is when the engine piston is located at top dead center (TDC) and the minimum volume occurs when the engine piston is located at bottom dead center (BDC). The steam inlet valve is set to emit 700 K , 5.5 MPa superheated water vapor for 24 crank angle degrees (CAD) which produces a cutoff ratio of entire steam chamber displacement of 5.2%. The steam piston's power stroke occurs during the IC engine piston's compression and exhaust strokes for a total of two steam power strokes per four-stroke engine cycle. The valve lift profile and the steam chamber clearance height throughout the four cycles are shown in Figure 3.3. The clearance height in the steam chamber is designed to be 0.5 mm to maximize efficiency. Figure 3.3 shows that the valves would come in contact with the steam piston unless the steam piston is designed to allow additional clearance in the location of the valve operating volume or the valve mechanism design is changed. Finally, the exhaust steam discharges into a condenser, which supplies the condensed working fluid to the pump.

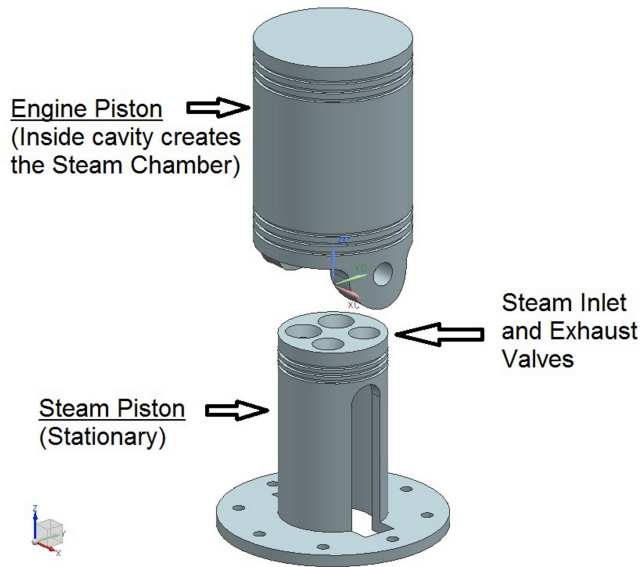


Figure 3.2: Schematic of the proposed waste heat recovery piston in piston design

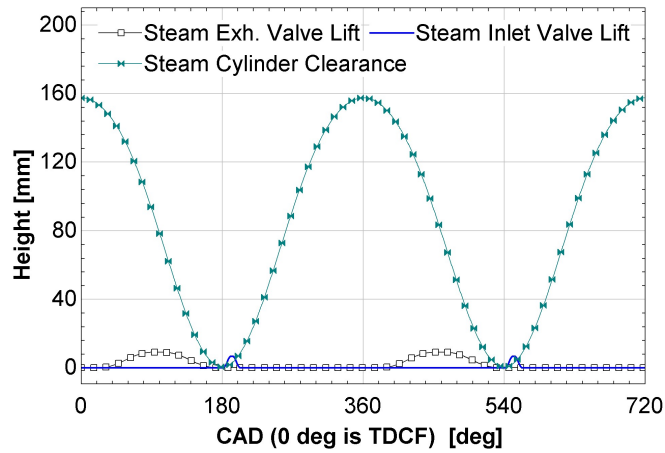


Figure 3.3: The steam inlet and exhaust valve profiles with the steam cylinder clearance height.

3.3.1 Steam Chamber

The expansion of the working fluid vapor within the steam chamber, located beneath the crown of the piston, during the compression and exhaust strokes has the potential to increase the power output of the engine by reducing the pumping losses associated with a traditional IC engine. The steam chamber employed an approximately zero clearance (0.51 mm), zero compression design to allow a practically instantaneous steam inlet pressure to occupy the first 5% of the total volume of the steam chamber before expanding within the steam chamber. This also minimizes the parasitic energy losses during the return stroke to diminish any compression work losses by leaving the steam exhaust valve open within the steam chamber.

The GT-Power model of the steam chamber has four valves per steam chamber (two inlets and two outlets with dimensions of 33% and 29% of the bore size, respectively). Utilizing four valves increases the valve area per piston area, which increases the speed at which the engine power is flow limited [53]. This WHR system was evaluated at an engine speed of 1,500 *RPM* which is the engine speed at a cruise condition for the Class-8 diesel engine. [54]

3.3.2 Working Fluid

The mass flow rate of the working fluid is determined by computing the amount of thermal exergy (available energy) within the coolant and exhaust system of the engine and the required energy needed to supply superheated working fluid (water) into the steam chamber at 700 K and 5.5 MPa . Water was chosen as the working fluid since it has a higher Rankine cycle efficiency compared to organic fluids at temperatures above 643 K . [37, 38]

Two of the six cylinders are equipped with a steam chamber to minimize the required mass flow rate of the steam. This also decreases the ratio between the displacement volume of the combustion chamber and the displacement volume of the steam chamber, which reduces the required thickness and weight of the engine piston skirt. A single steam cylinder configuration was not analyzed due to an anticipated significant imbalance of forces.

3.3.3 Coolant Heat Exchanger:

The coolant heat exchanger raises the temperature of the working fluid by extracting the thermal energy from the engine coolant. The mass flow rate of the working fluid through the coolant heat exchanger is assumed constant because the multiple-cylinder WHR engine configuration helps to normalize fluctuations. The coolant heat exchanger is assumed to be 80% efficient with a 5% pressure drop for the working fluid. Since the pressure of the

working fluid is designated to be 5.5 MPa as it enters the steam chamber, the working fluid pressure entering the coolant heat exchanger is high enough to prevent a phase change (from liquid to vapor), due to the relatively low peak temperature of 393 K within the engine coolant. The working fluid has a temperature of 393 K leaving the coolant heat exchanger, which reduced the required size of the exhaust heat exchanger, thus reducing back pressure on the engine to expel the exhaust gas.

3.3.4 Exhaust Heat Exchanger:

The exhaust heat exchanger superheats the working fluid by extracting the thermal energy from the exhaust system. A compact heat exchanger was chosen for the gas-to-gas heat exchange process to ensure the vapor of the working fluid exited as superheated. The heat transfer to the working fluid within the exhaust heat exchanger is divided into three processes; increasing the temperature of the working fluid to a saturated liquid, evaporation, and superheat. The specific heat of the working fluid during these processes was calculated by the average temperature for each process. The back-pressure of the exhaust heat exchanger is swept in the calculations from zero to an amount in which all generated power is canceled out by the parasitic loss created by the waste heat recovery system. This allows for analysis of the work potential of this WHR technique that is independent from the highly variable back-pressure within compact heat exchanger designs.

3.3.5 Condenser, Pump, and Piping

The exhaust steam expels into the condenser, which is set to an atmospheric pressure of 101 *kPa*. This condenser pressure insures that the saturated vapor exhaust steam condenses to saturated liquid with ambient air temperatures. If the condenser pressure were set below atmospheric pressure, there would be a chance that the ambient air temperatures would not be low enough to condense the vapor to liquid and a vacuum increases the chance of air leakage into the system. Any increase in condenser pressure negatively influences the thermal efficiency of the Rankine cycle [55]. For this reason, condenser pressures above atmospheric were not evaluated.

The circulation pump increases the pressure of the working fluid to a level that maximized the amount of thermal energy recovered and thus maximized the amount of work done during the polytropic expansion in the steam chamber.

The pipes contributed to a 5% pressure drop between each apparatus to account for inherent working fluid pumping losses. The 5% pressure drop between each apparatus was chosen as an estimate since this analysis was based on a simulation and the exact pipe material, diameter, length, and orientation could all be customized for each engine assembly and vehicle.

3.4 Compression Ignition Engine

A Class-8 diesel engine was modeled in GT-Power to predict the operational characteristics of the engine's power distribution (thermal and mechanical) as well as exhaust gas characteristics (temperature, mass flow rate, and specific heat). The engine selected was the Caterpillar Inc. C-13 on-highway diesel engine with ACERT Technology, which is a 12.5 L, in-line six-cylinder, four-stroke diesel with a 130 mm bore, 157 mm stroke, and an advertised power of 227 kW [54]. The model was calibrated by attaining brake torque and power curves that were within 5% of the manufacture's documentation. The engine simulation did not perfectly match all characteristics found in the C-13 engine because the engine was modeled without proprietary data, such as valve timing and intake/exhaust manifold design. This difference was acceptable because the overall goal of the model was to attain operating characteristics that only closely resembled a typical Class-8 diesel engine.

The model was set to operate at full engine load in order to maximize the potential of this WHR system. This is also a more typical load condition for Class-8 diesels in actual operation. The pertinent exhaust characteristics were attained at an engine speed of 1,500 RPM as this was the maximum recommended engine speed [54]. The exhaust gas temperature, mass flow rate, specific heat, and density over a range of engine speeds are shown in Figure 3.4 and Figure 3.5. These values were measured in the exhaust

pipe downstream of the after-treatment devices and before the muffler. This location was selected to maximize the recoverable heat energy while not impeding the after-treatment devices that have operational thermal requirements.

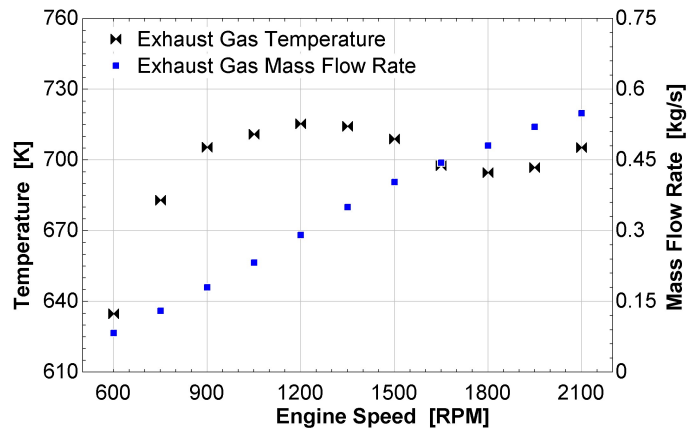


Figure 3.4: Exhaust gas temperature and mass flow rate located in the exhaust system between after-treatment devices and the muffler for the C-13 diesel engine operating at full load

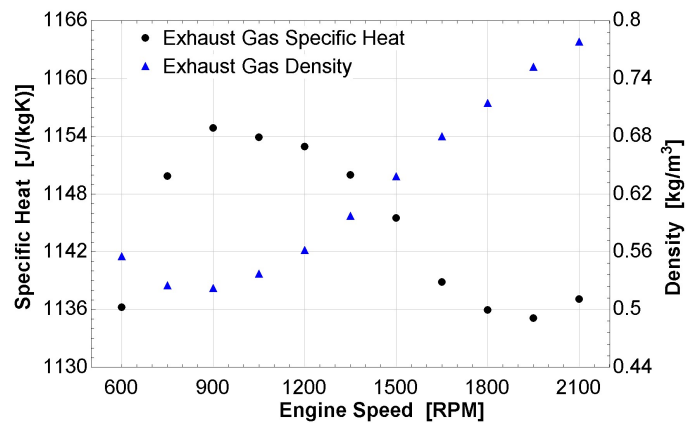


Figure 3.5: Exhaust gas specific heat and density located in the exhaust system between after-treatment devices and the muffler for the C-13 diesel engine operating at full load

3.5 Data Analysis

3.5.1 Steam Generation

The energy required to evaporate and superheat the working fluid within the exhaust heat exchanger was approximately 650% greater than the energy required to raise the temperature of the working fluid to 393 K within the coolant heat exchanger. For this reason, the exhaust heat exchanger was the determining component to compute the mass flow rate of the working fluid. Using the simulated engine exhaust gas characteristics at 1,500 RPM and full load with the low temperature set to 393 K, the exhaust gas contained approximately 145 kW of usable waste heat. Equation (3.1) was used to determine the mass flow rate of water based on a 80% efficient exhaust gas heat exchanger. Note that the specific heat of the working fluid was calculated at the average temperature for each process and the working fluid entered the exhaust heat exchanger at a temperature of 393 K. ($C_{p,468.7K} = 4.446 \frac{kJ}{kgK}$, $\Delta H_{vap,5.5MPa} = 1605 \frac{kJ}{kg}$, $C_{p,621.5K} = 2.774 \frac{kJ}{kgK}$, $Power_{exh} = 145$ kW, $\eta_{HE} = 0.80$, $\Delta T_f = 149$ K, $\Delta T_g = 156$ K)

$$\dot{m}_{wf} = \frac{Power_{exh} * \eta_{HE}}{C_{p,f} * \Delta T_f + \Delta H_{vap} + C_{p,g} * \Delta T_g} \quad (3.1)$$

The total in-cylinder heat transfer in the C-13 engine simulation was 100 kW . With the mass flow rate of the working fluid determined to be 0.043 kg/s , the amount of recoverable heat energy from the coolant was calculated next. In Figure 3.6, the starting temperature of the working fluid from the pump was varied to illustrate the affect it had on the amount of waste heat recovered from the coolant and the percentage of total coolant thermal energy recovered. The maximum starting temperature of 373 K was chosen because the condenser pressure was set to atmospheric and any steam with a temperature above 373 K would not condense at this pressure. The results show that the maximum recovered coolant energy is less than 18% of the total in-cylinder heat transfer, which means a traditional air-to-liquid radiator would still be required to remove the remaining thermal energy from the coolant.

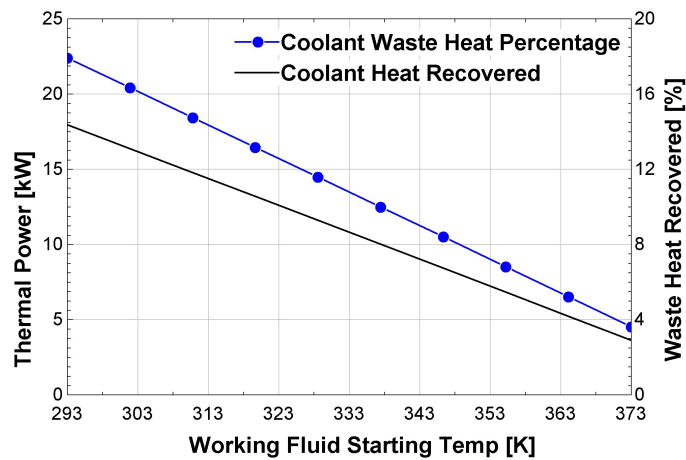


Figure 3.6: The amount of waste heat recovered and the percentage of the total rejected in-cylinder heat transfer from 100 kW over a range of starting working fluid temperatures.

3.5.2 Steam Chamber Analysis

The steam chamber simulation was designed to utilize the maximum mass flow rate of the working fluid, which was achieved by implementing a steam chamber bore diameter of 90 mm. This gave the steam chamber a volume of 999 cm³ and a displacement ratio of the combustion chamber to the steam chamber a value of 2.1. The mass of steam that occupied the steam chamber throughout the four-stroke cycle is shown in Figure 3.7 with the steam inlet and exhaust valve lift profiles. The lift profiles were modeled after cycloidal follower equations [56]. With this profile, the exhaust valve profile opened after the maximum steam chamber volume to minimize the total work required during the steam exhaust stroke. The late opening of the exhaust valve shortened the exhaust valve duration. This reduced the compression of the working fluid at the end of the stroke which was more significant than the negative compression work of the late valve opening. The steam chamber pressure and temperature are shown in Figure 3.8. The pressure and temperature exceeded the target values of 700 K and 5.5 MPa at the time of the steam inlet opening. This may have been the result of momentum of the incoming steam or a possible calculation error within the 1-D engine simulation software.

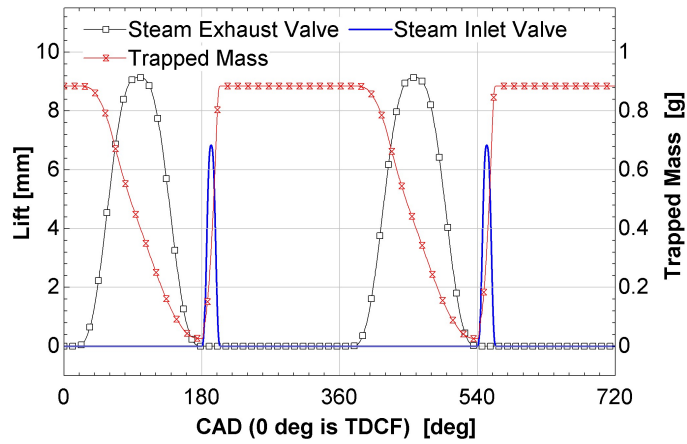


Figure 3.7: Steam chamber valve lift profiles and trapped working fluid mass within the steam chamber

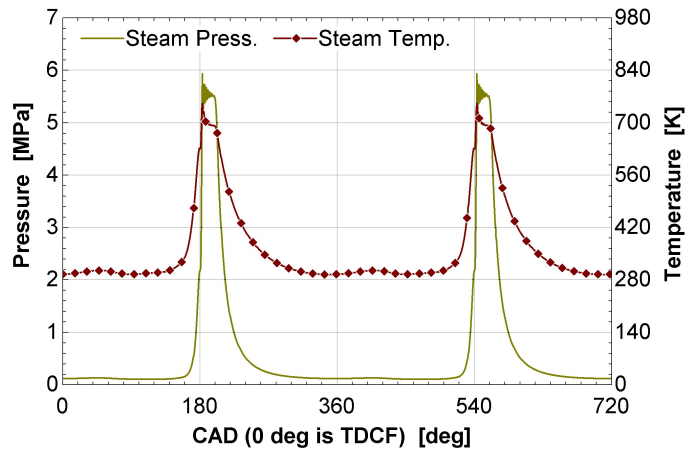


Figure 3.8: Steam chamber pressure and working fluid temperature

Tracking the quality of the steam throughout the four-cycle process was important in order to avoid having an incompressible liquid condensate in the steam chamber that had nearly zero clearance. If the steam condensed to a liquid within the steam chamber, it would likely cause mechanical failure. The quality and pressure of the steam throughout the engine cycle are shown in Figure 3.9. The high temperature, high pressure steam was injected into the cylinder and remained 100% vapor for a short period after the inlet steam valve was

closed and the steam was allowed to expand. The data shows significant duration during the four-stroke cycle in which the steam condenses to liquid, although the compression at the end of the exhaust stroke vaporizes the liquid water as the steam piston approached the critical location of BDC.

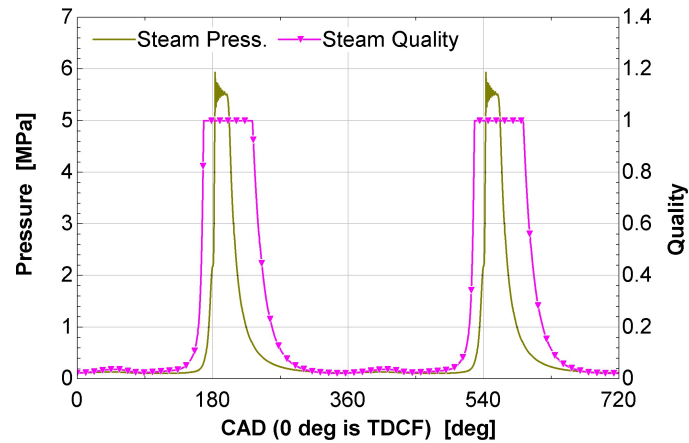


Figure 3.9: The steam chamber pressure and steam quality throughout the four engine cycles. (Quality of 1 correlates to 100% steam per mass ratio and a quality of 0 correlates to 0% steam per mass ratio.)

3.5.3 Power Generation

The net power generation for the C-13 diesel engine operating two cylinders with steam chambers and a steam power stroke every crank shaft revolution was evaluated. The generated brake power for the steam chambers was determined from the GT-Power simulation model for the steam cylinder and scaled with the number of cylinders. The brake power from the steam chambers without any parasitic losses was determined to be 26.7 kW with the engine operating at 1,500 RPM and full load.

The parasitic losses outside of the steam chamber in this WHR system primarily came from the working fluid pump and the additional back pressure caused by the exhaust heat exchanger, which the engine must overcome during the exhaust stroke. The loss from the pump was calculated with the assumption that there would be a 5% drop in pressure across each pipe and heat exchanger from the pump to the steam chamber. This required the pump to increase the pressure of the water from the condenser from 101 *kPa* to roughly 7.1 *MPa*. The pump was considered 80% efficient and the alternator that would supply the electrical power to the pump was 80% efficient. The power required to operate the working fluid pump with the assumptions stated was 0.4 *kW*. The loss from the exhaust heat exchanger was calculated by sweeping the back pressure from zero to an amount in which the total loss of the system would nullify any power generated from the steam chamber. The results, shown in Figure 3.10, show that the maximum brake fuel conversion efficiency that can be attained was 37.5% when there was no additional back pressure on the engine from the exhaust heat exchanger. The results also show that as long as the additional back pressure to the engine is below 41.8 *kPa*, then there will be an improvement in brake fuel conversion efficiency. The additional back pressure from an exhaust heat exchanger could possibly compare to the back pressure of a muffler, which was set to 30 *kPa* in the C-13 diesel engine model.

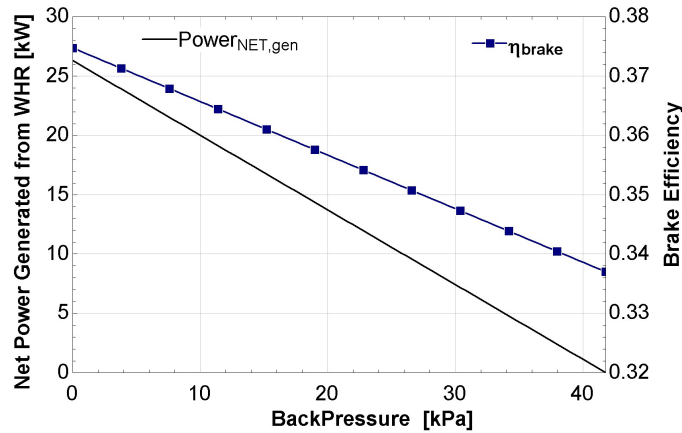


Figure 3.10: Net power generated from WHR and corresponding fuel conversion efficiency over a range of exhaust back pressures resulting from an exhaust heat exchanger.

3.6 Conclusions

A diesel engine with a piston-in-piston WHR method was evaluated with the use of GT-Power and EES. The simulation showed that a Class-8 diesel engine at full load could be implemented with this WHR technology. This diesel engine running at 1,500 *RPM* at full load (1,496 *Nm*) had a brake power increase of up to 26.7 *kW* with the addition of this engine technology on two of the six cylinders, actuated twice per four-stroke engine cycle. This increased power equated to an improvement in brake fuel conversion efficiency from 34.4% up to a maximum of 37.5% (3.1% increase). The analysis of the steam chamber throughout the engine cycles showed that the water vapor condensed during certain portions of the cycle. The formation of liquid in the steam chamber has the potential to reduce the efficiency of the system and to cause a mechanical failure if not properly removed from the

cylinder (hydraulic lock) during steam chamber compression. The validity of this WHR engine technology during transient conditions (start-up and accelerations) as well as the extent of the impact of condensation within the steam chamber requires further simulation as well as experimental testing.

Chapter 4

Thermoelectric Generators: Cylinder Walls

This chapter was written in preparation to be submitted as a journal article ¹. Utilizing thermoelectric generators to recover the heat energy from the cylinder walls of an IC engine has many possible advantages over existing WHR systems. In addition, this technique has not been previously evaluated according to a thorough literature review. This type of WHR system has a minimal impact on current engine designs and reduces or eliminates several of the characteristic disadvantages of current automotive WHR systems, which are described in Chapter 2. The goal of this project is to understand the effect of the TEG on the energy distribution, cylinder wall temperatures, and TEG power conversion potential.

¹The material contained in this chapter was written/designed for a journal article submission.

Supplemental information for this experiment can be found in Appendix A.

Automotive Cylinder Wall Waste Heat Recovery with Thermoelectric Generators

John R. Armstead

Michigan Technological University
Houghton, Michigan, USA

Scott A. Miers

Michigan Technological University
Houghton, Michigan, USA

4.1 Abstract

This article investigated the impact of implementing thermoelectric generators (TEG) on the outer cylinder walls of a liquid-cooled internal combustion engine. The research focused on the empirical trends in fuel energy distribution, cylinder wall temperatures, and TEG power generation with the addition of a TEG surrogate material over a range of engine speeds and loads in a two cylinder, 19.4 kW, liquid-cooled, spark-ignition engine. One 30 mm x 30 mm TEG was installed on the outside of each cylinder wall while a TEG surrogate material, which had similar thermal resistance as the actual TEG, covered the remaining outside cylinder surface area. Engine oil analysis was performed to assess the possible negative effects of increased cylinder wall temperature on the oil quality. The electrical power generated from the TEGs was scaled to simulate the effect of covering the entire cylinder surface with TEGs.

The cylinder wall temperatures increased by 17% to 44% which correlated well to the 4.3%

to 9.5% decrease in coolant heat transfer. Approximately 23.3%-28.2% of the heat transfer to the coolant came through the TEG and TEG surrogate material. The gross indicated work decreased by 0.4% to 1.0% which was attributed to the decrease in friction energy. The exhaust gas energy decreased by 0% to 2.6% because of the decreased combustion duration which resulted in more in-cylinder heat transfer from the combustion gas and increase in mechanical efficiency. The scaled electrical output of the TEG represented 0.0007 – 0.0014% of the fuel energy at 40 *Nm* and 0.0015 – 0.0059% of the fuel energy at 20 *Nm*. The low energy production of the TEG was likely due to the way the TEG's were installed.

4.2 Introduction / Background

The internal combustion (IC) engine converts approximately one third of the chemical energy in fuel to mechanical work. The fuel energy that is not converted to mechanical work during the combustion process is expelled from the engine as heat, predominately through the cooling and exhaust systems [25]. Figure 4.1 shows a diagram of the typical fuel energy distribution for a spark ignited (SI) engine, which includes the total indicated work (mechanical work), heat transfer (in-cylinder heat transfer), and the net transfer out due to flows (heat and kinetic energy in the exhaust gas). Since heat energy can not be converted completely into useable energy, this figure also illustrates the amount of theoretical useful energy (availability) within each of these systems. In an effort to utilize

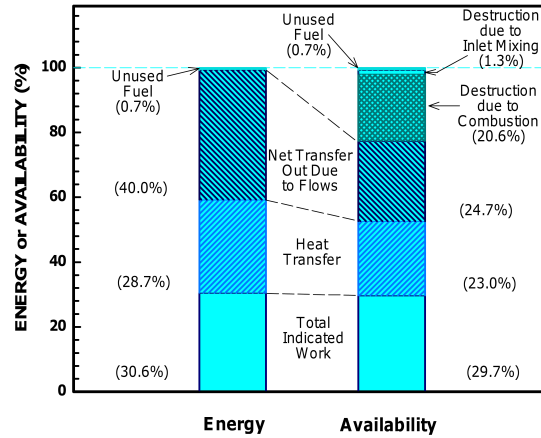


Figure 4.1: Energy and exergy (availability) for a SI engine. [57]

a larger percentage of this fuel energy and therefore reduce fossil fuel consumption, there are waste heat recovery (WHR) techniques that can capture unutilized heat and convert it into usable electrical or mechanical work. Stobart, et al. [30] estimated that a 1.3 kW WHR system could eliminate the alternator on a small, passenger-sized vehicle, which is beneficial to fuel conversion efficiency because the alternator is a parasitic load on the engine.

Thermoelectric generators (TEG), which are solid-state devices made from alternating elements of n-type (negative) and p-type (positive) semiconductors, have the potential to become a useful WHR tool to convert waste heat energy from internal combustion engines to electrical energy. When there is a temperature gradient across a TEG, the system converts a portion of the heat energy into an electric current. The efficiencies of TEGs are evaluated by the dimensionless figure of merit (ZT) [34] which is calculated using Equation (4.1). The current value of ZT for TEG systems is around 1.0. However, to be competitive with traditional mechanical recovery systems, such as turbochargers, the ZT value for

TEG systems needs to be around 3 – 4 [34]. The maximum efficiency ($\eta_{max,TEG}$) of the TEG power conversion for a given ZT value and hot-side/cold-side temperatures can be calculated with Equation (4.2) [58]. (Equation nomenclature: S = Seebeck coefficient, σ = electrical conductivity, T = average operating temperature, T_H = hot-side temperature, T_C = cold-side temperature, and κ = thermal conductivity)

$$ZT = \frac{S^2 * \sigma * T}{\kappa} \quad (4.1)$$

$$\eta_{max,TEG} = \frac{T_H - T_C}{T_H} * \frac{\sqrt{1 + ZT_{avg}} - 1}{\sqrt{1 + ZT_{avg}} + \frac{T_C}{T_H}} \quad (4.2)$$

TEG automotive WHR techniques have been primarily focused on exhaust system installations [30, 36, 26, 47, 59, 60]. This is due to the higher exhaust gas temperatures, which increase the potential power conversion of TEGs, compared to the coolant system. Even with less overall potential compared to the exhaust system, the coolant system has garnered TEG research. Some advantages of coolant system WHR is that exhaust heat exchangers put more back-pressure on the engine which increase the pumping work, and there is less variability in temperature and energy streams which degrades TEG and Rankine cycle efficiencies. One study by Crane et al. [29] explored the possibility of TEGs within the coolant system by designing a modified radiator simulation with a series of TEGs. The hot-side reservoir was the coolant while the cold-side reservoir was the

ambient air. The results indicated that a 1 kW system can be achieved with a cross flow heat exchanger with a power density to heat exchanger volume of approximately $45 \text{ kW}/\text{m}^3$. This research explored a coolant-based TEG WHR system located on the outer cylinder walls of an IC engine to convert a portion of this heat energy to electricity. This TEG system technique is a thermal insulator to heat transfer and any resulting reduction in heat transfer to the cylinder walls will have an affect on the engine performance, efficiency, and emissions. Also, by reducing the heat transfer through the cylinder walls, the combustion-side temperature of the cylinder walls would increase, which could potentially degrade the engine oil quality and also lead to an increased chance of auto-ignition (knock).

There have been numerous research studies since the 1970's to investigate the potential of increasing the fuel conversion efficiency by reducing in-cylinder heat transfer. This concept is known as low heat rejection (LHR), which theoretically would increase the fuel conversion efficiency of the engine by increasing the combustion gas temperatures and pressures by reducing the in-cylinder heat transfer. A LHR engine would attempt to minimize or eliminate the need for a traditional coolant system by coating the cylinder surfaces with a high temperature, low thermal conductivity material that could withstand the combustion gas temperatures. The LHR technique was generally not tested in SI engines because of the knock limitation of gasoline but was tested on compression ignition (CI) engines [61, 62, 63, 64, 65, 66, 67, 68]. LHR engine research had mixed results as the fuel conversion efficiency would only either slightly increase or slightly decrease depending on the engine parameters such as injection timing, total amount of in-cylinder

heat transfer reduction, and valve timing adjustments. The reduction in heat energy which was once conventionally removed by the coolant system did not consistently result in more mechanical work output but rather was expelled in the form of increased exhaust gas temperatures and the increased combustion gas temperature reduced nearly all exhaust emissions other than NO_x for LHR engines [69]. Buyukkaya et al. [70] achieved a 1 – 6% reduction in brake specific fuel consumption (BSFC) with a thermal barrier coating on all in-cylinder surfaces. The authors delayed the injection timing from the original setting of 20° before top dead center (BTDC) to 18° BTDC, on a six cylinder, direct injection, turbocharged diesel engine. The NO_x was reduced by 11% when the injection timing was set to 18° BTDC and 26% on average for 16° BTDC. The LHR research indicates that installing TEGs on the outer cylinder walls would not necessarily improve the fuel conversion efficiency but the reduction in heat transfer to the coolant would be expelled from the cylinder by higher temperature exhaust gas. The reduction in heat transfer to the coolant will not be as significant as LHR research (50 – 65% reduction) because the cylinder wall insulation is on the outer cylinder wall, which allows the engine block and head to absorb the heat before being hindered.

4.3 Experimental Design

This research used a two-cylinder, 19.4 kW, liquid-cooled, spark-ignition engine. The cylinder dimensions included an 80 mm bore, 67 mm stroke, a total displacement of 674 cc,

with a compression ratio of 8.5 : 1 [71]. The water-jacket was approximately 40 *mm* deep with a width that varied from 5 – 7 *mm* at the top of the water-jacket and 3 – 5 *mm* at the bottom.

To map the fuel energy distribution, cylinder wall temperatures, and TEG power output, a number of transducers were installed on the engine. A total of sixteen temperature measurements were performed with ungrounded, sheathed K-type thermocouples with an uncertainty of 1.1°C or 0.4% (whichever value is greater). These thermocouples measured temperature of key locations within the coolant system, exhaust system, oil, and the intake air. The mass flow rate of the coolant was measured with a turbine type flow meter with an uncertainty of 3%. An electro-chemical oxygen sensor was used to measure the relative air/fuel ratio, λ , from 0.62 to 1.10. The actual air/fuel ratio (AFR) was computed by multiplying the relative air/fuel ratio, λ , by the stoichiometric air/fuel ratio (14.6) of the Tier II EEE U.S. Federal emission certification fuel used in the experiment. Equation (4.3) shows the calculation for AFR based on the λ measurement and the stoichiometric ratio of the fuel.

$$AFR = \lambda * 14.6 \quad (4.3)$$

The range of AFR measurement was 9.052 to 16.06. The mass flow rate of the air was

determined by multiplying the fuel flow rate, which was measured with a Coriolis-type flow meter with 0.1% uncertainty, by the computed air/fuel ratio, which had an absolute uncertainty of 0.1 AFR. The total mass flow rate of the exhaust gas was determined by adding the mass flow rate of the fuel to the mass flow rate of the air.

Each cylinder had two 1.6 *mm* diameter thermocouples recessed into the cylinder walls. The tips of the thermocouples were located 3 *mm* and 15 *mm* down from the cylinder head surface nearest to the exhaust valve. These thermocouples were used to measure cylinder wall temperatures. One 1.6 *mm* diameter thermocouple was adhered at the center location of the TEG to measure the "cold-side" coolant temperature. The exhaust gas temperature was measured with thermocouples located 35 *mm* downstream from the exhaust valve of each engine cylinder. This measurement was used to determine the amount of available heat that was expelled from each cylinder into the exhaust system.

4.3.1 TEG / Surrogate Selection and Installation

The TEG used in this experiment was a Seebeck Thermoelectric Generator from the company; Custom Thermoelectric based out of Bishopville, Maryland. The top and bottom plate had dimensions of 30 *mm* by 30 *mm* with a lapped height of 3.5 *mm* while having a thermal conductivity of 3.88 *W/mK*. The TEGs are typically installed with 1.275 *MPa* of compression between two heat sinks. Due to the limited amount of space within the

water-jacket the TEGs were installed with JB Weld. Because this TEG application was submerged into coolant and adhered directly to the cylinder wall, the pre-applied thermal interface material (graphite foil) was removed at the recommendation of the manufacturer. The hot side and cold side of this TEG were rated at a continuous temperature of 300°C and 180°C, respectively. The ZT value was calculated to be 0.64. To install the TEG on a flat surface, the outer surface of the cylinder wall was machined, shown in Figure 4.2(a) and Figure 4.2(b). A total of 3.8 *mm* of material was removed from the side of the cylinder wall

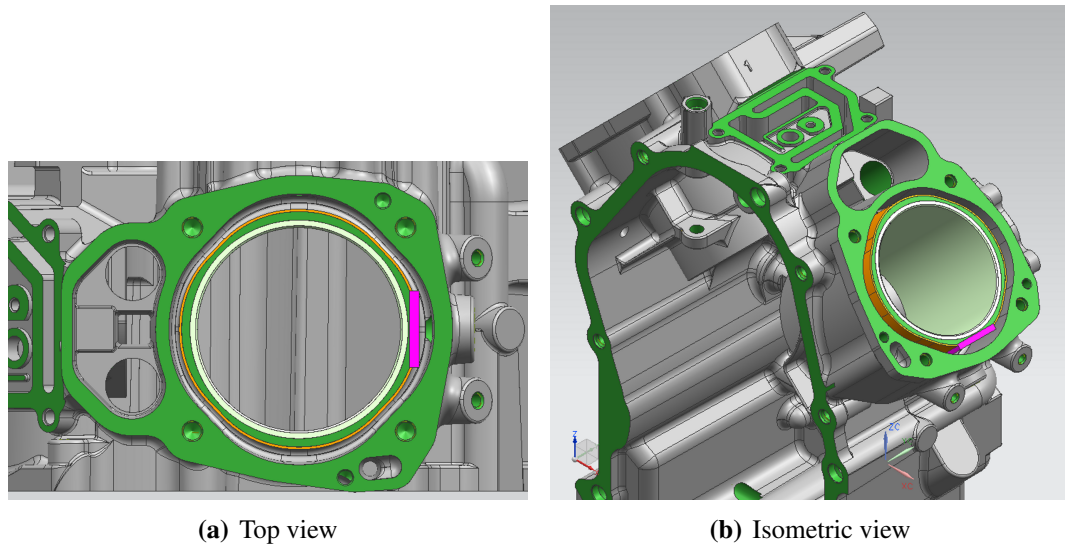


Figure 4.2: Engine block water-jacket with a TEG (magenta) and a TEG surrogate material (orange) installed.

for a depth of 35 *mm*. There was a concern that the removal of part of the aluminum cylinder wall could cause the cylinder bore to deform due to uneven heat transfer. If the cylinder liner did deform, it would lead to excessive oil consumption and increased blow-by, which were not noted in the testing. This would not be a concern in a production application as the cylinder walls would be designed for the TEG application.

ThermaCool TC100 from Saint-Gobain was selected as the TEG surrogate that was used to cover the remaining exposed outer cylinder wall. This material is an unsupported solid silicone rubber with a thermal conductivity of 1.3 W/mK . The nominal thickness of 0.81 mm gave the surrogate material a thermal resistance per unit area that was 32% lower than the thermal resistance per unit area of the TEG. The reduced thermal resistance of the surrogate material allowed more heat to transfer to the coolant compared to the TEG, which reduced the increase in cylinder wall temperature that was predicted. However, this was the best match available that could withstand the expected temperature at the outer cylinder wall. The surrogate itself would not sufficiently adhere to the aluminum cylinder walls without a thin coat (approximately $0.1 - 0.15 \text{ mm}$) of JB Weld, which had a thermal conductivity of 5 W/mK . Because the adhesive thermal conductivity was almost four times greater than the surrogate material, variations in adhesive thickness had a minimal impact on the heat transfer through this portion of the cylinder. The recessed thermocouples in the cylinder walls helped to ensure the TEG surrogate could lie flat on the cylinder walls and minimize the obstruction in the cooling passage.

4.4 Test Matrix / Procedure

The test matrix included a combination of engine speeds of 3600, 3000, 2400, and 1800 *RPM* at engine loads of 40 *Nm* and 20 *Nm*. The engine speeds of 3600 and 2400 *RPM* are significant because the peak power and peak torque are found at those engine speeds,

respectively. The engine loads were selected to increase the likelihood that both the baseline and the TEG testing would be able to reach and maintain the most demanding test modes. Wide open throttle was not implemented because the resulting power may not have been consistent between rounds or between the baseline and TEG testing. Baseline (no TEG/surrogate installed) testing for 25 cycles was conducted, followed by 25 TEG/surrogate cycles. After 25 rounds of baseline testing were recorded, the engine head was removed and the TEG and surrogate material were installed. The engine was then again operated for another 25 rounds for the TEG testing.

The engine speed, engine load, fuel supply pressure, and inlet coolant temperature were controlled throughout the testing. The engine speed and load depended on the desired mode point. The fuel pressure supplied to the engine fuel pump was set and maintained at 1.5 *psig* as suggested by the engine manufacturer. The inlet coolant temperature going into the engine was set to 90°C ($\pm 2^\circ\text{C}$) because the factory coolant thermostat would typically be fully open at this temperature. For all the experiments, the thermostat was blocked open to reduce variability in coolant flow. Once the oil temperature stabilized while the engine was operating at 3600 *RPM* and 40 *Nm*, three minutes of engine data was recorded at a sampling frequency of 10 *Hz*. At approximately the one minute mark of data acquisition, the combustion analyzer software was engaged to record three hundred engine cycles of in-cylinder pressure and crankshaft location data. After the specific engine speed/load data was successfully recorded, the engine speed and engine torque were changed to the next desired setting and allowed to stabilize for no less than five minutes before the next data

recording. The following analysis provides details on the impact of the TEG and surrogate related to in-cylinder heat transfer, gross work output, exhaust energy, oil analysis, and TEG conversion efficiency.

4.5 Fuel Energy Distribution

A flowchart of the fuel energy distribution can be seen in Figure 4.3. During the combustion

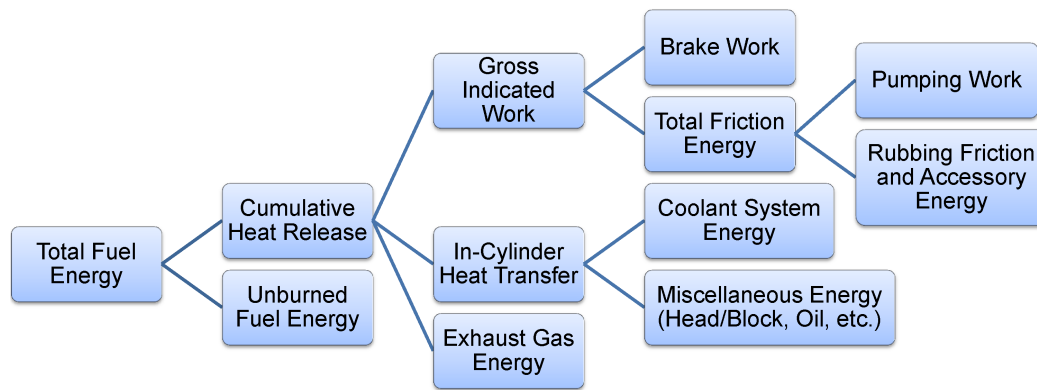


Figure 4.3: Fuel energy distribution flowchart

process, a portion of the chemical energy in the fuel is released as heat while the rest of the chemical energy travels through the engine as unburned fuel. Although detrimental to brake specific fuel consumption (BSFC), excess fuel can be beneficial to the lifespan of engine components, such as pistons and exhaust valves, because the cooling effect of the fuel's heat of vaporization assists in keeping the engine components from overheating. The cumulative heat release, the fuel chemical energy released as heat from 30 crank angle degrees before top dead center firing to 90 crank angle degrees after top dead center firing, is distributed

into three areas; gross indicated work, in-cylinder heat transfer, and exhaust gas energy. The gross indicated work is the work delivered to the piston during the compression and expansion strokes only, which is equal to the summation of the brake work (crankshaft work) and total friction energy (pumping, rubbing friction, and accessory work). The in-cylinder heat transfer includes the energy to the coolant and to miscellaneous locations such as the block, head, and oil reservoir. The exhaust gas energy is the difference in energy from the high temperature exhaust gas to the thermodynamic dead state of 25°C. All of the fuel energy distributions are reported in this analysis as the energy per four-stroke engine cycle (two revolutions of the crankshaft). The trend lines within the figures are separated by engine loads. The baseline testing results (BL) and TEG testing results were plotted on the same figure.

The total fuel energy per cycle was determined using Equation (4.4) (Nomenclature: \dot{m}_{fuel} = mass flow rate of fuel, LHV = lower heating value of the fuel, n_R = number of crankshaft revolutions per cycle, N = rotational speed of the crankshaft) while the cumulative heat release was determined using the in-cylinder pressure data, crank angle encoder, and engine displacement.

$$Energy_{Fuel,Total,Cycle} = \frac{\dot{m}_{fuel} * LHV * n_R}{N} \quad (4.4)$$

The combustion efficiency, which is the ratio of the cumulative heat release to the total supplied fuel energy, is shown in Figure 4.4(a). This combustion efficiency only appears low because the factory calibration of the engine was fuel-rich with lambda below the stoichiometric equivalent of 1, which can be seen in Figure 4.4(b). The data for the combustion efficiency and lambda is summarized in Table 4.1. The trend lines in Figure 4.4(a) and Figure 4.4(b) show that as the engine operated closer to stoichiometric, the overall combustion efficiency improved due to less fuel being wasted for engine component cooling.

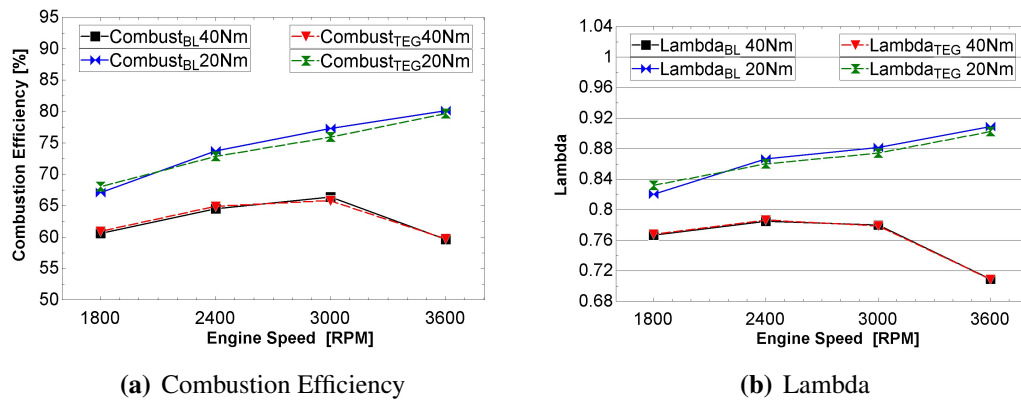


Figure 4.4: Combustion efficiency and lambda for the baseline testing and the resulting change after TEG installation

Table 4.1
Data summary of the combustion efficiency and lambda

	Baseline			Change with TEG (%)		
Combustion efficiency (%)	Low	High	Average	Low	High	Average
20 Nm	67.1	80.1	74.6	-1.7	1.4	-0.5
40 Nm	59.6	66.4	62.8	-0.9	0.6	0.1
Lambda	Low	High	Average	Low	High	Average
20 Nm	0.82	0.91	0.87	-0.8	1.5	-0.2
40 Nm	0.71	0.78	0.76	-0.1	0.2	0.1

The combustion efficiency had a high correlation to lambda, seen in Figure 4.5(a), with a 93.58% linear coefficient of determination. Figure 4.5(b) shows that the change in lambda and change in combustion efficiency after the TEG addition had a 80.46% linear coefficient of determination. This indicates that the installation of the TEG and surrogate did not directly influence the combustion efficiency but rather the combustion efficiency was influenced by the carburetor calibration. The changes in engine operation, which is described in the next several sections, affected the how the carburetor interacted with the change in the incoming air.

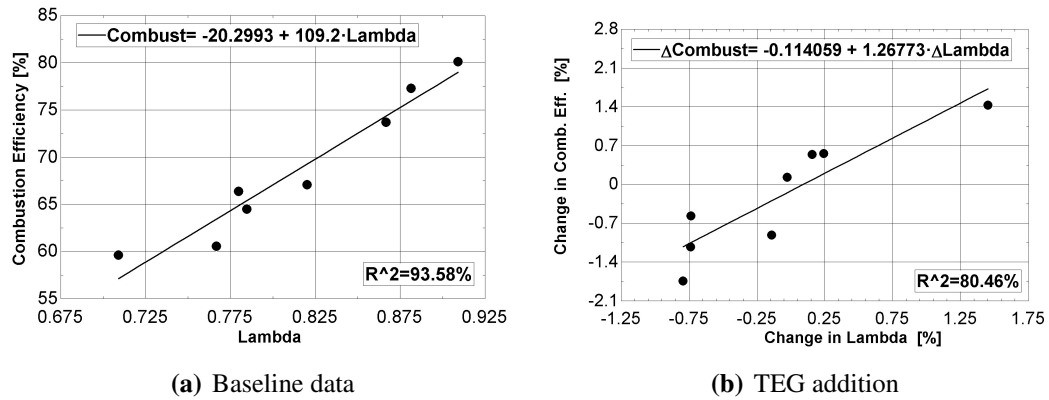


Figure 4.5: Relations between combustion efficiency and lambda

4.5.1 In-Cylinder Heat Transfer

The addition of the TEG and surrogate material on the outer cylinder walls directly impacted the cylinder wall temperatures and the overall in-cylinder heat transfer. To determine the temperature of the cylinder walls, the thermocouples within the cylinder

walls from both cylinders were averaged together from their respective locations (3 *mm* down from the cylinder head (Upper) and 15 *mm* down from the cylinder head (Lower)). The cylinder wall temperatures for the baseline testing are shown in Figure 4.6(a) with the TEG testing are shown in Figure 4.6(b) and the percent change in the cylinder wall temperatures is shown in Figure 4.6(c). The data summary for the cylinder wall temperatures are shown in Table 4.2. The trend lines during the TEG testing for the cylinder wall temperatures do not follow the same trend as the baseline testing. This was due to the additional thermal resistance from the TEG and TEG surrogate which was much larger than the thermal resistance of the cylinder wall material (steel liner with cast aluminum walls). Heat transfer would now require a larger difference from the cylinder walls through the TEG to remain constant.

Table 4.2
Data summary of the Upper (3mm) and Lower (15mm) outer cylinder wall temperature

	Baseline			TEG			Change with TEG (%)		
Upper (°C)	Low	High	Avg.	Low	High	Avg.	Low	High	Avg.
20 <i>Nm</i>	108.2	109.1	108.5	131.6	149.3	140.1	21.6	36.8	29.1
40 <i>Nm</i>	110.0	111.6	110.6	144.3	159.0	151.4	29.3	44.0	36.9
Lower (°C)	Low	High	Avg.	Low	High	Avg.	Low	High	Avg.
20 <i>Nm</i>	109.8	112.1	110.7	128.4	145.4	136.5	17.0	30.0	23.3
40 <i>Nm</i>	112.0	113.2	112.6	139.0	153.6	146.1	23.2	35.6	29.7

Additional thermocouples were installed to measure the coolant temperature leaving the water-jacket as the coolant entered the cylinder head in an attempt to differentiate the two in-cylinder heat transfers; from the cylinder walls and from the cylinder head. The

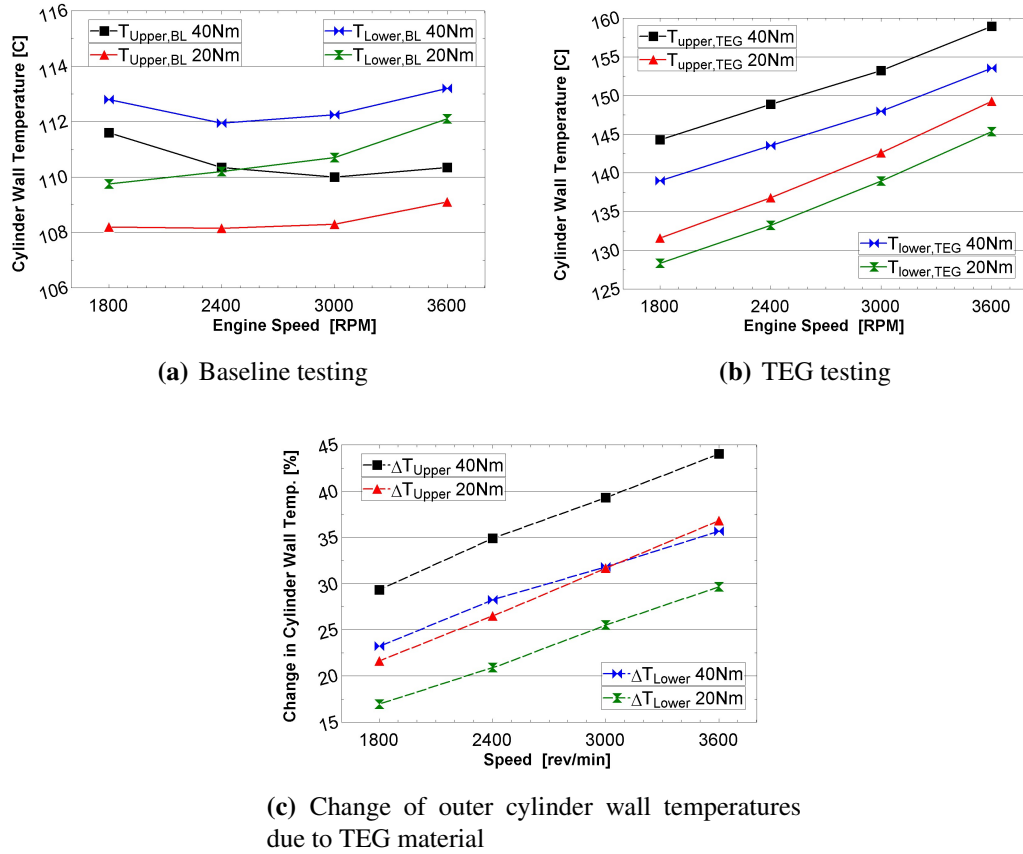


Figure 4.6: Upper (3mm) and lower (15mm) outer cylinder wall temperatures

temperature difference between the thermocouple measurements entering the cylinder head and leaving the cylinder head were within the uncertainty of the thermocouples. Thus the coolant system analysis could not effectively distinguish the two heat transfer paths. This finding also indicated that the in-cylinder heat transfer to the cylinder head was not primarily rejected into the coolant system but rather rejected into the combination of the circulating engine oil within the cylinder head and from natural/forced convection to the ambient air.

The in-cylinder heat transfer to the coolant system was calculated using Equation (4.5). (Nomenclature: $Heat_{cool}$ = coolant energy, \dot{V}_{cool} = volumetric flow rate of the coolant, $\rho_{cool,95C}$ = density of 50/50 mixture of water and ethylene glycol at an average temperature of 95°C, $cp_{cool,95C}$ = specific heat of a 50/50 mixture of water and ethylene glycol at an average temperature of 95°C, $T_{Head,Out}$ = coolant temperature leaving cylinder head, $T_{WJ,In}$ = coolant temperature entering the water-jacket)

$$Heat_{cool} = \frac{\dot{V}_{cool} * \rho_{cool,95C} * cp_{cool,95C} * (T_{Head,Out} - T_{WJ,In}) * n_R}{N} \quad (4.5)$$

Figure 4.7 illustrates the energy removed by the coolant system for the baseline testing and the resulting change after the TEG installation while the data summary is found in Table 4.3. The trend of increasing energy removed by the coolant system as the engine speed decreases is due to the fact that the high-temperature combustion gas has more time for heat transfer within the combustion chamber [40].

Table 4.3
Data summary of the energy to coolant

	Baseline			Change with TEG (%)		
Coolant system (J)	Low	High	Average	Low	High	Average
20 Nm	229.7	248.0	240.7	-9.5	-4.6	-6.8
40 Nm	252.1	339.7	298.4	-7.5	-4.3	-6.0

The smaller than expected drop in heat transfer to the coolant system was an interesting

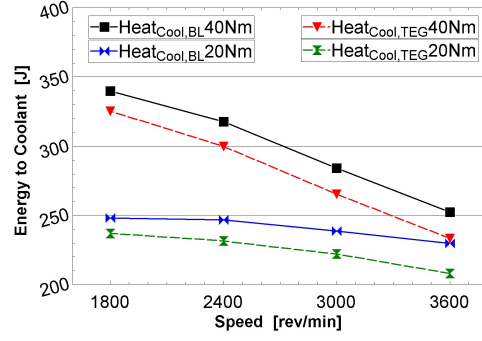


Figure 4.7: Heat transfer to the coolant system for the baseline testing and the resulting change after TEG installation

finding. To further understand the heat path, the heat transfer through the TEG material was calculated with Equation (4.6) (Nomenclature: T_{lower} = lower position cylinder wall temperature, T_{TEG} = cold-side temperature from TEG, $R_{surrogate}$ = thermal resistance of TEG surrogate material, R_{JBWeld} = thermal resistance of JB Weld).

$$Heat_{Thru,TEG} = \frac{T_{lower} - T_{TEG}}{R_{surrogate} + R_{JBWeld}} * \frac{n_R}{N} \quad (4.6)$$

The heat transfer through the TEG material is shown in Figure 4.8 with the data summary in Table 4.4. The result indicates that after the TEG was installed the in-cylinder heat transfer was typically bypassing the direct route through the cylinder wall to the coolant system. The engine block and head must have acted as a heat sink and helped to dissipate the in-cylinder energy and allowed rest of the water-jacket surfaces to transfer the heat.

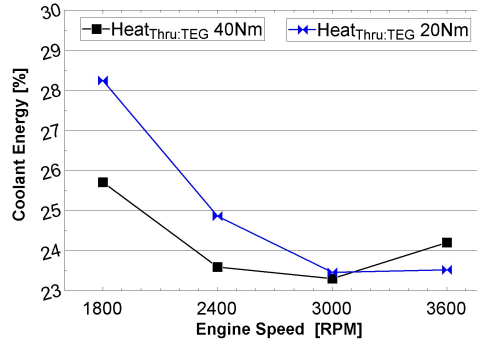


Figure 4.8: Percentage of the heat energy within the coolant system that was transferred through the TEG material

Table 4.4

Data summary of the percentage of the energy within the coolant system that was transferred through the TEG material data summary

	Baseline		
Coolant Energy Percent (%)	Low	High	Average
20 Nm	23.5	28.2	25.0
40 Nm	23.3	25.7	24.2

4.5.2 Gross Indicated Work

The gross indicated work was affected by the increase in cylinder wall temperatures and the change in the laboratory test environment. The gross indicated work, Equation (4.7), was determined by using the in-cylinder pressure data, crank angle encoder, and engine geometry, while the brake work was determined by using the brake torque, measured by the dynamometer strain gage, engine speed, measured by the dynamometer magnetic pick-up, and engine displacement. Figure 4.9(a) shows the trends in gross indicated work and brake work. Brake torque and engine speed were control parameters during testing, therefore there was only minimal variation in brake work from the baseline to the TEG. The stable

brake work and the decrease in gross indicated work for all engine modes means that the mechanical efficiency, Equation (4.8), increased when the TEG was installed. The increase in mechanical efficiency caused a decrease in the BSFC, as shown in Figure 4.9(b). The data summary for the gross indicated work and BSFC is shown in Table 4.5.

$$Work_{Gross,Indicated} = Work_{Brake} + Work_{Friction,Total} \quad (4.7)$$

$$\eta_{mechanical} = \frac{Work_{Brake}}{Work_{Gross,Indicated}} \quad (4.8)$$

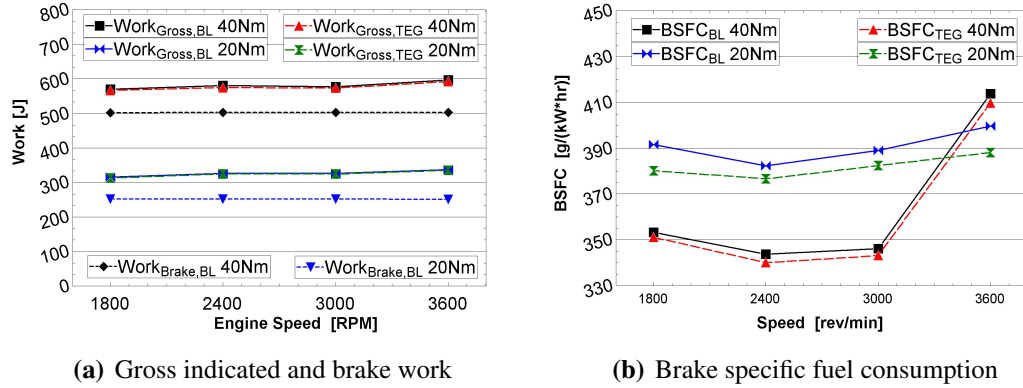


Figure 4.9: Gross indicated and brake work and BSFC for the baseline testing and the resulting change after TEG installation

Table 4.5

Data summary of the gross indicated work, brake work, and brake specific fuel consumption

	Baseline			Change with TEG (%)		
Gross indicated work (J)	Low	High	Average	Low	High	Average
20 Nm	315.5	337.0	326.0	-0.9	-0.4	-0.6
40 Nm	569.5	596.5	580.8	-1.0	-0.6	-0.8
Brake work (J)	Low	High	Average	Low	High	Average
20 Nm	251.2	251.7	251.5	-0.1	0.1	0.0
40 Nm	501.8	502.8	502.5	-0.1	0.0	0.0
BSFC (g/(kW * hr))	Low	High	Average	Low	High	Average
20 Nm	382.3	399.6	390.6	-2.9	-1.5	-2.3
40 Nm	346.1	413.7	364.2	-1.0	-0.6	-0.9

4.5.2.1 Remaining Friction Energy and Pumping Work

Since the brake work was held constant at each particular test point, the change in gross indicated work after the TEG installation must be attributed to a change in total friction energy, which encompasses the pumping work and the remaining friction energy (rubbing friction and accessory energy). The baseline remaining friction energy and the pumping work with the percent change due to the TEG can be found in Figure 4.10(a) and Figure 4.10(b), respectively. The data summary for the remaining friction energy and pumping work is shown in Table 4.6. The engine mode with 2400 *RPM* and 20 *Nm* was the only mode had a slight increase in pumping work.

The remaining friction energy decreased for all engine modes which could have been caused by a decrease in engine oil viscosity due to higher oil overall temperatures and on the cylinder walls. The oil used during testing was Castrol GTX 10W-30, which had

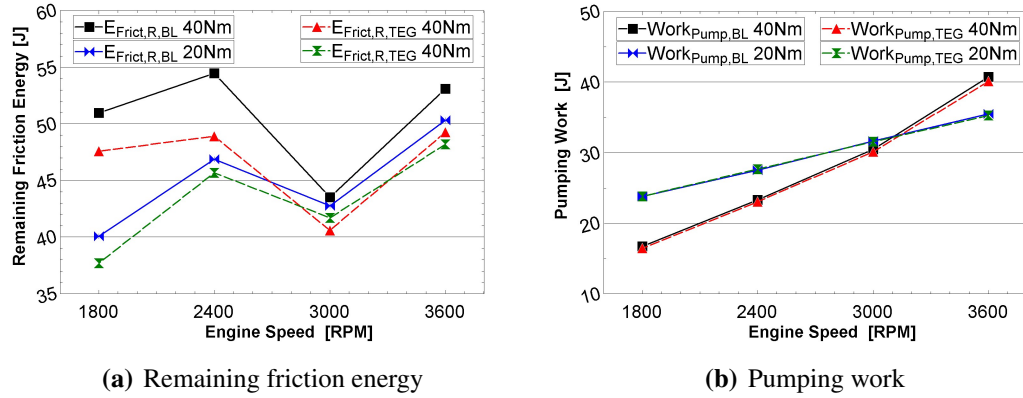


Figure 4.10: Remaining friction energy and pumping work for the baseline testing and the resulting change after TEG installation

Table 4.6
Data summary of the remaining friction energy and pumping work

	Baseline			Change with TEG (%)		
Remaining friction energy (J)	Low	High	Average	Low	High	Average
20 Nm	40.1	50.3	45.0	−5.9	−2.5	−3.8
40 Nm	43.5	54.5	50.5	−10.3	−6.6	−7.7
Pumping work (J)	Low	High	Average	Low	High	Average
20 Nm	23.8	35.5	29.6	−0.6	0.4	−0.1
40 Nm	16.7	40.7	27.8	−1.5	−1.2	−1.4

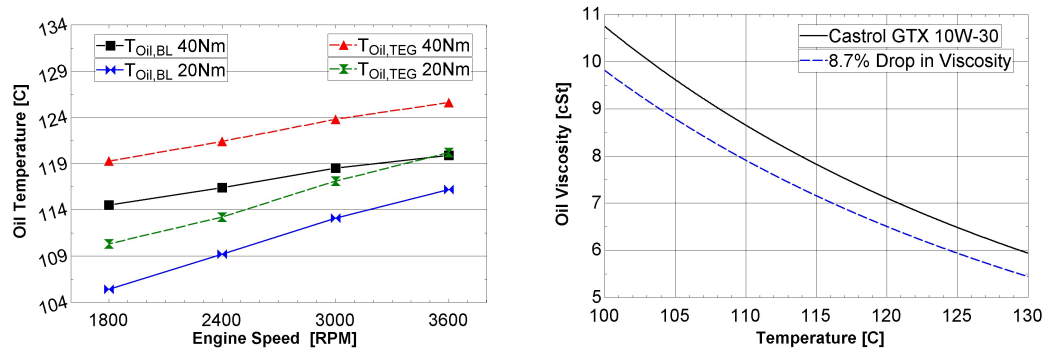
published viscosities of 70.05cSt at 40°C and 10.75cSt at 100°C [72]. The oil analysis for the baseline and TEG testing did not indicate any noteworthy oil degradation but the baseline oil viscosity was measured to be 8.7% less than the TEG oil viscosity. A possible cause of the lower baseline oil viscosity at the testing temperature of 100°C was from a minor amount of fuel dilution (raw, unburned fuel in the oil) measured from the baseline testing oil. Fuel dilution lowers the oil's viscosity and flash point, which could increase friction. The oil analysis report suggested that the cause of unburned fuel in the oil could have been from excessive idling. Although the oil viscosity for the baseline

testing was lower than the TEG testing when at the same temperature, the increased overall oil temperature for the TEG testing resulted in nearly the identical overall oil viscosity. The oil temperatures for the baseline testing and resulting change with the TEG, shown in Figure 4.11(a). The increased oil temperature due to the TEG and surrogate installation decreased the oil viscosity. The oil viscosity for the two tests, seen in Figure 4.11(b), was created with the published viscosity data, the reported reduced viscosity results from the baseline testing due to fuel dilution, and the basic equation linking viscosity (in centistokes [cSt]) and temperature (in Kelvin), seen in Equation (4.9).

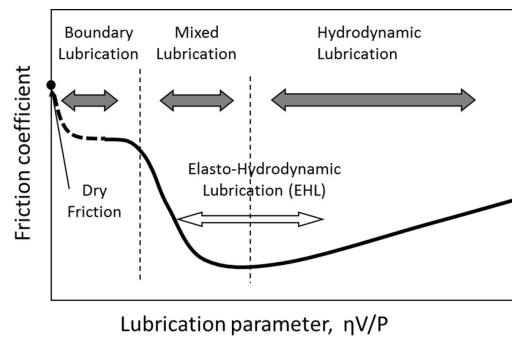
$$\log(\log(\text{Viscosity} + 0.7)) = A - B * \log(\text{Temperature}_{\text{absolute}}) \quad (4.9)$$

This increased cylinder wall temperatures for the TEG, shown in Figure 4.6(b), would have decreased the local oil viscosity more than the baseline oil on the cylinder walls, which could have caused the overall decrease in rubbing friction energy. The Stribeck diagram, shown in Figure 4.11(c), shows that as oil viscosity decreases from the hydrodynamic lubrication zone, the friction coefficient would decrease unless the viscosity become too low and enters the mixed lubrication or boundary lubrication zones. It should be noted that piston rings on the cylinder wall operate in the hydrodynamic lubrication zone at all crank angles except at top dead center and bottom dead center where the piston slows to a

stop before changing directions while the piston skirt stays in the hydrodynamic lubrication zone at all crank angles. [40].



(a) Oil temperature for the baseline testing and the (b) Oil viscosity over a range of temperatures resulting change after TEG installation including 8.7% reduction in viscosity for BL oil fuel dilution



(c) Stribeck diagram [73]

Figure 4.11: Oil to friction relations

Table 4.7

Data summary of the oil temperature

	Baseline			TEG			Change with TEG (%)		
Oil (°C)	Low	High	Avg.	Low	High	Avg.	Low	High	Avg.
20 Nm	105.2	116.2	111.0	110.3	120.2	115.2	3.4	4.6	3.8
40 Nm	114.5	119.9	117.3	119.3	125.6	122.5	4.2	4.8	4.4

The changes in the pumping work were a result of the change in air density, throttle

position, and mechanical efficiency during the baseline and TEG testing. The increase in mechanical efficiency during the TEG testing means that the engine required less fuel and air to produce the same desired brake work. To reduce the amount of fuel and air consumed in a carbureted engine, the throttle would have had to close more, which would have increased the pressure drop across the throttle, which that would have caused an increase in the pumping work for the engine. The test results for pumping work, shown in Figure 4.10(b), did not show an increase during the TEG testing as expected but rather resulted in a drop in pumping work. This phenomenon was a due to the change in the laboratory test environment between the baseline and TEG testing. The baseline and TEG testing were performed weeks apart and the air density changed, shown in Figure 4.12(a). The change in air density was due to changes in atmospheric pressure, relative humidity and temperature. The reduced air density during the TEG testing would not had same potential in flow pressure to draw out the fuel from the carburetor. This means that even though the engine required less overall fuel to produce the same brake work, the throttle, shown in Figure 4.12(b), had to open more to properly operate the carburetor. The data summary for the air density and throttle position can be seen in Table 4.8. Because the throttle cable was removed numerous times while the engine was being serviced, the data for the throttle position and change in throttle position should only be used for overall trends.

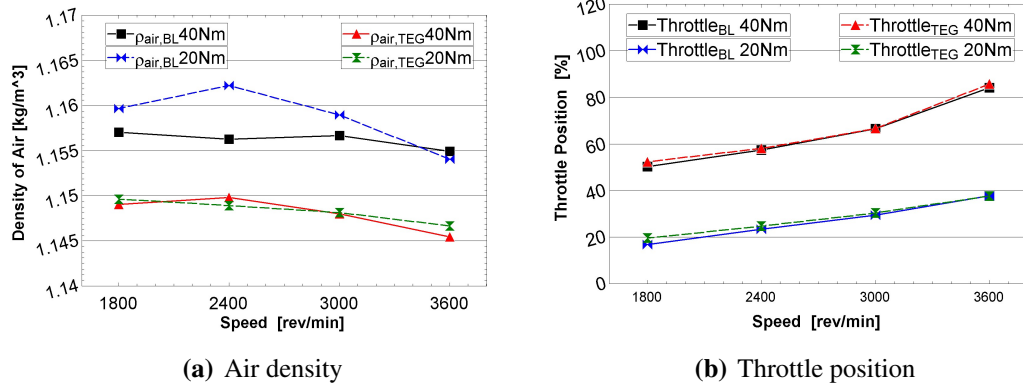


Figure 4.12: Air density and throttle position for the baseline testing and the resulting change after TEG installation

Table 4.8
Data summary of the air density and throttle position

	Baseline			Change with TEG (%)		
Air density (kg/m^3)	Low	High	Average	Low	High	Average
20 Nm	1.15	1.16	1.16	−1.1	−0.6	−0.9
40 Nm	1.16	1.16	1.16	−0.8	−0.6	−0.7
Throttle position (%)	Low	High	Average	Low	High	Average
20 Nm	16.8	37.8	26.9	−0.2	16.7	6.3
40 Nm	50.2	84.1	64.6	0.3	4.2	1.9

4.5.3 Exhaust Gas Energy

The exhaust gas energy was affected by the change in gross indicated work and the in-cylinder heat transfer. The exhaust gas energy was determined using the average thermocouple temperature measurements in the exhaust from both cylinders and the mass flow rate of the exhaust gas. In order to compute the enthalpy of the exhaust gas, an assumption was made for the exhaust gas composition comprised of 70% N_2 , 15% CO_2 , and 15% H_2O by mole fraction (67.8% N_2 , 22.8% CO_2 , and 9.4% H_2O by

mass fraction). This information was used to determine the change in enthalpy at the average exhaust temperature and the thermodynamic dead state of 25°C with the use of the software program Engineering Equation Solver, EES. Because the engine operates rich of stoichiometric conditions, carbon monoxide (CO) would be significant in the exhaust. However, the addition of CO was not used in the calculations because the change in enthalpy for CO_2 and CO were within a few percentage points of each other. Therefore, the resulting energy analysis would not have been altered with varying levels of CO that would have replaced CO_2 . The exhaust gas energy, shown in Figure 4.13(a), dropped because of the combination of the changes in exhaust gas temperatures, shown in Figure 4.13(b), and a drop in exhaust gas mass flow rate due to increased mechanical efficiency with the TEG and surrogate material. The data summary for the exhaust gas energy and exhaust gas temperatures can be seen in Table 4.9.

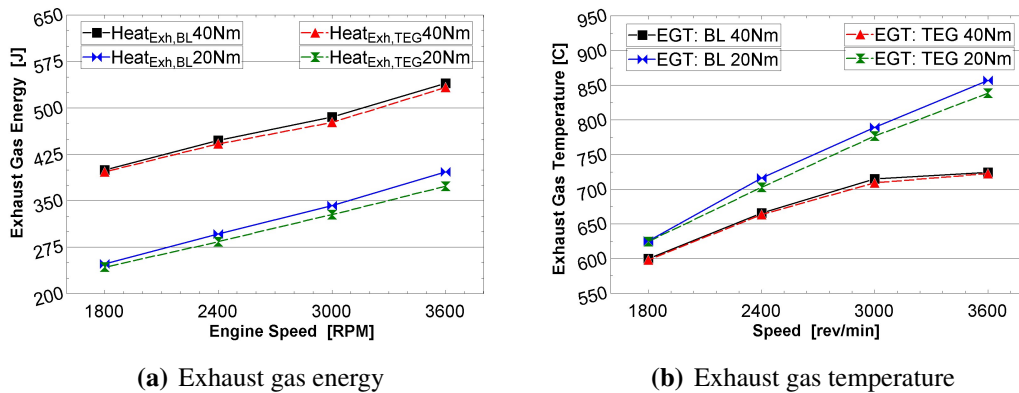


Figure 4.13: Exhaust gas energy and temperature for the baseline testing and the resulting change after TEG installation

Combustion analysis helps to explain the changes in the exhaust gas temperatures.

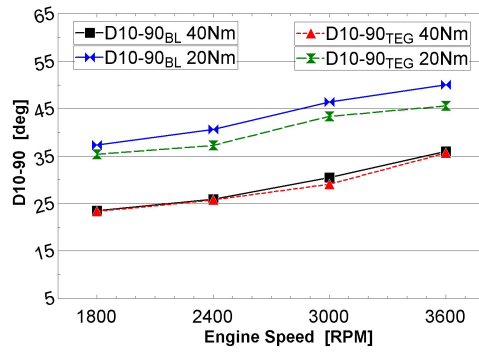
Table 4.9

Data summary of the exhaust gas energy and temperature

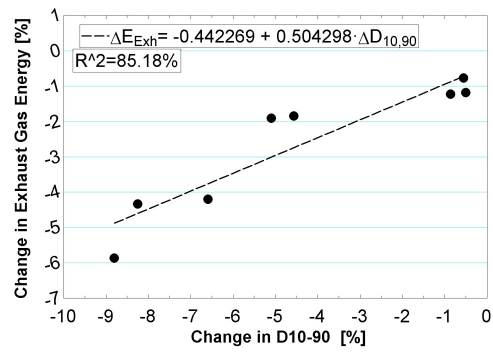
	Baseline			Change with TEG (%)		
Exhaust gas energy (J)	Low	High	Average	Low	High	Average
20 <i>Nm</i>	247.7	396.4	320.6	−5.9	−1.9	−4.1
40 <i>Nm</i>	399.8	539.9	468.1	−1.8	−0.8	−1.3
Exhaust gas temp (°C)	Low	High	Average	Low	High	Average
20 <i>Nm</i>	625.2	857.0	747.0	−2.2	0.1	−1.4
40 <i>Nm</i>	599.9	724.3	676.2	−0.8	−0.2	−0.4

Figure 4.14(a) shows the combustion duration from 10% and 90% of mass fraction burned.

The data summary of the combustion duration is shown in Table 4.10. The combustion duration decreased for all test points during the TEG testing. This was caused by the increased cylinder wall temperature. With a decreased combustion duration and a fix spark timing, the combustion gas temperature and pressure increased earlier in the expansion stroke. An example of this was observed in the in-cylinder pressure trace, shown in Figure 4.15, during the engine speed of 3000 *RPM* and engine load of 40 *Nm*. Soon after the start of combustion the overall cylinder pressure increased which would have also increased the combustion gas temperature. The combustion duration ended earlier in the process leaving the increased combustion gas temperature more crank angles for heat transfer before the exhaust valve opens. When this happened the in-cylinder pressure during the TEG testing dropped below the in-cylinder pressure of the BL testing. Which means the exhaust gas temperatures would have been lower due to the decreases combustion duration. This was verified in Figure 4.14(b), which shows that the change in the exhaust gas energy had a linear coefficient of determination of 85.18% to the change in the burn duration.



(a) Combustion duration



(b) Change in exhaust gas energy and change in combustion duration correlation

Figure 4.14: Combustion duration for the baseline testing and the resulting change after TEG installation and the relation to the change in exhaust gas energy

Table 4.10

Data summary of the combustion duration

	Baseline			Change with TEG (%)		
Combustion duration (deg)	Low	High	Average	Low	High	Average
20 Nm	37.3	50.0	43.6	-8.8	-5.1	-7.2
40 Nm	23.5	36.0	29.0	-4.6	-0.5	-1.6

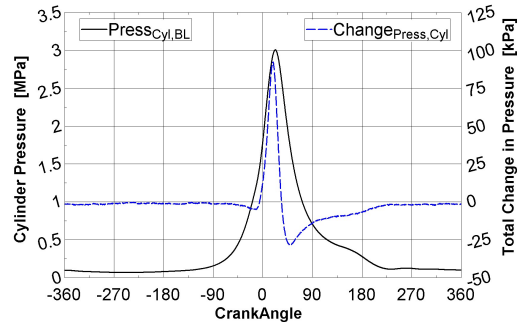


Figure 4.15: Cylinder pressure trace and the total change after TEG installation for engine speed of 3000 RPM and 40 Nm

4.5.4 Miscellaneous Energy

The cumulative heat release that was not accounted for within the brake work, pumping work, coolant system energy, and exhaust gas heat was considered as miscellaneous energy. The miscellaneous energy included any in-cylinder heat transfer that did not get removed by the coolant system and the total friction loss from the rubbing friction and accessory energy. Examples include heat transfer to the cylinder head, engine block, and oil sump reservoir. Figure 4.16 shows the miscellaneous energy and the data summary is shown in Table 4.11. It was expected that the miscellaneous energy would increase with increased engine speed and load because the coolant system would not have adequate time to properly remove the heat. The change in miscellaneous energy is due to a reduction in exhaust gas energy due to the decreased combustion duration. This increased miscellaneous energy can also be seen by the increase in the oil sump temperature in Figure 4.11(a).

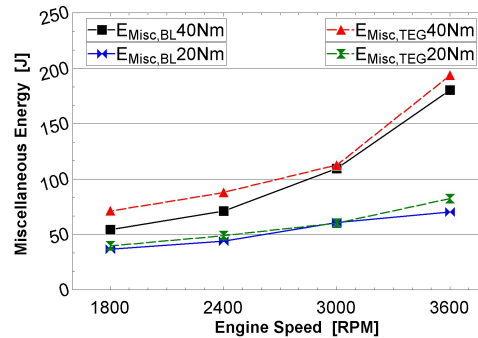


Figure 4.16: Miscellaneous power for the baseline testing and the resulting change after TEG installation

Table 4.11
Miscellaneous energy and temperature data summary

	Baseline			Change with TEG (%)		
Miscellaneous energy (J)	Low	High	Average	Low	High	Average
20 <i>Nm</i>	36.7	70.3	53.0	−0.9	16.9	9.0
40 <i>Nm</i>	54.4	180.2	103.7	2.9	31.2	16.4

4.6 TEG Energy Conversion

To maximize power production, each TEG was load matched with a 5.4 Ω electrical resistor, which was installed in series with each TEG. Using the voltage reading across the electrical resistors from the two TEGs, combined with the electric resistance, the TEG power was calculated. The TEG power was then converted to energy over each engine cycle (720 CAD). The TEG energy was scaled to simulate the complete coverage of both outer cylinder walls with TEGs. This TEG energy was then compared to the amount of cumulative heat release to determine the increase in fuel conversion efficiency. The results can be seen in Figure 4.17(a). Using the lower cylinder wall temperatures behind the surrogate material, the outer TEG temperature, and documentation from the TEG manufacturer, the predicted total TEG energy output for this application was determined, as shown in Figure 4.17(b). The data summary for both the experimental and predicted TEG output is shown in Table 4.12.

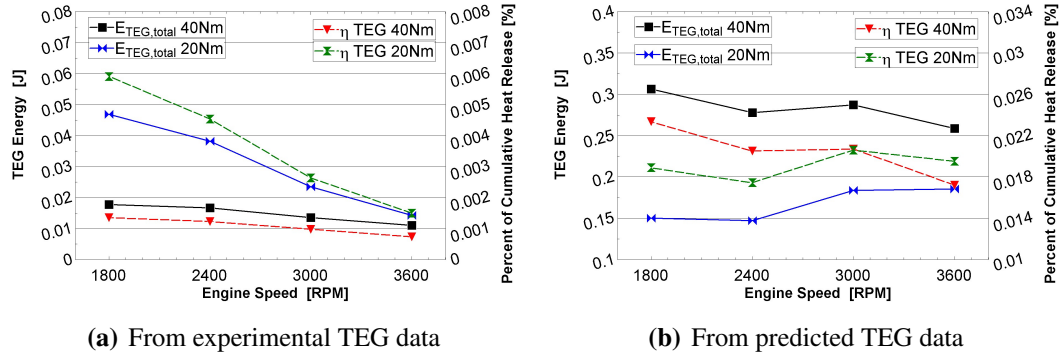


Figure 4.17: Scaled TEG energy output and fuel energy conversion

Table 4.12
Data summary of the TEG energy output and fuel energy conversion

	TEG energy conversion			Fuel percentage (%)		
TEG Experimental (J)	Low	High	Average	Low	High	Average
20 Nm	0.014	0.047	0.031	0.0015	0.0059	0.0036
40 Nm	0.011	0.018	0.015	0.0007	0.0014	0.0011
TEG Prediction (J)	Low	High	Average	Low	High	Average
20 Nm	0.147	0.185	0.167	0.017	0.021	0.019
40 Nm	0.259	0.306	0.282	0.017	0.023	0.020

4.6.1 TEG Malfunction

The low energy production of the TEG in the experimental testing compared to the fully predicted was a cause for concern. Possible reasons for the energy production discrepancy included; the TEG modules were installed not under compression, possible coolant contamination, and possible temperature difference smaller than measured.

The TEG manufacturer recommends that the TEG be compressed between two heat sinks with a pressure of 1.275 MPa (equates to a 1148 N force on the TEG), which was

not possible during this testing because of space limitations in the water-jacket. An independent test was done on a TEG under compression between two aluminum plates with embedded thermocouples to study the effect of compression on TEG output. When the hot side was subjected to a hot-plate the TEG produced voltages and power outputs that compared favorably with the manufacturer's documentation over similar temperature ranges, as shown in Table 4.13. Another independent test was done with the TEG adhered with JB Weld to one aluminum plate with the cold-side thermocouple attached to the TEG with a minimum amount of JB Weld, as shown in Figure 4.18. This is representative of the technique used during the TEG testing on the engine. Although the temperature conditions during the TEG engine testing were not able to be reproduced with this origination, the TEG (smaller delta temperature) produced voltages and power outputs comparable with the manufacturer's documentation. Table 4.13 documents the results of the compression and non-compression tests. The conclusion from these independent compression tests were that the output of the TEG is consistent with the manufacturers specifications and the no compression case still produced consistent results.

Table 4.13
TEG voltage output validation with and without compression

	Hot-side Temp [°C]	Cold-side Temp [°C]	Measured Voltage [V]	Predicted Voltage [V]	Difference [%]
Compression	166	85	1.75	1.75	0.0
	160	90	1.45	1.50	3.4
	170	95	1.55	1.59	2.6
No Compression	131	105	0.50	0.4	-20.0

There was a possibility that the engine coolant was able to penetrate the TEG module



Figure 4.18: TEG validation test without compression

and disrupt the operation. To test this, the TEGs were removed from the cylinder wall for visual inspection. It was discovered that the cold-side of the TEGs were open to the internal thermal electric modules, which can be seen in Figure 4.19. New TEGs were installed on

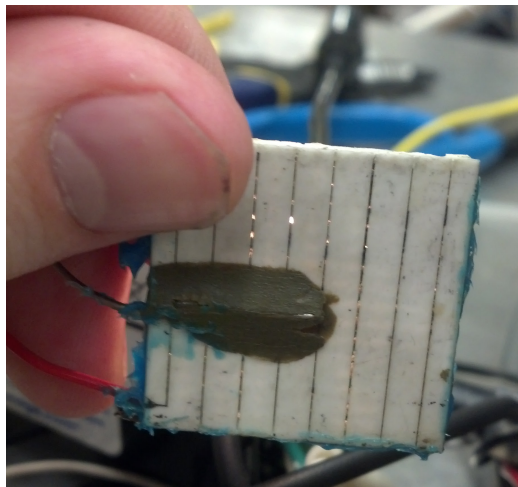


Figure 4.19: Location for coolant penetration into TEG

the cylinder walls which did not have the graphite foil removed from the cold-side of the TEG. It was believed that the graphite foil would help seal the TEG from the coolant. In addition, one thermocouple was installed directly behind the TEG on cylinder 2 to

verify the hot-side temperature. The predicted hot-side temperature for this location was previously obtained by using the data from the embedded thermocouples in the cylinder walls which were located 90 degrees from the TEG. It was possible that the hot-side cylinder wall temperature for the TEG was smaller than the temperature measurements from the other cylinder wall location. This would have caused a smaller temperature gradient and the TEG voltage and power output would have decreased. One full round of testing was completed with the new TEGs and the new embedded thermocouple. One of the TEGs failed before the engine was thermally stable for the first engine mode. With the proper electrical load matching, the TEG voltage output for this test compared to the predicted voltage output, as can be seen in Figure 4.20. The results show that the voltage output remained low compared to the predicted values. Furthermore, the thermocouple embedded in the cylinder wall behind the TEG measured temperatures 9.8% to 17.7% lower than the cylinder wall temperature measured behind the surrogate during the same test, shown in Figure 4.21(a). Considering that temperature discrepancy could suggest that coolant once again entered the TEG and increased its thermal conductivity, one more full round of engine testing was performed with the TEG replaced with the TEG surrogate material. During this test the thermocouple embedded in the cylinder wall behind the TEG measured temperatures only 0.3% to 3.1% below the lower cylinder wall temperature behind the surrogate. These results indicate that coolant must have entered the TEGs during testing, which would account for low energy production and that the cylinder wall temperature at the TEG location does not significantly reduce compared to the cylinder

wall measurements behind the surrogate. Therefore, a TEG with no coolant contamination would be predicted to produce the energy shown in Figure 4.17(b).

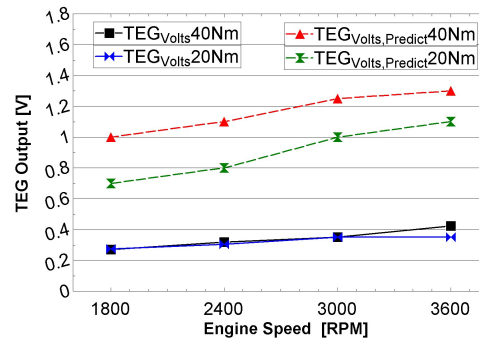


Figure 4.20: TEG measured voltage compared to the predicted TEG voltage

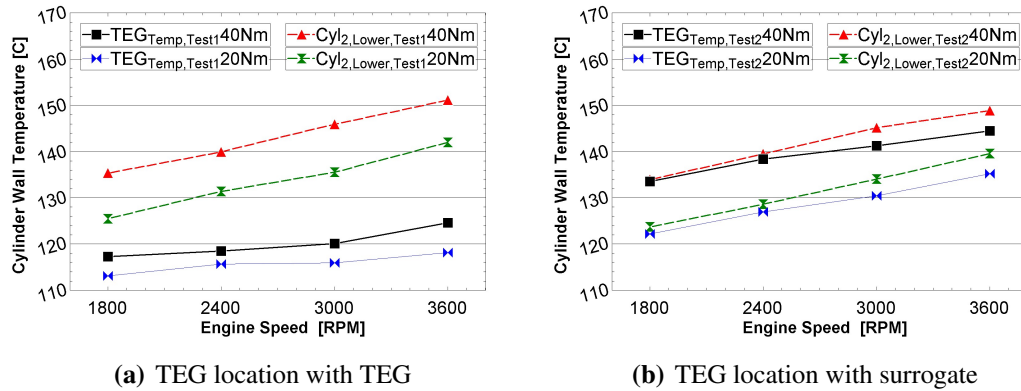


Figure 4.21: Comparison of cylinder wall temperatures for cylinder 2 using the TEG as a thermal insulator and using the TEG surrogate material as a thermal insulator

4.7 Conclusions

The research focused on the empirical trends in fuel energy distribution, cylinder wall temperatures, and TEG power generation with the addition of the TEG / surrogate material over a range of engine speeds and loads in a two cylinder, 19.4 kW, liquid-cooled, spark-ignition engine.

The cylinder wall temperatures increased by 17% to 44% depending on the reduction of the coolant heat transfer. The coolant heat transfer decreased by 4.3% to 9.5% depending on the engine setting. The amount of heat transfer through the outer cylinder wall contributed approximately 23.3% to 28.2%, indicating that a significant amount of heat transfer going to the coolant does not come directly from the outer cylinder walls but from the engine block. The gross indicated work decreased by 0.4% to 1.0% which was attributed to the decrease in the remaining friction energy and pumping work. The remaining friction energy decreased because the overall oil viscosity decreased due to the increased oil temperatures on the cylinder walls. The decrease in pumping work was a result of the change in air density during testing and not because of the TEG installation. The exhaust gas energy decreased by 0.8% to 5.9% because of the decreased combustion duration which allowed more time for in-cylinder heat transfer from the high temperature combustion gas. In addition, fuel conversion efficiency increased, which reduced the fuel flow and thus reduced the exhaust energy.

The scaled output of the TEG was less than $0.1 J$. The low energy production of the TEG was due to coolant contamination. The predicted TEG energy output using a hot-side and cold-side temperature measurement in the engine ranged from $0.1 J$ to $0.3 J$. This corresponds to less than 0.1% of the cumulative heat release.

Chapter 5

Conclusions and Recommendations

5.1 Conclusions

This dissertation focused on the potential energy recovery, engineering challenges, and the new advancements in automotive waste heat recovery methods. Chapter 2 defined current automotive waste heat recovery techniques using Rankine cycles and thermoelectric generators and outlined the engineering challenges with the technologies. Chapter 3 quantified the potential improvement in vehicle fuel economy with a combination of a coolant and exhaust-based Rankine cycle which utilizes a recently patented piston in piston engine technology. Chapter 4 investigated the impact of implementing thermoelectric generators (TEG) on the outer cylinder walls of a liquid-cooled internal combustion engine.

Automobile WHR systems have shown considerable potential to increase fuel economy. The two main WHR systems for automotive applications were found to be thermoelectric generators and Rankine cycle electrical generators. The design considerations for these systems include; backpressure, weight, thermal power fluctuations, cold reservoir reliability, DC-DC converter losses, type of engine, coolant or exhaust energy streams, expense, complexity, and size. Additional considerations for thermoelectric material, longevity, and stress are needed for thermoelectric generators while working fluid selection, component design, system pressure, and safety are needed for Rankine cycles.

The Rankine cycle research project had a hypothesis that there would be enough steam generation that all six cylinders of the C-13 diesel engine could be equipped with a secondary steam chamber and that fuel conversion efficiency would increase by 2.0%. The simulation showed that a Class-8 diesel engine at full load could be implemented with this WHR technology but the steam generation from the coolant and exhaust heat exchangers was not substantial enough to operate all six cylinders. The Class-8 diesel engine running at 1,500 *RPM* at full load (1,496 Nm) had a net increase of up to 26.7 *kW* with the addition of this engine technology on two of the six cylinders, actuated twice per four-stroke engine cycle. This increased power equated to an improvement in brake fuel conversion efficiency from 34.4% up to a maximum of 37.5% (3.1% increase). The hypothesis of a 2% increase in fuel conversion efficiency was shown to be possible depending on the design of the exhaust heat exchanger. The analysis of the steam chamber throughout the engine cycles showed that the water vapor condensed during certain portions of the cycle. The formation

of liquid in the steam chamber has the potential to reduce the efficiency of the system and to cause a mechanical failure if not properly removed from the cylinder (hydraulic lock).

The TEG research project had a hypotheses that the fuel conversion efficiency will improve by 0.5% and that the majority of the displaced cylinder wall heat transfer will be expelled through the exhaust system in a two cylinder, 19.4 kW, liquid-cooled, spark-ignition engine. The research focused on the empirical trends in fuel energy distribution, cylinder wall temperatures, and TEG power generation with the addition of the TEG / surrogate material over a range of engine speeds and loads. The cylinder wall temperatures increased by 17% to 44% depending on the reduction of the coolant heat transfer. The coolant heat transfer decreased by 4% to 9% depending on the engine setting. The amount of heat transfer through the outer cylinder wall contributed approximately 23%-28%, indicating that a significant amount of heat transfer going to the coolant does not come directly from the outer cylinder walls but from the engine block. The gross indicated work decreased by 0.4% to 1.0% which was attributed to the decrease in the remaining friction energy and pumping work. The remaining friction work decreased because the overall oil viscosity decreased due to the increased oil temperatures on the cylinder walls. The decrease in pumping work was a result of the change in air density during testing and not because of the TEG installation. The exhaust gas energy decreased by 0% to 2.6%. The reduction of exhaust gas energy with the reduction in coolant energy was not expected. The reduction in exhaust gas energy was caused by the decreased combustion duration which allowed more time for in-cylinder heat transfer from the combustion gas and the increase in mechanical

efficiency. The miscellaneous energy changed by -0.9% to 31.2% . The scaled output of the TEG was less than 0.1 J . The low energy production of the TEG was due to coolant contamination. A surrogate material was used in place of the TEG and the predicted output reached 0.3 J . This accounted for less than 0.1% of the cumulative heat release. Higher TEG conversion efficiencies, combined with greater control of heat transfer paths, would be needed in order to improve energy output and make this a viable waste heat recovery technique.

5.2 Recommendations for Future Work

The experiments evaluated in this dissertation assisted in furthering the concept of automotive waste heat recovery. As most research does, the results open new questions that could be explored in the future. The following is a list of recommendations for future work for both WHR techniques.

5.2.1 Rankine Cycle: Steam Assisted Engine

The issue of having water condensing within the steam chamber during expansion could have unknown effects and cause damage to the system. The working fluid mixture did evaporate in this simulation when the steam chamber approached the clearance height of

0.5 mm (TDC). Wetting over a number of cycles could induce a collection of water droplets in the steam chamber. This could cause a loss of efficiency or possible mechanical failure which would warrant laboratory experiments to determine the severity of the issue.

The analysis of this WHR technique was done under steady-state conditions. Transient situations would impose additional challenges. In particular, the cold-start regime would require a steam by-pass valve, allowing the recovery system to warm up and produce the required steam properties before being put into operation.

The design geometry and increased mass of the pistons with the steam chambers could affect the performance, durability, and mechanical vibration of the engine. The magnitude of any negative affects are unknown at this point.

The lift profile of the intake valve has a disconcertingly short crank angle duration and the valve would come in contact with the piston without the piston being modified to have two small pockets to encompass the inlet valve. The short crank angle duration causes increased valve velocities and accelerations that may not be favorable to long valve life.

5.2.2 Thermoelectric Generators: Cylinder Walls

The design of using adhesive to join the TEG to the cylinder wall did not yield the expected output energy. A redesigned cylinder wall profile and water-jacket would allow for a

traditional TEG installation under recommended compression pressure.

The oil analysis did not signal any significant degradation with the increased cylinder walls during the 42 hours of TEG testing. Endurance testing a range of oil weights could offer more insight on optimal oil selection and possible long time usage issues.

Due to availability and resources, the proof-of-concept WHR technique was implemented on a small SI engine. The original concept was envisioned on a Class 8 diesel engine. The WHR potential under those conditions deserves consideration for future research.

Using the energy distribution trends found in this dissertation as a guide, a simulation based research project would give insight on the impact on the engine with a variation in TEG thermal resistances.

References

- [1] EIA. Annual energy outlook 2013 Technical report, April , **2013**.
- [2] EIA. Alternatives to traditional transportation fuels 1999 Technical report, U.S. Energy Information Administration, **2001**.
- [3] EIA. Alternatives to traditional transportation fuels 2000 Technical report, U.S. Energy Information Administration, **2002**.
- [4] EIA. Alternatives to traditional transportation fuels 2002 Technical report, U.S. Energy Information Administration, **2004**.
- [5] EIA. Alternatives to traditional transportation fuels 2007 Technical report, U.S. Energy Information Administration, **2009**.
- [6] EIA. Alternatives to traditional transportation fuels 2009 Technical report, U.S. Energy Information Administration, **2011**.
- [7] de Paula Pignatti, T. T.; Miziara, W.; de Cunha, R. E. Reduced friction for a four cylinder two valve otto engine valve train Technical report, 10 , **2011**.

- [8] Hoshikawa, J.; Kato, K.; Miyamoto, K.; Higashi, H.; Ito, A. A study of friction reduction by soft skirt piston Technical report, 08 , **2011**.
- [9] Kimura, Y.; Murakami, M. Analysis of piston friction - effects of cylinder bore temperature distribution and oil temperature 08 , **2011**.
- [10] Selvaraj, B.; Sridhara, S. N.; Indraprakash, G.; Senthilkumar, A.; Pangaonkar, A. Effects of intake port geometry on the performance of an si engine 11 , **2011**.
- [11] Wyszynski, L. P.; Stone, C. R.; Kalghatgi, G. T. The volumetric efficiency of direct and port injection gasoline engines with different fuels 03 , **2002**.
- [12] Turin, R. C.; Zhang, R.; Chang, M.-F. Volumetric efficiency model for variable cam-phasing and variable valve lift applications 04 , **2008**.
- [13] Martensson, J.; Flardh, O. Modeling the effect of variable cam phasing on volumetric efficiency, scavenging and torque generation 04 , **2010**.
- [14] Taglialatela-Scafati, F.; Cesario, N.; Lavorgna, M.; Mancaruso, E.; Vaglieco, B. M. Diagnosis and control of advanced diesel combustions using engine vibration signal 04 , **2011**.
- [15] Fathi, M.; Saray, R. K.; Pourfallah, M.; Kheyrollahi, J.; Javadirad, G. Egr and intake charge temperature effects on dual-fuel hcci combustion and emissions characteristics 09 , **2011**.

- [16] Improvement of performance and emission characteristics of a di diesel engine with turbulence induced piston (internal jet piston) using biodiesel blends. 12 **2009**.
- [17] Sadakane, S.; Sugiyama, M.; Kishi, H.; Abe, S.; Harada, J.; Sonoda, Y. Development of a new v-6 high performance stoichiometric gasoline direct injection engine 04 , **2005**.
- [18] Iijima, A.; Yoshida, K.; Shoji, H. A comparative study of hcci and atac combustion characteristics based on experimentation and simulations influence of the fuel octane number and internal egr on combustion 10 , **2005**.
- [19] Wei, D.; Lu, X.; Lu, Z.; Gu, J. Performance analysis and optimization of organic rankine cycle (orc) for waste heat recovery Technical report, Elsevier, **2007**.
- [20] Ringler, J.; Seifert, M.; Guyotot, V.; Hubner, W. Rankine cycle for waste heat recovery of ic engines Technical Report 2009-01-0174, **2009**.
- [21] Boretti, A. Improving the efficiency of lpg compression ignition engines for passenger cars through waste heat recovery 12 , **2011**.
- [22] Endo, T.; Kawajiri, S.; Kojima, Y.; Takahashi, K.; Baba, T.; Ibaraki, S.; Takahashi, T.; Shinohara, M. Study on maximizing exergy in automotive engines Technical Report 2007-01-0257, **2007**.
- [23] EIA. Annual energy outlook 2010 Technical report, U.S. Energy Information Administration, April , **2010**.

- [24] Armstead, J. R.; Miers, S. A. In *N/A*, 2010.
- [25] Chammas, R. E.; Clodic, D. Combined cycle for hybrid vehicles Technical Report 2005-01-1171, **2005**.
- [26] Yu, C.; Chau, K. Thermoelectric automotive waste heat energy recovery using maximum power point tracking Technical report, **2009**.
- [27] Yang, J.; Stabler, F. R. Automotive applications of thermoelectric materials Technical Report 7, **2009**.
- [28] Hatzikraniotis, E.; Zorbas, K. T.; Samaras, I.; Kyratsi, T. H.; Paraskevopoulos, K. M. Efficiency study of a commercial thermoelectric power generator teg under thermal cycling Technical report, **2009**.
- [29] Crane, D. T.; Jackson, G. S. Optimization of cross flow heat exchangers for thermoelectric waste heat recovery Technical report, **2003**.
- [30] Stobart, R.; Milner, D. The potential for thermo-electric regeneration of energy in vehicles Technical Report 2009-01-1333, **2009**.
- [31] Mori, M.; Yamagami, T.; Oda, N.; Hattori, M.; Sorazawa, M.; Haraguchi, T. Current possibilities of thermoelectric technology relative to fuel economy Technical Report 2009-01-0170, **2009**.
- [32] Rowe, D. *Thermoelectrics Handbook: Macro to Nano*; Boca Raton, 2006.

- [33] Headings, L. M.; Midlam-Mohler, S.; Washington, G. N.; Heremans, J. P. High temperature thermoelectric auxiliary power unit for automotive applications October 28-30 , **2008**.
- [34] LaManna, J.; Ortiz, D.; Livelli, M.; Haas, S.; Chikwem, C.; Ray, B.; Stevens, R. Feasibility of thermoelectric waste heat recovery in large scale systems October 31 - November 6 , **2008**.
- [35] Srinivasan, M.; Praslad, S. M. In *Power Electronics and Drives Systems, 2005. PEDS 2005. International Conference on*, Vol. 2, pages 977–982, 2005.
- [36] Saqr, K. M.; Mansour, M. K.; Musa, M. N. Thermal design of automobile exhaust based thermoelectric generators: Objectives and challenges Technical Report 2, **2008**.
- [37] Hung, T. C.; Shai, T. Y.; Wang, S. K. A review of organic rankine cycles (orcs) for the recovery of low-grade waste heat Technical Report 7, **1997**.
- [38] Liu, B.-T.; Chien, K.-H.; Wang, C.-C. Effect of working fluids on organic rankine cycle for waste heat recovery Technical report, **2004**.
- [39] Schuster, A.; Karellas, S.; Kakaras, E.; Spliethoff, H. Energetic and economic investigation of organic rankine cycle applications Technical report, **2009**.
- [40] Heywood, J. B. *Internal Combustion Engine Fundamentals*; McGraw-Hill, Inc, 1988.
- [41] Crane, D. T.; Bell, L. E. Design to maximize performance of a thermoelectric power generator with a dynamic thermal power source Technical report, **2009**.

- [42] Crane, D. T.; Jackson, G. S.; Holloway, D. Towards optimization of automotive waste heat recovery using thermoelectrics Technical Report 2001-01-1021, SAE Technical Paper, **2001**.
- [43] Wojciechowski, K. T.; Schhmidt, M.; Zybala, R.; Merkisz, J.; Fuc, P.; Lijewski, P. Comparison of waste heat recovery from the exhaust of a spark ignition and a diesel engine Technical report, **2009**.
- [44] Teng, H.; Regner, G.; Cowland, C. Achieving high engine efficiency for heavy-duty diesel engines by waste heat recovery using supercritical organic-fluid rankine cycle Technical Report 2006-01-3522, **2006**.
- [45] Smith, K.; Thornton, M. Feasibility of thermoelectrics for waste heat recovery in conventional vehicles Technical report, April , **2009**.
- [46] Yang, J. In *International Conference on Thermoelectrics*, Vol. N/A, page N/A, 2005.
- [47] Hussain, Q. E.; Brigham, D. R.; Maranville, C. W. Thermoelectric exhaust heat recovery for hybrid vehicles Technical Report 2009-01-1327, **2009**.
- [48] Arias, D. A.; Shedd, T. A.; Jester, R. K. Theoretical analysis of waste heat recovery from an internal combustion engine in a hybrid vehicle Technical Report 2006-01-1605, **2006**.

- [49] Teng, H.; Regner, G.; Cowland, C. Waste heat recovery of heavy-duty diesel engines by organic rankine cycle part i: Hybrid energy system of diesel and rankine engines Technical Report 2007-01-0537, **2007**.
- [50] Mago, P. J.; Srinivasan, K. K.; Chamra, L. M.; Somayaji, C. An examination of exergy destruction in organic rankine cycles Technical report, **2008**.
- [51] Weight category definitions from 49cfr565.5. Oak Ridge National Laboratory, C. f. T. A. **2000**.
- [52] Internal combustion engine with auxillary steam power recovered from waste heat. Harmon SR., J. V.; Harmon JR., J. V.; Harmon, S. C. **2011**.
- [53] Ferguson, C. R.; Kirkpatrick, A. T. *Internal Combustion Engines*; John Wiley & Sons, Inc, 2nd ed., 2001.
- [54] C-13 on-highway diesel engine with acert technology. Caterpillar, I. **2007**.
- [55] Cengel, Y. A.; Boles, M. A. *Thermodynamics An Engineering Approach*; Jeans, Suzanne, 6th ed., 2008.
- [56] Waldron, K. J.; Kinzel, G. L. *Kinematics, Dynamics, and Design of Machinery*; 2nd ed., 2004.
- [57] Caton, J. A. Results from the second-law of thermodynamics for a spark-ignition engine using a cycle simulation October , **1999**.

- [58] Angrist, S. *Direct energy conversion*, Allyn and Bacon series in mechanical engineering and applied mechanics; Allyn and Bacon, 1982.
- [59] Ikoma, K.; Munekiyo, M.; Furuya, K.; Kobayashi, M.; Izumi, T.; Shinohara, K. Thermoelectric module and generator for gasoline engine vehicles May 24-28 , **1998**.
- [60] Fleurial, J.-P. Thermoelectric power generation materials: Technology and application opportunities Technical report, **2009**.
- [61] Gatowski, J. A.; Jones, J. D.; Siegl, D. C. Evaluation of the fuel economy potential of the low-heat-rejection diesel engine for passenger-car application February , **1987**.
- [62] Bruns, L.; Bryzik, W.; Kamo, R. Performance assessment of us. army truck with adiabatic diesel engine February , **1989**.
- [63] Hoag, K. L.; Brands, M. C.; Bryzik, W.; Army, U. Cummins/tacom adiabatic engine program Technical report.
- [64] Kamo, R.; Bryzik, W.; Glance, P. Adiabatic engine trends-worldwide February , **1987**.
- [65] Khoshrovan, E. Heat transfer studies in an adiabatic diesel engine November , **1991**.
- [66] Modi, A. J.; Gosai, D. Experimental study on thermal barrier coated diesel engine performance with blends of diesel and palm biodiesel Technical report, SAE International, **2010**.

- [67] Parlak, A. The effect of heat transfer on performance of the diesel cycle and exergy of the exhaust gas stream in a lhr diesel engine at the optimum injection timing Technical Report 2, **2005**.
- [68] Taymaz, I. An experimental study of energy balance in low heat rejection diesel engine Technical Report 2-3, **2006**.
- [69] Descombes, G.; Maroteaux, F.; Feidt, M. Study of the interaction between mechanical energy and heat exchanges applied to ic engines Technical Report 16, **2003**.
- [70] Büyükkaya, E.; Engin, T.; Cerit, M. Effects of thermal barrier coating on gas emissions and performance of a lhr engine with different injection timings and valve adjustments Technical Report 9-10, **2006**.
- [71] Kohler aegis lh630-775 service manual. 09 **2006**.
- [72] Stewardship, P. Material safety data sheet: Castrol gtx 10w-30 Technical Report 459835-VE12, August , **2012**.
- [73] Kondo, Y.; Koyama, T.; Sasaki, S. *Ionic Liquids - New Aspects for the Future*; 2013.
- [74] Characterized control valves (ccv): Features and benefits. Belimo Aircontrols, I.; May , **2012**.
- [75] Ftb370 series. Omega. Omega.com.

- [76] Teg specification sheet: Seebeck thermoelectric generator: Part number 1261g-7l31-04cl. Inc, C. T. Y. T. P.; Custom Thermoelectric: Your Thermoelectric Partner Inc,, **2011**.
- [77] Dynamite accessories price list. Land-And-Sea. December , **2011**.
- [78] Pressure sensors for combustion analysis product catalog - edition 2011. AVL. **2011**.

Appendix A

Supplemental Information

This section within the appendix is to give supplemental information related to Chapter 4 in regards to engine specifications, laboratory test cell, transducer instrumentation, and experimental results. The condensed nature of the journal article did not allow for detailed explanation and justifications for the aforementioned criteria.

A.1 Engine Specifications

The engine that was used for this research was a 19.4kW, two-cylinder, liquid-cooled, spark-ignition model. The engine was donated to Michigan Technological University from the Kohler Company. The engine specifications can be found in Table A.1.

Table A.1

Engine specifications for the Kohler LH690 horizontal-shaft, liquid-cooled SI engine. NOTE: All listed dimensions and tolerances are measured at 20°C. [71]

Engine type	Spark ignition
Power	Maximum 19.4 kW (26 HP) @3600 RPM
	Recommended 16.5 kW (22.1 HP)
Peak Torque	58.1 Nm (42.9 ftlb.) @2400 RPM
Bore	80 mm (3.15 in.)
Stroke	67 mm (2.64 in)
Displacement	674 cubic centimeters (41.1 cubic inches)
Compression Ratio	8.5 : 1
Dry Weight	51.7 kg (114 lb)
Oil Capacity	1.6 – 1.8 L (1.7 – 1.9 U.S. qt)
Coolant Capacity	2.0 L (2.18 U.S. qt)
Maximum Angle of Operation	20 degrees
Dimensions L x W x H	17.0 in x 18.1 in x 26.5 in

Two views of the unmodified stock engine is shown in Figure A.1(a) and Figure A.1(b).

In this configuration, the engine coolant circulates through the coolant system by a pump that is belt-driven from the camshaft. The coolant flow separates after the pump into two cooling circuits that remove heat energy from each of the two cylinder water-jackets. The coolant exits the water-jacket around the cylinder through openings in the head gasket. These openings lead to the engine head and out a passage within the intake manifold where the two circuits merge. When the thermostat is open the coolant flows into the radiator

and then back into the pump. The stock thermostat remains closed until the engine reaches the temperature of 79.4°C and will be fully open at 90.5°C. The radiator is cooled with ambient air by a cooling fan that is belt driven off the flywheel. [71]

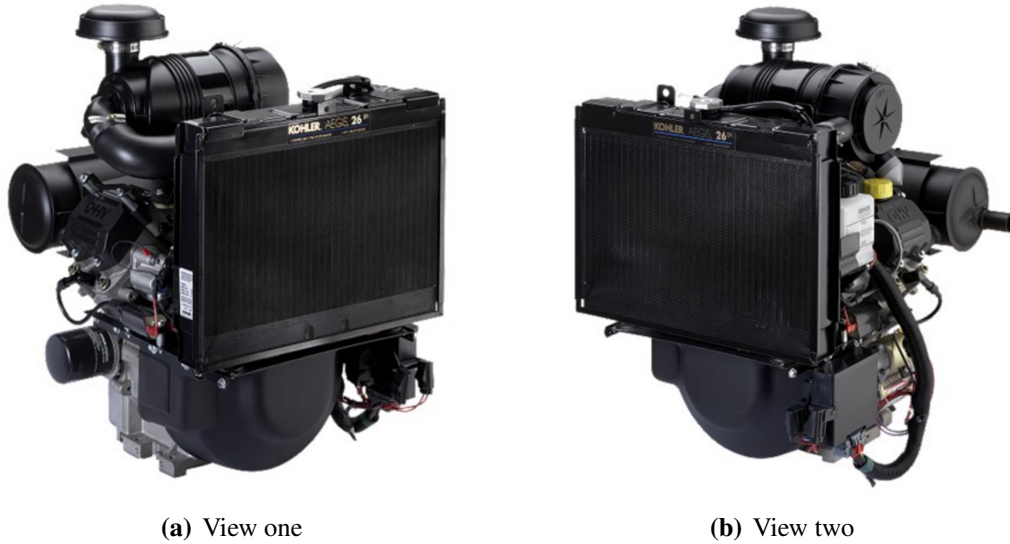


Figure A.1: Kohler AEGIS LH690 Liquid-Cooled Horizontal Crankshaft Engine [71]

A.2 Laboratory Test Cell

The laboratory test cell description is divided into three systems include the cooling system, exhaust system, and mechanical system.

A.2.1 Cooling System

The cooling system was designed to control the temperature of the coolant as it enters the engine which allowed for repeatable results. This was accomplished by removing the traditional air-to-liquid radiator and installing a custom liquid-to-liquid heat exchanger system. The coolant system equipment is explained below with figure references that show the installation locations.

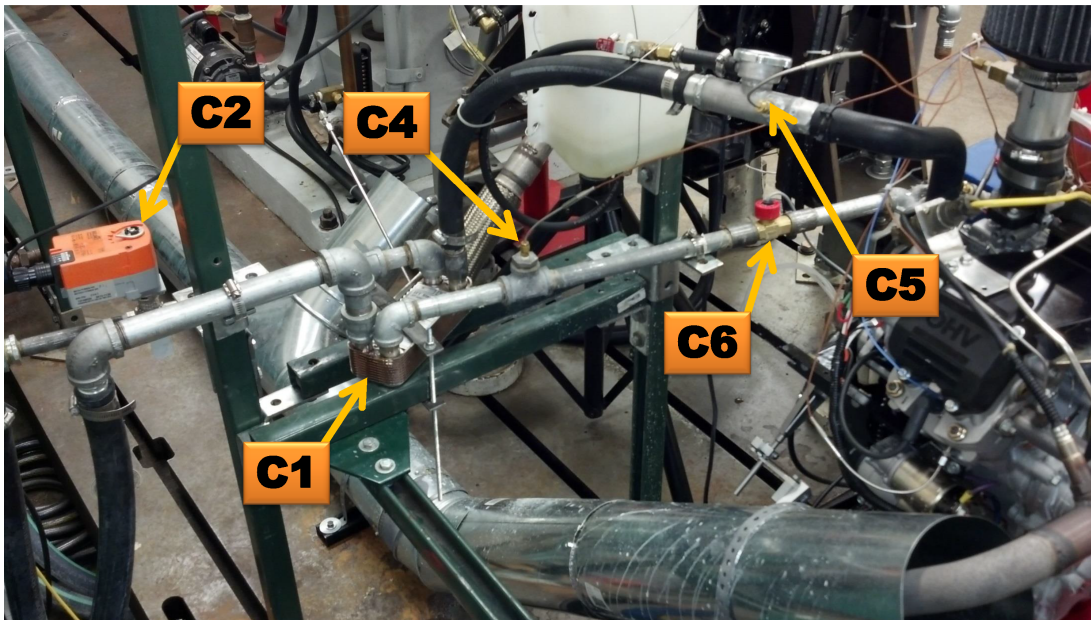


Figure A.2: View 1 of the coolant system.

C1 (Figure A.2) The liquid-to-liquid cross flow heat exchanger was from ITT Industries, Inc. It was a Standard Xchange Brazepak, brazed plate heat exchanger with a part number of BP400-20.

C2 (Figure A.2) The characterized control valve was from the company Belimo Aircontrols (USA), Inc. and had a part number of B213+TFRB24-SR+NO. The nomenclature for this characterized control valve states that this part number has the following; Valve: 2-way, Valve Size: 1/2 inch npt, Trim Material: stainless steel trim, Actuator Type: spring return, Power Supply: 24 VAC/DC, Control: 2 – 10 VDC, Spring Return: normally open. The flow coefficient (C_V), which is a dimensionless parameter which relates geometrically similar pumps, was 4.7. The equation for C_V can be found in Equation (A.1). Q is the volumetric flow rate in gallons per minutes, SG is the specific gravity and $\Delta Press$ is the pressure drop across the valve in psi. [74]

$$C_V = Q * \frac{SG}{\sqrt{\Delta Press}} \quad (A.1)$$

C3 (Not shown) A proportional-integral-derivative (PID) controller was used to monitor the coolant inlet temperature and regulate the characterized control valve to maintain a setpoint coolant supply temperature. The PID temperature controller was purchased from Omega Engineering, Inc. with a part number of CN77543. The nomenclature for this part number states the following: CN77 series PID controller, Case Type: NEMA 4 bezel for 1/16 DIN panel cutout 45mm x 45mm, Control Output #1: non-isolated 1 to 10VDC or 0 – 20mA 500 Ω max, Control Output #2 (Direct or Reverse Acting): relay from "C" 5A 120VAC, 3A 240 VAC. The control output

#1 was used to control the characterized control valve. One K-type thermocouple (C4), which was used by the PID controller, was installed in the coolant loop directly after the coolant heat exchanger. This arrangement allowed for a faster response to a change in coolant temperature compared to a thermocouple location at the inlet of the engine. The PID controller had a temperature set point one degree Celsius higher than the desired temperature of the inlet coolant. This was done because there is over 1m length of galvanized piping between the heat exchanger and the inlet to the engine and this length is prone to heat transfer to the surrounding environment.

C4 (Figure A.2) K-type thermocouple to measure the coolant temperature after the Standard Xchange Brazepak heat exchanger. This reading was utilized by the PID temperature controller. All sixteen temperature measurements were performed with ungrounded, sheathed K-type thermocouples. These thermocouples, purchased from Omega.com, are denoted as having special limits which, “Meets or exceeds special limits of error (SLE) and EN 60584 – 2: Tolerance Class 1”. These K-type thermocouples have an uncertainty of 1.1°C or 0.4% (whichever value is greater). The standard limits for K-Type thermocouples were not used because of the increased uncertainty of 2.2°C or 2.0% (whichever value is greater).

C5 (Figure A.2) K-type thermocouple to measure the coolant as it leaves the engine going to the Standard Xchange Brazepak heat exchanger.

C6 (Figure A.2) The mass flow rate of the coolant was measured and recorded with a hall effect turbine-type flow meter designed to handle the expected coolant temperatures.

This piece of equipment was purchased from Omega Engineering, Inc. and the model number was FTB371. The fittings were 3/4 mNPT. The flow range was 1.9 to 39.4 liters per minute with an uncertainty of $\pm 3\%$. The maximum operational temperature is 85°C at 0.689 bar and the maximum pressure is 9.997 bar at 29.4°C. The calibrated K-Factor of 869 Pulses/Liter was used during testing. [75]

C7 (Figure A.3) K-type thermocouple to measure the coolant as it leaves the water-jacket and enters the cylinder head.

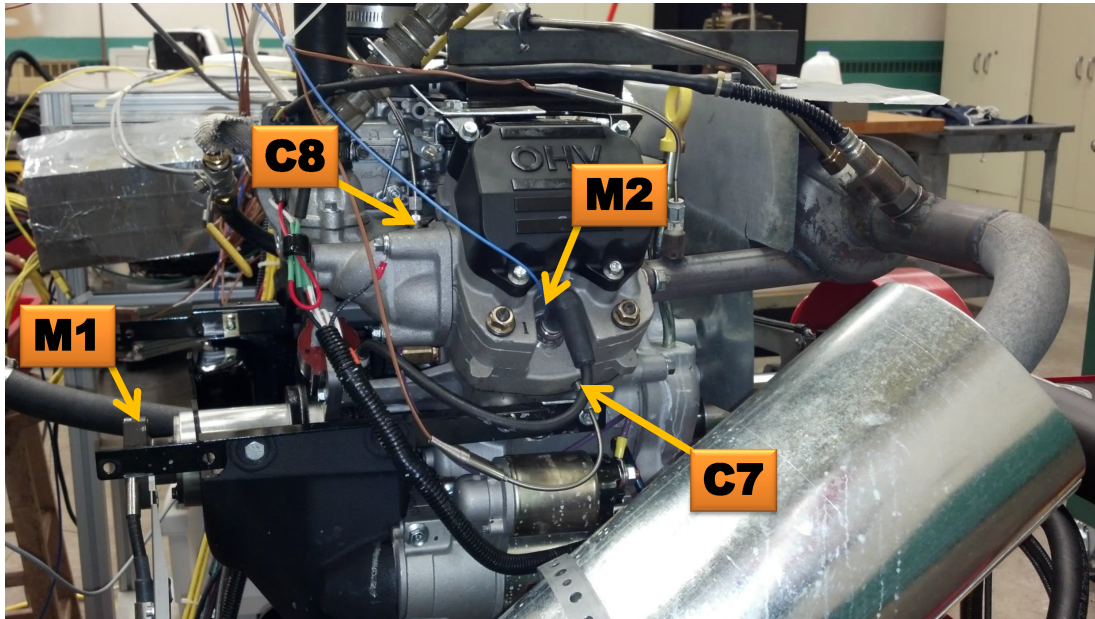


Figure A.3: View 2 of the coolant system

C8 (Figure A.3) K-type thermocouple to measure the coolant as it leaves the cylinder head and enters the intake manifold. The two cylinder coolant flows converge in the intake manifold and exit the engine to the plate heat exchanger.

C9 (Figure A.4) K-type thermocouple to measure the coolant as it enters the engine before

the coolant pump and before the coolant flow splits to cylinder 1 and cylinder 2.

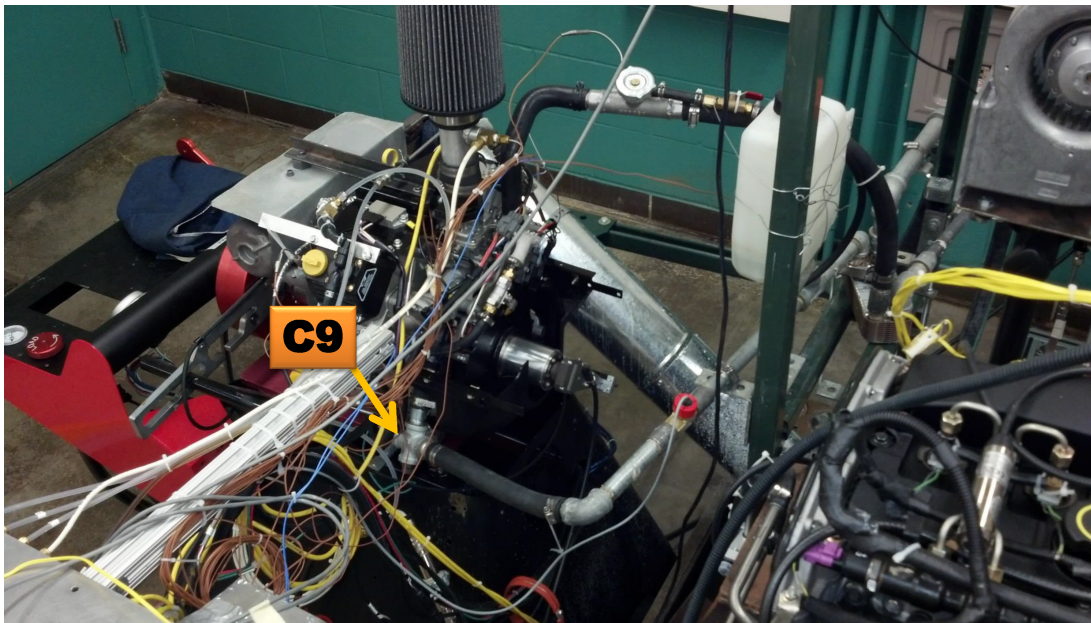


Figure A.4: View 3 of the coolant system

A.2.1.1 Cylinder Walls

The TEG used in this experiment was a stock Seebeck Thermoelectric Generator from the company; Custom Thermoelectric based out of Bishopville, Maryland. The part number for this Seebeck Thermoelectric Generator was 1261G-7L31-04CL. The performance output for this TEG is shown in Figure A.5.

In order to install the TEG and measure the outer cylinder wall temperatures, some machining of the aluminum was required. Figure A.6(a) shows the grooves that were machined that allowed the 1/16 inch diameter thermocouple to be installed in the cylinder

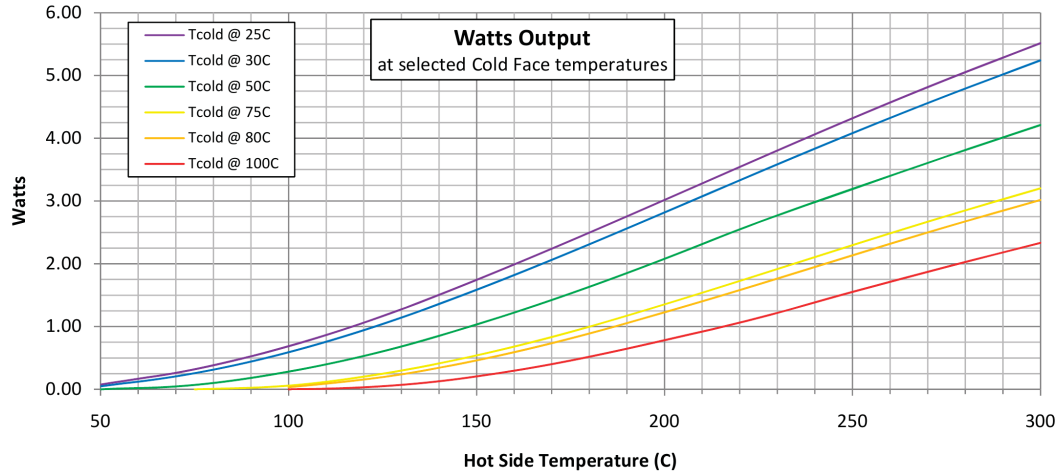
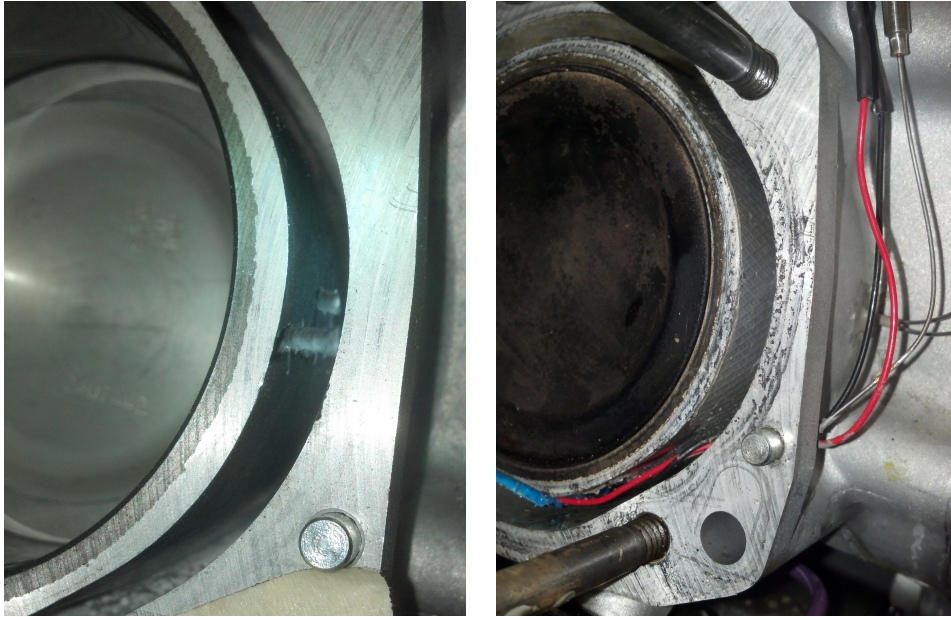


Figure A.5: TEG performance output in Watts over a range of hot and cold-side temperatures [76]

walls. The two thermocouples that were installed on each cylinder were located 3mm and 15mm from the top of the cylinder wall. The thermocouple located 15mm from the top of the cylinder wall was to measure the outer cylinder wall temperature that coincides with the middle of the 30mm tall TEG. This temperature measurement was used for the heat transfer calculation for the "hot-side" wall temperature. The thermocouple located 3mm from the top of the cylinder wall was intended to measure the highest temperature reading. This thermocouple measurement was used as a safety precaution to insure that the TEG surrogate was not being subjected to cylinder wall temperatures above the maximum temperature of 200°C. Figure A.6(b) shows the same cylinder wall location of Figure A.6(a) but after the thermocouples were installed with JB Weld.

The thermocouples were recessed into the cylinder walls to help ensure the TEG surrogate could evenly cover the cylinder walls at the location, as shown in Figure A.7(a). The



(a) Location of thermocouples within cylinder wall (exhaust side) (b) Thermocouples installed with JB Weld

Figure A.6: Cylinder #1 outer wall thermocouple installation

surrogate adhered to the cylinder wall with a thin layer (0.1 – 0.15mm) of JB Weld on the cylinder wall. This technique was performed previously with another type of surrogate material (which did not hold up to testing). The JB Weld was not able to be removed without possible damage done to the cylinder walls, which means there was a previous (0.1 – 0.15 mm) layer of JB Weld. The TEGs were installed with only one layer of JB Weld, shown in Figure A.7(b). One K-Type 1/16 inch diameter thermocouple was adhered at the center location of the TEG. This temperature reading was used in the heat transfer calculation for the "cold-side" coolant temperature.



(a) TEG surrogate (light blue) installed



(b) TEG and TEG thermocouple installed (close up)

Figure A.7: Cylinder #1 TEG and TEG surrogate installation

A.2.1.2 Cold-Junction Compensation

The Land-and-Sea dynamometer data acquisition (DAQ) system was used to measure and record all thermocouple outputs. This DAQ system did not have electronic cold-junction compensation (CJC). The K-type thermocouples plugged into a junction where there is a transition to copper wires connected to the DAQ system. Since thermocouple junctions are created when two dissimilar metals are connected, this arrangement creates two new thermocouple junctions. The system can be calibrated if these junctions are kept at a constant temperature, but that is not a realistic situation in a laboratory setting. Therefore, the junctions between the copper wires and the K-type thermocouples were connected at



Figure A.8: Terminal block of the K-type thermocouple to copper wire connections. Bag is filled with a dielectric fluid.

terminal blocks, which were submerged in an ice water bath to maintain a constant junction temperature. Figure A.8 shows that the terminal blocks were first placed in a plastic bag, which was filled with a dielectric fluid (vegetable oil), then submerged in an ice bath. This was done to isolate the electric current from the individual thermocouples. Once the terminal block is allowed sufficient time (approximately 30 minutes) to acclimate to the ice water temperature, the calibrated junctions provided repeatable temperature measurements.

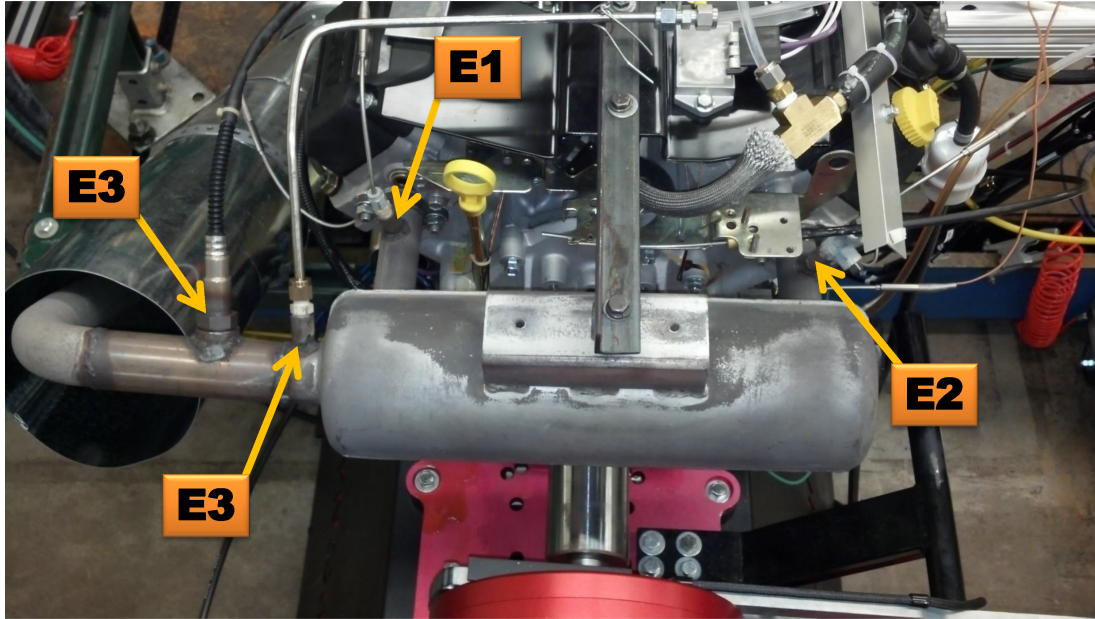


Figure A.9: Exhaust system schematic

A.2.2 Exhaust System

E1 and E2 (Figure A.9) The exhaust gas temperature, 35mm downstream the exhaust valve, was measured with two K-type thermocouples. These temperature measurements were used to determine the available useful energy that is expelled from each cylinder into the exhaust system. (E1 location measures EGT1, E2 location measures EGT2)

E3 (Figure A.9) The electrochemical oxygen sensor with a product name of Powerdex AFX Air-Fuel Monitor, was used to measure equivalent ratio. The actual sensor was an NTK wide-band oxygen sensor. This transducer, which is shown in Figure A.9, has the ability to determine the equivalent ratio from 0.62 to 1.10. It has an

uncertainty of 0.1 AFR.

E4 (Figure A.9) Exhaust pressure measurement with a static pressure transducer capable of measuring 0 – 30psia.

A.2.3 Mechanical System

The specification on the dynamometer is shown in Table A.2.

M1 (Figure A.3) The crank angle encoder that was from AVL and the part number of AVL 356C. The maximum engine speed that the product can measure is 20,000 RPM. The operational temperature range was –400 to 700°C for the electronics and -400 to +1200°C for the mechanics and optics. The selectable output per revolution was 3600, 1800, 720,... 36. [78]

M2 (Figure A.3) AVL In-Cylinder Pressure Transducer had a part number of AVL GH13Z-24. The operating temperature range was –40 to 400 °C and had a pressure range of 250 bar. The cyclic temperature drift was $< \pm 0.5$ bar. The natural frequency was 115 kHz. The sensitivity was 16 pC/bar and the thermal sensitivity change was $\leq 2\%$ at 20 to 400°C and $\leq \pm 0.5\%$ at 20 to 400°C. [78]

Table A.2
9" water brake dynamometer information [77]

Part #	Part	Description
430 – 341	DYNOMite-Pro DAQ	Advanced, precision, 16-bit 28-channel capable data-acquisition computer and power supply for integration (via DYNO-MAX) into sophisticated engine and chassis dynamometer systems (or other custom applications). Internally samples RPM (and optional full-bridge torque transducer) at up to 1,000Hz
430 – 310	Auto Load Servo	Provides convenient one-hand for (throttle) operation during dynamometer test sessions. Input your sweep rate and holding RPM, give it the throttle, and let the computer take over loading the engine - automatically!
425 – 280	28-channel Data Harness	Allows the DYNOMite Pro 28-channel data-acquisition computer to record EGT, fuel-flow, pressures, etc. and control other advanced functions when used with appropriate sensors, controls, and/or software upgrades.
430 – 465	Weather Station Module	For automatic entry of air temperature, barometric pressure, and relative humidity atmospheric conditions when the TEST button is pressed. (Requires Full-Function Cable part #425 – 250 and current EPROM update).
430 – 137	Dyno Rotor RPM Pick-up Kit	These kits include a screw in pickup that feeds a square-wave RPM signal into the DYNOMite data-acquisition computer's jackshaft RPM channel. (fits 9" absorbers)
430 – 343	Toroid 7 & 9" P/U Kit	
709 – 011	9" Torque Arm	
801 – 200	DYNO-MAX 2010 Software	Standard-version data-acquisition software for integrating a 64-bit (or 32-bit) Windows 7 (Vista, or XP)-equipped PC with the DYNOMite computer. Features: multiple environments, graphing, dampening, etc. (Does not include formula editor, overlaying, report designer, import/export, and many other advanced-configuration features.)

A.3 Oil Analysis

Oil Analyzers, Inc. performed oil analysis on two oil samples. The engine was broken in with new oil and a new oil filter for approximately 60 hours before any baseline testing was performed. This was done to properly seat the piston rings on the inner cylinder walls, which increases the stability of the engine performance and fuel conversion efficiency. Both the baseline testing and the TEG testing were completed in approximately 42 hours each with freshly changed oil and oil filter. The oil analysis focused on five categories; wear metals, contaminant metals, multi-source metals, additive metals, contaminants, and fluid properties. The wear metals included iron, chromium, nickel, aluminum, copper, lead, tin, cadmium, silver, and vanadium. For both oil samples, all the wear metal reports were rated to be at normal levels. It should be noted that the amount (ppm) of each wear metal was reduced with the TEG testing and that could have been caused by the engine still being broken in during baseline testing even though 60 hours of break-in time was accumulated. The contaminant metals include silicon, sodium, and potassium. All were within normal levels for both tests except for the potassium reading which went from 2 ppm for the baseline oil to 27 ppm for the TEG oil, which was flagged with 1 out of 4 for a severity issue. The potassium source was most likely from coolant. The engine was required to be opened multiple times during the testing period and some coolant could have introduced to the oil inadvertently. The multi-source metals include titanium, molybdenum, antimony, manganese, lithium, and boron. All multi-source metals were within normal

levels. The additive metals include magnesium, calcium, barium, phosphorous, and zinc which were all within normal levels. The contaminants include fuel dilution, soot, and water. While all levels were normal, a minor amount of fuel dilution was flagged with a 1 out of 4 for a severity issue during the baseline testing. Fuel dilution is when raw, unburned fuel ends up in the crankcase. This will lower the oil's viscosity and flash point, which can result in increased friction. The report suggested that the cause could have been from excessive idling but if the piston rings were not fully seated at the beginning of the baseline testing, small amounts of unburned fuel could have blown by the piston rings. The fluid properties of the oil include viscosity at 40°C, viscosity at 100°C, acid number, base number, oxidation, and nitration. All the fluid properties were within normal levels. The viscosity at 100°C becomes interesting due to the previous levels of fuel dilution. The baseline oil viscosity was 8.7% less than the TEG oil viscosity. It is important to note that the oxidation number and nitration number did not change between the two tests. The oxidation number measures the breakdown of the lubricant and nitration levels, which would have indicated excessive blow-by from between the cylinder walls and compression rings. One of the concerns of installing the TEG / TEG surrogates was that the increased cylinder wall temperature could have distorted the cylinders. The consistent levels of nitrogen indicate that cylinder wall distortion did not occur due to the lack of blow-by constituents in the oil.

WHR Sensor Layout

Updated: April 25, 2013

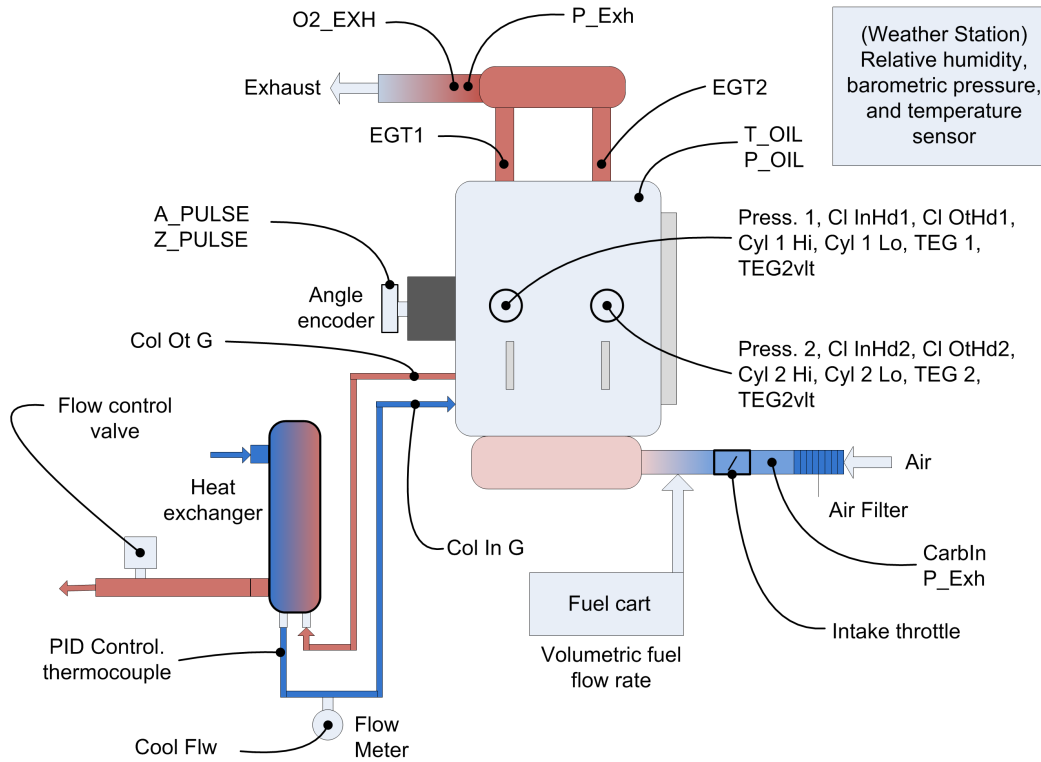


Figure A.10: Transducer locations

A.4 Test Variable Nomenclature / Data

A schematic of the transducers can be seen in Figure A.10. The nomenclature for the variable names are explained below.

Mode The mode number of the experiment that coincides with the engine speed and engine load, seen in Table A.3.

Hold Spd (Hold Speed) The desired engine speed of the testing mode.

Table A.3

Engine testing mode numbers and the corresponding engine speed and load

Engine Speed (RPM)	Mode #	Engine Load (Nm)	Mode #	Engine Load (Nm)
3600	1	40	5	20
3000	2	40	6	20
2400	3	40	7	20
1800	4	40	8	20

Eng Spd (Engine Speed) The measured engine speed using the magnetic pick-up on the dynamometer.

Throttle (%) The throttle position from 0 – 100%.

Hold Trq (N-m) (Hold Torque (Nm)) The desired engine load of the testing mode.

Tq Obs (ft-lb) (Torque Observed (ft-lb)) The measured engine torque from the dynamometer strain gage.

Tq Obs (N-m) (Torque Observed (N-m)) The measured engine torque from the dynamometer strain gage.

Pwr Obs (Hp) (Power Observed (Hp)) The measured engine power by the dynamometer.

Pwr Obs (kW) (Power Observed (kW)) The measured engine power by the dynamometer.

SAE-Fact (Factor) (SAE Factor) The correction factor used to adjust the torque and power from the engine with a standard density of air. This is used for repeatability in different ambient environments.

Trq Corr (ft-lb) (Torque Corrected (ft-lb)) The corrected engine torque from the observed engine torque.

Trq Corr (N-m) (Torque Corrected (N-m)) The corrected engine torque from the observed engine torque.

Pwr Corr (Hp) (Power Corrected (Hp)) The corrected engine power from the observed engine power.

Pwr Corr (kW) (Power Observed (kW)) The corrected engine power from the observed engine power.

CarbIn (Degree C) (Carburetor In (Degree C)) The thermocouple temperature measurement of the inlet air 150mm upstream of the carburetor.

P CarbIn (PSI) (Pressure Carburetor In (psi)) The static pressure measurement of the inlet air 150mm upstream of the carburetor.

EGT1 (Degree C) (Exhaust Gas Temperature 1 (Degree C)] The exhaust gas temperature of cylinder 1. The thermocouple was installed 35mm downstream of the exhaust valve.

EGT2 (Degree C) (Exhaust Gas Temperature 2 (Degree C)] The exhaust gas temperature of cylinder 2. The thermocouple was installed 35mm downstream of the exhaust valve.

P Exh (PSI) (Pressure Exhaust (PSI)) The exhaust gas pressure measurement.

Col In G (Degree C) (Coolant In Global (Degree C)) The coolant temperature entering the engine.

Col Ot G (Degree C) (Coolant Out Global (Degree C)) The coolant temperature exiting the engine.

Cl InHd1 (Degree C) (Coolant In Head 1 (Degree C)) The coolant temperature exiting the water-jacket and entering the cylinder head in cylinder #1.

Cl InHd2 (Degree C) (Coolant In Head 2 (Degree C)) The coolant temperature exiting the water-jacket and entering the cylinder head in cylinder #2.

Cl OtHd1 (Degree C) (Coolant Out Head 1 (Degree C)) The coolant temperature exiting cylinder #1 head.

Cl OtHd2 (Degree C) (Coolant Out Head 2 (Degree C)) The coolant temperature exiting cylinder #2 head.

Cyl 1 Hi (Degree C) (Cylinder 1 High (Degree C)) The exhaust-side cylinder wall temperature measurement located 3mm down from the top of the cylinder.

Cyl 2 Hi (Degree C) (Cylinder 2 High (Degree C)) The exhaust-side cylinder wall temperature measurement located 3mm down from the top of the cylinder.

Cyl 1 Lo (Degree C) (Cylinder 1 Low (Degree C)) The exhaust-side cylinder wall temperature measurement located 15mm down from the top of the cylinder.

Cyl 2 Lo (Degree C) (Cylinder 2 Low (Degree C)) The exhaust-side cylinder wall temperature measurement located 15mm down from the top of the cylinder.

TEG 1 (Degree C) Thermocouple temperature measurement located at the center of the 30mm X 30mm TEG on cylinder 1.

TEG 2 (Degree C) Thermocouple temperature measurement located at the center of the 30mm X 30mm TEG on cylinder 2.

Oil (Degree C) The oil temperature measurement located after the oil pump and before the oil filter.

P-Oil (PSI) (Pressure Oil (PSI)) The oil pressure measurement located after the oil pump and before the oil filter.

TEG1vlt (Volts) (TEG 1 Volt (Volts)) The voltage output from TEG located on cylinder #1.

TEG2vlt (Volts) (TEG 2 Volt (Volts)) The voltage output from TEG located on cylinder #2.

P Fuel (PSI) (Pressure Fuel (PSI)) The absolute fuel pressure after the OEM fuel pump and before the carburetor.

Fuel Flw (kg/h) (Fuel Flow (kg/h)) The mass flow rate of the fuel measured by the fuel cart.

BSFC (g/kWh) (Brake Specific Fuel Consumption (g/kWh)) Mass flow rate of fuel divided by the uncorrected power output of the engine.

Lambda An electrochemical oxygen sensor was used to measure relative air/fuel ratio, λ .

AFR (Air Fuel Ratio) Calculated within dynamometer software with λ and stoichiometric properties of the fuel.

M Air (kg/h) (Mass Air (kg/h)) The mass flow rate of the incoming air which was calculated using the fuel flow rate and air fuel ratio.

BMEP WHR (Bar) (Brake Mean Effective Pressure Waste Heat Recovery (Bar)) The brake work per cycle divided by the engine displacement per cycle.

Ambient (Degree C) The ambient air temperature measured with the weather station. The weather station was located 1 foot above the engine to determine the thermodynamic properties of the incoming air. This data was used to calculate the SAE correction factor.

Baro (mBar) (Barometric Pressure (mBar)) The barometric pressure measurement from the weather station.

Humid (%) (Humidity (%)) The relative humidity measurement from the weather station.

P-Fuel-I (PSI) (Pressure Fuel Inlet (PSI)) The fuel pressure supplied from the fuel cart to the engine fuel pump. Fuel pressure supply was set at 1.5psig.

SPEED (rpm) The engine speed measured by the AVL 365C shaft encoder.

IMEPH1 (bar) The gross indicated mean effective pressure for cylinder #1.

IMEPH2 (bar) The gross indicated mean effective pressure for cylinder #2.

IMEPL1 (bar) The pumping indicated mean effective pressure for cylinder #1.

IMEPL2 (bar) The pumping indicated mean effective pressure for cylinder #2.

IMEP1 (bar) The net indicated mean effective pressure for cylinder #1.

IMEP2 (bar) The net indicated mean effective pressure for cylinder #2.

COVIMEP1 (%) The coefficient of variation in the 300 engine cycles of the indicated mean effective pressure for cylinder #1.

COVIMEP2 (%) The coefficient of variation in the 300 engine cycles of the indicated mean effective pressure for cylinder #2.

PMAX1 (bar) The maximum pressure for cylinder #1.

PMAX2 (bar) The maximum pressure for cylinder #2.

APMAX1 (deg) The crank angle degree of the maximum pressure for cylinder #1.

APMAX2 (deg) The crank angle degree of the maximum pressure for cylinder #2.

RMAX1 (bar/deg) The maximum rate of pressure rise for cylinder #1.

RMAX2 (bar/deg) The maximum rate of pressure rise for cylinder #2.

ARMAX1 (deg) The crank angle degree location of the maximum rate of pressure rise for cylinder #1.

ARMAX2 (deg) The crank angle degree location of the maximum rate of pressure rise for cylinder #2.

MFB10-1 (deg) (Mass Fraction Burned 10% Cylinder #1) Crank angle location where 10% of the fuel's cumulative heat is released in cylinder #1.

MFB10-2 (deg) (Mass Fraction Burned 10% Cylinder #2) Crank angle location where 10% of the fuel's cumulative heat is released in cylinder #2.

MFB50-1 (deg) (Mass Fraction Burned 50% Cylinder #1) Crank angle location where 50% of the fuel's cumulative heat is released in cylinder #1.

MFB50-2 (deg) (Mass Fraction Burned 50% Cylinder #2) Crank angle location where 50% of the fuel's cumulative heat is released in cylinder #2.

MFB90-1 (deg) (Mass Fraction Burned 90% Cylinder #1) Crank angle location where 90% of the fuel's cumulative heat is released in cylinder #1.

MFB90-2 (deg) (Mass Fraction Burned 90% Cylinder #2) Crank angle location where 90% of the fuel's cumulative heat is released in cylinder #2.

D10 – 90-1 (deg) (Difference 10% – 90% Cylinder #1) Total crank angle degrees between 10% mass fraction burned and 90% mass fraction burned for cylinder #1.

D10 – 90-2 (deg) (Difference 10% – 90% Cylinder #2) Total crank angle degrees between 10% mass fraction burned and 90% mass fraction burned for cylinder #2.

A.4.1 Raw Data Statistics

The following sixteen pages include the statistical data from all the outputs (calibrated transducer data and software calculations) for both the baseline and TEG testing.

Results for: BL - Mode 1

Descriptive Statistics:

Variable	Mean	StDev	CoefVar	Minimum	Maximum	Range	Skewness	Kurtosis
Mode	1.0000	0.000000	0.00	1.0000	1.0000	0.000000	*	*
Hold Spd	3600.0	0.000000	0.00	3600.0	3600.0	0.000000	*	*
Eng Spd (RPM)	3601.1	0.805	0.02	3599.5	3602.9	3.36	0.15	-0.33
Throttle (%)	84.081	2.433	2.89	80.635	90.155	9.519	0.87	0.51
Hold Trq (N-m)	40.000	0.000000	0.00	40.000	40.000	0.000000	*	*
Tq Obs (ft-lb)	29.486	0.0379	0.13	29.421	29.563	0.141	0.22	-0.49
Tq Obs (N-m)	39.977	0.0515	0.13	39.890	40.082	0.192	0.23	-0.48
Pwr Obs (Hp)	20.217	0.0265	0.13	20.171	20.265	0.0932	0.12	-0.80
Pwr Obs (kW)	15.076	0.0198	0.13	15.042	15.111	0.0695	0.13	-0.80
SAE-Fact (Factor)	1.0010	0.00976	0.97	0.9790	1.0240	0.0450	0.04	0.64
Trq Corr (ft-lb)	29.486	0.0379	0.13	29.421	29.563	0.141	0.22	-0.49
Trq Corr (N-m)	39.977	0.0515	0.13	39.890	40.082	0.192	0.23	-0.48
Pwr Corr (Hp)	20.217	0.0265	0.13	20.171	20.265	0.0932	0.12	-0.80
Pwr Corr (kW)	15.076	0.0198	0.13	15.042	15.111	0.0695	0.13	-0.80
CarbIn (Degree C)	26.160	2.770	10.59	19.980	32.783	12.804	-0.49	1.33
P_CarbIn (PSI)	14.512	0.0847	0.58	14.339	14.627	0.288	-1.06	-0.05
EGT1 (Degree C)	711.29	5.86	0.82	700.92	718.30	17.38	-0.49	-1.30
EGT2 (Degree C)	737.31	6.18	0.84	723.33	744.24	20.91	-1.19	0.33
P_Exh (PSI)	14.801	0.0766	0.52	14.633	14.931	0.298	-0.48	-0.25
Col In G (Degree C)	89.667	1.160	1.29	87.557	91.800	4.243	0.21	-0.79
Col Ot G (Degree C)	98.108	1.231	1.25	95.667	100.073	4.406	0.11	-0.79
Cool Flw (gal/min)	3.8518	0.1457	3.78	3.6645	4.2362	0.5717	0.71	0.27
Cl InHd1 (Degree C)	99.377	1.148	1.15	97.017	101.487	4.470	0.09	-0.54
Cl InHd2 (Degree C)	97.540	1.191	1.22	95.115	99.570	4.455	0.05	-0.64
Cl OtHd1 (Degree C)	98.084	1.244	1.27	95.549	100.221	4.672	0.05	-0.66
Cl OtHd2 (Degree C)	99.060	1.303	1.32	96.369	101.224	4.855	0.04	-0.62
Cyl 1 Hi (Degree C)	116.75	0.727	0.62	115.71	117.95	2.23	0.15	-1.28
Cyl 2 Hi (Degree C)	103.90	1.62	1.56	99.96	106.35	6.38	-0.98	0.58
Cyl 1 Lo (Degree C)	111.99	0.885	0.79	110.22	113.53	3.31	-0.09	-0.59
Cyl 2 Lo (Degree C)	114.36	0.953	0.83	112.47	116.01	3.54	-0.33	-0.67
TEG 1 (Degree C)	-0.291	0.779	-267.98	-1.121	2.987	4.109	3.21	13.54
TEG 2 (Degree C)	0.5242	0.4072	77.68	-0.3508	1.2055	1.5564	-0.45	-0.45
Oil (Degree C)	119.90	0.965	0.80	117.61	121.47	3.86	-0.29	-0.25
P_Oil (PSI)	41.684	0.338	0.81	40.893	42.327	1.434	0.09	-0.02
TEG1vlt (Volts)	0.000000	0.000000	*	0.000000	0.000000	0.000000	*	*
TEG2vlt (Volts)	0.000000	0.000000	*	0.000000	0.000000	0.000000	*	*
P_Fuel (PSI)	17.139	0.181	1.06	16.569	17.418	0.850	-1.28	2.90
Fuel Flw (kg/h)	6.2382	0.1168	1.87	6.0797	6.5093	0.4296	0.89	0.12
BSFC (g/kWh)	413.85	7.61	1.84	404.20	431.98	27.78	1.03	0.39
Lambda	0.70900	0.00775	1.09	0.69376	0.72061	0.02685	-0.57	-0.60
AFR	10.332	0.112	1.08	10.113	10.501	0.389	-0.59	-0.67
M_Air (kg/h)	64.442	0.541	0.84	63.803	65.825	2.021	1.03	0.74
BMEP_WHR (Bar)	7.4605	0.00938	0.13	7.4420	7.4812	0.0392	0.05	-0.13
Ambient (Degree C)	25.629	3.135	12.23	20.285	37.164	16.878	1.72	7.38
Baro (mBar)	998.91	5.17	0.52	988.53	1006.02	17.49	-0.79	-0.13
Humid (%)	25.710	2.943	11.45	20.767	30.524	9.757	0.24	-1.05
P_Fuel_I (PSI)	1.5059	0.0195	1.30	1.4633	1.5421	0.0789	-0.22	-0.55
SPEED (rpm)	3602.2	1.81	0.05	3598.6	3605.6	6.97	0.21	-0.03
IMEPH1 (bar)	8.7071	0.0706	0.81	8.6066	8.8591	0.2525	0.55	-0.42
IMEPH2 (bar)	8.9919	0.0463	0.51	8.9056	9.0955	0.1899	0.41	-0.12
IMEPL1 (bar)	-0.61901	0.00183	-0.30	-0.62317	-0.61452	0.00865	-0.15	1.08
IMEPL2 (bar)	-0.58889	0.00311	-0.53	-0.59358	-0.58248	0.01110	0.25	-0.99
IMEP1 (bar)	8.0911	0.0703	0.87	7.9927	8.2427	0.2500	0.55	-0.44
IMEP2 (bar)	8.4060	0.0457	0.54	8.3162	8.5070	0.1909	0.30	-0.14
COVIMEP1 (%)	4.4441	0.3240	7.29	3.8753	5.0772	1.2019	0.08	-0.61
COVIMEP2 (%)	3.9209	0.3053	7.79	3.4693	4.6047	1.1354	0.61	-0.13
PMAX1 (bar)	27.805	0.609	2.19	26.653	28.821	2.168	-0.23	-0.81
PMAX2 (bar)	29.251	0.507	1.73	28.419	30.302	1.883	0.24	-0.75
APMAX1 (deg)	23.238	0.424	1.82	22.497	23.927	1.430	-0.10	-1.09
APMAX2 (deg)	24.337	0.281	1.15	23.750	24.770	1.020	-0.51	-0.46
RMAX1 (bar/deg)	0.66494	0.03608	5.43	0.60047	0.73078	0.13031	-0.03	-0.88
RMAX2 (bar/deg)	0.69398	0.02705	3.90	0.65375	0.74920	0.09545	0.23	-0.81
ARMAX1 (deg)	3.3544	0.4476	13.34	2.5733	4.2500	1.6767	0.25	-0.60
ARMAX2 (deg)	4.4715	0.4872	10.90	3.2500	5.8833	2.6333	0.12	3.48
MFB10_1 (deg)	3.0290	0.2916	9.63	2.5158	3.6608	1.1450	0.34	-0.33
MFB10_2 (deg)	3.0828	0.1993	6.47	2.7858	3.4408	0.6550	0.21	-1.03
MFB50_1 (deg)	21.138	0.656	3.10	20.128	22.558	2.429	0.45	-0.55
MFB50_2 (deg)	20.306	0.484	2.39	19.592	21.343	1.751	0.41	-0.68
MFB90_1 (deg)	40.554	0.942	2.32	38.927	42.552	3.625	0.25	-0.64
MFB90_2 (deg)	37.514	0.820	2.19	36.257	39.643	3.387	0.58	0.29
D10-90_1 (deg)	37.525	0.701	1.87	36.347	38.891	2.544	0.06	-0.90
D10-90_2 (deg)	34.431	0.653	1.90	33.407	36.252	2.844	0.70	1.01

Results for: BL - Mode 2

Descriptive Statistics:

Variable	Mean	StDev	CoefVar	Minimum	Maximum	Range	Skewness	Kurtosis
Mode	2.0000	0.000000	0.00	2.0000	2.0000	0.000000	*	*
Hold Spd	3000.0	0.000000	0.00	3000.0	3000.0	0.000000	*	*
Eng Spd (RPM)	3000.2	0.989	0.03	2998.4	3002.3	3.88	0.34	0.11
Throttle (%)	66.509	1.677	2.52	63.903	70.189	6.287	0.68	0.06
Hold Trq (N-m)	40.000	0.000000	0.00	40.000	40.000	0.000000	*	*
Tq Obs (ft-lb)	29.501	0.0438	0.15	29.427	29.641	0.214	1.03	3.26
Tq Obs (N-m)	39.998	0.0593	0.15	39.898	40.188	0.290	1.04	3.31
Pwr Obs (Hp)	16.852	0.0237	0.14	16.812	16.926	0.114	0.99	2.78
Pwr Obs (kW)	12.566	0.0176	0.14	12.537	12.622	0.0851	1.02	2.92
SAE-Fact (Factor)	1.0010	0.00976	0.97	0.9790	1.0240	0.0450	0.04	0.64
Trq Corr (ft-lb)	29.501	0.0438	0.15	29.427	29.641	0.214	1.03	3.26
Trq Corr (N-m)	39.998	0.0593	0.15	39.898	40.188	0.290	1.04	3.31
Pwr Corr (Hp)	16.852	0.0237	0.14	16.812	16.926	0.114	0.99	2.78
Pwr Corr (kW)	12.566	0.0176	0.14	12.537	12.622	0.0851	1.02	2.92
CarbIn (Degree C)	25.682	2.743	10.68	16.202	30.623	14.421	-1.88	5.77
P_CarbIn (PSI)	14.526	0.0819	0.56	14.365	14.636	0.271	-0.86	-0.37
EGT1 (Degree C)	696.08	2.76	0.40	690.47	701.52	11.05	0.28	-0.25
EGT2 (Degree C)	733.21	10.24	1.40	712.88	756.67	43.78	-0.04	0.06
P_Exh (PSI)	14.744	0.0814	0.55	14.584	14.880	0.296	-0.50	-0.22
Col In G (Degree C)	89.606	1.112	1.24	87.802	92.071	4.269	0.17	-0.35
Col Ot G (Degree C)	97.946	1.142	1.17	95.879	100.172	4.292	-0.02	-0.48
Cool Flw (gal/min)	3.6605	0.1584	4.33	3.4537	4.0121	0.5584	0.90	-0.04
Cl InHd1 (Degree C)	99.304	1.071	1.08	97.357	101.396	4.038	-0.06	-0.47
Cl InHd2 (Degree C)	97.676	1.070	1.10	95.752	99.788	4.036	0.10	-0.52
Cl OtHd1 (Degree C)	97.829	1.170	1.20	95.714	100.136	4.422	-0.04	-0.50
Cl OtHd2 (Degree C)	98.772	1.194	1.21	96.493	101.086	4.593	-0.04	-0.35
Cyl 1 Hi (Degree C)	116.13	0.705	0.61	114.65	117.13	2.48	-0.37	-0.69
Cyl 2 Hi (Degree C)	103.93	1.93	1.86	100.13	108.54	8.40	0.02	0.37
Cyl 1 Lo (Degree C)	111.24	0.744	0.67	109.68	112.42	2.74	-0.30	-0.50
Cyl 2 Lo (Degree C)	113.29	0.728	0.64	111.70	114.50	2.80	-0.30	-0.48
TEG 1 (Degree C)	-0.284	0.835	-293.65	-1.167	3.266	4.433	3.32	14.24
TEG 2 (Degree C)	0.5400	0.4017	74.39	-0.2000	1.3994	1.5994	0.15	-0.62
Oil (Degree C)	118.46	1.05	0.89	116.63	120.36	3.73	0.15	-1.00
P_Oil (PSI)	39.819	0.268	0.67	39.297	40.499	1.202	0.61	0.70
TEG1vlt (Volts)	0.000000	0.000000	*	0.000000	0.000000	0.000000	*	*
TEG2vlt (Volts)	0.000000	0.000000	*	0.000000	0.000000	0.000000	*	*
P_Fuel (PSI)	17.577	0.264	1.50	16.830	17.932	1.102	-1.10	1.49
Fuel Flw (kg/h)	4.3496	0.1038	2.39	4.1567	4.5889	0.4322	0.33	0.02
BSFC (g/kWh)	346.16	8.11	2.34	331.51	364.64	33.13	0.33	-0.10
Lambda	0.77987	0.01027	1.32	0.76167	0.80400	0.04233	0.33	-0.25
AFR	11.363	0.149	1.32	11.103	11.712	0.609	0.33	-0.31
M_Air (kg/h)	49.407	0.581	1.18	48.510	50.950	2.440	0.87	0.99
BMEP_WHR (Bar)	7.4638	0.0117	0.16	7.4428	7.5010	0.0582	0.98	3.21
Ambient (Degree C)	25.285	3.239	12.81	17.257	36.521	19.263	0.99	6.71
Baro (mBar)	999.24	5.12	0.51	988.86	1006.45	17.59	-0.78	-0.11
Humid (%)	26.144	2.902	11.10	21.337	30.705	9.369	0.20	-1.29
P_Fuel_I (PSI)	1.5134	0.0181	1.20	1.4800	1.5433	0.0633	-0.00	-1.28
SPEED (rpm)	3001.3	0.656	0.02	3000.2	3002.6	2.36	0.32	-0.79
IMEPH1 (bar)	8.3453	0.0779	0.93	8.2259	8.5505	0.3247	1.15	1.51
IMEPH2 (bar)	8.7696	0.0456	0.52	8.6988	8.8741	0.1754	0.51	0.03
IMEPL1 (bar)	-0.46449	0.00259	-0.56	-0.47096	-0.45827	0.01269	-0.30	1.31
IMEPL2 (bar)	-0.43909	0.00371	-0.84	-0.44389	-0.43275	0.01114	0.36	-1.43
IMEP1 (bar)	7.8838	0.0786	1.00	7.7649	8.0919	0.3270	1.16	1.55
IMEP2 (bar)	8.3336	0.0431	0.52	8.2668	8.4335	0.1667	0.53	0.13
COVIMEP1 (%)	2.6929	0.1690	6.28	2.3833	3.0418	0.6585	-0.11	-0.61
COVIMEP2 (%)	1.9819	0.1374	6.93	1.7498	2.2155	0.4657	0.23	-0.99
P_MAX1 (bar)	28.778	0.383	1.33	28.046	29.533	1.488	0.22	-0.35
P_MAX2 (bar)	32.308	0.404	1.25	31.539	33.089	1.550	-0.05	-0.67
AP_MAX1 (deg)	22.935	0.217	0.94	22.463	23.397	0.933	0.26	-0.02
AP_MAX2 (deg)	22.747	0.290	1.27	22.183	23.217	1.033	-0.27	-1.05
R_MAX1 (bar/deg)	0.73375	0.01708	2.33	0.69918	0.76360	0.06442	-0.35	-0.59
R_MAX2 (bar/deg)	0.88554	0.02373	2.68	0.84184	0.93364	0.09180	0.06	-0.79
AR_MAX1 (deg)	3.3371	0.2942	8.82	2.8733	4.0267	1.1533	0.57	-0.31
AR_MAX2 (deg)	5.4053	0.4851	8.97	4.4933	6.4633	1.9700	0.01	-0.41
MFB10_1 (deg)	1.0589	0.1393	13.16	0.7583	1.3358	0.5775	-0.07	-0.18
MFB10_2 (deg)	0.7270	0.2636	36.26	0.1833	1.0958	0.9125	-0.68	-0.34
MFB50_1 (deg)	17.621	0.287	1.63	16.843	18.167	1.324	-0.40	1.08
MFB50_2 (deg)	15.493	0.382	2.47	14.830	16.173	1.343	0.01	-1.15
MFB90_1 (deg)	33.905	0.521	1.54	32.440	34.703	2.263	-0.79	1.07
MFB90_2 (deg)	28.819	0.614	2.13	27.733	30.046	2.313	0.02	-0.79
D10-90_1 (deg)	32.846	0.449	1.37	31.682	33.368	1.686	-0.69	0.11
D10-90_2 (deg)	28.092	0.518	1.85	27.217	29.083	1.867	-0.17	-0.99

Results for: BL - Mode 3

Descriptive Statistics:

Variable	Mean	StDev	CoefVar	Minimum	Maximum	Range	Skewness	Kurtosis
Mode	3.0000	0.000000	0.00	3.0000	3.0000	0.000000	*	*
Hold Spd	2400.0	0.000000	0.00	2400.0	2400.0	0.000000	*	*
Eng Spd (RPM)	2400.5	1.24	0.05	2398.4	2402.9	4.52	-0.02	-1.02
Throttle (%)	57.377	2.196	3.83	53.538	63.617	10.079	0.78	1.27
Hold Trq (N-m)	40.000	0.000000	0.00	40.000	40.000	0.000000	*	*
Tq Obs (ft-lb)	29.485	0.0344	0.12	29.420	29.548	0.128	0.45	-0.43
Tq Obs (N-m)	39.976	0.0467	0.12	39.887	40.061	0.174	0.44	-0.43
Pwr Obs (Hp)	13.476	0.0154	0.11	13.447	13.507	0.0597	0.25	-0.23
Pwr Obs (kW)	10.049	0.0114	0.11	10.028	10.072	0.0438	0.24	-0.23
SAE-Fact (Factor)	1.0010	0.00976	0.97	0.9790	1.0240	0.0450	0.04	0.64
Trq Corr (ft-lb)	29.485	0.0344	0.12	29.420	29.548	0.128	0.45	-0.43
Trq Corr (N-m)	39.976	0.0467	0.12	39.887	40.061	0.174	0.44	-0.43
Pwr Corr (Hp)	13.476	0.0154	0.11	13.447	13.507	0.0597	0.25	-0.23
Pwr Corr (kW)	10.049	0.0114	0.11	10.028	10.072	0.0438	0.24	-0.23
CarbIn (Degree C)	25.478	2.404	9.44	16.439	27.993	11.554	-2.66	8.33
P_CarbIn (PSI)	14.529	0.0842	0.58	14.356	14.627	0.271	-0.90	-0.25
EGT1 (Degree C)	645.78	3.07	0.47	640.43	651.45	11.02	-0.05	-0.90
EGT2 (Degree C)	685.47	5.24	0.76	675.36	694.84	19.48	0.01	-0.62
P_Exh (PSI)	14.721	0.0857	0.58	14.568	14.875	0.307	-0.33	-0.27
Col In G (Degree C)	89.560	0.779	0.87	88.238	91.238	3.000	0.25	-0.78
Col Ot G (Degree C)	97.710	0.766	0.78	96.510	99.475	2.965	0.29	-0.49
Cool Flw (gal/min)	3.3506	0.0416	1.24	3.2559	3.4335	0.1775	-0.14	0.20
Cl InHd1 (Degree C)	98.963	0.707	0.71	97.732	100.389	2.657	0.01	-0.67
Cl InHd2 (Degree C)	97.735	0.704	0.72	96.602	99.291	2.689	0.34	-0.64
Cl OtHd1 (Degree C)	97.644	0.769	0.79	96.299	99.283	2.983	0.13	-0.65
Cl OtHd2 (Degree C)	98.522	0.773	0.78	97.207	100.282	3.074	0.27	-0.42
Cyl 1 Hi (Degree C)	115.42	0.780	0.68	114.06	116.83	2.77	0.31	-0.62
Cyl 2 Hi (Degree C)	105.30	1.53	1.45	101.83	107.77	5.94	-1.06	0.38
Cyl 1 Lo (Degree C)	110.72	0.789	0.71	109.65	112.31	2.66	0.38	-0.85
Cyl 2 Lo (Degree C)	113.20	0.606	0.54	111.48	113.97	2.50	-1.20	1.80
TEG 1 (Degree C)	-0.202	0.876	-433.89	-1.202	3.613	4.814	3.60	16.04
TEG 2 (Degree C)	0.5480	0.3450	62.96	-0.1011	1.0996	1.2007	-0.27	-0.91
Oil (Degree C)	116.38	0.916	0.79	114.03	117.86	3.83	-0.62	0.29
P_Oil (PSI)	36.650	0.243	0.66	36.131	37.286	1.154	0.50	0.79
TEG1vlt (Volts)	0.000000	0.000000	*	0.000000	0.000000	0.000000	*	*
TEG2vlt (Volts)	0.000000	0.000000	*	0.000000	0.000000	0.000000	*	*
P_Fuel (PSI)	17.801	0.293	1.65	17.071	18.249	1.178	-0.76	0.18
Fuel Flw (kg/h)	3.4535	0.0766	2.22	3.2821	3.6173	0.3352	-0.07	0.11
BSFC (g/kWh)	343.70	7.59	2.21	326.18	359.15	32.97	-0.16	0.08
Lambda	0.78473	0.00835	1.06	0.76916	0.79972	0.03056	0.06	-0.72
AFR	11.434	0.121	1.06	11.199	11.650	0.450	0.02	-0.69
M_Air (kg/h)	39.479	0.568	1.44	38.178	40.510	2.332	-0.54	-0.04
BMEP_WHR (Bar)	7.4578	0.00970	0.13	7.4406	7.4764	0.0358	0.50	-0.48
Ambient (Degree C)	25.378	2.415	9.52	18.662	33.066	14.404	0.07	6.37
Baro (mBar)	999.30	5.03	0.50	988.95	1006.70	17.75	-0.77	-0.07
Humid (%)	26.346	3.105	11.79	21.195	34.400	13.205	0.76	0.23
P_Fuel_I (PSI)	1.5102	0.0219	1.45	1.4691	1.5616	0.0924	0.51	0.32
SPEED (rpm)	2400.4	0.542	0.02	2399.0	2401.2	2.18	-0.52	0.08
IMEPH1 (bar)	8.4425	0.0548	0.65	8.3414	8.5762	0.2349	0.66	0.79
IMEPH2 (bar)	8.7761	0.0482	0.55	8.6899	8.8755	0.1856	0.20	-0.39
IMEPL1 (bar)	-0.34685	0.00212	-0.61	-0.35278	-0.34189	0.01090	-0.36	2.07
IMEPL2 (bar)	-0.34486	0.00238	-0.69	-0.35010	-0.33932	0.01078	0.38	0.44
IMEP1 (bar)	8.0987	0.0556	0.69	7.9976	8.2342	0.2366	0.68	0.76
IMEP2 (bar)	8.4342	0.0481	0.57	8.3505	8.5374	0.1869	0.31	-0.24
COVIMEP1 (%)	1.6940	0.1096	6.47	1.4618	1.9508	0.4890	0.03	0.52
COVIMEP2 (%)	1.1975	0.0872	7.28	1.0736	1.3815	0.3079	0.44	-0.63
PMAX1 (bar)	33.426	0.294	0.88	32.703	33.914	1.211	-0.52	0.15
PMAX2 (bar)	36.420	0.284	0.78	35.779	37.023	1.245	0.03	0.58
APMAX1 (deg)	20.422	0.250	1.22	20.067	20.987	0.920	0.88	0.03
APMAX2 (deg)	19.443	0.229	1.18	19.040	19.963	0.923	0.27	-0.09
RMAX1 (bar/deg)	0.97914	0.01978	2.02	0.93148	1.01294	0.08146	-0.59	-0.06
RMAX2 (bar/deg)	1.1379	0.0206	1.81	1.0909	1.1725	0.0816	-0.48	-0.12
ARMAX1 (deg)	4.6443	0.3245	6.99	4.0367	5.1667	1.1300	0.07	-1.05
ARMAX2 (deg)	4.7259	0.2235	4.73	4.3000	5.2233	0.9233	0.20	-0.35
MFB10_1 (deg)	-1.1566	0.1652	-14.28	-1.4792	-0.8100	0.6692	0.25	0.00
MFB10_2 (deg)	-1.9649	0.1520	-7.74	-2.1942	-1.6825	0.5117	0.05	-1.01
MFB50_1 (deg)	12.960	0.350	2.70	12.445	13.712	1.267	0.92	-0.17
MFB50_2 (deg)	11.325	0.256	2.26	10.910	11.887	0.977	0.14	-0.29
MFB90_1 (deg)	25.820	0.686	2.66	24.911	27.338	2.428	0.99	-0.12
MFB90_2 (deg)	22.846	0.355	1.55	22.325	23.666	1.341	0.32	-0.35
D10-90_1 (deg)	26.976	0.558	2.07	26.162	28.148	1.987	0.90	-0.15
D10-90_2 (deg)	24.811	0.237	0.95	24.443	25.348	0.905	0.39	-0.64

Results for: BL - Mode 4

Descriptive Statistics:

Variable	Mean	StDev	CoefVar	Minimum	Maximum	Range	Skewness	Kurtosis
Mode	4.0000	0.000000	0.00	4.0000	4.0000	0.000000	*	*
Hold Spd	1800.0	0.000000	0.00	1800.0	1800.0	0.000000	*	*
Eng Spd (RPM)	1798.1	0.174	0.01	1797.7	1798.3	0.661	-0.24	-0.19
Throttle (%)	50.228	1.848	3.68	46.334	55.827	9.493	1.09	3.12
Hold Trq (N-m)	40.000	0.000000	0.00	40.000	40.000	0.000000	*	*
Tq Obs (ft-lb)	29.485	0.0355	0.12	29.419	29.566	0.146	0.35	-0.21
Tq Obs (N-m)	39.977	0.0480	0.12	39.888	40.086	0.198	0.35	-0.19
Pwr Obs (Hp)	10.094	0.0125	0.12	10.071	10.123	0.0525	0.33	-0.09
Pwr Obs (kW)	7.5273	0.00918	0.12	7.5101	7.5490	0.0389	0.34	-0.04
SAE-Fact (Factor)	1.0010	0.00976	0.97	0.9790	1.0240	0.0450	0.04	0.64
Trq Corr (ft-lb)	29.485	0.0355	0.12	29.419	29.566	0.146	0.35	-0.21
Trq Corr (N-m)	39.977	0.0480	0.12	39.888	40.086	0.198	0.35	-0.19
Pwr Corr (Hp)	10.094	0.0125	0.12	10.071	10.123	0.0525	0.33	-0.09
Pwr Corr (kW)	7.5273	0.00918	0.12	7.5101	7.5490	0.0389	0.34	-0.04
CarbIn (Degree C)	25.649	2.399	9.35	18.187	29.097	10.910	-2.23	5.46
P_CarbIn (PSI)	14.538	0.0817	0.56	14.374	14.631	0.257	-0.95	-0.26
EGT1 (Degree C)	580.94	2.35	0.41	576.41	585.34	8.93	-0.17	-0.59
EGT2 (Degree C)	618.84	2.59	0.42	614.10	624.40	10.29	0.09	-0.09
P_Exh (PSI)	14.670	0.0693	0.47	14.525	14.780	0.255	-0.40	-0.06
Col In G (Degree C)	89.493	1.177	1.31	86.807	91.604	4.798	-0.02	-0.15
Col Ot G (Degree C)	98.087	1.094	1.12	95.416	99.889	4.473	-0.22	0.10
Cool Flw (gal/min)	2.5473	0.00744	0.29	2.5332	2.5641	0.0310	0.42	0.24
Cl InHd1 (Degree C)	99.204	0.921	0.93	96.868	100.852	3.984	-0.25	0.37
Cl InHd2 (Degree C)	98.421	1.018	1.03	95.927	100.002	4.074	-0.25	-0.01
Cl OtHd1 (Degree C)	98.086	1.063	1.08	95.294	99.948	4.654	-0.27	0.81
Cl OtHd2 (Degree C)	98.947	1.112	1.12	96.219	100.751	4.532	-0.19	0.12
Cyl 1 Hi (Degree C)	115.84	0.873	0.75	113.94	116.98	3.04	-0.72	-0.53
Cyl 2 Hi (Degree C)	107.43	1.53	1.42	103.75	109.99	6.24	-0.54	0.07
Cyl 1 Lo (Degree C)	111.52	0.812	0.73	109.28	112.67	3.39	-0.85	0.82
Cyl 2 Lo (Degree C)	114.13	0.743	0.65	112.50	115.00	2.51	-1.01	0.20
TEG 1 (Degree C)	-0.130	0.914	-701.59	-0.900	3.891	4.791	3.75	16.72
TEG 2 (Degree C)	0.5997	0.3686	61.47	0.0150	1.1811	1.1661	-0.02	-1.28
Oil (Degree C)	114.48	1.15	1.00	112.20	116.07	3.87	-0.33	-0.85
P_Oil (PSI)	31.814	0.422	1.33	30.971	32.802	1.832	0.06	0.47
TEG1vlt (Volts)	0.000000	0.000000	*	0.000000	0.000000	0.000000	*	*
TEG2vlt (Volts)	0.000000	0.000000	*	0.000000	0.000000	0.000000	*	*
P_Fuel (PSI)	18.144	0.254	1.40	17.374	18.461	1.087	-1.27	2.51
Fuel Flw (kg/h)	2.6586	0.0526	1.98	2.5803	2.7700	0.1897	0.46	-0.55
BSFC (g/kWh)	353.19	6.95	1.97	342.79	368.41	25.62	0.50	-0.42
Lambda	0.76678	0.00587	0.77	0.75514	0.77891	0.02377	-0.09	-0.29
AFR	11.171	0.0843	0.75	11.004	11.344	0.340	-0.10	-0.31
M_Air (kg/h)	29.696	0.415	1.40	28.950	30.662	1.712	0.82	0.49
BMEP_WHR (Bar)	7.4557	0.0112	0.15	7.4353	7.4851	0.0498	0.44	0.50
Ambient (Degree C)	25.155	2.237	8.89	18.693	31.435	12.743	-0.66	5.22
Baro (mBar)	999.21	4.89	0.49	988.89	1005.99	17.10	-0.77	-0.04
Humid (%)	26.527	3.468	13.07	22.627	35.646	13.019	1.18	0.92
P_Fuel_I (PSI)	1.5080	0.0222	1.47	1.4634	1.5591	0.0956	0.57	0.40
SPEED (rpm)	1799.2	0.570	0.03	1798.1	1800.3	2.20	-0.32	-0.09
IMEPH1 (bar)	8.2627	0.0539	0.65	8.1989	8.4180	0.2192	1.19	1.28
IMEPH2 (bar)	8.6350	0.0534	0.62	8.5484	8.7902	0.2418	0.91	1.64
IMEPL1 (bar)	-0.24986	0.00388	-1.55	-0.25439	-0.23732	0.01707	1.85	3.96
IMEPL2 (bar)	-0.24575	0.00391	-1.59	-0.25116	-0.23515	0.01600	1.35	2.06
IMEP1 (bar)	8.0159	0.0573	0.71	7.9498	8.1836	0.2338	1.25	1.50
IMEP2 (bar)	8.3923	0.0556	0.66	8.3054	8.5578	0.2525	1.02	1.92
COVIMEP1 (%)	1.3179	0.1161	8.81	1.1150	1.6173	0.5023	0.26	0.57
COVIMEP2 (%)	0.7750	0.0698	9.00	0.6226	0.9282	0.3056	0.00	0.47
PMAX1 (bar)	36.116	0.404	1.12	35.437	36.796	1.359	-0.00	-1.04
PMAX2 (bar)	40.018	0.345	0.86	39.464	40.734	1.270	0.27	-0.63
APMAX1 (deg)	17.858	0.342	1.91	17.320	18.410	1.090	0.18	-1.37
APMAX2 (deg)	16.337	0.374	2.29	15.620	16.983	1.363	-0.42	-0.56
RMAX1 (bar/deg)	1.1775	0.0340	2.89	1.1219	1.2372	0.1153	-0.06	-1.29
RMAX2 (bar/deg)	1.4052	0.0401	2.86	1.3308	1.4825	0.1517	0.33	-0.47
ARMAX1 (deg)	4.4868	0.3694	8.23	3.5700	5.1733	1.6033	-0.44	0.14
ARMAX2 (deg)	3.9395	0.1836	4.66	3.6067	4.3400	0.7333	-0.16	-0.07
MFB10_1 (deg)	-3.0991	0.2468	-7.96	-3.5133	-2.6792	0.8342	0.10	-1.02
MFB10_2 (deg)	-4.3224	0.2124	-4.91	-4.7550	-4.0208	0.7342	-0.65	-0.37
MFB50_1 (deg)	9.9158	0.4370	4.41	9.1950	10.6133	1.4183	0.23	-1.35
MFB50_2 (deg)	7.8543	0.4107	5.23	7.0983	8.5608	1.4625	-0.34	-0.72
MFB90_1 (deg)	21.475	0.848	3.95	20.089	22.851	2.762	0.26	-1.20
MFB90_2 (deg)	18.026	0.589	3.27	16.992	18.874	1.883	-0.30	-0.89
D10-90_1 (deg)	24.574	0.630	2.56	23.367	25.650	2.283	0.14	-0.94
D10-90_2 (deg)	22.349	0.397	1.77	21.687	22.930	1.243	-0.02	-1.12

Results for: BL - Mode 5

Descriptive Statistics:

Variable	Mean	StDev	CoefVar	Minimum	Maximum	Range	Skewness	Kurtosis
Mode	5.0000	0.000000	0.00	5.0000	5.0000	0.000000	*	*
Hold Spd	3600.0	0.000000	0.00	3600.0	3600.0	0.000000	*	*
Eng Spd (RPM)	3601.1	0.383	0.01	3600.5	3602.0	1.54	0.43	0.04
Throttle (%)	37.770	1.561	4.13	34.630	41.906	7.276	0.39	1.25
Hold Trq (N-m)	20.000	0.000000	0.00	20.000	20.000	0.000000	*	*
Tq Obs (ft-lb)	14.737	0.0328	0.22	14.694	14.792	0.0984	0.24	-1.54
Tq Obs (N-m)	19.981	0.0446	0.22	19.922	20.054	0.132	0.24	-1.55
Pwr Obs (Hp)	10.105	0.0221	0.22	10.077	10.142	0.0658	0.26	-1.54
Pwr Obs (kW)	7.5352	0.0167	0.22	7.5141	7.5631	0.0491	0.25	-1.56
SAE-Fact (Factor)	1.0010	0.00976	0.97	0.9790	1.0240	0.0450	0.04	0.64
Trq Corr (ft-lb)	14.737	0.0328	0.22	14.694	14.792	0.0984	0.24	-1.54
Trq Corr (N-m)	19.981	0.0446	0.22	19.922	20.054	0.132	0.24	-1.55
Pwr Corr (Hp)	10.105	0.0221	0.22	10.077	10.142	0.0658	0.26	-1.54
Pwr Corr (kW)	7.5352	0.0167	0.22	7.5141	7.5631	0.0491	0.25	-1.56
CarbIn (Degree C)	26.311	2.525	9.60	18.620	30.563	11.943	-2.02	5.08
P_CarbIn (PSI)	14.536	0.0810	0.56	14.364	14.630	0.266	-0.94	-0.22
EGT1 (Degree C)	862.85	3.71	0.43	854.20	872.18	17.98	0.65	1.94
EGT2 (Degree C)	851.22	4.36	0.51	844.49	862.70	18.21	0.68	0.65
P_Exh (PSI)	14.743	0.0713	0.48	14.596	14.831	0.235	-0.92	-0.23
Col In G (Degree C)	89.887	1.320	1.47	87.896	92.548	4.651	0.62	-0.14
Col Ot G (Degree C)	97.737	1.430	1.46	95.713	100.462	4.750	0.47	-0.66
Cool Flw (gal/min)	3.7731	0.1399	3.71	3.5467	4.0657	0.5191	0.13	-0.76
Cl InHd1 (Degree C)	99.111	1.270	1.28	96.992	101.480	4.487	0.32	-0.53
Cl InHd2 (Degree C)	96.250	1.316	1.37	94.283	98.772	4.489	0.50	-0.49
Cl OtHd1 (Degree C)	97.870	1.457	1.49	95.633	100.671	5.038	0.46	-0.55
Cl OtHd2 (Degree C)	98.164	1.504	1.53	95.934	101.063	5.128	0.49	-0.56
Cyl 1 Hi (Degree C)	115.68	0.686	0.59	114.68	117.06	2.38	0.25	-0.65
Cyl 2 Hi (Degree C)	102.46	1.72	1.68	98.95	105.48	6.53	-0.21	-0.05
Cyl 1 Lo (Degree C)	111.55	0.920	0.83	109.78	113.18	3.40	-0.12	-0.44
Cyl 2 Lo (Degree C)	112.65	0.793	0.70	111.18	114.47	3.30	0.25	0.10
TEG 1 (Degree C)	-0.2469	0.4679	-189.56	-1.3939	1.1244	2.5183	0.34	2.95
TEG 2 (Degree C)	0.6278	0.3673	58.52	-0.3156	1.1206	1.4361	-0.83	0.56
Oil (Degree C)	116.15	1.03	0.89	114.29	118.06	3.77	0.30	-0.81
P_Oil (PSI)	42.445	0.248	0.58	41.886	43.101	1.216	0.29	1.19
TEG1vlt (Volts)	0.000000	0.000000	*	0.000000	0.000000	0.000000	*	*
TEG2vlt (Volts)	0.000000	0.000000	*	0.000000	0.000000	0.000000	*	*
P_Fuel (PSI)	17.892	0.284	1.59	16.948	18.339	1.391	-1.47	4.32
Fuel Flw (kg/h)	3.0113	0.0289	0.96	2.9553	3.0691	0.1138	-0.17	-0.30
BSFC (g/kWh)	399.75	4.09	1.02	391.38	408.39	17.01	-0.23	0.11
Lambda	0.90914	0.00532	0.59	0.89500	0.92155	0.02655	0.18	2.29
AFR	13.246	0.0785	0.59	13.038	13.429	0.391	0.18	2.24
M_Air (kg/h)	39.887	0.432	1.08	39.132	40.833	1.702	0.19	-0.49
BMEP_WHR (Bar)	3.7273	0.00849	0.23	3.7156	3.7406	0.0250	0.26	-1.54
Ambient (Degree C)	26.103	3.254	12.47	19.027	38.958	19.932	2.12	11.19
Baro (mBar)	999.85	4.92	0.49	989.57	1006.53	16.96	-0.82	-0.09
Humid (%)	25.887	2.960	11.44	21.129	31.497	10.368	0.45	-0.93
P_Fuel_I (PSI)	1.4942	0.0123	0.82	1.4698	1.5235	0.0537	0.16	1.19
SPEED (rpm)	3602.9	3.25	0.09	3597.3	3609.1	11.8	-0.08	-0.66
IMEPH1 (bar)	5.2620	0.0366	0.70	5.1877	5.3214	0.1337	-0.24	-0.83
IMEPH2 (bar)	4.7373	0.0585	1.23	4.6676	4.9057	0.2381	1.00	1.42
IMEPL1 (bar)	-0.53053	0.00276	-0.52	-0.53534	-0.52446	0.01088	0.21	-0.28
IMEPL2 (bar)	-0.52238	0.00571	-1.09	-0.52930	-0.50864	0.02066	1.01	0.03
IMEP1 (bar)	4.7345	0.0373	0.79	4.6564	4.7962	0.1398	-0.25	-0.80
IMEP2 (bar)	4.2179	0.0633	1.50	4.1433	4.4000	0.2567	1.05	1.43
COVIMEP1 (%)	8.677	0.526	6.06	7.801	9.674	1.872	0.24	-0.73
COVIMEP2 (%)	8.648	0.529	6.12	7.661	9.839	2.178	0.23	-0.47
PMAX1 (bar)	13.693	0.133	0.97	13.440	13.907	0.467	-0.02	-0.60
PMAX2 (bar)	12.662	0.183	1.44	12.394	13.204	0.810	0.81	1.73
APMAX1 (deg)	22.092	0.541	2.45	20.847	22.917	2.070	-0.56	-0.18
APMAX2 (deg)	20.577	0.567	2.75	19.130	21.820	2.690	-0.17	0.86
RMAX1 (bar/deg)	0.25193	0.00512	2.03	0.24492	0.26274	0.01782	0.64	-0.55
RMAX2 (bar/deg)	0.23035	0.00458	1.99	0.22269	0.23760	0.01491	0.13	-1.16
ARMAX1 (deg)	-13.361	0.802	-6.00	-14.853	-12.133	2.720	0.02	-1.05
ARMAX2 (deg)	-14.708	0.828	-5.63	-16.007	-13.090	2.917	0.10	-0.95
MFB10_1 (deg)	9.2779	0.2989	3.22	8.8125	9.8567	1.0442	0.44	-0.66
MFB10_2 (deg)	8.8802	0.2109	2.37	8.4850	9.2558	0.7708	-0.05	-0.78
MFB50_1 (deg)	33.811	0.534	1.58	33.007	34.840	1.833	0.12	-0.89
MFB50_2 (deg)	33.748	0.629	1.86	32.648	34.904	2.256	0.11	-0.82
MFB90_1 (deg)	58.765	0.921	1.57	57.312	60.875	3.563	0.32	-0.25
MFB90_2 (deg)	59.375	1.073	1.81	57.559	61.647	4.087	0.17	-0.66
D10-90_1 (deg)	49.487	0.762	1.54	48.374	51.318	2.944	0.54	-0.16
D10-90_2 (deg)	50.495	0.923	1.83	49.074	52.682	3.608	0.28	-0.27

Results for: BL - Mode 6

Descriptive Statistics:

Variable	Mean	StDev	CoefVar	Minimum	Maximum	Range	Skewness	Kurtosis
Mode	6.0000	0.000000	0.00	6.0000	6.0000	0.000000	*	*
Hold Spd	3000.0	0.000000	0.00	3000.0	3000.0	0.000000	*	*
Eng Spd (RPM)	3001.1	0.345	0.01	3000.4	3001.7	1.26	-0.30	-0.68
Throttle (%)	29.429	1.462	4.97	26.343	32.452	6.109	-0.16	0.06
Hold Trq (N-m)	20.000	0.000000	0.00	20.000	20.000	0.000000	*	*
Tq Obs (ft-lb)	14.759	0.0343	0.23	14.696	14.812	0.116	-0.11	-0.92
Tq Obs (N-m)	20.010	0.0465	0.23	19.924	20.082	0.158	-0.11	-0.92
Pwr Obs (Hp)	8.4334	0.0196	0.23	8.3970	8.4646	0.0676	-0.14	-0.82
Pwr Obs (kW)	6.2888	0.0147	0.23	6.2617	6.3123	0.0507	-0.12	-0.84
SAE-Fact (Factor)	1.0010	0.00976	0.97	0.9790	1.0240	0.0450	0.04	0.64
Trq Corr (ft-lb)	14.759	0.0343	0.23	14.696	14.812	0.116	-0.11	-0.92
Trq Corr (N-m)	20.010	0.0465	0.23	19.924	20.082	0.158	-0.11	-0.92
Pwr Corr (Hp)	8.4334	0.0196	0.23	8.3970	8.4646	0.0676	-0.14	-0.82
Pwr Corr (kW)	6.2888	0.0147	0.23	6.2617	6.3123	0.0507	-0.12	-0.84
CarbIn (Degree C)	25.155	3.325	13.22	15.752	29.406	13.654	-1.51	1.80
P_CarbIn (PSI)	14.534	0.0868	0.60	14.358	14.658	0.300	-0.79	-0.37
EGT1 (Degree C)	792.11	3.14	0.40	786.52	797.95	11.44	0.01	-1.12
EGT2 (Degree C)	786.56	4.21	0.54	779.12	797.13	18.01	0.54	0.56
P_Exh (PSI)	14.708	0.0809	0.55	14.537	14.843	0.305	-0.65	0.04
Col In G (Degree C)	89.663	0.960	1.07	88.298	91.816	3.517	0.35	-0.62
Col Ot G (Degree C)	96.609	0.997	1.03	94.954	98.686	3.732	0.14	-0.61
Cool Flw (gal/min)	3.6894	0.1526	4.14	3.5016	4.0547	0.5530	1.04	0.27
Cl InHd1 (Degree C)	98.203	0.981	1.00	96.487	100.367	3.881	0.05	-0.29
Cl InHd2 (Degree C)	95.698	0.918	0.96	94.233	97.679	3.447	0.13	-0.47
Cl OtHd1 (Degree C)	96.806	1.025	1.06	95.074	99.209	4.135	0.21	-0.13
Cl OtHd2 (Degree C)	96.879	1.027	1.06	94.979	99.087	4.108	-0.05	-0.22
Cyl 1 Hi (Degree C)	114.42	0.660	0.58	113.10	115.76	2.66	0.04	-0.19
Cyl 2 Hi (Degree C)	102.19	1.90	1.86	100.20	109.49	9.29	2.50	8.58
Cyl 1 Lo (Degree C)	110.39	0.894	0.81	108.57	112.26	3.69	-0.50	0.34
Cyl 2 Lo (Degree C)	110.96	0.599	0.54	109.57	111.82	2.25	-0.65	0.29
TEG 1 (Degree C)	-0.3113	0.3874	-124.45	-1.2539	0.3000	1.5539	-0.68	-0.00
TEG 2 (Degree C)	0.6191	0.3897	62.94	-0.3006	1.1689	1.4694	-0.85	0.50
Oil (Degree C)	113.08	1.17	1.03	110.95	115.40	4.46	0.21	-0.38
P_Oil (PSI)	41.006	0.290	0.71	40.314	41.744	1.430	0.33	1.53
TEG1vlt (Volts)	0.000000	0.000000	*	0.000000	0.000000	0.000000	*	*
TEG2vlt (Volts)	0.000000	0.000000	*	0.000000	0.000000	0.000000	*	*
P_Fuel (PSI)	18.035	0.281	1.56	17.288	18.399	1.111	-1.05	0.73
Fuel Flw (kg/h)	2.4460	0.0204	0.84	2.4018	2.4860	0.0842	-0.21	0.10
BSFC (g/kWh)	389.05	3.41	0.88	381.16	395.92	14.76	0.02	0.49
Lambda	0.88151	0.00605	0.69	0.86796	0.89791	0.02996	0.54	1.51
AFR	12.844	0.0879	0.68	12.651	13.085	0.435	0.60	1.56
M_Air (kg/h)	31.415	0.367	1.17	30.794	32.170	1.376	0.30	-0.71
BMEP_WHR (Bar)	3.7350	0.00887	0.24	3.7171	3.7494	0.0323	-0.23	-0.47
Ambient (Degree C)	24.947	3.866	15.50	15.942	36.964	21.022	0.40	3.91
Baro (mBar)	999.83	4.90	0.49	989.52	1006.71	17.19	-0.76	-0.09
Humid (%)	26.473	3.545	13.39	21.548	35.100	13.551	0.89	0.21
P_Fuel_I (PSI)	1.5128	0.0162	1.07	1.4759	1.5382	0.0623	-0.61	-0.19
SPEED (rpm)	3001.9	1.36	0.05	2999.7	3004.3	4.62	0.43	-0.90
IMEPH1 (bar)	5.2471	0.0273	0.52	5.1947	5.2892	0.0945	0.03	-0.95
IMEPH2 (bar)	4.4251	0.0564	1.28	4.3541	4.5694	0.2154	0.90	0.44
IMEPL1 (bar)	-0.45112	0.00396	-0.88	-0.45896	-0.44175	0.01721	0.28	0.40
IMEPL2 (bar)	-0.48733	0.00626	-1.28	-0.49513	-0.47134	0.02378	1.28	1.38
IMEP1 (bar)	4.7991	0.0274	0.57	4.7449	4.8422	0.0973	-0.11	-1.04
IMEP2 (bar)	3.9408	0.0618	1.57	3.8675	4.1013	0.2338	1.02	0.68
COVIMEP1 (%)	5.7971	0.2605	4.49	5.3329	6.2127	0.8799	-0.24	-1.00
COVIMEP2 (%)	7.369	0.519	7.05	6.036	8.384	2.348	-0.58	1.06
PMAX1 (bar)	14.332	0.175	1.22	13.954	14.617	0.663	-0.36	-0.43
PMAX2 (bar)	12.217	0.169	1.38	12.021	12.723	0.701	1.44	2.51
APMAX1 (deg)	24.055	0.336	1.39	23.317	24.817	1.500	0.10	0.57
APMAX2 (deg)	20.995	0.591	2.82	20.257	22.627	2.370	1.08	1.12
RMAX1 (bar/deg)	0.27121	0.00762	2.81	0.25684	0.28511	0.02827	-0.12	-0.84
RMAX2 (bar/deg)	0.22375	0.00477	2.13	0.21476	0.23075	0.01599	-0.15	-1.43
ARMAX1 (deg)	-5.893	1.027	-17.43	-8.343	-4.233	4.110	-0.78	0.35
ARMAX2 (deg)	-11.953	0.872	-7.30	-13.383	-10.000	3.383	0.33	-0.49
MFB10_1 (deg)	7.1186	0.3722	5.23	6.5425	7.8275	1.2850	0.56	-0.52
MFB10_2 (deg)	7.8148	0.1856	2.37	7.4450	8.3133	0.8683	0.62	1.24
MFB50_1 (deg)	29.349	0.573	1.95	28.237	30.684	2.448	0.45	0.05
MFB50_2 (deg)	31.583	0.553	1.75	30.010	32.370	2.360	-1.02	1.26
MFB90_1 (deg)	51.610	0.903	1.75	49.793	53.654	3.862	0.31	0.17
MFB90_2 (deg)	56.168	1.182	2.11	53.126	58.032	4.906	-0.96	0.64
D10-90_1 (deg)	44.492	0.665	1.50	43.250	45.914	2.664	0.35	-0.07
D10-90_2 (deg)	48.353	1.127	2.33	45.543	50.105	4.562	-0.98	0.55

Results for: BL - Mode 7

Descriptive Statistics:

Variable	Mean	StDev	CoefVar	Minimum	Maximum	Range	Skewness	Kurtosis
Mode	7.0000	0.000000	0.00	7.0000	7.0000	0.000000	*	*
Hold Spd	2400.0	0.000000	0.00	2400.0	2400.0	0.000000	*	*
Eng Spd (RPM)	2401.0	0.455	0.02	2400.2	2401.9	1.69	-0.14	-0.90
Throttle (%)	23.409	1.317	5.63	20.101	25.383	5.282	-0.75	0.15
Hold Trq (N-m)	20.000	0.000000	0.00	20.000	20.000	0.000000	*	*
Tq Obs (ft-lb)	14.745	0.0426	0.29	14.675	14.824	0.149	0.29	-0.87
Tq Obs (N-m)	19.991	0.0579	0.29	19.897	20.100	0.203	0.31	-0.87
Pwr Obs (Hp)	6.7406	0.0190	0.28	6.7099	6.7751	0.0651	0.25	-0.97
Pwr Obs (kW)	5.0265	0.0141	0.28	5.0039	5.0522	0.0483	0.24	-1.00
SAE-Fact (Factor)	1.0010	0.00976	0.97	0.9790	1.0240	0.0450	0.04	0.64
Trq Corr (ft-lb)	14.745	0.0426	0.29	14.675	14.824	0.149	0.29	-0.87
Trq Corr (N-m)	19.991	0.0579	0.29	19.897	20.100	0.203	0.31	-0.87
Pwr Corr (Hp)	6.7406	0.0190	0.28	6.7099	6.7751	0.0651	0.25	-0.97
Pwr Corr (kW)	5.0265	0.0141	0.28	5.0039	5.0522	0.0483	0.24	-1.00
CarbIn (Degree C)	24.541	3.635	14.81	14.450	28.887	14.437	-1.66	1.91
P_CarbIn (PSI)	14.540	0.0830	0.57	14.372	14.657	0.284	-0.95	-0.07
EGT1 (Degree C)	722.65	7.74	1.07	710.77	737.31	26.54	-0.13	-1.23
EGT2 (Degree C)	709.87	6.52	0.92	700.03	721.30	21.28	-0.09	-1.21
P_Exh (PSI)	14.670	0.0749	0.51	14.510	14.779	0.269	-0.76	-0.19
Col In G (Degree C)	89.838	1.117	1.24	87.606	92.138	4.531	-0.35	0.05
Col Ot G (Degree C)	96.100	1.006	1.05	94.092	98.042	3.950	-0.36	-0.09
Cool Flw (gal/min)	3.3871	0.0278	0.82	3.3269	3.4281	0.1012	-0.57	-0.57
Cl InHd1 (Degree C)	97.691	0.995	1.02	95.573	99.641	4.068	-0.16	-0.05
Cl InHd2 (Degree C)	95.577	0.993	1.04	93.459	97.449	3.990	-0.39	-0.01
Cl OtHd1 (Degree C)	96.262	1.056	1.10	94.103	98.294	4.191	-0.21	-0.15
Cl OtHd2 (Degree C)	96.404	1.059	1.10	94.229	98.471	4.242	-0.29	-0.06
Cyl 1 Hi (Degree C)	113.77	0.763	0.67	112.09	115.16	3.07	-0.21	-0.39
Cyl 2 Hi (Degree C)	102.52	1.33	1.30	99.08	104.35	5.27	-0.99	0.72
Cyl 1 Lo (Degree C)	109.31	0.971	0.89	106.91	111.08	4.16	-0.30	0.02
Cyl 2 Lo (Degree C)	111.05	0.568	0.51	109.68	112.05	2.38	-0.53	0.42
TEG 1 (Degree C)	-0.3633	0.4500	-123.88	-1.2494	0.3000	1.5494	-0.52	-0.75
TEG 2 (Degree C)	0.5792	0.4453	76.88	-0.4867	1.1160	1.6027	-0.82	-0.02
Oil (Degree C)	109.18	1.06	0.97	107.38	111.78	4.39	-0.04	0.16
P_Oil (PSI)	38.866	0.396	1.02	37.931	39.706	1.775	-0.06	0.12
TEG1vlt (Volts)	0.000000	0.000000	*	0.000000	0.000000	0.000000	*	*
TEG2vlt (Volts)	0.000000	0.000000	*	0.000000	0.000000	0.000000	*	*
P_Fuel (PSI)	18.140	0.255	1.41	17.653	18.527	0.874	-0.58	-0.84
Fuel Flw (kg/h)	1.9222	0.0487	2.53	1.8683	2.0111	0.1428	0.70	-1.11
BSFC (g/kWh)	382.47	9.65	2.52	370.37	401.91	31.54	0.75	-0.91
Lambda	0.86671	0.01694	1.95	0.84106	0.89370	0.05264	-0.23	-1.38
AFR	12.630	0.246	1.95	12.257	13.023	0.766	-0.23	-1.38
M_Air (kg/h)	24.267	0.406	1.67	23.281	24.964	1.683	-0.77	1.19
BMEP_WHR (Bar)	3.7289	0.00954	0.26	3.7128	3.7500	0.0372	0.49	-0.29
Ambient (Degree C)	24.222	3.746	15.46	14.523	33.770	19.248	-0.57	2.37
Baro (mBar)	999.83	4.89	0.49	989.37	1006.40	17.02	-0.86	-0.01
Humid (%)	26.511	3.529	13.31	21.125	36.360	15.235	0.89	0.79
P_Fuel_I (PSI)	1.5108	0.0138	0.91	1.4809	1.5323	0.0514	-0.48	-0.61
SPEED (rpm)	2401.7	0.485	0.02	2400.8	2402.7	1.93	0.19	-0.29
IMEPH1 (bar)	5.2353	0.0434	0.83	5.1348	5.3368	0.2020	0.01	0.79
IMEPH2 (bar)	4.4307	0.0362	0.82	4.3249	4.4985	0.1737	-0.87	2.37
IMEPL1 (bar)	-0.37698	0.00343	-0.91	-0.38246	-0.36888	0.01358	0.71	0.01
IMEPL2 (bar)	-0.43983	0.00581	-1.32	-0.44645	-0.42576	0.02068	1.06	0.19
IMEP1 (bar)	4.8613	0.0451	0.93	4.7586	4.9710	0.2124	0.12	0.94
IMEP2 (bar)	3.9938	0.0384	0.96	3.8837	4.0633	0.1795	-0.86	1.93
COVIMEP1 (%)	3.8967	0.3045	7.81	3.3145	4.3881	1.0736	-0.16	-0.87
COVIMEP2 (%)	5.4631	0.3281	6.01	4.7508	6.0256	1.2748	-0.32	-0.40
PMAX1 (bar)	15.639	0.241	1.54	15.188	16.107	0.919	0.37	-0.64
PMAX2 (bar)	13.302	0.151	1.13	12.980	13.657	0.677	-0.20	0.97
APMAX1 (deg)	24.589	0.369	1.50	23.720	25.247	1.527	-0.23	0.41
APMAX2 (deg)	22.966	0.375	1.63	22.253	23.717	1.463	0.34	-0.15
RMAX1 (bar/deg)	0.32455	0.00849	2.62	0.31177	0.34254	0.03077	0.60	-0.26
RMAX2 (bar/deg)	0.25699	0.00485	1.89	0.24688	0.26568	0.01881	-0.07	-0.33
ARMAX1 (deg)	0.143	0.567	395.91	-0.970	1.323	2.293	0.10	-0.33
ARMAX2 (deg)	-3.455	0.690	-19.96	-4.760	-2.147	2.613	0.29	-0.45
MFB10_1 (deg)	4.6626	0.2553	5.48	4.2208	5.1967	0.9758	-0.03	-0.63
MFB10_2 (deg)	5.4252	0.1853	3.42	5.0758	5.7442	0.6683	-0.29	-0.61
MFB50_1 (deg)	24.575	0.541	2.20	23.441	25.730	2.289	-0.25	0.06
MFB50_2 (deg)	26.254	0.407	1.55	25.518	26.998	1.481	-0.06	-0.77
MFB90_1 (deg)	44.076	0.972	2.21	42.339	46.523	4.183	0.24	0.48
MFB90_2 (deg)	47.242	0.717	1.52	45.964	48.820	2.856	0.20	-0.37
D10-90_1 (deg)	39.413	0.783	1.99	38.078	41.631	3.553	0.70	1.52
D10-90_2 (deg)	41.816	0.603	1.44	40.750	43.227	2.477	0.31	-0.02

Results for: BL - Mode 8

Descriptive Statistics:

Variable	Mean	StDev	CoefVar	Minimum	Maximum	Range	Skewness	Kurtosis
Mode	8.0000	0.000000	0.00	8.0000	8.0000	0.000000	*	*
Hold Spd	1800.0	0.000000	0.00	1800.0	1800.0	0.000000	*	*
Eng Spd (RPM)	1800.9	0.0796	0.00	1800.7	1801.0	0.334	-0.25	-0.33
Throttle (%)	16.844	1.834	10.89	13.964	20.196	6.232	0.02	-1.00
Hold Trq (N-m)	20.000	0.000000	0.00	20.000	20.000	0.000000	*	*
Tq Obs (ft-lb)	14.762	0.0380	0.26	14.678	14.829	0.151	-0.55	-0.26
Tq Obs (N-m)	20.015	0.0516	0.26	19.900	20.105	0.205	-0.54	-0.27
Pwr Obs (Hp)	5.0619	0.0131	0.26	5.0328	5.0848	0.0520	-0.52	-0.26
Pwr Obs (kW)	3.7747	0.00978	0.26	3.7533	3.7920	0.0387	-0.51	-0.29
SAE-Fact (Factor)	1.0010	0.00976	0.97	0.9790	1.0240	0.0450	0.04	0.64
Trq Corr (ft-lb)	14.762	0.0380	0.26	14.678	14.829	0.151	-0.55	-0.26
Trq Corr (N-m)	20.015	0.0516	0.26	19.900	20.105	0.205	-0.54	-0.27
Pwr Corr (Hp)	5.0619	0.0131	0.26	5.0328	5.0848	0.0520	-0.52	-0.26
Pwr Corr (kW)	3.7747	0.00978	0.26	3.7533	3.7920	0.0387	-0.51	-0.29
CarbIn (Degree C)	25.407	1.712	6.74	21.532	29.303	7.770	-0.65	1.30
P_CarbIn (PSI)	14.547	0.0819	0.56	14.381	14.655	0.274	-0.92	-0.28
EGT1 (Degree C)	627.19	8.14	1.30	614.42	635.71	21.30	-0.39	-1.79
EGT2 (Degree C)	623.23	6.32	1.01	612.87	631.91	19.04	-0.42	-1.49
P_Exh (PSI)	14.636	0.0717	0.49	14.470	14.745	0.275	-0.71	0.18
Col In G (Degree C)	98.926	1.160	1.30	86.856	91.333	4.477	0.66	-0.16
Col Ot G (Degree C)	95.186	1.080	1.13	93.380	97.714	4.334	0.81	0.28
Cool Flw (gal/min)	2.5552	0.00920	0.36	2.5440	2.5769	0.0328	1.07	0.32
Cl InHd1 (Degree C)	97.039	1.059	1.09	95.388	99.562	4.174	0.80	0.35
Cl InHd2 (Degree C)	95.050	1.088	1.14	93.275	97.501	4.225	0.86	0.35
Cl OtHd1 (Degree C)	95.477	1.118	1.17	93.786	98.141	4.355	0.92	0.45
Cl OtHd2 (Degree C)	95.499	1.134	1.19	93.753	98.102	4.349	0.87	0.28
Cyl 1 Hi (Degree C)	112.98	0.975	0.86	111.31	114.86	3.55	0.56	-0.49
Cyl 2 Hi (Degree C)	103.35	1.40	1.36	100.64	105.99	5.35	-0.05	-0.42
Cyl 1 Lo (Degree C)	108.97	1.11	1.02	106.55	111.13	4.59	0.05	-0.03
Cyl 2 Lo (Degree C)	110.47	0.802	0.73	108.77	112.21	3.44	0.03	0.19
TEG 1 (Degree C)	-0.3413	0.4901	-143.61	-1.3000	0.3939	1.6939	-0.35	-1.06
TEG 2 (Degree C)	0.548	0.503	91.70	-0.816	1.155	1.971	-1.13	1.03
Oil (Degree C)	105.41	1.22	1.16	102.15	107.09	4.94	-1.00	0.79
P_Oil (PSI)	35.109	0.565	1.61	33.207	35.927	2.721	-1.55	4.39
TEG1vlt (Volts)	0.000000	0.000000	*	0.000000	0.000000	0.000000	*	*
TEG2vlt (Volts)	0.000000	0.000000	*	0.000000	0.000000	0.000000	*	*
P_Fuel (PSI)	18.334	0.186	1.01	17.844	18.545	0.701	-1.13	1.10
Fuel Flw (kg/h)	1.4785	0.0583	3.95	1.4098	1.5728	0.1630	0.31	-1.72
BSFC (g/kWh)	391.75	15.27	3.90	374.02	418.83	44.82	0.35	-1.63
Lambda	0.82021	0.02198	2.68	0.78955	0.84263	0.05307	-0.32	-1.96
AFR	11.951	0.322	2.69	11.504	12.278	0.774	-0.32	-1.96
M_Air (kg/h)	17.652	0.276	1.57	17.194	18.208	1.014	0.44	-0.82
BMEP_WHR (Bar)	3.7318	0.0114	0.31	3.7117	3.7532	0.0415	-0.18	-0.52
Ambient (Degree C)	24.720	1.892	7.65	21.255	31.210	9.955	1.12	5.44
Baro (mBar)	999.56	4.88	0.49	989.22	1006.38	17.16	-0.80	0.00
Humid (%)	26.044	3.285	12.62	20.415	32.462	12.047	0.44	-0.64
P_Fuel_I (PSI)	1.5133	0.0176	1.16	1.4771	1.5418	0.0648	-0.27	-0.49
SPEED (rpm)	1801.6	0.504	0.03	1800.7	1802.6	1.94	0.12	-0.45
IMEPH1 (bar)	5.1517	0.0386	0.75	5.0909	5.2427	0.1518	0.67	-0.13
IMEPH2 (bar)	4.2110	0.0281	0.67	4.1572	4.2665	0.1093	-0.08	0.02
IMEPL1 (bar)	-0.32217	0.00443	-1.37	-0.32778	-0.31148	0.01630	0.98	0.33
IMEPL2 (bar)	-0.38397	0.00623	-1.62	-0.39260	-0.36995	0.02265	0.83	0.03
IMEP1 (bar)	4.8326	0.0420	0.87	4.7681	4.9331	0.1650	0.70	-0.02
IMEP2 (bar)	3.8300	0.0308	0.80	3.7735	3.8970	0.1235	0.16	0.27
COVIMEP1 (%)	2.5800	0.2655	10.29	2.1363	3.2551	1.1188	0.68	0.40
COVIMEP2 (%)	4.978	0.550	11.05	4.204	6.299	2.095	0.81	0.18
PMAX1 (bar)	17.874	0.284	1.59	17.305	18.708	1.403	0.69	2.41
PMAX2 (bar)	13.636	0.174	1.27	13.316	13.892	0.576	-0.43	-0.89
APMAX1 (deg)	23.056	0.310	1.34	22.500	23.650	1.150	0.08	-0.62
APMAX2 (deg)	21.349	0.454	2.13	20.507	22.050	1.543	-0.62	-0.54
RMAX1 (bar/deg)	0.42697	0.01434	3.36	0.40234	0.46798	0.06564	0.88	1.45
RMAX2 (bar/deg)	0.28557	0.00760	2.66	0.27349	0.29825	0.02476	0.15	-1.14
ARMAX1 (deg)	1.9007	0.3466	18.24	1.1833	2.6700	1.4867	0.42	0.32
ARMAX2 (deg)	-1.597	0.629	-39.39	-2.947	-0.657	2.290	-0.32	-0.66
MFB10_1 (deg)	1.4729	0.2604	17.68	0.9125	1.8583	0.9458	-0.39	-0.81
MFB10_2 (deg)	3.5756	0.1751	4.90	3.3450	3.9950	0.6500	0.65	0.05
MFB50_1 (deg)	18.668	0.579	3.10	17.300	19.773	2.473	-0.24	0.18
MFB50_2 (deg)	23.778	0.596	2.51	22.743	24.828	2.084	0.01	-0.97
MFB90_1 (deg)	35.033	0.899	2.57	32.997	37.128	4.132	0.27	0.96
MFB90_2 (deg)	44.604	1.329	2.98	42.358	46.965	4.607	0.09	-0.82
D10-90_1 (deg)	33.560	0.695	2.07	32.084	35.381	3.297	0.70	1.55
D10-90_2 (deg)	41.028	1.212	2.95	38.912	43.158	4.247	0.11	-0.77

Results for: TEG - Mode 1

Descriptive Statistics:

Variable	Mean	StDev	CoefVar	Minimum	Maximum	Range	Skewness	Kurtosis
Mode	1.0000	0.000000	0.00	1.0000	1.0000	0.000000	*	*
Hold Spd	3600.0	0.000000	0.00	3600.0	3600.0	0.000000	*	*
Eng Spd (RPM)	3601.1	0.769	0.02	3599.9	3602.5	2.65	0.53	-0.64
Throttle (%)	85.667	2.204	2.57	81.807	89.838	8.032	-0.19	-0.80
Hold Trq (N-m)	40.000	0.000000	0.00	40.000	40.000	0.000000	*	*
Tq Obs (ft-lb)	29.499	0.0490	0.17	29.405	29.628	0.223	0.51	0.75
Tq Obs (N-m)	39.996	0.0664	0.17	39.868	40.170	0.302	0.51	0.76
Pwr Obs (Hp)	20.226	0.0344	0.17	20.163	20.322	0.159	0.65	1.22
Pwr Obs (kW)	15.083	0.0257	0.17	15.035	15.154	0.119	0.65	1.25
SAE-Fact (Factor)	1.0073	0.00609	0.60	0.9930	1.0150	0.0220	-0.59	-0.45
Trq Corr (ft-lb)	29.499	0.0490	0.17	29.405	29.628	0.223	0.51	0.75
Trq Corr (N-m)	39.996	0.0664	0.17	39.868	40.170	0.302	0.51	0.76
Pwr Corr (Hp)	20.226	0.0344	0.17	20.163	20.322	0.159	0.65	1.22
Pwr Corr (kW)	15.083	0.0257	0.17	15.035	15.154	0.119	0.65	1.25
CarbIn (Degree C)	27.946	1.297	4.64	24.242	29.539	5.297	-1.36	2.16
P_CarbIn (PSI)	14.429	0.0766	0.53	14.277	14.559	0.282	-0.27	-0.97
EGT1 (Degree C)	717.63	4.36	0.61	712.04	730.57	18.53	1.01	1.56
EGT2 (Degree C)	727.62	3.42	0.47	723.06	738.26	15.21	1.29	2.47
P_Exh (PSI)	14.724	0.0819	0.56	14.565	14.879	0.314	0.09	-0.73
Col In G (Degree C)	90.752	0.983	1.08	88.941	92.320	3.379	-0.27	-0.80
Col Ot G (Degree C)	98.748	0.967	0.98	96.978	100.353	3.375	-0.32	-0.78
Cool Flw (gal/min)	3.7592	0.0789	2.10	3.6310	3.9307	0.2996	0.39	-0.44
Cl InHd1 (Degree C)	100.29	0.833	0.83	98.73	101.67	2.94	-0.28	-0.68
Cl InHd2 (Degree C)	97.172	0.924	0.95	95.465	98.500	3.035	-0.39	-0.82
Cl OtHd1 (Degree C)	99.058	0.962	0.97	97.183	100.610	3.427	-0.35	-0.72
Cl OtHd2 (Degree C)	99.540	1.005	1.01	97.673	101.064	3.391	-0.39	-0.78
Cyl 1 Hi (Degree C)	164.58	1.56	0.95	162.91	168.70	5.79	1.12	0.40
Cyl 2 Hi (Degree C)	153.26	1.67	1.09	148.30	156.30	8.01	-0.88	2.14
Cyl 1 Lo (Degree C)	154.41	1.09	0.71	152.67	157.34	4.66	0.46	0.71
Cyl 2 Lo (Degree C)	152.73	1.26	0.82	148.91	154.49	5.58	-1.22	2.49
TEG 1 (Degree C)	94.023	0.797	0.85	92.342	95.314	2.972	-0.60	-0.28
TEG 2 (Degree C)	96.296	0.841	0.87	94.659	97.547	2.888	-0.03	-0.87
Oil (Degree C)	125.64	0.364	0.29	124.83	126.37	1.54	-0.29	0.02
P_Oil (PSI)	40.719	0.216	0.53	40.348	41.131	0.783	0.15	-0.55
TEG1vlt (Volts)	0.27468	0.02652	9.65	0.19092	0.31445	0.12353	-1.54	3.58
TEG2vlt (Volts)	0.26263	0.01400	5.33	0.24516	0.29473	0.04956	0.65	-0.17
P_Fuel (PSI)	16.984	0.234	1.38	16.508	17.417	0.908	-0.51	-0.33
Fuel Flw (kg/h)	6.1776	0.1300	2.10	5.8254	6.3736	0.5482	-0.65	0.96
BSFC (g/kWh)	409.62	8.48	2.07	386.33	422.63	36.30	-0.73	0.99
Lambda	0.70878	0.00854	1.20	0.69742	0.73654	0.03912	1.50	3.42
AFR	10.327	0.124	1.20	10.155	10.724	0.569	1.44	3.21
M_Air (kg/h)	63.783	0.636	1.00	62.480	64.903	2.422	0.10	-0.32
BMEP_WHR (Bar)	7.4635	0.0131	0.18	7.4373	7.4956	0.0583	0.20	0.45
Ambient (Degree C)	26.407	1.155	4.37	23.194	27.800	4.606	-1.38	1.63
Baro (mBar)	994.39	4.97	0.50	984.75	1002.01	17.26	-0.11	-1.08
Humid (%)	27.645	3.158	11.42	22.930	32.297	9.367	-0.01	-1.54
P_Fuel_I (PSI)	1.5127	0.0115	0.76	1.4931	1.5348	0.0417	-0.01	-0.62
SPEED (rpm)	3601.6	2.14	0.06	3597.4	3607.8	10.4	0.56	2.10
IMEPH1 (bar)	8.5463	0.0480	0.56	8.4807	8.6357	0.1550	0.20	-1.17
IMEPH2 (bar)	9.0212	0.0511	0.57	8.9089	9.1156	0.2067	-0.26	0.14
IMEPL1 (bar)	-0.61142	0.00277	-0.45	-0.61604	-0.60610	0.00995	0.38	-0.42
IMEPL2 (bar)	-0.57830	0.00376	-0.65	-0.58762	-0.57055	0.01708	-0.43	0.75
IMEP1 (bar)	7.9379	0.0477	0.60	7.8702	8.0232	0.1530	0.15	-1.23
IMEP2 (bar)	8.4458	0.0500	0.59	8.3335	8.5389	0.2054	-0.27	0.37
COVIMEP1 (%)	4.3983	0.3237	7.36	3.8473	5.1777	1.3304	0.70	0.40
COVIMEP2 (%)	3.6491	0.3278	8.98	3.0522	4.1577	1.1055	0.06	-1.23
PMAX1 (bar)	26.808	0.485	1.81	25.905	28.012	2.107	0.42	0.46
PMAX2 (bar)	30.591	0.552	1.81	29.556	31.595	2.039	-0.03	-0.93
APMAX1 (deg)	23.569	0.201	0.85	23.160	23.877	0.717	-0.29	-0.96
APMAX2 (deg)	23.903	0.180	0.75	23.553	24.350	0.797	0.19	0.64
RMAX1 (bar/deg)	0.60744	0.02283	3.76	0.57022	0.67027	0.10006	0.78	1.17
RMAX2 (bar/deg)	0.75680	0.03052	4.03	0.70129	0.81075	0.10946	-0.13	-0.99
ARMAX1 (deg)	3.0275	0.4142	13.68	2.2467	3.7500	1.5033	-0.33	-0.66
ARMAX2 (deg)	5.2579	0.4375	8.32	4.4200	6.2600	1.8400	-0.04	-0.30
MFB10_1 (deg)	3.4545	0.2643	7.65	2.7150	3.9158	1.2008	-0.61	1.35
MFB10_2 (deg)	2.4619	0.2833	11.51	2.0483	3.1258	1.0775	0.58	-0.56
MFB50_1 (deg)	22.076	0.717	3.25	20.273	23.377	3.104	-0.28	0.62
MFB50_2 (deg)	18.919	0.620	3.28	17.992	20.162	2.170	0.37	-1.17
MFB90_1 (deg)	42.138	1.346	3.19	39.062	44.525	5.463	-0.11	0.08
MFB90_2 (deg)	35.113	1.136	3.24	33.583	37.229	3.647	0.37	-1.29
D10-90_1 (deg)	38.683	1.104	2.85	36.347	40.609	4.263	-0.01	-0.21
D10-90_2 (deg)	32.651	0.875	2.68	31.517	34.103	2.586	0.31	-1.39

Results for: TEG - Mode 2

Descriptive Statistics:

Variable	Mean	StDev	CoefVar	Minimum	Maximum	Range	Skewness	Kurtosis
Mode	2.0000	0.000000	0.00	2.0000	2.0000	0.000000	*	*
Hold Spd	3000.0	0.000000	0.00	3000.0	3000.0	0.000000	*	*
Eng Spd (RPM)	3000.1	0.573	0.02	2999.1	3001.8	2.70	0.76	1.73
Throttle (%)	66.701	1.209	1.81	64.303	69.080	4.777	-0.19	0.06
Hold Trq (N-m)	40.000	0.000000	0.00	40.000	40.000	0.000000	*	*
Tq Obs (ft-lb)	29.478	0.0392	0.13	29.414	29.566	0.152	0.29	-0.49
Tq Obs (N-m)	39.966	0.0532	0.13	39.880	40.086	0.206	0.28	-0.51
Pwr Obs (Hp)	16.838	0.0210	0.12	16.805	16.885	0.0804	0.14	-0.49
Pwr Obs (kW)	12.556	0.0156	0.12	12.532	12.591	0.0590	0.13	-0.51
SAE-Fact (Factor)	1.0073	0.00609	0.60	0.9930	1.0150	0.0220	-0.59	-0.45
Trq Corr (ft-lb)	29.478	0.0392	0.13	29.414	29.566	0.152	0.29	-0.49
Trq Corr (N-m)	39.966	0.0532	0.13	39.880	40.086	0.206	0.28	-0.51
Pwr Corr (Hp)	16.838	0.0210	0.12	16.805	16.885	0.0804	0.14	-0.49
Pwr Corr (kW)	12.556	0.0156	0.12	12.532	12.591	0.0590	0.13	-0.51
CarbIn (Degree C)	27.237	1.875	6.88	21.432	29.237	7.806	-1.75	3.15
P_CarbIn (PSI)	14.442	0.0736	0.51	14.313	14.572	0.258	-0.09	-1.05
EGT1 (Degree C)	690.67	2.11	0.31	686.91	694.29	7.38	-0.09	-0.64
EGT2 (Degree C)	727.59	5.33	0.73	719.79	736.71	16.92	0.16	-1.48
P_Exh (PSI)	14.663	0.0712	0.49	14.477	14.783	0.306	-0.59	0.56
Col In G (Degree C)	90.174	1.094	1.21	88.436	92.950	4.514	0.79	0.37
Col Ot G (Degree C)	98.055	1.086	1.11	96.287	100.888	4.601	0.78	0.52
Cool Flw (gal/min)	3.6109	0.1161	3.21	3.4135	3.7953	0.3818	0.01	-1.12
Cl InHd1 (Degree C)	99.915	0.956	0.96	98.045	102.321	4.276	0.62	0.54
Cl InHd2 (Degree C)	96.693	1.017	1.05	95.044	99.222	4.178	0.77	0.28
Cl OtHd1 (Degree C)	98.345	1.139	1.16	96.446	101.312	4.865	0.78	0.53
Cl OtHd2 (Degree C)	98.668	1.121	1.14	96.867	101.529	4.662	0.77	0.38
Cyl 1 Hi (Degree C)	158.11	0.789	0.50	156.78	159.50	2.72	-0.00	-0.66
Cyl 2 Hi (Degree C)	148.32	1.53	1.03	145.92	150.94	5.02	0.34	-1.11
Cyl 1 Lo (Degree C)	148.43	0.704	0.47	147.04	149.65	2.61	-0.33	-0.53
Cyl 2 Lo (Degree C)	147.46	1.20	0.81	145.40	149.51	4.10	0.20	-1.14
TEG 1 (Degree C)	93.620	0.973	1.04	91.911	95.921	4.010	0.62	0.10
TEG 2 (Degree C)	95.782	1.027	1.07	94.207	98.142	3.935	0.70	-0.26
Oil (Degree C)	123.85	0.536	0.43	122.73	125.20	2.47	0.08	0.86
P_Oil (PSI)	38.814	0.224	0.58	38.374	39.406	1.032	0.30	1.19
TEG1vlt (Volts)	0.27763	0.02792	10.06	0.20622	0.30878	0.10256	-1.11	0.55
TEG2vlt (Volts)	0.26580	0.01499	5.64	0.23022	0.29061	0.06039	-0.60	0.16
P_Fuel (PSI)	17.305	0.245	1.41	16.870	17.869	0.999	0.15	-0.23
Fuel Flw (kg/h)	4.3105	0.0489	1.14	4.2290	4.3959	0.1668	-0.21	-1.12
BSFC (g/kWh)	343.32	3.87	1.13	336.27	350.30	14.03	-0.27	-0.96
Lambda	0.77877	0.00548	0.70	0.76994	0.78933	0.01939	0.14	-0.99
AFR	11.347	0.0791	0.70	11.222	11.498	0.276	0.16	-1.13
M_Air (kg/h)	48.908	0.305	0.62	48.412	49.547	1.135	0.49	-0.67
BMEP_WHR (Bar)	7.4579	0.0104	0.14	7.4356	7.4783	0.0428	-0.11	-0.42
Ambient (Degree C)	25.870	1.821	7.04	20.058	27.200	7.142	-1.93	3.76
Baro (mBar)	994.74	4.96	0.50	984.79	1002.33	17.53	-0.21	-0.97
Humid (%)	28.142	3.401	12.09	23.393	33.819	10.427	0.11	-1.48
P_Fuel_I (PSI)	1.5015	0.0114	0.76	1.4777	1.5282	0.0506	0.24	0.59
SPEED (rpm)	3001.3	0.693	0.02	2999.5	3002.5	3.00	-0.68	0.87
IMEPH1 (bar)	8.2866	0.0356	0.43	8.2121	8.3512	0.1391	0.05	-0.52
IMEPH2 (bar)	8.7177	0.0304	0.35	8.6675	8.7788	0.1114	0.35	-0.51
IMEPL1 (bar)	-0.45870	0.00177	-0.39	-0.46158	-0.45511	0.00648	0.29	-1.06
IMEPL2 (bar)	-0.43431	0.00107	-0.25	-0.43607	-0.43170	0.00438	0.04	0.11
IMEP1 (bar)	7.8310	0.0353	0.45	7.7559	7.8937	0.1378	-0.04	-0.49
IMEP2 (bar)	8.2864	0.0299	0.36	8.2388	8.3460	0.1072	0.37	-0.56
COVIMEP1 (%)	2.5528	0.1591	6.23	2.2479	2.8613	0.6134	-0.03	-0.50
COVIMEP2 (%)	1.8454	0.1175	6.37	1.6144	2.1869	0.5725	0.66	2.09
PMAX1 (bar)	29.615	0.505	1.70	28.588	30.680	2.092	0.28	-0.18
PMAX2 (bar)	32.958	0.272	0.83	32.412	33.388	0.977	-0.12	-0.96
APMAX1 (deg)	22.589	0.236	1.04	22.123	23.077	0.953	0.19	-0.23
APMAX2 (deg)	22.087	0.200	0.91	21.717	22.547	0.830	0.35	-0.02
RMAX1 (bar/deg)	0.77449	0.02722	3.51	0.72367	0.83091	0.10724	0.34	-0.19
RMAX2 (bar/deg)	0.93143	0.01785	1.92	0.88873	0.96352	0.07479	-0.25	-0.12
ARMAX1 (deg)	4.2085	0.4261	10.13	3.5267	4.9067	1.3800	0.11	-1.16
ARMAX2 (deg)	6.0808	0.2694	4.43	5.6600	6.5300	0.8700	-0.04	-1.23
MFB10_1 (deg)	0.7244	0.1982	27.36	0.3075	1.2008	0.8933	0.09	0.41
MFB10_2 (deg)	0.5042	0.1321	26.20	0.2258	0.7458	0.5200	-0.00	-0.45
MFB50_1 (deg)	16.583	0.508	3.06	15.645	17.714	2.069	0.15	-0.24
MFB50_2 (deg)	14.652	0.240	1.64	14.258	15.227	0.968	0.37	-0.06
MFB90_1 (deg)	31.832	0.943	2.96	30.122	33.719	3.598	-0.03	-0.53
MFB90_2 (deg)	27.554	0.367	1.33	26.910	28.374	1.464	0.26	-0.24
D10-90_1 (deg)	31.107	0.758	2.44	29.728	32.518	2.790	-0.10	-0.67
D10-90_2 (deg)	27.050	0.272	1.00	26.558	27.661	1.103	0.17	-0.16

Results for: TEG - Mode 3

Descriptive Statistics:

Variable	Mean	StDev	CoefVar	Minimum	Maximum	Range	Skewness	Kurtosis
Mode	3.0000	0.000000	0.00	3.0000	3.0000	0.000000	*	*
Hold Spd	2400.0	0.000000	0.00	2400.0	2400.0	0.000000	*	*
Eng Spd (RPM)	2400.6	1.55	0.06	2396.7	2402.6	5.95	-1.23	1.14
Throttle (%)	57.996	1.731	2.98	54.767	60.910	6.143	-0.38	-0.67
Hold Trq (N-m)	40.000	0.000000	0.00	40.000	40.000	0.000000	*	*
Tq Obs (ft-lb)	29.485	0.0301	0.10	29.433	29.533	0.101	-0.03	-0.66
Tq Obs (N-m)	39.976	0.0408	0.10	39.906	40.042	0.136	-0.03	-0.68
Pwr Obs (Hp)	13.477	0.0128	0.10	13.450	13.499	0.0488	-0.58	-0.04
Pwr Obs (kW)	10.050	0.00963	0.10	10.029	10.066	0.0370	-0.58	-0.02
SAE-Fact (Factor)	1.0073	0.00609	0.60	0.9930	1.0150	0.0220	-0.59	-0.45
Trq Corr (ft-lb)	29.485	0.0301	0.10	29.433	29.533	0.101	-0.03	-0.66
Trq Corr (N-m)	39.976	0.0408	0.10	39.906	40.042	0.136	-0.03	-0.68
Pwr Corr (Hp)	13.477	0.0128	0.10	13.450	13.499	0.0488	-0.58	-0.04
Pwr Corr (kW)	10.050	0.00963	0.10	10.029	10.066	0.0370	-0.58	-0.02
CarbIn (Degree C)	26.851	2.276	8.48	20.433	29.074	8.641	-2.05	3.48
P_CarbIn (PSI)	14.448	0.0746	0.52	14.295	14.563	0.268	-0.27	-0.65
EGT1 (Degree C)	644.56	3.72	0.58	637.09	650.03	12.94	-0.24	-0.98
EGT2 (Degree C)	682.16	4.88	0.72	674.98	690.36	15.38	0.20	-1.32
P_Exh (PSI)	14.641	0.0810	0.55	14.488	14.810	0.322	-0.08	-0.55
Col In G (Degree C)	89.907	0.838	0.93	88.216	92.056	3.840	0.17	0.92
Col Ot G (Degree C)	97.604	0.811	0.83	95.925	99.495	3.570	0.05	0.29
Cool Flw (gal/min)	3.3495	0.0401	1.20	3.2576	3.4215	0.1639	-0.47	0.13
Cl InHd1 (Degree C)	99.458	0.665	0.67	97.885	100.848	2.963	-0.33	0.63
Cl InHd2 (Degree C)	96.917	0.716	0.74	95.403	98.712	3.309	0.16	0.72
Cl OtHd1 (Degree C)	97.898	0.834	0.85	96.260	99.921	3.660	0.17	0.42
Cl OtHd2 (Degree C)	98.153	0.829	0.84	96.466	100.201	3.735	0.16	0.56
Cyl 1 Hi (Degree C)	154.21	2.34	1.51	150.76	158.70	7.93	0.27	-0.96
Cyl 2 Hi (Degree C)	143.51	1.07	0.75	141.38	145.83	4.44	0.10	-0.07
Cyl 1 Lo (Degree C)	145.20	2.11	1.45	142.30	148.66	6.36	0.13	-1.36
Cyl 2 Lo (Degree C)	141.90	1.19	0.84	139.72	144.21	4.48	0.11	-0.37
TEG 1 (Degree C)	93.636	0.688	0.73	92.231	95.308	3.077	0.03	0.55
TEG 2 (Degree C)	95.967	0.986	1.03	94.409	98.779	4.370	1.17	1.86
Oil (Degree C)	121.42	0.784	0.65	119.30	122.68	3.38	-0.38	0.95
P_Oil (PSI)	35.792	0.340	0.95	35.178	36.739	1.560	0.36	1.55
TEG1vlt (Volts)	0.28403	0.02760	9.72	0.20828	0.32232	0.11404	-1.02	1.36
TEG2vlt (Volts)	0.25341	0.01732	6.84	0.21378	0.28685	0.07307	-0.41	0.53
P_Fuel (PSI)	17.753	0.199	1.12	17.300	18.101	0.800	-0.14	-0.36
Fuel Flw (kg/h)	3.4178	0.0585	1.71	3.3011	3.5223	0.2212	0.01	-0.73
BSFC (g/kWh)	340.11	5.77	1.70	328.54	350.39	21.85	0.00	-0.70
Lambda	0.78660	0.00712	0.91	0.77683	0.80083	0.02400	0.39	-0.91
AFR	11.461	0.105	0.92	11.315	11.666	0.351	0.35	-0.98
M_Air (kg/h)	39.164	0.423	1.08	38.243	39.969	1.726	-0.04	-0.49
BMEP_WHR (Bar)	7.4573	0.00816	0.11	7.4437	7.4733	0.0296	0.17	-0.72
Ambient (Degree C)	25.534	1.931	7.56	19.321	27.200	7.879	-2.09	4.29
Baro (mBar)	994.76	5.05	0.51	984.80	1003.13	18.33	-0.18	-0.93
Humid (%)	27.738	3.333	12.02	20.931	34.360	13.429	-0.11	-0.81
P_Fuel_I (PSI)	1.5029	0.0105	0.70	1.4822	1.5224	0.0402	-0.59	-0.06
SPEED (rpm)	2400.6	0.879	0.04	2398.5	2402.1	3.60	-0.45	0.56
IMEPH1 (bar)	8.3327	0.0393	0.47	8.2728	8.4262	0.1534	0.50	-0.17
IMEPH2 (bar)	8.7120	0.0398	0.46	8.6266	8.7703	0.1437	-0.49	-0.76
IMEPL1 (bar)	-0.34411	0.00279	-0.81	-0.34909	-0.33886	0.01023	0.24	-0.83
IMEPL2 (bar)	-0.33934	0.00249	-0.73	-0.34431	-0.33543	0.00887	-0.32	-0.70
IMEP1 (bar)	7.9917	0.0403	0.50	7.9334	8.0894	0.1560	0.55	-0.13
IMEP2 (bar)	8.3758	0.0392	0.47	8.2894	8.4361	0.1467	-0.46	-0.71
COVIMEP1 (%)	1.7924	0.1749	9.76	1.5673	2.2265	0.6592	1.09	1.25
COVIMEP2 (%)	1.1512	0.0988	8.58	0.9345	1.3590	0.4245	0.12	0.35
PMAX1 (bar)	33.022	0.253	0.76	32.458	33.828	1.370	0.80	4.09
PMAX2 (bar)	36.506	0.350	0.96	35.617	37.159	1.542	-0.35	0.52
APMAX1 (deg)	20.356	0.244	1.20	19.823	20.907	1.083	0.17	0.16
APMAX2 (deg)	19.160	0.246	1.29	18.717	19.540	0.823	-0.41	-1.02
RMAX1 (bar/deg)	0.95759	0.01618	1.69	0.91993	1.00602	0.08609	0.33	3.61
RMAX2 (bar/deg)	1.1586	0.0238	2.06	1.1073	1.1995	0.0922	-0.04	-0.56
ARMAX1 (deg)	4.7028	0.2968	6.31	3.8933	5.2000	1.3067	-0.74	1.11
ARMAX2 (deg)	5.1920	0.2566	4.94	4.7233	5.6433	0.9200	0.07	-0.65
MFB10_1 (deg)	-1.1607	0.2288	-19.71	-1.4958	-0.6267	0.8692	0.62	-0.21
MFB10_2 (deg)	-1.9388	0.1765	-9.10	-2.3025	-1.5767	0.7258	-0.23	-0.11
MFB50_1 (deg)	12.993	0.286	2.20	12.285	13.726	1.441	0.27	1.63
MFB50_2 (deg)	11.061	0.272	2.46	10.567	11.557	0.990	-0.29	-0.81
MFB90_1 (deg)	25.970	0.381	1.47	25.025	27.010	1.985	0.44	2.19
MFB90_2 (deg)	22.460	0.380	1.69	21.759	23.221	1.462	-0.09	-0.73
D10-90_1 (deg)	27.131	0.249	0.92	26.521	27.670	1.149	-0.01	1.36
D10-90_2 (deg)	24.399	0.240	0.98	24.000	24.797	0.797	-0.08	-1.09

Results for: TEG - Mode 4

Descriptive Statistics:

Variable	Mean	StDev	CoefVar	Minimum	Maximum	Range	Skewness	Kurtosis
Mode	4.0000	0.000000	0.00	4.0000	4.0000	0.000000	*	*
Hold Spd	1800.0	0.000000	0.00	1800.0	1800.0	0.000000	*	*
Eng Spd (RPM)	1798.2	0.168	0.01	1797.8	1798.5	0.734	-0.39	0.64
Throttle (%)	52.334	1.236	2.36	48.256	54.735	6.479	-1.12	4.16
Hold Trq (N-m)	40.000	0.000000	0.00	40.000	40.000	0.000000	*	*
Tq Obs (ft-lb)	29.490	0.0359	0.12	29.391	29.561	0.170	-0.56	1.67
Tq Obs (N-m)	39.983	0.0487	0.12	39.849	40.080	0.231	-0.56	1.68
Pwr Obs (Hp)	10.097	0.0124	0.12	10.062	10.119	0.0569	-0.78	1.76
Pwr Obs (kW)	7.5293	0.00923	0.12	7.5029	7.5456	0.0427	-0.81	1.88
SAE-Fact (Factor)	1.0073	0.00609	0.60	0.9930	1.0150	0.0220	-0.59	-0.45
Trq Corr (ft-lb)	29.490	0.0359	0.12	29.391	29.561	0.170	-0.56	1.67
Trq Corr (N-m)	39.983	0.0487	0.12	39.849	40.080	0.231	-0.56	1.68
Pwr Corr (Hp)	10.097	0.0124	0.12	10.062	10.119	0.0569	-0.78	1.76
Pwr Corr (kW)	7.5293	0.00923	0.12	7.5029	7.5456	0.0427	-0.81	1.88
CarbIn (Degree C)	27.153	1.249	4.60	23.950	28.696	4.745	-1.26	1.12
P_CarbIn (PSI)	14.459	0.0737	0.51	14.301	14.582	0.281	-0.16	-0.64
EGT1 (Degree C)	580.47	3.12	0.54	575.17	586.03	10.86	-0.03	-0.95
EGT2 (Degree C)	615.73	3.36	0.55	609.79	622.48	12.70	0.39	-0.36
P_Exh (PSI)	14.594	0.0729	0.50	14.452	14.715	0.263	-0.30	-0.61
Col In G (Degree C)	90.445	0.983	1.09	88.664	92.793	4.128	0.48	0.06
Col Ot G (Degree C)	98.711	0.883	0.89	97.001	100.604	3.603	0.24	-0.32
Cool Flw (gal/min)	2.5351	0.00950	0.37	2.5145	2.5487	0.0342	-0.63	-0.52
Cl InHd1 (Degree C)	100.07	0.696	0.70	98.85	101.57	2.71	0.25	-0.57
Cl InHd2 (Degree C)	98.219	0.818	0.83	96.559	100.063	3.505	0.26	-0.06
Cl OtHd1 (Degree C)	99.176	0.889	0.90	97.438	100.999	3.560	0.19	-0.42
Cl OtHd2 (Degree C)	99.263	0.923	0.93	97.466	101.305	3.839	0.31	-0.16
Cyl 1 Hi (Degree C)	149.95	3.00	2.00	145.37	154.30	8.93	0.22	-1.46
Cyl 2 Hi (Degree C)	138.70	0.883	0.64	136.97	140.71	3.74	0.04	-0.06
Cyl 1 Lo (Degree C)	141.08	2.33	1.65	137.90	144.84	6.94	0.41	-1.37
Cyl 2 Lo (Degree C)	136.86	1.09	0.79	134.97	138.67	3.70	0.04	-0.82
TEG 1 (Degree C)	94.252	0.914	0.97	92.344	96.459	4.115	0.23	0.39
TEG 2 (Degree C)	97.276	1.005	1.03	95.375	99.131	3.756	0.05	-0.66
Oil (Degree C)	119.30	0.759	0.64	117.64	120.73	3.08	-0.22	-0.61
P_Oil (PSI)	30.857	0.494	1.60	29.624	31.332	1.708	-1.47	1.43
TEG1vlt (Volts)	0.25846	0.02040	7.89	0.20411	0.28383	0.07972	-0.86	0.61
TEG2vlt (Volts)	0.22122	0.01606	7.26	0.19341	0.24650	0.05309	-0.05	-1.20
P_Fuel (PSI)	18.025	0.204	1.13	17.642	18.458	0.816	-0.09	-0.38
Fuel Flw (kg/h)	2.6426	0.0357	1.35	2.5780	2.7135	0.1355	0.34	-0.76
BSFC (g/kWh)	350.98	4.79	1.36	342.48	360.50	18.02	0.30	-0.82
Lambda	0.76797	0.00557	0.72	0.75800	0.77989	0.02189	0.21	-0.21
AFR	11.188	0.0825	0.74	11.042	11.363	0.321	0.20	-0.22
M_Air (kg/h)	29.564	0.221	0.75	29.176	30.029	0.853	0.18	-0.87
BMEP_WHR (Bar)	7.4574	0.0104	0.14	7.4309	7.4771	0.0462	-0.51	0.74
Ambient (Degree C)	25.683	1.085	4.22	23.110	26.700	3.590	-1.25	0.62
Baro (mBar)	994.60	5.06	0.51	984.43	1002.42	18.00	-0.25	-0.94
Humid (%)	27.335	2.843	10.40	22.015	31.361	9.346	-0.28	-1.45
P_Fuel_I (PSI)	1.4942	0.0136	0.91	1.4664	1.5193	0.0529	-0.20	-0.01
SPEED (rpm)	1799.3	0.567	0.03	1798.0	1801.1	3.04	0.68	3.79
IMEPH1 (bar)	8.2094	0.0251	0.31	8.1742	8.2500	0.0758	0.28	-1.37
IMEPH2 (bar)	8.5849	0.0314	0.37	8.5280	8.6455	0.1175	-0.00	-0.95
IMEPL1 (bar)	-0.24800	0.00307	-1.24	-0.25264	-0.24310	0.00954	0.15	-1.48
IMEPL2 (bar)	-0.24001	0.00391	-1.63	-0.24622	-0.23355	0.01266	0.32	-1.26
IMEP1 (bar)	7.9645	0.0266	0.33	7.9264	8.0085	0.0820	0.33	-1.30
IMEP2 (bar)	8.3480	0.0327	0.39	8.2868	8.4140	0.1272	0.08	-0.76
COVIMEP1 (%)	1.3218	0.0917	6.94	1.1533	1.5868	0.4335	0.64	1.81
COVIMEP2 (%)	0.7774	0.0518	6.66	0.6817	0.9193	0.2375	0.83	1.07
PMAX1 (bar)	36.125	0.429	1.19	35.380	36.977	1.597	0.00	-0.96
PMAX2 (bar)	39.900	0.286	0.72	39.055	40.401	1.345	-0.93	1.90
APMAX1 (deg)	17.757	0.335	1.89	17.187	18.307	1.120	0.06	-1.40
APMAX2 (deg)	16.271	0.186	1.14	15.863	16.560	0.697	-0.26	-0.56
RMAX1 (bar/deg)	1.1804	0.0340	2.88	1.1222	1.2437	0.1215	-0.02	-1.09
RMAX2 (bar/deg)	1.4052	0.0245	1.74	1.3377	1.4610	0.1233	-0.36	1.81
ARMAX1 (deg)	4.5388	0.2091	4.61	4.0867	4.9667	0.8800	-0.09	0.70
ARMAX2 (deg)	4.1392	0.2253	5.44	3.6700	4.5967	0.9267	0.01	-0.49
MFB10_1 (deg)	-3.1661	0.2344	-7.40	-3.5867	-2.8450	0.7417	-0.12	-1.43
MFB10_2 (deg)	-4.2767	0.1506	-3.52	-4.5667	-4.0350	0.5317	-0.38	-0.67
MFB50_1 (deg)	9.7860	0.4312	4.41	9.0342	10.5300	1.4958	0.08	-1.28
MFB50_2 (deg)	7.8221	0.2058	2.63	7.3883	8.1633	0.7750	-0.19	-0.52
MFB90_1 (deg)	21.215	0.753	3.55	20.009	22.623	2.613	0.27	-1.08
MFB90_2 (deg)	17.999	0.326	1.81	17.237	18.773	1.536	0.10	0.92
D10-90_1 (deg)	24.381	0.539	2.21	23.503	25.468	1.964	0.42	-0.67
D10-90_2 (deg)	22.275	0.265	1.19	21.687	23.017	1.330	0.55	1.74

Results for: TEG - Mode 5

Descriptive Statistics:

Variable	Mean	StDev	CoefVar	Minimum	Maximum	Range	Skewness	Kurtosis
Mode	5.0000	0.000000	0.00	5.0000	5.0000	0.000000	*	*
Hold Spd	3600.0	0.000000	0.00	3600.0	3600.0	0.000000	*	*
Eng Spd (RPM)	3601.3	0.332	0.01	3600.7	3601.8	1.08	-0.10	-1.40
Throttle (%)	37.691	1.278	3.39	35.603	40.356	4.752	0.39	-0.26
Hold Trq (N-m)	20.000	0.000000	0.00	20.000	20.000	0.000000	*	*
Tq Obs (ft-lb)	14.748	0.0329	0.22	14.691	14.826	0.135	0.13	-0.08
Tq Obs (N-m)	19.996	0.0448	0.22	19.919	20.102	0.183	0.14	-0.10
Pwr Obs (Hp)	10.113	0.0226	0.22	10.074	10.167	0.0929	0.14	-0.06
Pwr Obs (kW)	7.5410	0.0168	0.22	7.5125	7.5814	0.0689	0.15	-0.04
SAE-Fact (Factor)	1.0073	0.00609	0.60	0.9930	1.0150	0.0220	-0.59	-0.45
Trq Corr (ft-lb)	14.748	0.0329	0.22	14.691	14.826	0.135	0.13	-0.08
Trq Corr (N-m)	19.996	0.0448	0.22	19.919	20.102	0.183	0.14	-0.10
Pwr Corr (Hp)	10.113	0.0226	0.22	10.074	10.167	0.0929	0.14	-0.06
Pwr Corr (kW)	7.5410	0.0168	0.22	7.5125	7.5814	0.0689	0.15	-0.04
CarbIn (Degree C)	27.558	1.097	3.98	24.725	28.925	4.200	-0.96	0.55
P_CarbIn (PSI)	14.454	0.0753	0.52	14.321	14.581	0.260	-0.09	-0.90
EGT1 (Degree C)	850.90	3.93	0.46	843.90	859.16	15.26	0.18	-0.61
EGT2 (Degree C)	826.13	3.14	0.38	821.40	831.88	10.48	0.42	-0.72
P_Exh (PSI)	14.658	0.0925	0.63	14.456	14.798	0.342	-0.43	-0.50
Col In G (Degree C)	90.604	0.791	0.87	89.161	92.100	2.939	0.09	-0.38
Col Ot G (Degree C)	97.780	0.864	0.88	96.340	99.579	3.239	0.48	-0.17
Cool Flw (gal/min)	3.7345	0.1149	3.08	3.5147	3.9942	0.4796	0.02	0.06
Cl InHd1 (Degree C)	99.474	0.761	0.76	98.146	100.955	2.809	0.22	-0.51
Cl InHd2 (Degree C)	95.899	0.797	0.83	94.506	97.465	2.959	0.30	-0.32
Cl OtHd1 (Degree C)	98.236	0.915	0.93	96.624	100.200	3.576	0.43	-0.10
Cl OtHd2 (Degree C)	98.019	0.939	0.96	96.454	99.946	3.493	0.46	-0.26
Cyl 1 Hi (Degree C)	156.98	1.12	0.72	155.39	159.33	3.94	0.87	0.06
Cyl 2 Hi (Degree C)	141.54	0.896	0.63	139.77	143.05	3.28	-0.02	-0.81
Cyl 1 Lo (Degree C)	148.18	1.45	0.98	145.64	151.10	5.45	0.35	-0.68
Cyl 2 Lo (Degree C)	142.54	1.03	0.72	140.67	144.80	4.13	0.51	-0.11
TEG 1 (Degree C)	94.203	0.913	0.97	92.823	96.038	3.215	0.28	-0.96
TEG 2 (Degree C)	95.325	1.000	1.05	93.391	97.449	4.058	0.24	-0.11
Oil (Degree C)	120.15	0.644	0.54	119.09	121.64	2.55	0.65	-0.02
P_Oil (PSI)	41.809	0.155	0.37	41.456	42.020	0.564	-0.61	-0.49
TEG1vlt (Volts)	0.31976	0.04326	13.53	0.24356	0.39486	0.15130	0.19	-1.17
TEG2vlt (Volts)	0.28859	0.02002	6.94	0.24650	0.31606	0.06956	-0.58	-0.30
P_Fuel (PSI)	17.656	0.263	1.49	17.198	18.165	0.967	-0.37	-0.61
Fuel Flw (kg/h)	2.9265	0.0280	0.96	2.8869	2.9912	0.1044	0.60	-0.60
BSFC (g/kWh)	388.15	3.48	0.90	382.62	395.82	13.20	0.52	-0.62
Lambda	0.90242	0.00425	0.47	0.89572	0.91128	0.01556	0.43	-0.31
AFR	13.149	0.0625	0.48	13.052	13.280	0.229	0.43	-0.32
M_Air (kg/h)	38.481	0.346	0.90	37.927	39.273	1.345	0.77	-0.10
BMEP_WHR (Bar)	3.7304	0.00847	0.23	3.7160	3.7494	0.0334	0.20	-0.31
Ambient (Degree C)	26.321	0.936	3.56	24.053	27.200	3.147	-0.87	-0.19
Baro (mBar)	995.12	5.03	0.51	984.71	1002.86	18.15	-0.31	-0.83
Humid (%)	27.586	2.867	10.39	22.987	32.539	9.552	-0.08	-1.43
P_Fuel_I (PSI)	1.5027	0.0111	0.74	1.4739	1.5226	0.0487	-0.42	0.49
SPEED (rpm)	3602.0	2.96	0.08	3596.5	3608.5	11.9	0.22	-0.12
IMEPH1 (bar)	5.2300	0.0466	0.89	5.1366	5.2996	0.1630	-0.25	-0.83
IMEPH2 (bar)	4.7054	0.0635	1.35	4.6117	4.8221	0.2104	0.36	-1.15
IMEPL1 (bar)	-0.52337	0.00337	-0.64	-0.52826	-0.51656	0.01169	0.27	-1.02
IMEPL2 (bar)	-0.52313	0.00493	-0.94	-0.53052	-0.51431	0.01621	0.20	-1.22
IMEP1 (bar)	4.7095	0.0459	0.97	4.6202	4.7832	0.1630	-0.23	-0.83
IMEP2 (bar)	4.1853	0.0670	1.60	4.0935	4.3093	0.2158	0.41	-1.12
COVIMEP1 (%)	8.4464	0.4544	5.38	7.4686	9.4347	1.9660	0.02	0.20
COVIMEP2 (%)	7.8453	0.3848	4.91	7.3195	8.9528	1.6333	1.15	1.50
PMAX1 (bar)	13.978	0.295	2.11	13.494	14.466	0.972	-0.16	-1.25
PMAX2 (bar)	12.904	0.188	1.46	12.562	13.190	0.628	-0.17	-1.10
APMAX1 (deg)	23.861	0.756	3.17	21.840	25.063	3.223	-0.72	0.67
APMAX2 (deg)	23.369	0.420	1.80	22.497	24.083	1.587	-0.55	-0.40
RMAX1 (bar/deg)	0.25697	0.00729	2.84	0.24440	0.26838	0.02397	0.12	-1.34
RMAX2 (bar/deg)	0.23248	0.00370	1.59	0.22602	0.23881	0.01280	-0.00	-1.12
ARMAX1 (deg)	-10.612	1.649	-15.54	-13.593	-8.140	5.453	-0.30	-0.95
ARMAX2 (deg)	-11.341	0.836	-7.37	-13.100	-9.877	3.223	-0.68	0.47
MFB10_1 (deg)	8.8609	0.3203	3.62	8.3517	9.4633	1.1117	0.18	-1.10
MFB10_2 (deg)	8.3176	0.2129	2.56	8.0067	8.8867	0.8800	1.03	0.86
MFB50_1 (deg)	31.734	1.020	3.21	30.333	33.689	3.357	0.39	-1.05
MFB50_2 (deg)	30.897	0.425	1.38	30.279	31.888	1.609	0.83	0.32
MFB90_1 (deg)	54.685	1.850	3.38	51.985	58.651	6.666	0.50	-0.83
MFB90_2 (deg)	53.701	0.820	1.53	52.521	55.383	2.862	0.86	-0.03
D10-90_1 (deg)	45.824	1.553	3.39	43.556	49.387	5.831	0.61	-0.57
D10-90_2 (deg)	45.384	0.760	1.68	44.392	47.147	2.754	0.87	-0.14

Results for: TEG - Mode 6

Descriptive Statistics:

Variable	Mean	StDev	CoefVar	Minimum	Maximum	Range	Skewness	Kurtosis
Mode	6.0000	0.000000	0.00	6.0000	6.0000	0.000000	*	*
Hold Spd	3000.0	0.000000	0.00	3000.0	3000.0	0.000000	*	*
Eng Spd (RPM)	3000.9	0.280	0.01	3000.3	3001.3	0.954	-0.14	-1.07
Throttle (%)	30.305	1.352	4.46	28.411	32.528	4.116	0.15	-1.66
Hold Trq (N-m)	20.000	0.000000	0.00	20.000	20.000	0.000000	*	*
Tq Obs (ft-lb)	14.755	0.0369	0.25	14.680	14.814	0.134	-0.19	-0.44
Tq Obs (N-m)	20.005	0.0501	0.25	19.903	20.086	0.182	-0.19	-0.44
Pwr Obs (Hp)	8.4305	0.0210	0.25	8.3880	8.4656	0.0776	-0.20	-0.38
Pwr Obs (kW)	6.2865	0.0156	0.25	6.2549	6.3128	0.0579	-0.19	-0.39
SAE-Fact (Factor)	1.0073	0.00609	0.60	0.9930	1.0150	0.0220	-0.59	-0.45
Trq Corr (ft-lb)	14.755	0.0369	0.25	14.680	14.814	0.134	-0.19	-0.44
Trq Corr (N-m)	20.005	0.0501	0.25	19.903	20.086	0.182	-0.19	-0.44
Pwr Corr (Hp)	8.4305	0.0210	0.25	8.3880	8.4656	0.0776	-0.20	-0.38
Pwr Corr (kW)	6.2865	0.0156	0.25	6.2549	6.3128	0.0579	-0.19	-0.39
CarbIn (Degree C)	27.118	1.407	5.19	23.078	28.858	5.779	-1.16	1.46
P_CarbIn (PSI)	14.448	0.0764	0.53	14.286	14.574	0.288	-0.38	-0.61
EGT1 (Degree C)	778.12	2.91	0.37	773.40	783.79	10.40	0.34	-0.54
EGT2 (Degree C)	775.20	3.75	0.48	769.30	780.49	11.19	-0.26	-1.22
P_Exh (PSI)	14.616	0.0781	0.53	14.429	14.739	0.310	-0.57	0.09
Col In G (Degree C)	90.028	0.900	1.00	88.563	91.751	3.187	0.32	-0.81
Col Ot G (Degree C)	96.472	0.927	0.96	94.829	98.246	3.416	0.35	-0.66
Cool Flw (gal/min)	3.7038	0.1402	3.78	3.4726	3.9673	0.4947	0.25	-0.44
Cl InHd1 (Degree C)	98.350	0.845	0.86	96.960	99.928	2.968	0.35	-0.85
Cl InHd2 (Degree C)	95.044	0.779	0.82	93.861	96.502	2.641	0.38	-0.89
Cl OtHd1 (Degree C)	96.918	0.957	0.99	95.254	98.735	3.481	0.43	-0.72
Cl OtHd2 (Degree C)	96.584	0.935	0.97	94.885	98.318	3.434	0.29	-0.78
Cyl 1 Hi (Degree C)	149.60	1.59	1.06	147.15	153.19	6.05	0.51	-0.45
Cyl 2 Hi (Degree C)	135.57	0.834	0.61	133.87	136.88	3.00	-0.31	-0.92
Cyl 1 Lo (Degree C)	141.12	1.56	1.11	138.47	144.72	6.25	0.19	-0.19
Cyl 2 Lo (Degree C)	136.82	0.983	0.72	134.78	139.04	4.26	0.56	0.76
TEG 1 (Degree C)	93.284	0.932	1.00	91.894	95.165	3.270	0.35	-0.97
TEG 2 (Degree C)	94.837	1.031	1.09	93.107	97.359	4.252	0.70	0.12
Oil (Degree C)	117.06	0.658	0.56	115.62	118.47	2.85	0.25	0.16
P_Oil (PSI)	40.359	0.190	0.47	39.926	40.685	0.759	-0.63	0.03
TEG1vlt (Volts)	0.4096	0.0716	17.47	0.2751	0.5196	0.2445	-0.21	-0.90
TEG2vlt (Volts)	0.29645	0.01707	5.76	0.26061	0.32354	0.06293	-0.64	-0.22
P_Fuel (PSI)	17.682	0.250	1.41	17.247	18.328	1.081	0.48	0.48
Fuel Flw (kg/h)	2.4039	0.0222	0.92	2.3647	2.4453	0.0806	0.28	-0.88
BSFC (g/kWh)	382.50	3.78	0.99	376.52	388.69	12.17	0.11	-1.15
Lambda	0.87448	0.00617	0.71	0.86549	0.88411	0.01862	0.11	-1.42
AFR	12.741	0.0889	0.70	12.611	12.877	0.265	0.09	-1.42
M_Air (kg/h)	30.625	0.230	0.75	30.204	31.233	1.029	0.82	0.92
BMEP_WHR (Bar)	3.7337	0.00932	0.25	3.7161	3.7506	0.0344	-0.05	-0.66
Ambient (Degree C)	25.932	1.259	4.86	22.639	27.200	4.561	-1.04	0.35
Baro (mBar)	995.01	5.01	0.50	984.52	1002.73	18.21	-0.35	-0.76
Humid (%)	28.010	3.280	11.71	23.335	33.247	9.911	0.02	-1.53
P_Fuel_I (PSI)	1.4987	0.0108	0.72	1.4776	1.5186	0.0409	-0.06	-0.68
SPEED (rpm)	3001.9	1.45	0.05	2998.9	3006.4	7.47	0.98	3.20
IMEPH1 (bar)	5.2376	0.0276	0.53	5.1999	5.3045	0.1046	0.65	-0.14
IMEPH2 (bar)	4.3984	0.0377	0.86	4.3342	4.4807	0.1466	0.40	-0.42
IMEPL1 (bar)	-0.44824	0.00374	-0.84	-0.45476	-0.44287	0.01190	-0.18	-1.17
IMEPL2 (bar)	-0.48848	0.00487	-1.00	-0.49695	-0.48202	0.01493	-0.26	-1.25
IMEP1 (bar)	4.7924	0.0272	0.57	4.7574	4.8574	0.1000	0.64	-0.09
IMEP2 (bar)	3.9129	0.0395	1.01	3.8521	4.0018	0.1497	0.48	-0.24
COVIMEP1 (%)	5.5324	0.2217	4.01	5.1918	5.8808	0.6890	0.23	-1.19
COVIMEP2 (%)	7.0051	0.4150	5.92	5.9700	7.6608	1.6908	-0.62	0.40
PMAX1 (bar)	14.982	0.243	1.62	14.520	15.385	0.865	-0.45	-0.76
PMAX2 (bar)	12.391	0.132	1.07	12.153	12.708	0.554	0.61	-0.01
APMAX1 (deg)	25.562	0.317	1.24	24.827	26.087	1.260	-0.58	0.37
APMAX2 (deg)	22.163	0.475	2.14	21.463	23.107	1.643	0.46	-0.71
RMAX1 (bar/deg)	0.28908	0.00803	2.78	0.27530	0.30152	0.02622	-0.40	-1.16
RMAX2 (bar/deg)	0.22462	0.00345	1.54	0.21841	0.23216	0.01375	0.61	0.00
ARMAX1 (deg)	-2.883	0.987	-34.24	-4.747	-1.313	3.433	-0.37	-0.71
ARMAX2 (deg)	-10.060	1.004	-9.98	-11.903	-8.477	3.427	0.04	-1.02
MFB10_1 (deg)	6.3496	0.2209	3.48	6.0100	6.7317	0.7217	0.29	-0.88
MFB10_2 (deg)	7.2627	0.2429	3.35	6.8533	7.8742	1.0208	0.60	0.48
MFB50_1 (deg)	26.932	0.624	2.32	26.004	28.299	2.295	0.75	-0.34
MFB50_2 (deg)	30.000	0.499	1.66	29.101	30.844	1.743	-0.38	-1.00
MFB90_1 (deg)	47.153	1.097	2.33	45.467	49.732	4.265	0.89	0.28
MFB90_2 (deg)	53.180	0.956	1.80	51.437	54.549	3.113	-0.14	-1.18
D10-90_1 (deg)	40.803	0.912	2.23	39.457	43.000	3.543	1.07	0.87
D10-90_2 (deg)	45.917	0.930	2.02	44.289	47.297	3.008	-0.13	-1.17

Results for: TEG - Mode 7

Descriptive Statistics:

Variable	Mean	StDev	CoefVar	Minimum	Maximum	Range	Skewness	Kurtosis
Mode	7.0000	0.000000	0.00	7.0000	7.0000	0.000000	*	*
Hold Spd	2400.0	0.000000	0.00	2400.0	2400.0	0.000000	*	*
Eng Spd (RPM)	2401.2	0.520	0.02	2400.3	2402.1	1.80	-0.10	-1.01
Throttle (%)	24.776	1.122	4.53	22.179	26.802	4.623	-0.48	0.19
Hold Trq (N-m)	20.000	0.000000	0.00	20.000	20.000	0.000000	*	*
Tq Obs (ft-lb)	14.735	0.0402	0.27	14.684	14.798	0.115	0.16	-1.52
Tq Obs (N-m)	19.977	0.0544	0.27	19.908	20.064	0.156	0.16	-1.53
Pwr Obs (Hp)	6.7366	0.0183	0.27	6.7129	6.7650	0.0521	0.16	-1.50
Pwr Obs (kW)	5.0235	0.0137	0.27	5.0052	5.0447	0.0394	0.15	-1.49
SAE-Fact (Factor)	1.0073	0.00609	0.60	0.9930	1.0150	0.0220	-0.59	-0.45
Trq Corr (ft-lb)	14.735	0.0402	0.27	14.684	14.798	0.115	0.16	-1.52
Trq Corr (N-m)	19.977	0.0544	0.27	19.908	20.064	0.156	0.16	-1.53
Pwr Corr (Hp)	6.7366	0.0183	0.27	6.7129	6.7650	0.0521	0.16	-1.50
Pwr Corr (kW)	5.0235	0.0137	0.27	5.0052	5.0447	0.0394	0.15	-1.49
CarbIn (Degree C)	27.075	1.215	4.49	23.320	28.747	5.426	-1.36	2.46
P_CarbIn (PSI)	14.451	0.0747	0.52	14.289	14.584	0.295	-0.36	-0.45
EGT1 (Degree C)	710.58	7.58	1.07	696.77	719.40	22.63	-0.62	-0.91
EGT2 (Degree C)	695.30	7.27	1.05	682.04	706.63	24.59	-0.55	-0.91
P_Exh (PSI)	14.580	0.0754	0.52	14.417	14.700	0.282	-0.32	-0.39
Col In G (Degree C)	89.944	0.689	0.77	88.791	91.501	2.709	0.58	-0.17
Col Ot G (Degree C)	95.804	0.646	0.67	94.828	97.405	2.577	0.74	0.30
Cool Flw (gal/min)	3.3945	0.0225	0.66	3.3293	3.4292	0.0998	-1.19	1.59
Cl InHd1 (Degree C)	97.782	0.620	0.63	96.764	99.069	2.305	0.41	-0.50
Cl InHd2 (Degree C)	94.923	0.649	0.68	93.959	96.433	2.474	0.61	-0.14
Cl OtHd1 (Degree C)	96.236	0.675	0.70	95.274	97.841	2.566	0.72	0.02
Cl OtHd2 (Degree C)	95.872	0.676	0.71	94.821	97.433	2.612	0.65	-0.05
Cyl 1 Hi (Degree C)	143.06	1.78	1.25	140.17	146.45	6.28	0.40	-1.04
Cyl 2 Hi (Degree C)	130.49	0.496	0.38	129.24	131.24	2.00	-0.86	0.59
Cyl 1 Lo (Degree C)	135.06	1.55	1.15	133.31	138.45	5.14	0.76	-0.57
Cyl 2 Lo (Degree C)	131.41	0.688	0.52	130.37	133.10	2.73	0.38	-0.03
TEG 1 (Degree C)	92.380	0.872	0.94	91.292	95.226	3.933	1.53	3.46
TEG 2 (Degree C)	94.780	0.914	0.96	93.420	97.371	3.951	0.98	1.23
Oil (Degree C)	113.19	0.465	0.41	112.25	114.08	1.83	0.29	-0.45
P_Oil (PSI)	38.190	0.256	0.67	37.623	38.805	1.182	-0.44	1.19
TEG1vlt (Volts)	0.4979	0.0704	14.14	0.3225	0.5592	0.2367	-1.36	0.73
TEG2vlt (Volts)	0.29093	0.01920	6.60	0.22900	0.32071	0.09171	-1.39	3.48
P_Fuel (PSI)	18.003	0.229	1.27	17.365	18.372	1.007	-0.74	1.14
Fuel Flw (kg/h)	1.8919	0.0361	1.91	1.8408	1.9535	0.1127	0.34	-0.93
BSFC (g/kWh)	376.65	7.19	1.91	366.77	389.30	22.53	0.30	-0.95
Lambda	0.86034	0.01686	1.96	0.82980	0.88038	0.05059	-0.68	-0.94
AFR	12.535	0.245	1.95	12.088	12.828	0.740	-0.69	-0.93
M_Air (kg/h)	23.703	0.149	0.63	23.432	23.998	0.566	0.19	-0.73
BMEP_WHR (Bar)	3.7256	0.0103	0.28	3.7093	3.7417	0.0323	0.14	-1.23
Ambient (Degree C)	25.767	1.223	4.75	21.425	26.973	5.549	-2.17	5.79
Baro (mBar)	994.88	5.09	0.51	984.19	1002.63	18.44	-0.38	-0.73
Humid (%)	27.588	3.208	11.63	21.484	33.205	11.721	-0.11	-1.23
P_Fuel_I (PSI)	1.5005	0.0112	0.74	1.4824	1.5247	0.0422	0.14	-0.64
SPEED (rpm)	2401.8	0.762	0.03	2400.4	2404.3	3.94	1.64	4.43
IMEPH1 (bar)	5.1813	0.0332	0.64	5.1058	5.2487	0.1429	-0.08	0.29
IMEPH2 (bar)	4.4484	0.0342	0.77	4.3961	4.5167	0.1205	0.33	-1.09
IMEPL1 (bar)	-0.37686	0.00351	-0.93	-0.38283	-0.37063	0.01220	0.03	-1.26
IMEPL2 (bar)	-0.44298	0.00474	-1.07	-0.45101	-0.43494	0.01606	-0.08	-1.23
IMEP1 (bar)	4.8075	0.0324	0.67	4.7365	4.8734	0.1369	-0.03	0.20
IMEP2 (bar)	4.0085	0.0357	0.89	3.9608	4.0755	0.1147	0.44	-1.22
COVIMEP1 (%)	3.7918	0.1752	4.62	3.4545	4.0325	0.5780	-0.20	-1.16
COVIMEP2 (%)	4.7867	0.3416	7.14	4.3023	5.6255	1.3233	0.71	-0.04
PMAX1 (bar)	16.323	0.383	2.35	15.405	16.938	1.533	-0.47	-0.03
PMAX2 (bar)	14.175	0.206	1.45	13.690	14.625	0.935	-0.12	0.65
APMAX1 (deg)	24.490	0.311	1.27	24.023	25.017	0.993	0.20	-1.33
APMAX2 (deg)	23.459	0.219	0.93	23.087	23.957	0.870	0.66	0.59
RMAX1 (bar/deg)	0.35316	0.01694	4.80	0.31953	0.38318	0.06365	-0.07	-0.58
RMAX2 (bar/deg)	0.29199	0.00910	3.12	0.27042	0.31047	0.04005	-0.23	0.49
ARMAX1 (deg)	1.756	0.628	35.75	-0.010	2.823	2.833	-0.56	1.43
ARMAX2 (deg)	0.187	0.708	379.51	-1.093	1.337	2.430	-0.03	-1.01
MFB10_1 (deg)	3.8173	0.4458	11.68	2.9808	4.6283	1.6475	0.01	-0.86
MFB10_2 (deg)	4.4501	0.2931	6.59	3.9175	5.0717	1.1542	0.11	-0.06
MFB50_1 (deg)	22.465	0.839	3.74	21.119	24.409	3.290	0.41	-0.11
MFB50_2 (deg)	23.179	0.588	2.54	22.123	24.453	2.329	0.41	-0.20
MFB90_1 (deg)	40.677	1.190	2.93	38.798	43.593	4.794	0.57	0.19
MFB90_2 (deg)	42.125	0.944	2.24	40.560	44.023	3.463	0.23	-0.47
D10-90_1 (deg)	36.859	0.824	2.23	35.615	38.964	3.349	0.72	0.30
D10-90_2 (deg)	37.675	0.693	1.84	36.425	38.951	2.526	0.04	-0.50

Results for: TEG - Mode 8

Descriptive Statistics:

Variable	Mean	StDev	CoefVar	Minimum	Maximum	Range	Skewness	Kurtosis
Mode	8.0000	0.000000	0.00	8.0000	8.0000	0.000000	*	*
Hold Spd	1800.0	0.000000	0.00	1800.0	1800.0	0.000000	*	*
Eng Spd (RPM)	1800.8	0.0708	0.00	1800.7	1800.9	0.266	-0.06	-0.79
Throttle (%)	19.646	1.115	5.68	17.377	21.466	4.090	-0.41	-0.94
Hold Trq (N-m)	20.000	0.000000	0.00	20.000	20.000	0.000000	*	*
Tq Obs (ft-lb)	14.744	0.0535	0.36	14.569	14.815	0.245	-1.38	3.35
Tq Obs (N-m)	19.990	0.0727	0.36	19.753	20.086	0.334	-1.38	3.38
Pwr Obs (Hp)	5.0553	0.0184	0.36	4.9947	5.0793	0.0846	-1.43	3.59
Pwr Obs (kW)	3.7697	0.0137	0.36	3.7248	3.7881	0.0633	-1.41	3.48
SAE-Fact (Factor)	1.0073	0.00609	0.60	0.9930	1.0150	0.0220	-0.59	-0.45
Trq Corr (ft-lb)	14.744	0.0535	0.36	14.569	14.815	0.245	-1.38	3.35
Trq Corr (N-m)	19.990	0.0727	0.36	19.753	20.086	0.334	-1.38	3.38
Pwr Corr (Hp)	5.0553	0.0184	0.36	4.9947	5.0793	0.0846	-1.43	3.59
Pwr Corr (kW)	3.7697	0.0137	0.36	3.7248	3.7881	0.0633	-1.41	3.48
CarbIn (Degree C)	27.015	1.009	3.74	24.725	28.509	3.784	-0.95	0.26
P_CarbIn (PSI)	14.457	0.0718	0.50	14.313	14.571	0.259	-0.35	-0.81
EGT1 (Degree C)	625.22	3.42	0.55	612.36	630.23	17.87	-2.17	7.87
EGT2 (Degree C)	623.67	2.90	0.46	613.04	626.81	13.77	-2.16	6.78
P_Exh (PSI)	14.559	0.0801	0.55	14.370	14.682	0.313	-0.66	0.20
Col In G (Degree C)	90.215	0.950	1.05	88.912	92.825	3.913	1.11	1.20
Col Ot G (Degree C)	96.203	0.865	0.90	95.077	98.497	3.421	1.07	0.77
Cool Flw (gal/min)	2.5476	0.00958	0.38	2.5345	2.5670	0.0325	0.43	-0.95
Cl InHd1 (Degree C)	98.192	0.789	0.80	97.166	100.158	2.992	1.03	0.30
Cl InHd2 (Degree C)	95.580	0.869	0.91	94.471	97.828	3.357	0.99	0.53
Cl OtHd1 (Degree C)	96.765	0.878	0.91	95.667	99.059	3.392	1.06	0.66
Cl OtHd2 (Degree C)	96.268	0.894	0.93	95.108	98.660	3.552	1.07	0.86
Cyl 1 Hi (Degree C)	137.33	1.57	1.14	135.00	140.02	5.02	0.27	-1.19
Cyl 2 Hi (Degree C)	125.95	0.743	0.59	124.58	127.80	3.22	0.39	0.30
Cyl 1 Lo (Degree C)	130.13	1.27	0.98	128.29	132.70	4.41	0.26	-0.88
Cyl 2 Lo (Degree C)	126.65	0.615	0.49	125.52	127.82	2.30	0.24	-0.57
TEG 1 (Degree C)	92.586	0.931	1.01	91.334	94.846	3.511	0.76	0.04
TEG 2 (Degree C)	94.954	1.414	1.49	92.335	97.908	5.573	0.40	-0.32
Oil (Degree C)	110.32	1.03	0.93	107.74	111.83	4.09	-0.69	0.17
P_Oil (PSI)	34.430	0.397	1.15	33.645	35.319	1.675	-0.01	0.56
TEG1vlt (Volts)	0.46547	0.04915	10.56	0.31458	0.50933	0.19475	-1.67	2.60
TEG2vlt (Volts)	0.29944	0.04154	13.87	0.25324	0.39561	0.14237	1.05	0.23
P_Fuel (PSI)	18.113	0.227	1.25	17.727	18.526	0.798	-0.00	-1.00
Fuel Flw (kg/h)	1.4331	0.0219	1.53	1.4103	1.5107	0.1005	2.20	6.19
BSFC (g/kWh)	380.19	5.92	1.56	373.28	399.48	26.20	1.59	3.72
Lambda	0.83215	0.00843	1.01	0.79657	0.83844	0.04187	-3.45	13.90
AFR	12.124	0.123	1.01	11.604	12.219	0.614	-3.44	13.93
M_Air (kg/h)	17.371	0.118	0.68	17.217	17.635	0.419	0.49	-0.50
BMEP_WHR (Bar)	3.7267	0.0131	0.35	3.6887	3.7489	0.0601	-0.84	1.57
Ambient (Degree C)	25.579	0.952	3.72	23.112	26.700	3.588	-1.14	0.77
Baro (mBar)	994.71	5.10	0.51	983.89	1002.47	18.59	-0.40	-0.71
Humid (%)	27.299	2.790	10.22	22.388	30.592	8.204	-0.32	-1.63
P_Fuel_I (PSI)	1.4996	0.0111	0.74	1.4811	1.5233	0.0423	0.23	-0.59
SPEED (rpm)	1801.7	0.385	0.02	1800.9	1802.4	1.53	-0.26	-0.12
IMEPH1 (bar)	5.1034	0.0255	0.50	5.0372	5.1502	0.1130	-0.41	0.97
IMEPH2 (bar)	4.1786	0.0312	0.75	4.1269	4.2439	0.1170	0.02	-0.76
IMEPL1 (bar)	-0.32177	0.00365	-1.14	-0.32663	-0.31508	0.01155	0.24	-1.31
IMEPL2 (bar)	-0.38368	0.00499	-1.30	-0.39019	-0.37500	0.01519	0.17	-1.33
IMEP1 (bar)	4.7847	0.0259	0.54	4.7225	4.8300	0.1075	-0.19	0.37
IMEP2 (bar)	3.7979	0.0343	0.90	3.7398	3.8716	0.1318	-0.04	-0.54
COVIMEP1 (%)	2.1948	0.1595	7.26	1.9373	2.6073	0.6700	0.68	0.51
COVIMEP2 (%)	4.4533	0.2978	6.69	3.9599	5.1946	1.2347	0.56	0.16
PMAX1 (bar)	18.631	0.262	1.41	18.139	19.259	1.120	0.50	0.25
PMAX2 (bar)	13.830	0.198	1.43	13.444	14.168	0.723	-0.24	-0.62
APMAX1 (deg)	22.342	0.341	1.52	21.767	22.947	1.180	0.14	-0.80
APMAX2 (deg)	21.377	0.281	1.32	20.877	21.887	1.010	0.20	-0.98
RMAX1 (bar/deg)	0.46347	0.01529	3.30	0.43606	0.49541	0.05935	0.34	-0.44
RMAX2 (bar/deg)	0.29400	0.00701	2.38	0.28232	0.30829	0.02597	0.01	-0.74
ARMAX1 (deg)	2.8139	0.2755	9.79	2.3200	3.2167	0.8967	-0.19	-1.27
ARMAX2 (deg)	-0.7279	0.3592	-49.34	-1.5467	0.1333	1.6800	0.07	0.72
MFB10_1 (deg)	0.8251	0.3030	36.73	0.3267	1.3392	1.0125	0.01	-1.10
MFB10_2 (deg)	3.2277	0.2221	6.88	2.8308	3.6042	0.7733	0.19	-0.98
MFB50_1 (deg)	16.917	0.511	3.02	16.035	17.949	1.914	0.08	-0.60
MFB50_2 (deg)	22.597	0.500	2.21	21.740	23.330	1.590	0.16	-1.31
MFB90_1 (deg)	32.197	0.747	2.32	30.817	33.929	3.113	0.06	0.23
MFB90_2 (deg)	42.658	0.873	2.05	40.935	44.068	3.133	0.08	-0.99
D10-90_1 (deg)	31.372	0.487	1.55	30.398	32.671	2.273	0.21	1.50
D10-90_2 (deg)	39.430	0.710	1.80	38.010	40.472	2.462	-0.07	-1.05

Appendix B

Copyrights

Each of the figures and articles within this document are cataloged with the letters of permission (if required) for copyright purposes.

B.1 Copyright Not Required

The list of items that did not require copyright permissions can be seen in Table B.1.

Table B.1

List of figures and that **do not** require copyright permission

Reference	Citation	Reason for no permission required
Figure 1.1	[1, 2, 3, 4, 5, 6]	Figure created from data published by the USA federal government.
Figure 1.2(a)	[1]	This is public domain because it was created and published by the USA federal government.
Figure 1.2(b)	[1]	This is public domain because it was created and published by the USA federal government.
Chapter 2 journal article	[24]	Copyright transfer agreement signed by the authors provides the permission to reprint the material. Please refer to page 163 for a copy of the copyright transfer agreement.
Figure 4.11(c)	[73]	See page 169 for documentation that this material is in the public domain.

Copyright transfer agreement retains authors rights for reproduction of full journal

article: [24]

6/14/13

TSEA1022

COPYRIGHT AGREEMENT (as of March 2010)



Publishing • Three Park Avenue • New York, NY 10016
Please email this form to journalcopyright@asme.org or fax to 212-591-7292

Before publication of your paper in a conference proceeding or in a journal, ASME must receive your signed Copyright Agreement Form. For conference papers, this form should be received by the deadline indicated by the Conference. Other forms may NOT be substituted for this form, nor may any wording on the form be changed. HANDWRITTEN SIGNATURES ONLY are acceptable.

PAPER NUMBER (for conference/journal papers): TSEA-13-1022

TITLE: Review Of Waste Heat Recovery Mechanisms For Internal Combustion Engines

AUTHOR(s): John R. Armstead, Scott Miers

JOURNAL NAME: Journal of Thermal Science and Engineering Applications

COPYRIGHT ASSIGNMENT

The following terms of copyright assignment refer to Sections 1, 2, and 3. Sections 4 and 5 may not be subject to copyright.

The undersigned hereby assigns irrevocably to ASME all worldwide rights under copyright in the Paper.

Authors retain all proprietary rights in any idea, process, procedure, or articles of manufacture described in the Paper, including the right to seek patent protection for them. Authors may perform, lecture, teach, conduct related research and display all or part of the Paper, in print or electronic format. Authors may reproduce and distribute the Paper for non-commercial purposes only. Non-commercial applies only to the sale of the paper per se. For all copies of the Paper made by Authors, Authors must acknowledge ASME as original publisher and include the names of all author(s), the publication title, and an appropriate copyright notice that identifies ASME as the copyright holder.

PLEASE READ THE TERMS AND CONDITIONS WHICH ARE FULLY INCORPORATED IN THIS AGREEMENT.

ASME requests that authors/copyright owners assign copyright to ASME in order for a conference or journal paper to be published by ASME. Authors exempt from this request are direct employees of the U.S. Government, whereby papers are not subject to copyright protection in the U.S., or non-U.S. government employees, whose governments hold the copyright to the paper. Otherwise, the author/ copyright owner(s) of the Paper should sign this form as instructed below. Please refer to the section below "Who Should Sign" and also to ASME's [FAQs page](#) for more information regarding copyright ownership and the copyright process.

WHO SHOULD SIGN

Only the copyright owner(s) of the Paper, or an authorized representative, can sign this form. If one of the following applies you may not own the copyright of the paper, or you may not be authorized to sign this agreement, and may need to have the appropriate copyright owner(s) or organization representative sign this Agreement:

journaltool.asme.org/templates/Form1903.cfm?notoolbar=yes&paperid=55383

1/6

- (1) you created the Paper within the scope of your employment, and your employer is the copyright owner
 (2) you created the Paper under an independent contractor agreement**; or
 (3) you received a grant that funded your Paper.

Please review your company policies regarding copyright, and if you are not authorized to sign this agreement, please forward to the appropriate organization representative. Please review applicable company, institutional, and grant policies and your employment/independent contractor agreement to determine who holds the rights to your Paper. For more information, please refer to the [FAQs](#).

****Note to U.S. Government Contractors:** If you created the Paper under contract with the U.S. Government, e.g., U.S. Government labs, the paper may be subject to copyright, and you or your employer may own the copyright. Please review your company/institutional policies and your contractor agreement. Your Paper may require a footer acknowledging contract information and also the following statement:

"The United States Government retains, and by accepting the article for publication, the publisher acknowledges that the United States Government retains, a non-exclusive, paid-up, irrevocable, worldwide license to publish or reproduce the published form of this work, or allow others to do so, for United States Government purposes."

It is your responsibility to ensure that the final PDF version of the Paper you submit includes all necessary footers and statements required under your contract.

1. PAPERS OWNED BY ONE AUTHOR OR JOINT AUTHORS; DESIGNATED

AUTHORS (For jointly authored works, all authors should submit a signed Agreement, or one designated author (the lead author) may sign on behalf of the other authors, but ONLY IF the designated author has secured written authorization to do so from all other authors. The designated author must be able to produce such written authorization if requested.)

Designated authors, please sign below and list the names of the co-authors for whom you are signing. Please include full contact information for each author. Attach additional sheets if necessary.

Author(s)/co-author(s) not covered by the Designated author, please sign in the appropriate section below and provide full contact information. Attach additional sheets if necessary.

Author

Name : John R. Armstead Signature : [Redacted] Date : 6/14/2013
 Affiliation: Michigan Technological University Job Title : Graduate Student
 (Company or Institution)
 Address : 1400 Townsend Drive 815, R.L. Smith ME-EM Building City : Houghton
 State : MI Zip Code : 49931 Country : United States
 Phone : [Redacted] Fax : none Email : jarmste@mtu.edu

Author

Name : _____ Signature : _____ Date : _____
 Affiliation: _____ Job Title : _____

(Company or Institution)
 Address : _____ City : _____
 State : _____ Zip Code : _____ Country : _____
 Phone : _____ Fax : _____ Email : _____

Co-Author

Name : _____ Signature : _____ Date : _____
 Affiliation: _____ Job Title : _____
 (Company or Institution)
 Address : _____ City : _____
 State : _____ Zip Code : _____ Country : _____
 Phone : _____ Fax : _____ Email : _____

Co-Author

Name : Scott Miers Signature : [REDACTED] Date : 6/14/2013
 Affiliation: Michigan Technological University Job Title : Professor
 (Company or Institution)
 Address : 1400 Townsend Drive 815 RL Smith Building City : Houghton
 State : MI Zip Code : 49931 Country : United States
 Phone : [REDACTED] Fax : 9999999999 Email : samiers@mtu.edu

Name : _____ Signature : _____ Date : _____
 Affiliation: _____ Title : _____
 (Company or Institution)
 Address : _____ City : _____
 State : _____ Zip Code : _____ Country : _____
 Phone : _____ Fax : _____ Email : _____

Name : _____ Signature : _____ Date : _____
 Affiliation: _____ Title : _____
 (Company or Institution)
 Address : _____ City : _____
 State : _____ Zip Code : _____ Country : _____
 Phone : _____ Fax : _____ Email : _____

2. **PAPERS OWNED BY EMPLOYER OF AUTHOR(S)** (Author may sign if so authorized; otherwise, an officer or other authorized agent of the employer should sign below.)

Name : _____ Signature : _____ Date : _____
 Affiliation : _____ Job Title : _____
 (Company or Institution)
 Address : _____ City : _____
 State : _____ Zip Code : _____ Country : _____
 Phone: _____ Fax: _____ Email: _____

PAPERS NOT SUBJECT TO COPYRIGHT ASSIGNMENT

3. PAPERS CREATED BY U.S. FEDERAL GOVERNMENT EMPLOYEES (Please sign below if you created the Paper within your scope of your employment by the U.S. Federal Government, and you are authorized to sign on behalf of your agency or department; otherwise, an officer or authorized agent should sign. Please include the following footer on the final PDF version of the Paper you submit: "This material is declared a work of the U.S. Government and is not subject to copyright protection in the United States. Approved for public release; distribution is unlimited.")

Name: _____ Signature: _____ Date: _____
 Affiliation: _____ Title: _____
 (Company or Institution)
 Address: _____ City: _____
 State: _____ Zip Code: _____ Country: _____
 Phone: _____ Fax: _____ Email: _____
 Name(s) and affiliations of Author(s) (attach additional sheets if necessary):

4. PAPERS CREATED BY U.S. FEDERAL OR STATE GOVERNMENT CONTRACTORS (Please fill in and sign below if you created the Paper under contract with the U.S. Federal or State government (e.g., U.S. government labs) , and you are authorized to sign on behalf of your organization; otherwise, an officer or other authorized agent should sign. Please include any required footers on the final PDF version of your Paper.

Name: _____ Signature: _____ Date: _____

Affiliation: _____ Title: _____

(Company or Institution)

Address: _____ City : _____

State: _____ Zip Code : _____ Country : _____

Phone: _____ Fax: _____ Email: _____

Name(s) and affiliations of Author(s) (attach additional sheets if necessary):

Please fill in and sign below if you created the Paper within the scope of your duties as an officer or employee of a non-U.S. government, and you are authorized to sign on behalf of your government; otherwise, an officer or authorized agent should sign.

Name: _____ Signature: _____ Date: _____

Affiliation: _____ Job Title: _____

(Company or Institution)

Address: _____ City: _____

State: _____ Zip Code: _____ Country: _____

Phone: _____ Fax: _____ Email: _____

The following terms and conditions are fully incorporated into the Copyright Form. Please read them carefully.

You represent and acknowledge that:

- journaltool.asme.org/templates/Form1903.cfm?notoolbar=yes&paperid=55383

6. The Paper is not subject to any prior claim, encumbrance or form and is not under consideration for publication elsewhere.
7. You have appropriately cited and acknowledged all third parties who have contributed significantly in the Paper's technical aspects.
8. ASME is not responsible for any misrepresentation, errors or omissions by those signing this copyright form.
9. (I) All print and electronic copies of the Paper submitted to ASME become ASME's physical property regardless of whether or not ASME publishes the Paper, and that ASME is not obligated to publish your paper (see the Termination Section below if your paper is not published).
10. ASME is not responsible for any of your expenses incurred in connection with preparing the Paper or attending meetings to present it, nor will ASME pay you any financial compensation if it publishes your Paper.
11. Subject to and to the maximum extent permitted by law, you agree to indemnify and hold harmless ASME from any damage or expense related to a breach of any of the representations and warranties above.

TERMINATION

If ASME decides not to publish your Paper, this Form, including all of ASME's rights in your Paper, terminates and you are thereafter free to offer the Paper for publication elsewhere.

GENERAL PROVISIONS

This Copyright Form, the Terms & Conditions, and ASME Copyright Guidelines, constitutes the entire agreement between you and ASME, and supersedes all prior or current negotiations, understandings and representations, whether oral or written, between you and ASME concerning the Paper.

This Agreement is governed by, and should be construed in accordance with, the laws of the State of New York, United States of America, applicable to agreements made and performed there, except to the extent that your institution is prohibited by law from entering contracts governed by New York law, in which limited case this Agreement is governed by, and should be construed in accordance with, the laws of the jurisdiction in which your institution is located. Any claim, dispute, action or proceeding relating to this Agreement may be brought only in the applicable state and federal courts in the State and County of New York, and you expressly consent to personal jurisdiction and venue in any of those courts.



Creative Commons Legal Code

Attribution 3.0 Unported



CREATIVE COMMONS CORPORATION IS NOT A LAW FIRM AND DOES NOT PROVIDE LEGAL SERVICES. DISTRIBUTION OF THIS LICENSE DOES NOT CREATE AN ATTORNEY-CLIENT RELATIONSHIP. CREATIVE COMMONS PROVIDES THIS INFORMATION ON AN "AS-IS" BASIS. CREATIVE COMMONS MAKES NO WARRANTIES REGARDING THE INFORMATION PROVIDED, AND DISCLAIMS LIABILITY FOR DAMAGES RESULTING FROM ITS USE.

License

THE WORK (AS DEFINED BELOW) IS PROVIDED UNDER THE TERMS OF THIS CREATIVE COMMONS PUBLIC LICENSE ("CCPL" OR "LICENSE"). THE WORK IS PROTECTED BY COPYRIGHT AND/OR OTHER APPLICABLE LAW. ANY USE OF THE WORK OTHER THAN AS AUTHORIZED UNDER THIS LICENSE OR COPYRIGHT LAW IS PROHIBITED.

BY EXERCISING ANY RIGHTS TO THE WORK PROVIDED HERE, YOU ACCEPT AND AGREE TO BE BOUND BY THE TERMS OF THIS LICENSE. TO THE EXTENT THIS LICENSE MAY BE CONSIDERED TO BE A CONTRACT, THE LICENSOR GRANTS YOU THE RIGHTS CONTAINED HERE IN CONSIDERATION OF YOUR ACCEPTANCE OF SUCH TERMS AND CONDITIONS.

1. Definitions

- a. **"Adaptation"** means a work based upon the Work, or upon the Work and other pre-existing works, such as a translation, adaptation, derivative work, arrangement of music or other alterations of a literary or artistic work, or phonogram or performance and includes cinematographic adaptations or any other form in which the Work may be recast, transformed, or adapted including in any form recognizably derived from the original, except that a work that constitutes a Collection will not be considered an Adaptation for the purpose of this License. For the avoidance of doubt, where the Work is a musical work, performance or phonogram, the synchronization of the Work in timed-relation with a moving image ("synching") will be considered an Adaptation for the purpose of this License.
- b. **"Collection"** means a collection of literary or artistic works, such as encyclopedias and anthologies, or performances, phonograms or broadcasts, or other works or subject matter other than works listed in Section 1(f) below, which, by reason of the selection and arrangement of their contents, constitute intellectual creations, in which the Work is included in its entirety in unmodified form along with one or more other contributions, each constituting separate and independent works in themselves, which together are assembled into a collective whole. A work that constitutes a Collection will not be considered an Adaptation (as defined above) for the purposes of this License.
- c. **"Distribute"** means to make available to the public the original and copies of the Work or Adaptation, as appropriate, through sale or other transfer of ownership.
- d. **"Licensor"** means the individual, individuals, entity or entities that offer(s) the Work under the terms of this License.
- e. **"Original Author"** means, in the case of a literary or artistic work, the individual, individuals, entity or entities who created the Work or if no individual or entity can be identified, the publisher; and in addition (i) in the case of a performance the actors, singers, musicians, dancers, and other persons who act, sing, deliver, declaim, play in, interpret or otherwise perform literary or artistic works or expressions of folklore; (ii) in the case of a phonogram the producer being the person or legal entity who first fixes the sounds of a performance or other sounds; and, (iii) in the case of broadcasts, the organization that transmits the broadcast.
- f. **"Work"** means the literary and/or artistic work offered under the terms of this License including without limitation any production in the literary, scientific and artistic domain, whatever may be the mode or form of its expression including digital form, such as a book, pamphlet and other writing; a lecture, address, sermon or other work of the same nature; a dramatic or dramatico-musical work; a

choreographic work or entertainment in dumb show; a musical composition with or without words; a cinematographic work to which are assimilated works expressed by a process analogous to cinematography; a work of drawing, painting, architecture, sculpture, engraving or lithography; a photographic work to which are assimilated works expressed by a process analogous to photography; a work of applied art; an illustration, map, plan, sketch or three-dimensional work relative to geography, topography, architecture or science; a performance; a broadcast; a phonogram; a compilation of data to the extent it is protected as a copyrightable work; or a work performed by a variety or circus performer to the extent it is not otherwise considered a literary or artistic work.

- g. **"You"** means an individual or entity exercising rights under this License who has not previously violated the terms of this License with respect to the Work, or who has received express permission from the Licensor to exercise rights under this License despite a previous violation.
- h. **"Publicly Perform"** means to perform public recitations of the Work and to communicate to the public those public recitations, by any means or process, including by wire or wireless means or public digital performances; to make available to the public Works in such a way that members of the public may access these Works from a place and at a place individually chosen by them; to perform the Work to the public by any means or process and the communication to the public of the performances of the Work, including by public digital performance; to broadcast and rebroadcast the Work by any means including signs, sounds or images.
- i. **"Reproduce"** means to make copies of the Work by any means including without limitation by sound or visual recordings and the right of fixation and reproducing fixations of the Work, including storage of a protected performance or phonogram in digital form or other electronic medium.

2. Fair Dealing Rights. Nothing in this License is intended to reduce, limit, or restrict any uses free from copyright or rights arising from limitations or exceptions that are provided for in connection with the copyright protection under copyright law or other applicable laws.

3. License Grant. Subject to the terms and conditions of this License, Licensor hereby grants You a worldwide, royalty-free, non-exclusive, perpetual (for the duration of the applicable copyright) license to exercise the rights in the Work as stated below:

- a. to Reproduce the Work, to incorporate the Work into one or more Collections, and to Reproduce the Work as incorporated in the Collections;
- b. to create and Reproduce Adaptations provided that any such Adaptation, including any translation in any medium, takes reasonable steps to clearly label, demarcate or otherwise identify that changes were made to the original Work. For example, a translation could be marked "The original work was translated from English to Spanish," or a modification could indicate "The original work has been modified.";
- c. to Distribute and Publicly Perform the Work including as incorporated in Collections; and,
- d. to Distribute and Publicly Perform Adaptations.
- e. For the avoidance of doubt:
 - i. **Non-waivable Compulsory License Schemes.** In those jurisdictions in which the right to collect royalties through any statutory or compulsory licensing scheme cannot be waived, the Licensor reserves the exclusive right to collect such royalties for any exercise by You of the rights granted under this License;
 - ii. **Waivable Compulsory License Schemes.** In those jurisdictions in which the right to collect royalties through any statutory or compulsory licensing scheme can be waived, the Licensor waives the exclusive right to collect such royalties for any exercise by You of the rights granted under this License; and,
 - iii. **Voluntary License Schemes.** The Licensor waives the right to collect royalties, whether individually or, in the event that the Licensor is a member of a collecting society that administers voluntary licensing schemes, via that society, from any exercise by You of the rights granted under this License.

The above rights may be exercised in all media and formats whether now known or hereafter devised. The above rights include the right to make such modifications as are technically necessary to exercise the rights in other media and formats. Subject to Section 8(f), all rights not expressly granted by Licensor are hereby reserved.

4. Restrictions. The license granted in Section 3 above is expressly made subject to and limited by the following restrictions:

- a. You may Distribute or Publicly Perform the Work only under the terms of this License. You must include a copy of, or the Uniform Resource Identifier (URI) for, this License with every copy of the Work You Distribute or Publicly Perform. You may not offer or impose any terms on the Work that restrict the terms of this License or the ability of the recipient of the Work to exercise the rights granted to that recipient under the terms of the License. You may not sublicense the Work. You must keep intact all notices that refer to this License and to the disclaimer of warranties with every copy of the Work You Distribute or Publicly Perform. When You Distribute or Publicly Perform the Work, You may not impose any effective technological measures on the Work that restrict the ability of a recipient of the Work from You to exercise the rights granted to that recipient under the terms of the License. This Section 4(a) applies to the Work as incorporated in a Collection, but this does not require the Collection apart from the Work itself to be made subject to the terms of this License. If You create a Collection, upon notice from any Licensor You must, to the extent practicable, remove from the Collection any credit as required by Section 4(b), as requested. If You create an Adaptation, upon notice from any Licensor You must, to the extent practicable, remove from the Adaptation any credit as required by Section 4(b), as requested.
- b. If You Distribute, or Publicly Perform the Work or any Adaptations or Collections, You must, unless a request has been made pursuant to Section 4(a), keep intact all copyright notices for the Work and provide, reasonable to the medium or means You are utilizing: (i) the name of the Original Author (or pseudonym, if applicable) if supplied, and/or if the Original Author and/or Licensor designate another party or parties (e.g., a sponsor institute, publishing entity, journal) for attribution ("Attribution Parties") in Licensor's copyright notice, terms of service or by other reasonable means, the name of such party or parties; (ii) the title of the Work if supplied; (iii) to the extent reasonably practicable, the URI, if any, that Licensor specifies to be associated with the Work, unless such URI does not refer to the copyright notice or licensing information for the Work; and (iv) , consistent with Section 3(b), in the case of an Adaptation, a credit identifying the use of the Work in the Adaptation (e.g., "French translation of the Work by Original Author," or "Screenplay based on original Work by Original Author"). The credit required by this Section 4 (b) may be implemented in any reasonable manner; provided, however, that in the case of a Adaptation or Collection, at a minimum such credit will appear, if a credit for all contributing authors of the Adaptation or Collection appears, then as part of these credits and in a manner at least as prominent as the credits for the other contributing authors. For the avoidance of doubt, You may only use the credit required by this Section for the purpose of attribution in the manner set out above and, by exercising Your rights under this License, You may not implicitly or explicitly assert or imply any connection with, sponsorship or endorsement by the Original Author, Licensor and/or Attribution Parties, as appropriate, of You or Your use of the Work, without the separate, express prior written permission of the Original Author, Licensor and/or Attribution Parties.
- c. Except as otherwise agreed in writing by the Licensor or as may be otherwise permitted by applicable law, if You Reproduce, Distribute or Publicly Perform the Work either by itself or as part of any Adaptations or Collections, You must not distort, mutilate, modify or take other derogatory action in relation to the Work which would be prejudicial to the Original Author's honor or reputation. Licensor agrees that in those jurisdictions (e.g. Japan), in which any exercise of the right granted in Section 3(b) of this License (the right to make Adaptations) would be deemed to be a distortion, mutilation, modification or other derogatory action prejudicial to the Original Author's honor and reputation, the Licensor will waive or not assert, as appropriate, this Section, to the fullest extent permitted by the applicable national law, to enable You to reasonably exercise Your right under Section 3(b) of this License (right to make Adaptations) but not otherwise.

5. Representations, Warranties and Disclaimer

UNLESS OTHERWISE MUTUALLY AGREED TO BY THE PARTIES IN WRITING, LICENSOR OFFERS THE WORK AS-IS AND MAKES NO REPRESENTATIONS OR WARRANTIES OF ANY KIND CONCERNING THE WORK, EXPRESS, IMPLIED, STATUTORY OR OTHERWISE, INCLUDING, WITHOUT LIMITATION, WARRANTIES OF TITLE, MERCHANTABILITY, FITNESS FOR A PARTICULAR PURPOSE, NONINFRINGEMENT, OR THE ABSENCE OF LATENT OR OTHER DEFECTS, ACCURACY, OR THE PRESENCE OF ABSENCE OF ERRORS, WHETHER OR NOT DISCOVERABLE. SOME JURISDICTIONS DO NOT ALLOW THE EXCLUSION OF IMPLIED WARRANTIES, SO SUCH EXCLUSION MAY NOT APPLY TO YOU.

6. Limitation on Liability. EXCEPT TO THE EXTENT REQUIRED BY APPLICABLE LAW, IN NO EVENT WILL LICENSOR BE LIABLE TO YOU ON ANY LEGAL THEORY FOR ANY SPECIAL, INCIDENTAL, CONSEQUENTIAL, PUNITIVE OR EXEMPLARY DAMAGES ARISING OUT OF THIS LICENSE OR THE USE OF THE WORK, EVEN IF LICENSOR HAS BEEN ADVISED OF THE POSSIBILITY OF SUCH

DAMAGES.

7. Termination

- a. This License and the rights granted hereunder will terminate automatically upon any breach by You of the terms of this License. Individuals or entities who have received Adaptations or Collections from You under this License, however, will not have their licenses terminated provided such individuals or entities remain in full compliance with those licenses. Sections 1, 2, 5, 6, 7, and 8 will survive any termination of this License.
- b. Subject to the above terms and conditions, the license granted here is perpetual (for the duration of the applicable copyright in the Work). Notwithstanding the above, Licensor reserves the right to release the Work under different license terms or to stop distributing the Work at any time; provided, however that any such election will not serve to withdraw this License (or any other license that has been, or is required to be, granted under the terms of this License), and this License will continue in full force and effect unless terminated as stated above.

8. Miscellaneous

- a. Each time You Distribute or Publicly Perform the Work or a Collection, the Licensor offers to the recipient a license to the Work on the same terms and conditions as the license granted to You under this License.
- b. Each time You Distribute or Publicly Perform an Adaptation, Licensor offers to the recipient a license to the original Work on the same terms and conditions as the license granted to You under this License.
- c. If any provision of this License is invalid or unenforceable under applicable law, it shall not affect the validity or enforceability of the remainder of the terms of this License, and without further action by the parties to this agreement, such provision shall be reformed to the minimum extent necessary to make such provision valid and enforceable.
- d. No term or provision of this License shall be deemed waived and no breach consented to unless such waiver or consent shall be in writing and signed by the party to be charged with such waiver or consent.
- e. This License constitutes the entire agreement between the parties with respect to the Work licensed here. There are no understandings, agreements or representations with respect to the Work not specified here. Licensor shall not be bound by any additional provisions that may appear in any communication from You. This License may not be modified without the mutual written agreement of the Licensor and You.
- f. The rights granted under, and the subject matter referenced, in this License were drafted utilizing the terminology of the Berne Convention for the Protection of Literary and Artistic Works (as amended on September 28, 1979), the Rome Convention of 1961, the WIPO Copyright Treaty of 1996, the WIPO Performances and Phonograms Treaty of 1996 and the Universal Copyright Convention (as revised on July 24, 1971). These rights and subject matter take effect in the relevant jurisdiction in which the License terms are sought to be enforced according to the corresponding provisions of the implementation of those treaty provisions in the applicable national law. If the standard suite of rights granted under applicable copyright law includes additional rights not granted under this License, such additional rights are deemed to be included in the License; this License is not intended to restrict the license of any rights under applicable law.

Creative Commons Notice

Creative Commons is not a party to this License, and makes no warranty whatsoever in connection with the Work. Creative Commons will not be liable to You or any party on any legal theory for any damages whatsoever, including without limitation any general, special, incidental or consequential damages arising in connection to this license. Notwithstanding the foregoing two (2) sentences, if Creative Commons has expressly identified itself as the Licensor hereunder, it shall have all rights and obligations of Licensor.

Except for the limited purpose of indicating to the public that the Work is licensed under the CCPL, Creative Commons does not authorize the use by either party of the trademark "Creative Commons" or any related trademark or logo of Creative Commons without the prior written consent of Creative Commons. Any permitted use will be in compliance with Creative Commons' then-current trademark usage guidelines, as may be published on its website or otherwise made available upon request from time to time. For the avoidance of doubt, this trademark restriction does not form part of this License.

B.2 Copyright Permission

The list of items that required copyright permissions can be seen in Table B.1.

Table B.2
List of figures and that require copyright permission

Figure #	Citation	Please refer to permission letter on page
Figure 2.1	[25]	192
Figure 2.2	[20]	192
Figure 2.3	[31]	192
Figure 2.4	[32]	188
Figure 2.5,2.6	[30]	192
Figure 2.7, 2.8 2.9	[25]	192
Figure 2.10	[31]	192
Figure 2.12	[27]	190
Figure 2.13, 2.14, 2.15, 2.16	[28]	174
Figure 2.17, 2.18, 2.19, 2.20, 2.21	[41]	176
Figure 2.22, 2.23	[29]	179
Figure 2.24	[48]	192
Figure 2.25	[49]	192
Figure 2.26	[50]	184
Figure 4.1	[57]	176
Figure A.1(a), A.1(b)	[71]	195
Figure A.5	[76]	198

Copyright permission for Figures 2.13 2.14 2.15 2.16 [28]

SPRINGER LICENSE TERMS AND CONDITIONS

Jun 06, 2013

This is a License Agreement between John R Armstead ("You") and Springer ("Springer") provided by Copyright Clearance Center ("CCC"). The license consists of your order details, the terms and conditions provided by Springer, and the payment terms and conditions.

All payments must be made in full to CCC. For payment instructions, please see information listed at the bottom of this form.

License Number	3134300102448
License date	Apr 22, 2013
Licensed content publisher	Springer
Licensed content publication	Journal of Electronic Materials
Licensed content title	Efficiency Study of a Commercial Thermoelectric Power Generator (TEG) Under Thermal Cycling
Licensed content author	E. Hatzikraniotis
Licensed content date	Jan 1, 2009
Volume number	39
Issue number	9
Type of Use	Thesis/Dissertation
Portion	Figures
Author of this Springer article	No
Order reference number	None
Title of your thesis / dissertation	Novel Automotive Waste Heat Recovery Techniques
Expected completion date	May 2013
Estimated size(pages)	200
Total	0.00 USD

Terms and Conditions

Introduction

The publisher for this copyrighted material is Springer Science + Business Media. By clicking "accept" in connection with completing this licensing transaction, you agree that the following terms and conditions apply to this transaction (along with the Billing and Payment terms and conditions established by Copyright Clearance Center, Inc. ("CCC"), at the time that you opened your Rightslink account and that are available at any time at <http://myaccount.copyright.com>).

Limited License

With reference to your request to reprint in your thesis material on which Springer Science and Business Media control the copyright, permission is granted, free of charge, for the use indicated in your enquiry.

Licenses are for one-time use only with a maximum distribution equal to the number that you identified in the licensing process.

This License includes use in an electronic form, provided its password protected or on the university's intranet or repository, including UMI (according to the definition at the Sherpa website: <http://www.sherpa.ac.uk/romeo/>). For any other electronic use, please contact Springer at (permissions.dordrecht@springer.com or permissions.heidelberg@springer.com).

The material can only be used for the purpose of defending your thesis, and with a maximum of 100 extra copies in paper.

Although Springer holds copyright to the material and is entitled to negotiate on rights, this license is only valid, subject to a courtesy information to the author (address is given with the article/chapter) and provided it concerns original material which does not carry references to other sources (if material in question appears with credit to another source, authorization from that source is required as well).

Permission free of charge on this occasion does not prejudice any rights we might have to charge for reproduction of our copyrighted material in the future.

Altering/Modifying Material: Not Permitted

You may not alter or modify the material in any manner. Abbreviations, additions, deletions and/or any other alterations shall be made only with prior written authorization of the author(s) and/or Springer Science + Business Media. (Please contact Springer at

(permissions.dordrecht@springer.com or permissions.heidelberg@springer.com)

Reservation of Rights

Springer Science + Business Media reserves all rights not specifically granted in the combination of (i) the license details provided by you and accepted in the course of this licensing transaction, (ii) these terms and conditions and (iii) CCC's Billing and Payment terms and conditions.

Copyright Notice:Disclaimer

You must include the following copyright and permission notice in connection with any reproduction of the licensed material: "Springer and the original publisher /journal title, volume, year of publication, page, chapter/article title, name(s) of author(s), figure number(s), original copyright notice) is given to the publication in which the material was originally published, by adding; with kind permission from Springer Science and Business Media"

Warranties: None

Example 1: Springer Science + Business Media makes no representations or warranties with respect to the licensed material.

Example 2: Springer Science + Business Media makes no representations or warranties with respect to the licensed material and adopts on its own behalf the limitations and disclaimers established by CCC on its behalf in its Billing and Payment terms and conditions for this licensing transaction.

Indemnity

You hereby indemnify and agree to hold harmless Springer Science + Business Media and CCC, and their respective officers, directors, employees and agents, from and against any and all claims arising out of your use of the licensed material other than as specifically authorized pursuant to this license.

No Transfer of License

This license is personal to you and may not be sublicensed, assigned, or transferred by you to any other person without Springer Science + Business Media's written permission.

No Amendment Except in Writing

This license may not be amended except in a writing signed by both parties (or, in the case of Springer Science + Business Media, by CCC on Springer Science + Business Media's behalf).

Objection to Contrary Terms

Springer Science + Business Media hereby objects to any terms contained in any purchase order, acknowledgment, check endorsement or other writing prepared by you, which terms are inconsistent with these terms and conditions or CCC's Billing and Payment terms and conditions. These terms and conditions, together with CCC's Billing and Payment terms and conditions (which are incorporated herein), comprise the entire agreement between you and Springer Science + Business Media (and CCC) concerning this licensing transaction. In the event of any conflict between your obligations established by these terms and conditions and those established by CCC's Billing and Payment terms and conditions, these terms and conditions shall control.

Jurisdiction

All disputes that may arise in connection with this present License, or the breach thereof, shall be settled exclusively by arbitration, to be held in The Netherlands, in accordance with Dutch law, and to be conducted under the Rules of the 'Netherlands Arbitrage Instituut' (Netherlands Institute of Arbitration). **OR:**

All disputes that may arise in connection with this present License, or the breach thereof, shall be settled exclusively by arbitration, to be held in the Federal Republic of Germany, in accordance with German law.

Other terms and conditions:

v1.3

If you would like to pay for this license now, please remit this license along with your payment made payable to "COPYRIGHT CLEARANCE CENTER" otherwise you will be invoiced within 48 hours of the license date. Payment should be in the form of a check or money order referencing your account number and this invoice number RLNK501005137.

Once you receive your invoice for this order, you may pay your invoice by credit card. Please follow instructions provided at that time.

Make Payment To:

Copyright Clearance Center

Dept 001

P.O. Box 843006

Boston, MA 02284-3006

For suggestions or comments regarding this order, contact RightsLink Customer Support: customer@copyright.com or +1-877-622-5543 (toll free in the US) or +1-978-646-2777.

Gratis licenses (referencing \$0 in the Total field) are free. Please retain this printable license for your reference. No payment is required.



John Armstead <jrarmste@mtu.edu>

REVISED: ASME PUBLICATIONS PERMISSION REQUEST FORM SUBMISSION

Beth Darchi <DarchiB@asme.org>
To: "jrarmste@mtu.edu" <jrarmste@mtu.edu>
Cc: Michelle DeBlasi <DeBlasiM@asme.org>

Mon, Jun 17, 2013 at 2:54 PM

Dear Mr. Armstead,

This letter has been revised to reflect all requests. It is our pleasure to grant you permission to publish the following ASME materials:

- **Figures 6, 7, 10, 14, 15** from "Design to Maximize Performance of a Thermoelectric Power Generator With a Dynamic Thermal Power Source," by Douglas T. Crane and Lon E. Bell, Journal of Energy Resources Technology, Volume 131, 2009
- **1 Figure** from "Results from the Second-Law of Thermodynamics for a Spark-Ignition Engine Using a Thermodynamic Engine Cycle Simulation," by Jerald A. Caton, Paper Number 99-ICE-239, 1999

as cited in your letter for inclusion in a Doctoral Thesis entitled Novel Automotive Waste Heat Recovery Techniques to be published by Michigan Technological University.

Permission is granted for the specific use as stated herein and does not permit further use of the materials without proper authorization. Proper attribution must be made to the author(s) of the materials, and no alterations of the materials is permitted in any material manner. As is customary, we request that you ensure proper acknowledgment of the exact sources of this material, the authors, and ASME as original publisher. Acknowledgment must be retained on all pages printed and distributed.

In accordance with ASME policy, this permission is contingent upon payment of a **Doctoral Thesis Discount** royalty fee of **US\$35 for 6 figures** (\$20.00 for the first figure/table, \$10 thereafter – actual fee \$70). This is solely charged to non-authors of the requested ASME papers. We accept payments on all major credit cards such as: Visa, MasterCard, American Express, Discover, and Diners Club, or by check payable to ASME. Please send payment to the attention Michelle DeBlasi, ASME Accounting, 22 Law Drive, Fairfield, NJ 07007, and indicate that this is a permission payment. Should you have any questions regarding payment form or transfer, please contact Ms. DeBlasi; P: 973-244-2268, F: 973-882-4924; E:deblasim@asme.org.

Many thanks for your interest in ASME publications.

Sincerely,

Beth Darchi
Copyrights & Permissions
ASME International
Two Park Avenue
New York, NY 10016
P: 212-591-7700
F: 212-591-7292
E: darchib@asme.org

-----Original Message-----

From: webmaster@asme.org [mailto:webmaster@asme.org]
Sent: Monday, April 08, 2013 12:00 AM
To: permissions@asme.org
Cc: jarmste@mtu.edu
Subject: ASME PUBLICATIONS PERMISSION REQUEST FORM SUBMISSION

ASME PUBLICATIONS PERMISSION REQUEST FORM HAS BEEN SUBMITTED:

ASME Publication Title: Design to Maximize Performance of a Thermoelectric Power Generator With a Dynamic Thermal Power Source
Complete List of Authors: Douglas T. Crane and Lon E. Bell
Paper Title (Conference/Journal): Journal of Energy Resources Technology
Paper Number (Conference): 012401-1
Volume Number (Journal): 131
Page(s) in the publication of
the permission request:
Year of Publication: 2009
I would like to... Republish in a Doctoral Thesis
Portion to be used: Figure/Table
List Figure Numbers: 6, 7, 10, 14, 15
List Table Numbers: 0
Number of Copies: 4
Usage: Both

Title of outside publication: Novel Automotive Waste Heat Recovery Techniques

Publisher: Michigan Technological University

Comments: doi:10.1115/1.3066392

First Name: John

Last Name: Armstead

Address Line 1: 907 Birch St.

Address Line 2:

City: Hancock

State: MI

Zip: 49930

Phone: 

Fax:

Email: jarmste@mtu.edu

ELSEVIER LICENSE TERMS AND CONDITIONS

Jun 06, 2013

This is a License Agreement between John R Armstead ("You") and Elsevier ("Elsevier") provided by Copyright Clearance Center ("CCC"). The license consists of your order details, the terms and conditions provided by Elsevier, and the payment terms and conditions.

All payments must be made in full to CCC. For payment instructions, please see information listed at the bottom of this form.

Supplier	Elsevier Limited The Boulevard, Langford Lane Kidlington, Oxford, OX5 1GB, UK
Registered Company Number	1982084
Customer name	John R Armstead
Customer address	907 Birch St. Hancock, MI 49930
License number	3124000696951
License date	Apr 08, 2013
Licensed content publisher	Elsevier
Licensed content publication	Energy Conversion and Management
Licensed content title	Optimization of cross flow heat exchangers for thermoelectric waste heat recovery
Licensed content author	Douglas T. Crane, Gregory S. Jackson
Licensed content date	June 2004
Licensed content volume number	45
Licensed content issue number	9–10
Number of pages	18
Start Page	1565
End Page	1582
Type of Use	reuse in a thesis/dissertation
Intended publisher of new work	other
Portion	figures/tables/illustrations
Number of figures/tables/illustrations	2
Format	both print and electronic
Are you the author of this Elsevier article?	No
Will you be translating?	No
Order reference number	None
Title of your thesis/dissertation	Novel Automotive Waste Heat Recovery Techniques
Expected completion date	May 2013
Estimated size (number of pages)	200
Elsevier VAT number	GB 494 6272 12
Permissions price	0.00 USD
VAT/Local Sales Tax	0.0 USD / 0.0 GBP

Total 0.00 USD

Terms and Conditions

INTRODUCTION

1. The publisher for this copyrighted material is Elsevier. By clicking "accept" in connection with completing this licensing transaction, you agree that the following terms and conditions apply to this transaction (along with the Billing and Payment terms and conditions established by Copyright Clearance Center, Inc. ("CCC"), at the time that you opened your Rightslink account and that are available at any time at <http://myaccount.copyright.com>).

GENERAL TERMS

2. Elsevier hereby grants you permission to reproduce the aforementioned material subject to the terms and conditions indicated.

3. Acknowledgement: If any part of the material to be used (for example, figures) has appeared in our publication with credit or acknowledgement to another source, permission must also be sought from that source. If such permission is not obtained then that material may not be included in your publication/copies. Suitable acknowledgement to the source must be made, either as a footnote or in a reference list at the end of your publication, as follows:

"Reprinted from Publication title, Vol /edition number, Author(s), Title of article / title of chapter, Pages No., Copyright (Year), with permission from Elsevier [OR APPLICABLE SOCIETY COPYRIGHT OWNER]." Also Lancet special credit - "Reprinted from The Lancet, Vol. number, Author(s), Title of article, Pages No., Copyright (Year), with permission from Elsevier."

4. Reproduction of this material is confined to the purpose and/or media for which permission is hereby given.

5. Altering/Modifying Material: Not Permitted. However figures and illustrations may be altered/adapted minimally to serve your work.

Any other abbreviations, additions, deletions and/or any other alterations shall be made only with prior written authorization of Elsevier Ltd. (Please contact Elsevier at permissions@elsevier.com)

6. If the permission fee for the requested use of our material is waived in this instance, please be advised that your future requests for Elsevier materials may attract a fee.

7. Reservation of Rights: Publisher reserves all rights not specifically granted in the combination of (i) the license details provided by you and accepted in the course of this licensing transaction, (ii) these terms and conditions and (iii) CCC's Billing and Payment terms and conditions.

8. License Contingent Upon Payment: While you may exercise the rights licensed immediately upon issuance of the license at the end of the licensing process for the transaction, provided that you have disclosed complete and accurate details of your proposed use, no license is finally effective unless and until full payment is received from you (either by publisher or by CCC) as provided in CCC's Billing and Payment terms and conditions. If full payment is not received on a timely basis, then any license preliminarily granted shall be deemed automatically revoked and shall be void as if never granted. Further, in the event that you breach any of these terms and conditions or any of CCC's Billing and Payment terms and conditions, the license is automatically revoked and shall be void as if never granted. Use of materials as described in a revoked license, as well as any use of the materials beyond the scope of an unrevoked license, may constitute copyright infringement and publisher reserves the right to take any and all action to protect its copyright in the materials.

9. Warranties: Publisher makes no representations or warranties with respect to the licensed material.

10. Indemnity: You hereby indemnify and agree to hold harmless publisher and CCC, and their respective officers, directors, employees and agents, from and against any and all claims arising out of your use of the licensed material other than as specifically authorized pursuant to this license.

11. No Transfer of License: This license is personal to you and may not be sublicensed, assigned, or transferred by you to any other person without publisher's written permission.

12. No Amendment Except in Writing: This license may not be amended except in a writing signed by both parties (or, in the case of publisher, by CCC on publisher's behalf).

13. Objection to Contrary Terms: Publisher hereby objects to any terms contained in any purchase order, acknowledgment, check endorsement or other writing prepared by you, which terms are inconsistent with these terms and conditions or CCC's Billing and Payment terms and conditions. These terms and conditions, together with CCC's Billing and Payment terms and conditions (which are incorporated herein), comprise the entire agreement between you and publisher (and CCC) concerning this licensing transaction. In the event of any conflict between your obligations established by these terms and conditions and those established by CCC's Billing and Payment terms and conditions, these terms and conditions shall control.

14. Revocation: Elsevier or Copyright Clearance Center may deny the permissions described in this License at their sole discretion, for any reason or no reason, with a full refund payable to you. Notice of such denial will be made using the contact information provided by you. Failure to receive such notice will not alter or invalidate the denial. In no event will Elsevier or Copyright Clearance Center be responsible or liable for any costs, expenses or damage incurred by you as a result of a denial of your permission request, other than a refund of the amount(s) paid by you to Elsevier and/or Copyright Clearance Center for denied permissions.

LIMITED LICENSE

The following terms and conditions apply only to specific license types:

15. **Translation:** This permission is granted for non-exclusive world **English** rights only unless your license was granted for translation rights. If you licensed translation rights you may only translate this content into the languages you requested. A professional translator must perform all translations and reproduce the content word for word preserving the integrity of the article. If this license is to re-use 1 or 2 figures then permission is granted for non-exclusive world rights in all languages.

16. **Website:** The following terms and conditions apply to electronic reserve and author websites:

Electronic reserve: If licensed material is to be posted to website, the web site is to be password-protected and made available only

to bona fide students registered on a relevant course if:

This license was made in connection with a course,

This permission is granted for 1 year only. You may obtain a license for future website posting,

All content posted to the web site must maintain the copyright information line on the bottom of each image,

A hyper-text must be included to the Homepage of the journal from which you are licensing at

<http://www.sciencedirect.com/science/journal/xxxxx> or the Elsevier homepage for books at <http://www.elsevier.com> , and

Central Storage: This license does not include permission for a scanned version of the material to be stored in a central repository such as that provided by Heron/XanEdu.

17. **Author website** for journals with the following additional clauses:

All content posted to the web site must maintain the copyright information line on the bottom of each image, and the permission granted is limited to the personal version of your paper. You are not allowed to download and post the published electronic version of your article (whether PDF or HTML, proof or final version), nor may you scan the printed edition to create an electronic version. A hyper-text must be included to the Homepage of the journal from which you are licensing at

<http://www.sciencedirect.com/science/journal/xxxxx> . As part of our normal production process, you will receive an e-mail notice when your article appears on Elsevier's online service ScienceDirect (www.sciencedirect.com). That e-mail will include the article's Digital Object Identifier (DOI). This number provides the electronic link to the published article and should be included in the posting of your personal version. We ask that you wait until you receive this e-mail and have the DOI to do any posting.

Central Storage: This license does not include permission for a scanned version of the material to be stored in a central repository such as that provided by Heron/XanEdu.

18. **Author website** for books with the following additional clauses:

Authors are permitted to place a brief summary of their work online only.

A hyper-text must be included to the Elsevier homepage at <http://www.elsevier.com> . All content posted to the web site must maintain the copyright information line on the bottom of each image. You are not allowed to download and post the published electronic version of your chapter, nor may you scan the printed edition to create an electronic version.

Central Storage: This license does not include permission for a scanned version of the material to be stored in a central repository such as that provided by Heron/XanEdu.

19. **Website** (regular and for author): A hyper-text must be included to the Homepage of the journal from which you are licensing at <http://www.sciencedirect.com/science/journal/xxxxx> or for books to the Elsevier homepage at <http://www.elsevier.com>

20. **Thesis/Dissertation**: If your license is for use in a thesis/dissertation your thesis may be submitted to your institution in either print or electronic form. Should your thesis be published commercially, please reapply for permission. These requirements include permission for the Library and Archives of Canada to supply single copies, on demand, of the complete thesis and include permission for UMI to supply single copies, on demand, of the complete thesis. Should your thesis be published commercially, please reapply for permission.

21. **Other Conditions**:

v1.6

If you would like to pay for this license now, please remit this license along with your payment made payable to "COPYRIGHT CLEARANCE CENTER" otherwise you will be invoiced within 48 hours of the license date. Payment should be in the form of a check or money order referencing your account number and this invoice number None500994474.

Once you receive your invoice for this order, you may pay your invoice by credit card. Please follow instructions provided at that time.

Make Payment To:

Copyright Clearance Center

Dept 001

P.O. Box 843006

Boston, MA 02284-3006

For suggestions or comments regarding this order, contact RightsLink Customer Support: customer care@copyright.com or +1-877-622-5543 (toll free in the US) or +1-978-646-2777.

Gratis licenses (referencing \$0 in the Total field) are free. Please retain this printable license for your reference. No payment is required.

Elsevier and/or Copyright Clearance Center for denied permissions.

LIMITED LICENSE

The following terms and conditions apply only to specific license types:

15. **Translation:** This permission is granted for non-exclusive world **English** rights only unless your license was granted for translation rights. If you licensed translation rights you may only translate this content into the languages you requested. A professional translator must perform all translations and reproduce the content word for word preserving the integrity of the article. If this license is to re-use 1 or 2 figures then permission is granted for non-exclusive world rights in all languages.

16. **Website:** The following terms and conditions apply to electronic reserve and author websites:
Electronic reserve: If licensed material is to be posted to website, the web site is to be password-protected and made available only to bona fide students registered on a relevant course if:

This license was made in connection with a course,

This permission is granted for 1 year only. You may obtain a license for future website posting. All content posted to the web site must maintain the copyright information line on the bottom of each image,

A hyper-text must be included to the Homepage of the journal from which you are licensing at <http://www.sciencedirect.com/science/journal/xxxxx> or the Elsevier homepage for books at <http://www.elsevier.com> , and

Central Storage: This license does not include permission for a scanned version of the material to be stored in a central repository such as that provided by Heron/XanEdu.

17. **Author website** for journals with the following additional clauses:

All content posted to the web site must maintain the copyright information line on the bottom of each image, and the permission granted is limited to the personal version of your paper. You are not allowed to download and post the published electronic version of your article (whether PDF or HTML, proof or final version), nor may you scan the printed edition to create an electronic version. A hyper-text must be included to the Homepage of the journal from which you are licensing at <http://www.sciencedirect.com/science/journal/xxxxx> . As part of our normal production process, you will receive an e-mail notice when your article appears on Elsevier's online service ScienceDirect (www.sciencedirect.com). That e-mail will include the article's Digital Object Identifier (DOI). This number provides the electronic link to the published article and should be included in the posting of your personal version. We ask that you wait until you receive this e-mail and have the DOI to do any posting.

Central Storage: This license does not include permission for a scanned version of the material to be stored in a central repository such as that provided by Heron/XanEdu.

18. **Author website** for books with the following additional clauses:

Authors are permitted to place a brief summary of their work online only.

A hyper-text must be included to the Elsevier homepage at <http://www.elsevier.com> . All content

posted to the web site must maintain the copyright information line on the bottom of each image. You are not allowed to download and post the published electronic version of your chapter, nor may you scan the printed edition to create an electronic version.

Central Storage: This license does not include permission for a scanned version of the material to be stored in a central repository such as that provided by Heron/XanEdu.

19. **Website** (regular and for author): A hyper-text must be included to the Homepage of the journal from which you are licensing at <http://www.sciencedirect.com/science/journal/xxxxx> or for books to the Elsevier homepage at <http://www.elsevier.com>

20. **Thesis/Dissertation**: If your license is for use in a thesis/dissertation your thesis may be submitted to your institution in either print or electronic form. Should your thesis be published commercially, please reapply for permission. These requirements include permission for the Library and Archives of Canada to supply single copies, on demand, of the complete thesis and include permission for UMI to supply single copies, on demand, of the complete thesis. Should your thesis be published commercially, please reapply for permission.

21. **Other Conditions**:

v1.6

If you would like to pay for this license now, please remit this license along with your payment made payable to "COPYRIGHT CLEARANCE CENTER" otherwise you will be invoiced within 48 hours of the license date. Payment should be in the form of a check or money order referencing your account number and this invoice number RLNK500994474. Once you receive your invoice for this order, you may pay your invoice by credit card. Please follow instructions provided at that time.

Make Payment To:
Copyright Clearance Center
Dept 001
P.O. Box 843006
Boston, MA 02284-3006

For suggestions or comments regarding this order, contact RightsLink Customer Support: customercare@copyright.com or +1-877-622-5543 (toll free in the US) or +1-978-646-2777.

Gratis licenses (referencing \$0 in the Total field) are free. Please retain this printable license for your reference. No payment is required.

JOHN WILEY AND SONS LICENSE TERMS AND CONDITIONS

Jun 06, 2013

This is a License Agreement between John R Armstead ("You") and John Wiley and Sons ("John Wiley and Sons") provided by Copyright Clearance Center ("CCC"). The license consists of your order details, the terms and conditions provided by John Wiley and Sons, and the payment terms and conditions.

All payments must be made in full to CCC. For payment instructions, please see information listed at the bottom of this form.

License Number	3124001235771
License date	Apr 08, 2013
Licensed content publisher	John Wiley and Sons
Licensed content publication	International Journal of Energy Research
Licensed content title	An examination of exergy destruction in organic Rankine cycles
Licensed copyright line	Copyright © 2008 John Wiley & Sons, Ltd.
Licensed content author	P. J. Mago, K. K. Srinivasan, L. M. Chamra, C. Somayaji
Licensed content date	Feb 25, 2008
Start page	926
End page	938
Type of use	Dissertation/Thesis
Requestor type	University/Academic
Format	Print and electronic
Portion	Figure/table
Number of figures/tables	1
Original Wiley figure/table number(s)	Figure 1
Will you be translating?	No
Total	0.00 USD
Terms and Conditions	

TERMS AND CONDITIONS

This copyrighted material is owned by or exclusively licensed to John Wiley & Sons, Inc. or one of its group companies (each a "Wiley Company") or a society for whom a Wiley Company has exclusive publishing rights in relation to a particular journal (collectively "WILEY"). By clicking "accept" in connection with completing this licensing transaction, you agree that the following terms and conditions apply to this transaction (along with the billing and payment terms and conditions established by the Copyright Clearance Center Inc., ("CCC's Billing and Payment terms and conditions"), at the time that you opened your RightsLink account (these are available at any time at <http://myaccount.copyright.com>).

Terms and Conditions

1. The materials you have requested permission to reproduce (the "Materials") are protected by copyright.
2. You are hereby granted a personal, non-exclusive, non-sublicensable, non-transferable, worldwide, limited license to reproduce the Materials for the purpose specified in the licensing process. This license is for a one-time use only with a maximum distribution equal to the number that you identified in the licensing process. Any form of republication granted by this license must be completed within two years of the date of the grant of this license (although copies prepared before may be distributed thereafter). The Materials shall not be used in any other manner or for any other purpose. Permission is granted subject to an appropriate acknowledgement given to the author, title of the material/book/journal and the publisher. You shall also duplicate the copyright notice that appears in the Wiley publication in your use of the Material. Permission is also granted on the understanding that nowhere in the text is a previously published source acknowledged for all or part of this Material. Any third party material is expressly excluded from this permission.
3. With respect to the Materials, all rights are reserved. Except as expressly granted by the terms of the license, no part of the Materials may be copied, modified, adapted (except for minor reformatting required by the new Publication), translated, reproduced, transferred or distributed, in any form or by any means, and no derivative works may be made based on the Materials without the prior permission

of the respective copyright owner. You may not alter, remove or suppress in any manner any copyright, trademark or other notices displayed by the Materials. You may not license, rent, sell, loan, lease, pledge, offer as security, transfer or assign the Materials, or any of the rights granted to you hereunder to any other person.

4. The Materials and all of the intellectual property rights therein shall at all times remain the exclusive property of John Wiley & Sons Inc or one of its related companies (WILEY) or their respective licensors, and your interest therein is only that of having possession of and the right to reproduce the Materials pursuant to Section 2 herein during the continuance of this Agreement. You agree that you own no right, title or interest in or to the Materials or any of the intellectual property rights therein. You shall have no rights hereunder other than the license as provided for above in Section 2. No right, license or interest to any trademark, trade name, service mark or other branding ("Marks") of WILEY or its licensors is granted hereunder, and you agree that you shall not assert any such right, license or interest with respect thereto.

5. NEITHER WILEY NOR ITS LICENSORS MAKES ANY WARRANTY OR REPRESENTATION OF ANY KIND TO YOU OR ANY THIRD PARTY, EXPRESS, IMPLIED OR STATUTORY, WITH RESPECT TO THE MATERIALS OR THE ACCURACY OF ANY INFORMATION CONTAINED IN THE MATERIALS, INCLUDING, WITHOUT LIMITATION, ANY IMPLIED WARRANTY OF MERCHANTABILITY, ACCURACY, SATISFACTORY QUALITY, FITNESS FOR A PARTICULAR PURPOSE, USABILITY, INTEGRATION OR NON-INFRINGEMENT AND ALL SUCH WARRANTIES ARE HEREBY EXCLUDED BY WILEY AND ITS LICENSORS AND WAIVED BY YOU.

6. WILEY shall have the right to terminate this Agreement immediately upon breach of this Agreement by you.

7. You shall indemnify, defend and hold harmless WILEY, its Licensors and their respective directors, officers, agents and employees, from and against any actual or threatened claims, demands, causes of action or proceedings arising from any breach of this Agreement by you.

8. IN NO EVENT SHALL WILEY OR ITS LICENSORS BE LIABLE TO YOU OR ANY OTHER PARTY OR ANY OTHER PERSON OR ENTITY FOR ANY SPECIAL, CONSEQUENTIAL, INCIDENTAL, INDIRECT, EXEMPLARY OR PUNITIVE DAMAGES, HOWEVER CAUSED, ARISING OUT OF OR IN CONNECTION WITH THE DOWNLOADING, PROVISIONING, VIEWING OR USE OF THE MATERIALS REGARDLESS OF THE FORM OF ACTION, WHETHER FOR BREACH OF CONTRACT, BREACH OF WARRANTY, TORT, NEGLIGENCE, INFRINGEMENT OR OTHERWISE (INCLUDING, WITHOUT LIMITATION, DAMAGES BASED ON LOSS OF PROFITS, DATA, FILES, USE, BUSINESS OPPORTUNITY OR CLAIMS OF THIRD PARTIES), AND WHETHER OR NOT THE PARTY HAS BEEN ADVISED OF THE POSSIBILITY OF SUCH DAMAGES. THIS LIMITATION SHALL APPLY NOTWITHSTANDING ANY FAILURE OF ESSENTIAL PURPOSE OF ANY LIMITED REMEDY PROVIDED HEREIN.

9. Should any provision of this Agreement be held by a court of competent jurisdiction to be illegal, invalid, or unenforceable, that provision shall be deemed amended to achieve as nearly as possible the same economic effect as the original provision, and the legality, validity and enforceability of the remaining provisions of this Agreement shall not be affected or impaired thereby.

10. The failure of either party to enforce any term or condition of this Agreement shall not constitute a waiver of either party's right to enforce each and every term and condition of this Agreement. No breach under this agreement shall be deemed waived or excused by either party unless such waiver or consent is in writing signed by the party granting such waiver or consent. The waiver by or consent of a party to a breach of any provision of this Agreement shall not operate or be construed as a waiver of or consent to any other or subsequent breach by such other party.

11. This Agreement may not be assigned (including by operation of law or otherwise) by you without WILEY's prior written consent.

12. Any fee required for this permission shall be non-refundable after thirty (30) days from receipt

13. These terms and conditions together with CCC's Billing and Payment terms and conditions (which are incorporated herein) form the entire agreement between you and WILEY concerning this licensing transaction and (in the absence of fraud) supersedes all prior agreements and representations of the parties, oral or written. This Agreement may not be amended except in writing signed by both parties. This Agreement shall be binding upon and inure to the benefit of the parties' successors, legal representatives, and authorized assigns.

14. In the event of any conflict between your obligations established by these terms and conditions and those established by CCC's Billing and Payment terms and conditions, these terms and conditions shall prevail.

15. WILEY expressly reserves all rights not specifically granted in the combination of (i) the license details provided by you and accepted in the course of this licensing transaction, (ii) these terms and conditions and (iii) CCC's Billing and Payment terms and conditions.

16. This Agreement will be void if the Type of Use, Format, Circulation, or Requestor Type was misrepresented during the licensing process.

17. This Agreement shall be governed by and construed in accordance with the laws of the State of New York, USA, without regards to such state's conflict of law rules. Any legal action, suit or proceeding arising out of or relating to these Terms and Conditions or the breach thereof shall be instituted in a court of competent jurisdiction in New York County in the State of New York in the United States of America and each party hereby consents and submits to the personal jurisdiction of such court, waives any objection to venue in such court and consents to service of process by registered or certified mail, return receipt requested, at the last known address of such party.

Wiley Open Access Terms and Conditions

Wiley publishes Open Access articles in both its Wiley Open Access Journals program [<http://www.wileyopenaccess.com/view/index.html>] and as Online Open articles in its subscription journals. The majority of Wiley Open Access Journals have adopted the [Creative Commons Attribution License](#) (CC BY) which permits the unrestricted use, distribution, reproduction, adaptation and commercial exploitation of the article in any medium. No permission is required to use the article in this way provided that the article is properly cited and other license terms are observed. A small number of Wiley Open Access journals

have retained the [Creative Commons Attribution Non Commercial License](#) (CC BY-NC), which permits use, distribution and reproduction in any medium, provided the original work is properly cited and is not used for commercial purposes.

Online Open articles - Authors selecting Online Open are, unless particular exceptions apply, offered a choice of Creative Commons licenses. They may therefore select from the CC BY, the CC BY-NC and the [Attribution-NoDerivatives](#) (CC BY-NC-ND). The CC BY-NC-ND is more restrictive than the CC BY-NC as it does not permit adaptations or modifications without rights holder consent.

Wiley Open Access articles are protected by copyright and are posted to repositories and websites in accordance with the terms of the applicable Creative Commons license referenced on the article. At the time of deposit, Wiley Open Access articles include all changes made during peer review, copyediting, and publishing. Repositories and websites that host the article are responsible for incorporating any publisher-supplied amendments or retractions issued subsequently.

Wiley Open Access articles are also available without charge on Wiley's publishing platform, **Wiley Online Library** or any successor sites.

Conditions applicable to all Wiley Open Access articles:

- The authors' moral rights must not be compromised. These rights include the right of "paternity" (also known as "attribution" - the right for the author to be identified as such) and "integrity" (the right for the author not to have the work altered in such a way that the author's reputation or integrity may be damaged).
- Where content in the article is identified as belonging to a third party, it is the obligation of the user to ensure that any reuse complies with the copyright policies of the owner of that content.
- If article content is copied, downloaded or otherwise reused for research and other purposes as permitted, a link to the appropriate bibliographic citation (authors, journal, article title, volume, issue, page numbers, DOI and the link to the definitive published version on Wiley Online Library) should be maintained. Copyright notices and disclaimers must not be deleted.
 - Creative Commons licenses are copyright licenses and do not confer any other rights, including but not limited to trademark or patent rights.
- Any translations, for which a prior translation agreement with Wiley has not been agreed, must prominently display the statement: "This is an unofficial translation of an article that appeared in a Wiley publication. The publisher has not endorsed this translation."

Conditions applicable to non-commercial licenses (CC BY-NC and CC BY-NC-ND)

For non-commercial and non-promotional purposes individual non-commercial users may access, download, copy, display and redistribute to colleagues Wiley Open Access articles. In addition, articles adopting the CC BY-NC may be adapted, translated, and text- and data-mined subject to the conditions above.

Use by commercial "for-profit" organizations

Use of non-commercial Wiley Open Access articles for commercial, promotional, or marketing purposes requires further explicit permission from Wiley and will be subject to a fee. Commercial purposes include:

- Copying or downloading of articles, or linking to such articles for further redistribution, sale or licensing;
- Copying, downloading or posting by a site or service that incorporates advertising with such content;
- The inclusion or incorporation of article content in other works or services (other than normal quotations with an appropriate citation) that is then available for sale or licensing, for a fee (for example, a compilation produced for marketing purposes, inclusion in a sales pack)
- Use of article content (other than normal quotations with appropriate citation) by for-profit organizations for promotional purposes
- Linking to article content in e-mails redistributed for promotional, marketing or educational purposes;
- Use for the purposes of monetary reward by means of sale, resale, license, loan, transfer or other form of commercial exploitation such as marketing products
- Print reprints of Wiley Open Access articles can be purchased from: corporatesales@wiley.com

The modification or adaptation for any purpose of an article referencing the CC BY-NC-ND License requires consent which can be requested from RightsLink@wiley.com.

Other Terms and Conditions:

BY CLICKING ON THE "I AGREE..." BOX, YOU ACKNOWLEDGE THAT YOU HAVE READ AND FULLY UNDERSTAND EACH OF THE SECTIONS OF AND PROVISIONS SET FORTH IN THIS AGREEMENT AND THAT YOU ARE IN AGREEMENT WITH AND ARE WILLING TO ACCEPT ALL OF YOUR OBLIGATIONS AS SET FORTH IN THIS AGREEMENT.

v1.8

If you would like to pay for this license now, please remit this license along with your payment made payable to "COPYRIGHT CLEARANCE CENTER" otherwise you will be invoiced within 48 hours of the license date. Payment should be in the form of a check or money order referencing your account number and this invoice number None500994477.

Once you receive your invoice for this order, you may pay your invoice by credit card. Please follow instructions provided at that time.

Make Payment To:
Copyright Clearance Center
Dept 001
P.O. Box 843006
Boston, MA 02284-3006

For suggestions or comments regarding this order, contact RightsLink Customer Support: customercare@copyright.com or +1-877-622-5543 (toll free in the US) or +1-978-646-2777.

Gratis licenses (referencing \$0 in the Total field) are free. Please retain this printable license for your reference. No payment is required.

Copyright permission for Figure 2.4: [32]

4/21/13

Copyright Clearance Center



Confirmation Number: 11087256
Order Date: 04/21/2013

Customer Information

Customer: John Armstead
Account Number: 3000643386
Organization: John Armstead
Email: jarmste@mtu.edu
Phone: +1 [REDACTED]
Payment Method: Invoice

Order Details

Thermoelectrics handbook : macro to nano

Billing Status:
N/A

Order detail ID: 63617814
ISBN: 978-0-8493-2264-8
Publication Book
Type:
Publisher: TAYLOR & FRANCIS GROUP LLC
Author/Editor: ROWE, D.M.

Permission Status: ☒ **Granted**
Permission type: Republish or display content
Type of use: Republish in a thesis/dissertation
Order License Id: 3133921439459

Requestor type	Academic institution
Format	Print, Electronic
Portion	chart/graph/table/figure
Number of charts/graphs/tables/figures	1
Title or numeric reference of the portion(s)	(Exact figure # unknown) Schematic of single thermo-electric couple operating in Seebeck and Peltier modes respectively
Editor of portion(s)	N/A
Author of portion(s)	N/A
Volume of serial or monograph	N/A
Issue, if republishing an article from a serial	N/A
Page range of portion	N/A
Publication date of portion	May 2013
Rights for	Main product
Duration of use	Life of current edition
Creation of copies for the disabled	no
With minor editing privileges	no
For distribution to	United States
In the following language(s)	Original language of publication
With incidental promotional use	no
Lifetime unit quantity of new product	0 to 499

<https://www.copyright.com/printOrder.do?id=11087256>

1/2

4/21/13

Copyright Clearance Center

Made available in the following markets	education
The requesting person/organization	John R Armstead
Order reference number	
Author/Editor	John R Armstead
The standard identifier	?
The proposed price	\$0.00
Title	Novel Automotive Waste Heat Recovery Techniques
Publisher	Michigan Technological University
Expected publication date	May 2013
Estimated size (pages)	200

Note: This item was invoiced separately through our **RightsLink service**. [More info](#)

\$ 0.00

Total order items: 1

Order Total: \$0.00

[Get Permission](#) | [License Your Content](#) | [Products And Solutions](#) | [Partners](#) | [Education](#) | [About Us](#)
[Privacy Policy](#) | [Terms & Conditions](#)

Copyright 2013 Copyright Clearance Center

Copyright permission for Figure 2.12: [27]

SPRINGER LICENSE TERMS AND CONDITIONS

Jun 06, 2013

This is a License Agreement between John R Armstead ("You") and Springer ("Springer") provided by Copyright Clearance Center ("CCC"). The license consists of your order details, the terms and conditions provided by Springer, and the payment terms and conditions.

All payments must be made in full to CCC. For payment instructions, please see information listed at the bottom of this form.

License Number	3141400328944
License date	May 03, 2013
Licensed content publisher	Springer
Licensed content publication	Journal of Electronic Materials
Licensed content title	Automotive Applications of Thermoelectric Materials
Licensed content author	Jihui Yang
Licensed content date	Jan 1, 2009
Volume number	38
Issue number	7
Type of Use	Thesis/Dissertation
Portion	Figures
Author of this Springer article	No
Order reference number	None
Title of your thesis / dissertation	Novel Automotive Waste Heat Recovery Techniques
Expected completion date	May 2013
Estimated size(pages)	200
Total	0.00 USD

Terms and Conditions

Introduction

The publisher for this copyrighted material is Springer Science + Business Media. By clicking "accept" in connection with completing this licensing transaction, you agree that the following terms and conditions apply to this transaction (along with the Billing and Payment terms and conditions established by Copyright Clearance Center, Inc. ("CCC"), at the time that you opened your Rightslink account and that are available at any time at <http://myaccount.copyright.com>).

Limited License

With reference to your request to reprint in your thesis material on which Springer Science and Business Media control the copyright, permission is granted, free of charge, for the use indicated in your enquiry.

Licenses are for one-time use only with a maximum distribution equal to the number that you identified in the licensing process.

This License includes use in an electronic form, provided its password protected or on the university's intranet or repository, including UMI (according to the definition at the Sherpa website: <http://www.sherpa.ac.uk/romeo/>). For any other electronic use, please contact Springer at (permissions.dordrecht@springer.com or permissions.heidelberg@springer.com).

The material can only be used for the purpose of defending your thesis, and with a maximum of 100 extra copies in paper.

Although Springer holds copyright to the material and is entitled to negotiate on rights, this license is only valid, subject to a courtesy information to the author (address is given with the article/chapter) and provided it concerns original material which does not carry references to other sources (if material in question appears with credit to another source, authorization from that source is required as well).

Permission free of charge on this occasion does not prejudice any rights we might have to charge for reproduction of our copyrighted material in the future.

Altering/Modifying Material: Not Permitted

You may not alter or modify the material in any manner. Abbreviations, additions, deletions and/or any other alterations shall be made only with prior written authorization of the author(s) and/or Springer Science + Business Media. (Please contact Springer at

(permissions.dordrecht@springer.com or permissions.heidelberg@springer.com)

Reservation of Rights

Springer Science + Business Media reserves all rights not specifically granted in the combination of (i) the license details provided by you and accepted in the course of this licensing transaction, (ii) these terms and conditions and (iii) CCC's Billing and Payment terms and conditions.

Copyright Notice:Disclaimer

You must include the following copyright and permission notice in connection with any reproduction of the licensed material: "Springer and the original publisher /journal title, volume, year of publication, page, chapter/article title, name(s) of author(s), figure number(s), original copyright notice) is given to the publication in which the material was originally published, by adding; with kind permission from Springer Science and Business Media"

Warranties: None

Example 1: Springer Science + Business Media makes no representations or warranties with respect to the licensed material.

Example 2: Springer Science + Business Media makes no representations or warranties with respect to the licensed material and adopts on its own behalf the limitations and disclaimers established by CCC on its behalf in its Billing and Payment terms and conditions for this licensing transaction.

Indemnity

You hereby indemnify and agree to hold harmless Springer Science + Business Media and CCC, and their respective officers, directors, employees and agents, from and against any and all claims arising out of your use of the licensed material other than as specifically authorized pursuant to this license.

No Transfer of License

This license is personal to you and may not be sublicensed, assigned, or transferred by you to any other person without Springer Science + Business Media's written permission.

No Amendment Except in Writing

This license may not be amended except in a writing signed by both parties (or, in the case of Springer Science + Business Media, by CCC on Springer Science + Business Media's behalf).

Objection to Contrary Terms

Springer Science + Business Media hereby objects to any terms contained in any purchase order, acknowledgment, check endorsement or other writing prepared by you, which terms are inconsistent with these terms and conditions or CCC's Billing and Payment terms and conditions. These terms and conditions, together with CCC's Billing and Payment terms and conditions (which are incorporated herein), comprise the entire agreement between you and Springer Science + Business Media (and CCC) concerning this licensing transaction. In the event of any conflict between your obligations established by these terms and conditions and those established by CCC's Billing and Payment terms and conditions, these terms and conditions shall control.

Jurisdiction

All disputes that may arise in connection with this present License, or the breach thereof, shall be settled exclusively by arbitration, to be held in The Netherlands, in accordance with Dutch law, and to be conducted under the Rules of the 'Netherlands Arbitrage Instituut' (Netherlands Institute of Arbitration). **OR:**

All disputes that may arise in connection with this present License, or the breach thereof, shall be settled exclusively by arbitration, to be held in the Federal Republic of Germany, in accordance with German law.

Other terms and conditions:

v1.3

If you would like to pay for this license now, please remit this license along with your payment made payable to "COPYRIGHT CLEARANCE CENTER" otherwise you will be invoiced within 48 hours of the license date. Payment should be in the form of a check or money order referencing your account number and this invoice number RLNK501013832.

Once you receive your invoice for this order, you may pay your invoice by credit card. Please follow instructions provided at that time.

Make Payment To:

Copyright Clearance Center

Dept 001

P.O. Box 843006

Boston, MA 02284-3006

For suggestions or comments regarding this order, contact RightsLink Customer Support: customer care@copyright.com or +1-877-622-5543 (toll free in the US) or +1-978-646-2777.

Gratis licenses (referencing \$0 in the Total field) are free. Please retain this printable license for your reference. No payment is required.

Copyright permission for Figure 2.24: [48],

Figures 2.1 2.7 2.8 2.9: [25],

Figures 2.3 2.10: [31], Figure 2.2: [20], Figures 2.5 2.6: [30], Figure 2.25: [49]



John Armstead <jarmste@mtu.edu>

Request to reprint SAE Material in a PhD Dissertation

Terri Kelly <terri@sae.org>
To: John Armstead <jarmste@mtu.edu>

Tue, Apr 23, 2013 at 4:08 PM

Dear John,

Thank you for your correspondence requesting permission to reprint the figures noted below from several SAE paper numbers in your doctoral dissertation for Michigan Technological University entitled "Novel Automotive Waste Heat Recovery Techniques."

Permission is hereby granted, and subject to the following conditions:

- Permission is for this one time single use only. New requests are required to distribute additional copies of your dissertation, or for further use or distribution of the SAE material.
- The following credit statement must appear directly below the figures: "Reprinted with permission from SAE Paper No. XXXXXX* © 200X** SAE International." *please insert the paper number and **year of publication
- For each figure, you must provide a reference to the paper author(s), paper number and SAE in the reference section of your dissertation.
- This permission does not cover any third party copyrighted work which may appear in the material requested. If figures are referenced to another publication, permission must be obtained from the original source (paper author).

Please feel free to contact me if you need further assistance.

Best regards,

Terri Kelly

Intellectual Property Rights Administrator

SAE International | 400 Commonwealth Drive | Warrendale, PA 15096-0001 | USA

Office: +01 724-772-4095 | Fax: +01 724-776-9765

terri@sae.org | www.sae.org

From: John Armstead [mailto:jrarmste@mtu.edu]
Sent: Monday, April 08, 2013 12:52 AM
To: copyright
Subject: Request to reprint SAE Material in a PhD Dissertation

SAE Copyright Administrator
SAE International
400 Commonwealth Drive
Warrendale, PA 15096-0001 - USA
email: copyright@sae.org
fax: 724-776-9765

I am completing a doctoral dissertation at Michigan Technological University entitled "Novel Automotive Waste Heat Recovery Techniques." I would like your permission to reprint select figures from the following journal articles. This dissertation will be in both print and electronic format. The number of copies will be approximately four (personal use, adviser, department, university library) and the expected publication date is May 2013. Thank you!

- Arias, D., Shedd, T., and Jester, R., "Theoretical Analysis of Waste Heat Recovery from an Internal Combustion Engine in a Hybrid Vehicle," SAE Technical Paper 2006-01-1605, 2006, doi:10.4271/2006-01-1605.
 - Fig. 11: Effect of electric supply
 - Fig. 12: Effect of backpressure
- El Chammas, R. and Clodic, D., "Combined Cycle for Hybrid Vehicles," SAE Technical Paper 2005-01-1171, 2005, doi:10.4271/2005-01-1171.
 - Figure 1: Heat balance of a 1.4 Spark ignition internal combustion engine
 - Figure 2: Rankine system and its Ideal cycle
 - Figure 4: T-s diagram for dry, wet and isentropic fluids
 - Figure 5: Rankine cycle efficiency
- Mori, M., Yamagami, T., Oda, N., Hattori, M. et al., "Current Possibilities of Thermoelectric Technology Relative to Fuel Economy," SAE Technical Paper 2009-01-0170, 2009, doi:10.4271/2009-01-0170.
 - Fig. 11: Effect of electric supply
 - Fig. 12: Effect of backpressure
- Ringler, J., Seifert, M., Guyotot, V., and Hübner, W., "Rankine Cycle for Waste Heat Recovery of IC Engines," *SAE Int. J. Engines* 2(1):67-76, 2009, doi:10.4271/2009-01-0174.
 - Figure 4: Exhaust gas temperatures in the gasoline engine map
- Stobart, R. and Milner, D., "The Potential for Thermo-Electric Regeneration of Energy in Vehicles," SAE Technical Paper 2009-01-1333, 2009, doi:10.4271/2009-01-1333.
 - Fig 3a – Schematic showing cross-section of a typical multi-couple thermo-electric module
 - Fig 3b – Electrical and thermal conduction paths of a multi-couple thermo-electric module
- Teng, H., Regner, G., and Cowland, C., "Waste Heat Recovery of Heavy-Duty Diesel Engines by Organic Rankine Cycle Part I: Hybrid Energy System of Diesel and Rankine Engines," SAE Technical Paper 2007-01-0537, 2007, doi:10.4271/2007-01-0537.
 - Fig.10 An ORC-WHR system with integrated low-temperature cooling loop.

--

John R. Armstead, Ph.D. Candidate

Mechanical Engineering - Engineering Mechanics
MEEM3220 Energy Lab Coordinator
Michigan Technological University
1400 Townsend Drive
Office 823, R.L. Smith ME-EM Building
Houghton, MI 49931
jramste@mtu.edu

Nothing in this message is intended to constitute an electronic signature unless a specific statement to the contrary is included in this message. Confidentiality Note: This message is intended only for the person or entity to which it is addressed. It may contain confidential and/or proprietary material. Any review, transmission, dissemination or other use, or taking of any action in reliance upon this message by persons or entities other than the intended recipient is prohibited. If you received this message in error, please contact the sender and delete it from your computer.

Photography License Agreement

This Photography License Agreement ("Agreement") is made and entered into as of June 14th, 2013 ("Effective Date") by and between Kohler Co., a Wisconsin corporation, with its principal place of business at 444 Highland Drive, Kohler, WI 53044 ("Kohler") and John R. Armstead, an individual U.S. citizen, with an address of 1400 Townsend Drive, Office 823, R.L. Smith ME-EM Bldg., Houghton, MI 49931 ("Licensee").

BACKGROUND

- A. Kohler is the owner of all rights to the Photographs identified in Exhibit A ("Photographs"). Licensee desires to have the right to use and incorporate copies of the Photographs in a doctoral dissertation at Michigan Technological University ("Material").
- B. Kohler is willing to grant Licensee the right to use the Photographs in the Material as set forth in Exhibit A.

NOW THEREFORE, the parties hereby agree as follows:

1. GRANT OF LICENSE

- (a) Rights Granted to Licensee. Kohler grants to Licensee a limited, non-exclusive, perpetual, worldwide, fully paid-up, royalty free license and right to:
 - (1) reproduce, use, display (including publicly), publish and distribute the Photographs, as part of the Material, in print and electronic format; and
 - (2) use Kohler's name as set forth in Section 4 below, together with the Photographs, in the Material.
- (b) Rights Reserved to Kohler. Licensee acknowledges and agrees that Kohler retains all ownership rights, copyrights, and other rights to the Photographs and it has no rights in the Photographs except those expressly granted by this Agreement. Nothing herein shall be construed as restricting Kohler's right to sell, lease on a non-exclusive basis, license, modify, publish, or otherwise distribute the Photographs, in whole or in part, to any other person.
- (c) No Obligation to Use. Nothing herein will constitute any obligation on the part of Licensee to make any use of the rights set forth herein.

(d) No Endorsement. The parties acknowledge and agree that the use of the Photographs in the Materials and use of Kohler's name as set forth in Section 4 below shall not constitute, nor imply, an endorsement by Kohler of Licensee's Materials.

2. DELIVERY

Upon execution of this Agreement, Kohler will deliver copies of the Photographs to Licensee in the form of a digital high resolution file.

3. COMPENSATION

Kohler expressly acknowledges and agrees that the use of Kohler's name as set forth in Section 4 below shall be deemed sufficient consideration for the granting of the rights to Licensee hereunder.

4. CREDIT NOTICE

Licensee will give Kohler credit in the following form: "Photos Courtesy of Kohler Co."

5. INDEMNIFICATION

Licensee agrees to defend, indemnify and hold harmless Kohler against any damages, losses, or expenses (including but not limited to reasonable attorneys' fees) in connection with any use of the Material, except for any claims based solely upon ownership rights in and to the Photographs.

6. TERMINATION

(a) Termination for Breach. Either party may terminate this Agreement only in the event of a material breach of the terms or conditions of this Agreement by the other party, provided that such breach is not cured within ten (10) days of written notice from the non-breaching party. Licensee's use of the Photographs in any manner other than as contemplated by this Agreement shall be considered a material breach.

(b) Effect of Termination. Upon termination of this Agreement, Licensee will immediately cease use of the Photographs and production of copies of the Material containing the Photographs.

7. NO RIGHT TO SUBLICENSE OR ASSIGN

Licensee shall not have the right to sublicense or assign the rights granted to Licensee under this Agreement.

8. COMPLETE AGREEMENT

This Agreement constitutes the sole and entire agreement between the parties pertaining to the licensed Photographs and supersedes all prior negotiations and agreements of the parties. Any amendments to this Agreement shall not be valid unless made in writing and signed by both parties.

9. INVALIDITY

In the event that any provision herein or part thereof shall be deemed void or invalid by a court of competent jurisdiction, the remaining provisions or parts thereof shall be and remain in full force and effect.


10. GOVERNING LAW AND FORUM

This Agreement shall be governed by and construed in accordance with the laws of the State of Wisconsin. Any and all proceedings related to the subject matter shall be maintained in the state or federal courts of Wisconsin and the parties hereby consent and submit to the jurisdiction of such courts.

IN WITNESS WHEREOF, the parties have executed this Agreement as of the Effective Date.

KOHLER CO.

JOHN R. ARMSTEAD

By: 
Name: Scott L. Anderson
Title: Communications Director

By: 




John Armstead <jrarmste@mtu.edu>

Request to reprint copyright material

Cyndy Masters <cyndym@customthermoelectric.com>
To: John Armstead <jrarmste@mtu.edu>

Tue, Jun 4, 2013 at 5:41 PM

Good afternoon:

This company has no objection to you re-printing the TEG Spec Sheet. My position at this company is Secretary/Treasurer.

Thanks,

Cyndy M.



cyndym@customthermoelectric.com

This communication, including any attachments, may contain confidential information and is intended only for the individual or entity to whom it is addressed. Any review, dissemination, copying of this communication or action taken based on it by anyone other than the intended recipient is strictly prohibited. If you are not the intended recipient, please contact the sender by reply e-mail, delete and destroy all copies of the original message including any attachments

----- Original Message -----

From: John Armstead
To: temodule@customthermoelectric.com
Sent: Tuesday, June 04, 2013 3:36 PM
Subject: Request to reprint copyright material

Custom Thermoelectric
11941 Industrial Park Road, STE 5
Bishopville, MD 21813

I am completing a doctoral dissertation at Michigan Technological University entitled "Novel Automotive Waste Heat Recovery Techniques." I would like your permission to reprint a figure from a TEG specification sheet. This dissertation will be in both print and electronic format. The number of copies will be approximately four (personal use, adviser, department, and university library) and the expected publication date is June 2013. Thank you!

- TEG Specification Sheet: Seebeck Thermoelectric Generator – Part# 1261G-7L31-04CL (REV. 10-03-2011)
 - Figure title: Watts Output at selected Cold Face temperatures

—

John R. Armstead, Ph.D. Candidate
Mechanical Engineering - Engineering Mechanics
MEEM3220 Energy Lab Coordinator
Michigan Technological University
1400 Townsend Drive
Office 823, R.L. Smith ME-EM Building
Houghton, MI 49931
jrarmste@mtu.edu